Cost-based Linear Holding Practice and Collaborative Air Traffic Flow Management under Trajectory Based Operations

YAN XU

Master of Engineering

Advisor

DR. XAVIER PRATS I MENENDEZ

Doctorate program in Aerospace Science and Technology

Department of Physics – Aeronautics Division

Technical University of Catalonia – BarcelonaTech

A dissertation submitted for the degree of

Doctor of Philosophy

September 2018

Cost-based Linear Holding Practice and Collaborative Air Traffic Flow Management under Trajectory Based Operations

Author
Yan Xu

Advisor
Dr. Xavier Prats i Menéndez

Thesis committee
Dr. Lorenzo Castelli
Dr. Luis Delgado
Dr. Adeline de Montlaur

Doctorate program in Aerospace Science and Technology
Technical University of Catalonia – BarcelonaTech
September 2018

PhD. Thesis made in:
Department of Physics – Aeronautics Division
Esteve Terradas, 5.
08860 Castelldefels
Catalonia (Spain)

To my parents
Jianhua Xu and Lin Shi

Contents

List of Figures

Figures in Appendices

List of Tables

Tables in Appendices

List of Publications

The list of publications resulting from this PhD work is given in inverse chronological order as follows:

Journal Papers

- XU YAN & PRATS XAVIER. 2018. Trajectory Optimization for Airspace Flow Programs: A Case Study on Delay Absorption and Recovery. *IEEE Transactions on Intelligent Transportation Systems*. In press.
- XU YAN, DALMAU RAMON & PRATS XAVIER. 2018. Climb, Cruise, and Descent Speed Reduction for Airborne Delay Without Extra Fuel. *Journal of Aircraft*. **55(2)**, 1299–1304.
- XU YAN & PRATS XAVIER. 2017. Including Linear Holding in Air Traffic Flow Management for Flexible Delay Handling. *Journal of Air Transportation*. **25**, 123–137.
- XU YAN, DALMAU RAMON & PRATS XAVIER. 2017. Maximizing airborne delay at no extra fuel cost by means of linear holding. *Transportation Research Part C: Emerging Technologies*. **81**, 137–152.
- XU YAN & PRATS XAVIER. 2017. Effects of linear holding for reducing additional flight delays without extra fuel consumption. *Transportation Research Part D: Transport and Environment*. **53**, 388–397.

Conference Proceedings

- XU YAN & PRATS XAVIER. 2018 (Sept.). Synchronization of Traffic Flow and Sector Opening for Collaborative Demand and Capacity Balancing. *In: Proceedings of the 37th AIAA/IEEE Digital Avionics Systems Conference (DASC)*. AIAA/IEEE, London (UK).
- XU YAN, PRATS XAVIER & YIN JIANAN. 2018 (Sept.). Coordinated Trajectory Management for Integrated Control of Airport and Airspace Operations. *In: Proceedings of the 37th AIAA/IEEE Digital Avionics Systems Conference (DASC)*. AIAA/IEEE, London (UK).
- XU YAN, DALMAU RAMON, MELGOSA MARC, MONTLAUR ADELINE & PRATS XAVIER. 2018 (Jun.). Alternative Trajectory Options for Delay Reduction in Demand and Capacity

Balancing. *In: Proceedings of the 8th International Conference on Research in Air Transportation (ICRAT)*. FAA/Eurocontrol, Castelldefels, Barcelona (Spain).

- XU YAN, PRATS XAVIER, YANG LEI & ZHANG HONGHAI. 2018 (Jan.). Integration of ground, airborne and linear holding for a cost-efficient network air traffic flow management. *In: Proceedings of the Transportation Research Board 97th Annual Meeting*. Transportation Research Board, Washington D.C. (USA).

- XU YAN & PRATS XAVIER. 2017 (Jan.). Including linear holding in air traffic flow management for flexible delay handling. *In: Proceedings of the 12th USA/Europe Air Traffic Management R&D Seminar*. FAA/Eurocontrol, Seattle, Washington, (USA).

- XU YAN, YIN SUWAN, DALMAU RAMON, PRATS XAVIER & HAN KE. 2017 (Jan.). Linear holding for reducing additional delays experienced by flights subject to ground holding at no extra fuel cost. *In: Proceedings of the Transportation Research Board 96th Annual Meeting*. Transportation Research Board, Washington D.C. (USA).

- XU YAN, DALMAU RAMON & PRATS XAVIER. 2016 (Jun.). Effects of speed reduction in climb, cruise and descent phases to generate linear holding at no extra fuel cost. *In: Proceedings of the 7th International Conference on Research in Air Transportation (ICRAT)*. FAA/Eurocontrol, Philadelphia (USA).

Acknowledgment

First of all, I would like to thank Dr. Lorenzo Castelli at Università degli Studi di Trieste (Italy), Dr. Luis Delgado at University of Westminster (UK), and Dr. Adeline de Montlaur at the Technical University of Catalonia (Spain) to join the committee panel of my PhD defense. I do appreciate that they could spare time to review this thesis and to attend my final presentation sharing their subject expertise and invaluable experience with us.

This PhD work has been funded by the Chinese Scholarship Council (No. 201506830050) in a joint program with the Technical University of Catalonia (UPC) from September 2015. Back to that year, I still remember the first day when I came to this place. I met one PhD student in our building who had just passed his thesis defense. Folk wisdom says a watched pot never boils. I never waited for this last moment to come, just doing my job and enjoying things happened around in every single day, yet all of a sudden it turns out that my pot is already boiling.

Before I came here from China, I really had hardly any confidence in pursing my PhD, in a completely unfamiliar environment far away from my home. I didn't even believe that I could eventually draw a report of hundred pages in English. Fortunately, I have made it, and Dr. Xavier Prats is the one who I must thank the most. He has been always standing by my side supporting me, cheering me up when I was down, helping me to overcome so many difficulties, and leading me to finally achieve that goal.

My officemates and friends, Ramon Dalmau, Marc Melgosa and Leonardo Camargo, who breathe the same air with me all day long through the three years, are indeed the best guys. Ramon Dalmau let me see clearly the gap in our research field between Chinese and European graduate students, and thus has encouraged me to catch up with the average level as much as I can. Dalmau has been generously teaching me with his latest studies, carefully reviewing and co-authoring my study. Marc Melgosa has helped me with lots of things too, even though he was often quite busy in delivering projects and giving lectures. Also thanks to Marc, I could know better about the real Catalan and Spanish cultures. Leonardo Camargo shared his professional knowledge about high performance computing with me. This has helped to extend my current work to another promising branch, and I do appreciate Leo's contribution.

I am also very grateful for the help and support from my colleagues in UPC during all the work undertaken in this thesis: Dr. Adeline de Montlaur, Dr. Cristina Barrado, Dr. Sergio Ruiz and Raúl Sáez. They have been always very helpful and responsive. We have shared many hours of work and enjoyment, and I feel super lucky to have chances to join with them.

In addition, I should thank Dr. Daniel Delahaye who hosted my visiting study at Ecole Nationale de l'Aviation Civile (ENAC) in Toulouse (France). Dr. Delahaye was being very kind during my stay there, and also gave insightful comments to my study which has been presented in this thesis. The visiting study was sponsored by the La Caixa-UPC International Mobility Scholarship (Y4262159C). Thanks to this research stay, I met Dr. Andrija Vidosavljevic and Ji Ma whom I had delightful discussions with.

Dr. Luis Delgado should be particularly acknowledged. Dr. Delgado had done excellent work when he was still a PhD candidate in UPC, which casts the essential light to how to move the first step of my PhD.

I would like to also thank Dr. David Pino, the coordinator of the Doctoral Program of Aerospace Science and Technology, who has been helping me with all my PhD required procedures. Besides, I would like to thank Alícia Sánchez, the secretary of the doctoral program, for kindly proceeding with my administrative paperwork.

Finally, I do hope to specifically thank my family. None of this would have been even possible without their unconditional support. As said by an old proverb, like a butterfly wants to fly across the ocean, family is the sailboat.

Castelldefels, September 2018
Yan Xu

Abstract

The current air transportation system is reaching the capacity limit in many countries/regions across the world. It tends to be less efficient or even incapable sometimes to deal with the enormous air traffic demand that continues growing year by year. This has been evidenced by the record-breaking flight delays reported in various places in recent years, which, have resulted in notable economical loses. To mitigate this imbalance between demand and capacity, air traffic flow management (ATFM) is usually one of the most useful options. It regulates traffic flows according to air traffic control capacity while preserving safety and efficiency of flights.

ATFM initiatives can be considered well in advance of the flight execution - more than one year earlier - based on air traffic forecasts and capacity plans, and continue in effect, with information updated, to eventually the day of operation. This long effective period will inevitably allow substantial collaboration among different stakeholders, including the ATFM authority, airspace users (AUs), air navigation service providers (ANSPs), airports, etc. Under the forthcoming paradigm of trajectory based operations (TBO), the flight 4-Dimensional trajectory has been anticipated to further enhance the connection between flight planning and execution phases, thus fostering such collaboration in ATFM.

Moreover, under nowadays operations, ground holding is a typical measure undertaken in many widely-used ATFM programs. Even though holding on the ground, at the origin airport, has the advantage of fuel efficiency over the air holding, it turns out that its feature of low flexibility would, in some circumstances, affect the ATFM performance. Yet, with proper flight trajectory management, it is also possible to have delay airborne at no extra fuel cost than performing ground holding.

This PhD thesis firstly focuses on this trajectory management, specifically on a cost-based linear holding practice. The linear holding is realized progressively along the planned trajectory through precise speed control which can be enabled by aircraft trajectory optimization techniques. Some typical short/mid haul flights are simulated for achieving the maximum airborne delay that can be yielded using same fuel consumption as initially scheduled. Based on this, its potential applicability is demonstrated, such as improving the effectiveness of Airspace Flow Programs, and helping to neutralize the additional delays subject to fixed ground holding.

A network ATFM model is adapted from the well-studied Bertsimas Stock-Patterson (BSP) model, incorporating different types of delay (including the linear holding) to flexibly handle the traffic flow with a set of given (yet changeable) capacities. In order that the benefits of the model

can be fully realized, AUs are required to participate in the decision-making process, submitting for instance the maximum linear holding bound per flight along the planned trajectory. The procedures are illustrated through a case study, showing an amount of delay reduction compared to using the BSP model.

Next, increased AUs' participation is expected for a proposed Collaborative ATFM framework, in which not only various delay initiatives are considered, but also alternative trajectories which allow flights to route out of the identified hotspot areas. A centralized linear programming optimization model then computes for the best trajectory selections and the optimal delay distributions across all concerned flights. It is proved by numerical experiments that the inclusion of alternative trajectory options can remarkably reduce the amount of delays.

Finally, ANSPs' involvement is additionally considered for the framework, through dynamic airspace reconfiguration, further enhancing the collaboration between ATFM stakeholders. As such, the traffic flow regulation and sector opening scheduling are bounded into an integrated optimization model, and thus are conducted in a synchronized way. Results indicate that the performance of demand and capacity balancing can be even improved if compared with the previous ATFM models presented in this PhD thesis.

Resumen

El sistema de transporte aéreo actual está llegando a su límite de capacidad en muchos países y regiones del mundo. Como consecuencia, éste tiende a ser menos eficiente e incluso en ocasiones incapaz de afrontar la enorme demanda de tráfico aéreo que incluso hoy en día crece rápidamente. Este hecho se ha visto evidenciado por los enormes retrasos registrados en diferentes lugares los últimos años, lo cual ha comportado enormes pérdidas económicas para la sociedad. Una gestión del flujo del tráfico aéreo (ATFM) más adecuada podría mitigar este desequilibrio entre la demanda y la capacidad. La función del ATFM es regular los flujos de tráfico aéreo según la capacidad de control del tráfico aéreo, siempre asegurando que los vuelos sean seguros y eficientes.

Las regulaciones del sistema de ATFM se pueden aplicar mucho antes de la ejecución del vuelo – más de un año antes – en función de las previsiones de tráfico aéreo y de la capacidad esperada. Una vez aplicadas, estas regulaciones continuarán evolucionando, con información actualizada, hasta el día de su ejecución. El largo período entre la planificación del vuelo y su ejecución permitirá una importante colaboración entre los diferentes miembros implicados, incluida la autoridad del ATFM, los usuarios del espacio aéreo (AUs), los proveedores de servicios de navegación aérea (ANSP), los aeropuertos, etc. En el marco del futuro paradigma de las operaciones basadas en trayectorias, la introducción de vuelos con control sobre la trayectoria en las 4 dimensiones espera mejorar aún más la conexión entre las fases de planificación del vuelo y su ejecución, fomentando así la colaboración en el proceso de toma de decisiones del sistema ATFM.

En las operaciones de hoy en día la espera en tierra es una de las regulaciones que más se aplica en el sistema de ATFM con el fin de evitar congestiones en los aeropuertos o en los sectores del espacio aéreo. Aun teniendo en cuenta que esperar en tierra, en el aeropuerto de origen, tiene la ventaja de consumir menos combustible que esperar en el aire en el aeropuerto de destino, su poca flexibilidad podría afectar negativamente al rendimiento del ATFM en algunas circunstancias. Aun así, con una gestión adecuada de la trayectoria de vuelo, también es posible efectuar cierto retraso en el aire sin ningún coste adicional de combustible respecto a lo que resultaría esperando en tierra.

Esta tesis doctoral se centra en primer lugar en esta gestión de la trayectoria de vuelo, específicamente en una práctica de espera lineal considerando los costes para la aerolínea. . La espera lineal se efectúa progresivamente a lo largo de la trayectoria planificada mediante un control preciso de la velocidad. Las velocidades que generan la espera deseada durante el vuelo se calculan mediante técnicas de optimización. Algunos vuelos típicos de corto y medio alcance se

simulan para cuantificar el máximo retraso en el aire que se podría generar utilizando el mismo consumo de combustible que el previsto inicialmente. Basándose en los resultados obtenidos, se investiga su potencial aplicabilidad, como por ejemplo mejorar la planificación de programas de flujo del espacio aéreo, y ayudar a neutralizar los retrasos no deseados adicionales debidos a la incertidumbre del sistema.

Se desarrolla un modelo de la red de ATFM basado en el conocido modelo Bertsimas Stock-Patterson (BSP). Como novedad, el modelo desarrollado en esta tesis incorpora diferentes tipos de retraso (incluyendo la espera lineal) para gestionar de manera más flexible el flujo de tráfico dado un conjunto de capacidades predefinidas. Con el fin de explotar al máximo los beneficios del modelo propuesto en esta tesis, se assume que las aerolíneas participaran el el proceso de toma de decisiones, declarando, por ejemplo, la máxima espera lineal asociada a cada vuelo a lo largo de la trayectoria planeada. Este concepto se ilustra con un caso de estudio, donde se demuestra una reducción significativa de los retrasos, comparado con el modelo BSP.

Seguidamente, se incluye la participación de las aerolíneas en un sistema de ATFM colaborativo, en el cual no tan sólo se consideran diferentes tipos de retrasos para balancear la capacidad y la demanda, sino también trayectorias alternativas que permiten que los vuelos eviten de forma óptima los sectores del espacio aéreo congestionados. Un modelo de optimización centralizado basado en programación lineal calcula las mejores selecciones de la trayectoria y las distribuciones óptimas de retraso en todos los vuelos afectado por la regulación. Se demuestra que incluir trayectorias alternativas puede reducir notablemente la cantidad de retrasos.

Finalmente, se considera también la participación de los ANSP en el sistema de ATFM, a través de la configuración dinámica del espacio aéreo, mejorando aún más la colaboración entre los miembros implicados en el sistema. Como tales, la regulación del flujo de tráfico aéreo y la programación de apertura de los diferentes sectores del espacio aéreo se incluyen en un modelo integrado de optimización y, por lo tanto, se programan de manera sincronizada. El nuevo modelo de balance de demanda y capacidad mejora aún más los resultados, si se compara con los otros modelos ATFM presentados también en esta tesis doctoral.

Resum

El sistema de transport aeri actual està arribant al seu límit de capacitat en molts països i regions del món. En conseqüència, aquest sol ser menys eficient i en algunes ocasions incapaç d'afrontar l'enorme demanda de trànsit aeri que encara avui creix ràpidament. Aquest fet s'ha vist evidenciat pels enormes retards enregistrats en diversos llocs els últims anys, i que han comportat enormes pèrdues econòmiques per a la societat. Una gestió del flux de trànsit aeri (ATFM) més adequada podria mitigar aquest desequilibri entre la demanda i la capacitat. La funció de l'ATFM és regular els fluxos de trànsit aeri segons la capacitat de control del trànsit aeri, i alhora assegurar que els vols siguin segurs i eficients.

Les regulacions del sistema d'ATFM es poden aplicar molt abans de l'execució del vol - més d'un any abans - en funció de les previsions del trànsit aeri i de la capacitat esperada. Un cop aplicades, aquestes regulacions continuaran evolucionant, amb informació actualitzada, fins el dia de la seva execució. El llarg període entre la planificació del vol i la seva execució permetrà una important col·laboració entre els diferents membres implicats, inclosa l'autoritat de l'ATFM, els usuaris de l'espai aeri (AUs), els proveïdors de serveis de navegació aèria (ANSP), els aeroports, etc. En el marc del futur paradigma de les operacions basades en trajectòries, la introducció de vols amb control sobre la trajectòria en les 4 dimensions espera millorar encara més la connexió entre les fases de planificació de vol i execució, fomentant així la col·laboració en el procés de presa de decisions del sistema d'ATFM.

En les operacions d'avui en dia l'espera a terra és una de les regulacions que més aplica el sistema d'ATFM per tal d'evitar congestions als aeroports o sectors de l'espai aeri. Tot i que esperar a terra, a l'aeroport d'origen, té l'avantatge de consumir menys combustible que esperar a l'aire a l'aeroport de destí, la seva poca flexibilitat podria afectar negativament al rendiment de l'ATFM en algunes circumstàncies. Tanmateix, amb una gestió adequada de la trajectòria de vol, també és possible efectuar cert retard a l'aire sense cap cost addicional de combustible respecte al que resultaria esperant a terra.

Aquesta tesi doctoral s'enfoca en primer lloc en aquesta gestió de trajectòria de vol, específicament en una pràctica d'espera lineal tenint en compte els costos per l'aerolínea. L'espera lineal s'efectua progressivament al llarg de la trajectòria planificada mitjançant un control precís de la velocitat. Les velocitats que generen l'espera desitjada durant el vol és calculen mitjançant tècniques d'optimització. Alguns vols típics de curt i mig abast es simulen per quantificar el màxim retard a l'aire que es podria generar utilitzant el mateix consum de combustible que el

previst inicialment. Basant-se en els resultats obtinguts, s'explora la seva aplicabilitat potencial, com ara millorar la planificació dels programes de flux de l'espai aeri, i ajudar a neutralitzar els retards addicionals no desitjats deguts a l'incertesa del sistema.

Es desenvolupa un model de la xarxa d'ATFM basat en el conegut model de Bertsimas Stock-Patterson (BSP). Com a novetat, el model desenvolupat en aquesta tesi incorpora diferents tipus de retard (incloent-hi l'espera lineal) per gestionar de forma més flexible el flux de trànsit donat un conjunt de capacitats pre-definides. Per tal d'explotar al màxim els beneficis del model proposat en aquesta tesi, s'assumeix que les aerolínies participaran en el procés de presa de decisions, declarant, per exemple, la màxima espera lineal associada a cada vol al llarg de la trajectòria planejada. Aquest concepte queda il·lustrat amb un cas d'estudi, on es demostra una reducció significativa dels regards, si es compara amb el model BSP.

Tot seguit, s'inclou la participació dels AUs en un sistema d'ATFM col·laboratiu, en el qual no només es consideren diverses tipus de retard per balancejar la capacitat i la demanda, sinó també trajectòries alternatives que permeten que els vols evitin de forma òptima els sectors de l'espai aeri congestionats. Un model d'optimització centralitzat basat en programació lineal calcula les millors seleccions de trajectòria i les distribucions òptimes de retard en tots els vols afectats per la regulació. Es demostra que incloure trajectòries alternatives pot reduir notablement la quantitat de retards.

Finalment, es considera també la participació de l'ANSP en el sistema d'ATFM, a través de la configuració dinàmica de l'espai aeri, millorant encara més la col·laboració entre els membres implicats en el sistema. Com a tal, la regulació del flux de trànsit i la programació d'obertura dels diferents sectors de l'espai aeri s'inclouen en un model integrat d'optimització i, per tant, es programen de forma sincronitzada. Els resultats suggereixen que el rendiment del balanç de la demanda i la capacitat es pot millorar encara més amb aquest sistema ATFM col·laboratiu complert. El nou model de balanç de demanda i capacitat millora encara més els resultats, si es compara amb els altres models d'ATFM presentats també en aquesta tesi doctoral.

Zhāi Yào

当前的航空交通运输系统，在很多国家（或地区）已逐步逼近其运行容量的限制。处理日益增长的交通需求正成为一项低效甚至无法实现的任务。近年来各地不断刷新的延误记录即是最有力的证明，而这些延误，显然已经对经济社会的发展造成了相当程度的阻碍。为了缓解航空交通需求与容量之间的失衡，常为采用的一种有效方案，空中交通流量管理，即依据容量约束而实施对交通流的科学管控，同时确保航班运行的安全与高效。

空中交通流量管理的措施可在航班执行前较长一段时间内（超过一年）基于交通和容量等的预测数据进行统筹规划，且该过程也将会随着新的信息的获取而保持持续更新，直至航班运行的当日。显然，这一期间各相关方可以有充分的时间来深入合作，包括流量管理当局，空域用户，空中导航服务提供方，机场等。在即将到来的“基于航迹运行”空管新范式下，航空器的四维航迹预计将能够进一步增强航班计划与执行之间的联系，从而促进上述流量管理中各方的协作。

此外，就目前的运行条件下，地面等待仍然是一种较为常见的流量管理手段。虽然在地面上吸收延误有诸多的优势，例如较之空中盘旋等待而言燃油经济性更高，然而其本身较低的灵活性在一些特定的场景下会影响流量管理的效率。实际上，通过适当的飞行航迹的调整也可以在不消耗额外燃油的情况下实现空中延误吸收。

本文首先即着眼于这一飞行航迹调整方法，尤其是一种基于燃油成本考虑的空中线性等待策略。该策略作用于航班的原规划航迹，通过航空器轨迹优化技术实现精确的速度控制，从而达到渐进式吸收延误的目的。本文探究了一批典型的短/中程航班，在不增加原计划外燃油成本的情况下，计算了他们的最大线性等待能力，并基于此提出了部分该策略的潜在应用，例如提升Airspace Flow Programs的运行效率，以及能够中和地面等待所带来的附加延误等。

之后，本文在经典的Bertsimas Stock-Patterson (BSP)模型基础上，提出了一种网络交通流模型，其中融合了不同的延误吸收方式（包括上述线性等待策略）对交通流进行灵活地调控，使之满足一系列给定的（且可变的）容量限制。为使模型能够取得最大执行效果，空域用户需参与到这一决策制定过程中，并为每架受到影响的航班提供相关信息。案例分析显示，该方法较之原BSP模型可减少一定程度的延误。

接着，本文探索了一项协同流量管理框架，其中空域用户的积极参与可得到进一步体现，该协同框架在此前网络交通流模型基础上，增加了备选航迹的选项，即空域用户可为每架航空器自主设计多条航迹，从而避开空域中的热点区域，降低可能的延误。本文建立了全局性的线性规划模型，并针对全体受控航班计算最优的航迹选择及延误分配。实验证明，添加备选航迹的选项可大幅度降低系统所需延误。

最后，本文在上述协同流量管理框架下，又增加考虑了空中导航服务提供方参与决策的可能，进一步强化了各相关方之间的协作。其中，本文采用动态空域重构的方法，实现交通流管控与扇区开放时段的同步规划，且两方面因素被整合进一个统一的优化模型。结果显示，容流平衡的效能较之本文之前提出的模型得到再次提升。

Notation

a_f	airborne holding for flight f
$a \in A$	set of airports
$C^a_{arr}(\tau)$	the arrival capacity of airport a in period τ
$C^a_{dep}(\tau)$	the departure capacity of airport a in period τ
$C^s_{sec}(\tau)$	the capacity of sector s in period τ
$C_{\Delta F}$	cost of extra fuel consumption
$C_{\Delta R}$	cost of extra route charges
$C_{\Delta T}$	extra time related costs
D^i_n	along path distance of flight segment i in Case-n
$e \in S^\tau_l$	set of elementary sectors collapsing to operating sector l during τ
e^j_f	the length of feasible time window
$f \in \mathcal{F}$	set of flights
F_i	fuel consumption in flight segment i
F_{nom}	fuel consumption for the nominal flight trajectory
$FF(t)$	fuel flow
g_f	ground holding for flight f
h_f	arrival delay for flight f
H^i_n	altitude (flight level) of flight segment i in Case-n
$k \in K_f$	set of trajectory options of flight f
$j \in J$	set of control points
$j \in P_k$	set of defined positions that trajectory k traverses
$l \in L$	set of operating sectors
M	Mach number
m	aircraft mass
n_f	number of defined positions for flight f
n_k	number of defined positions for trajectory k
$P(f,i)$	$\begin{cases} \text{departure airport,} & \text{if } i = 1 \\ \text{arrival airport,} & \text{if } i = n_f \\ \text{sector positions,} & \text{if } 1 < i < n_f \end{cases}$

$P(k,i)$	$\begin{cases}\text{departure airport,} & \text{if } i=1\\ \text{arrival airport,} & \text{if } i=n_k\\ \text{intermediate designed positions,} & \text{if } 1<i<n_k\end{cases}$
P_f	positions along the scheduled f trajectory
r_f^j	scheduled time of flight f at position j
r_k^j	initially scheduled time of trajectory k at position j
$R(f)$	scheduled time of flight f in line with $P(f)$
RC_k^f	cost of route charges for trajectory k of flight f
RC_0^f	cost of route charges for initial trajectory of flight f
$s \in S$	set of sectors of capacity constrained
$S(k,l,\tau)$	the first entered elementary sector for trajectory k among those collapsed into operating sector l during time period τ
$t \in T$	set of time moments
$t_0^{(i)}$	start time of time window for flight segment i
$t_f^{(i)}$	final time of time window for flight segment i
$t_{(\tau+1)}$	start time of time period $(\tau+1)$
T_i	operational time in flight segment i
T_f^j	feasible time window for flight f at position j
T_k^j	feasible time window for trajectory k at position j
$\dot{T}_k^j$	assigned time for trajectory k departing from position j
$\underline{T}_f^j$	lower bound of the feasible time window for flight f at position j
$\underline{T}_k^j$	lower bound of the feasible time window for trajectory k at position j
$\overline{T}_f^j$	upper bound of the feasible time window for flight f at position j
$\overline{T}_k^j$	upper bound of the feasible time window for trajectory k at position j
T^r	aircraft thrust
$T(\tau)$	τ^{th} time period defined within T
TJ_k^f	cost of fuel consumption for trajectory k of flight f
TJ_0^f	cost of fuel consumption for initial trajectory of flight f
u^w	the maximum airborne holding time
$u_k^{j,j'}$	time bound of delay recovery within flight segment (j,j')
$v_f^{j,j'}$	the maximum LH bound of contiguous positions
$v_k^{j,j'}$	time bound of LH within flight segment (j,j')
V_{eq}	equivalent airspeed
V_{LS}	lowest selectable speed
V_{nom}	nominal airspeed
V_S	stalling airspeed
$w \in W$	set of defined positions of sector entrance
$\boldsymbol{x}^{(i)}$	aircraft state vector of flight segment i
$z_f^{j,j'}$	scheduled duration of contiguous positions j and j' for flight f
$z_k^{j,j'}$	scheduled duration of contiguous positions j and j' for trajectory k
α	weighted cost of airborne holding to ground holding
α_k	weighted cost of fuel consumption for trajectory k
β	weighted cost of linear holding to ground holding
β_k	weighted cost of route charges for trajectory k
ϵ	fairness factor
δ_k	weighted cost of airborne holding for trajectory k
Δt_{GDP}	assigned GDP/AFP delay
γ	aircraft path angle

γ_k	weighted cost of ground holding for trajectory k
$\tau \in \mathcal{T}$	set of periods for traffic demand
ζ	weighted cost of delay recovery for trajectory k

List of Acronyms

ACC	Area Control Center
ADS-B	Automatic Dependent Surveillance-Broadcast
AFP	Airspace Flow Program
AIRAC	Aeronautical Information Regulation And Control
ANS	Air Navigation Services
ANSP	Air Navigation Service Providers
ASM	Airspace Management
ATC	Air Traffic Control
ATCO	Air Traffic Control Officer
ATFM	Air Traffic Flow Management
ATM	Air Traffic Management
ATS	Air Traffic Service
BADA	Base Of Aircraft Data
BDT	Business Development Trajectory
CAS	Calibrated Airspeed
CASA	Computer Assisted Slot Allocation
CATFM	Collaborative Air Traffic Flow Management
CCO	Continuous Climb Operations
CDM	Collaborative Decision Making
CDO	Continuous Descent Operations
CFMU	Central Flow Management Unit
CI	Cost Index
CNS	Communication Navigation and Surveillance
CPU	Central Processing Unit
CTA	Controlled Time of Arrival
CTD	Controlled Time of Departure
CTO	Controlled Time Over
CTOP	Collaborative Trajectory Options Program
DCB	Demand and Capacity Balancing
DDR	Demand Data Repository
DOC	Direct Operating Costs
ECAC	European Civil Aviation Conference

EDCT	Expect Departure Clearance Time
ETA	Estimated Time of Arrival
ETOT	Estimated Take Off Time
FAA	Federal Aviation Administration
FCA	Flow Constrained Area
FF	Fuel Flow
FL	Flight Level
FMS	Flight Management System
GCD	Great Circle Distance
GD	Green Dot speed
GDP	Ground Delay Program
GH	Ground Holding
IAS	Indicated Airspeed
ICAO	International Civil Aviation Organization
ISA	International Standard Atmosphere
LH	Linear Holding
LP	Linear Programming
MILP	Mixed Integer Linear Programming
MIT	Miles-in-Trail
NAS	National Airspace System
NLP	Nonlinear Programming
NM	Network Manager
NOP	Network Operations Plan
PEP	Performance Engineering Program
RBD	Ration-By-Distance
RBS	Ration-By-Schedule
RBT	Reference Business Trajectory
SBT	Shared Business Trajectory
SESAR	Single European Sky ATM Research
SR	Specific Range
SWIM	System Wide Information Management
TAS	True Airspeed
TBO	Trajectory Based Operations
TMI	Traffic Management Initiative
TOC	Top Of Climb
TOD	Top Of Descent
TOS	Trajectory Options Set
UDPP	User Driven Prioritisation Process

千里之行始于足下

The journey of a thousand miles begins with one step

— Tao Te Ching · Lao Tze

I

Introduction

Air transportation is enabled by Air Navigation Services (ANS) that through the use of technology and human resources guarantee safe and efficient flights. ANS are provided by Air Navigation Service Providers (ANSPs), using a variety of Communication, Navigation and Surveillance (CNS) systems to realize Air Traffic Management (ATM) and Aeronautical Information Service (AIS). Among current ATM initiatives, Airspace Management (ASM), Air Traffic Flow Management (ATFM) and Air Traffic Service (ATS) are the main components concerning the organizational scope, procedures and concepts of operations, being Air Traffic Control (ATC) the most tactical service provided to the Airspace Users (AUs).

Nevertheless, the current air transportation system is faced with a significant strain from the fast-growing flight demand. This has been evidenced in recent years by severe flight delays and more commonly-seen network congestions. In Europe, year 2016 saw an average departure delay per flight of 11.3 minutes (and 29.1 minutes, per delayed flight, for the average arrival delay), representing an increase of 9% in comparison to 2015. Furthermore, the percentage of flights delayed more than 30 minutes from all-causes increased to 9.8%, while a monthly average of 1.9% of operational cancellations occurred (Eurocontrol, 2017).

Meanwhile, in the United States, 17% of the flights were delayed by more than 15 minutes in 2016, with another 1.2% canceled (US Department of Transportation, 2016a). Given an average delay cost of $62.55/min anticipated for the U.S. passenger carriers, the 60 million minutes of total delay in this year led to an estimated $3.8 billion direct aircraft operating costs (Airlines for America, 2016). Moreover, a report for a 30-year outlook to 2045 estimated that flight delays and congestion cost the U.S. economy more than $20 billion each year (US Department of Transportation, 2015). As analyzed in (Ball *et al.*, 2010a), among the total costs, passengers normally absorb 50% in lost time, missed connections, and unexpected food and lodging expenses; while

airlines undertake 25% in additional labor, fuel, and maintenance; and people who avoid air travel because of delays cost nearly 10% of the total economy costs.

As another example, being of almost the same size to the United States' airspace, China suffers also a severe issue of enormous flight delays, even though its flight demand accounts for only around 1/3 to that in the U.S.. Statistics reported that in China the percentage of flights that maintained their original flight plans was eventually increased from the previous year to 76% in 2016, which however was the highest number in the nearest 5 years. An average of 16 minutes of delays was issued in that year, and the number was worse, i.e., 21 minutes, in 2015 (Civil Aviation Administration of China, 2016). Indeed, such problems occur not only in these countries/regions, but also in many places across the world, perhaps just on different levels.

I.1 Efforts to balance demand and capacity

One of the primary causes for above-mentioned delays and congestion is that the number of flights (demand) often exceeds the supply of the airspace accommodation (capacity). Besides average traffic volumes have experienced a sustained growth in the last decades, air traffic demand also shows some seasonal or exceptional peaks (holiday seasons, major sport events, etc.). Conversely, convective weather, airspace restrictions, overloaded airports and ATC industrial actions, to name a few, can temporarily reduce this supply. The effort thereby to achieve demand and capacity balancing (DCB) is typically known as ATFM.

Examples of commonly-seen ATFM initiatives include Ground Delay Programs (GDPs) and Airspace Flow Programs (AFPs) in the United States National Airspace System (NAS). Similar initiatives exist in Europe, implemented by Eurocontrol's Central Flow Management Unit (CFMU), which is known as the Network Manager (NM) nowadays. GDPs control the arrival rate at an affected airport by assigning departure delays to flights at their origin airports (FAA, 2009). Similarly, an AFP identifies constraints in the en-route system, regulating flights filed into the Flow Constrained Area (FCA) (Libby *et al.*, 2005). While a flight has no choice but to end up at its destination airport, a capacity-constrained en-route sector can often be bypassed by selecting an alternative route. A trade-off thus exists between more costs in fuel (due to flying a longer route or a non optimal flight level if taking the alternative route) and less costs from delays. To that aim, AFPs specify available reroutes that avoid the FCA. Flight operators may choose to accept the delay for an affected flight, or to take the available reroute (Pourtaklo & Ball, 2009).

On basis of the existing GDP/AFP, a newly-introduced Collaborative Trajectory Options Program (CTOP) has been recently deployed in the United States since 2014, which could handle multiple FCAs within a single program and allow different parts of the program to be adjusted independently as conditions change (FAA, 2014). One major highlight of the CTOP is that airlines are allowed to submit a set of preferred trajectory options, which is the so-called Trajectory Options Set (TOS), in prior to the issuance of the program. This means that, instead of simply taking departure delays on the ground or yielding to an ATC reroute instruction en route, the operators could use a list of trajectories planned by themselves to bypass the constrained area(s) and accordingly avoid possible delays. In general, a CTOP automatically assigns delays and/or reroutes around one or more FCA-based airspace constraints in order to balance demand with available capacity (Miller & Hall, 2015).

I.1.1 On-going ATM paradigm shift

In Europe, a substantial change of the ATM paradigm is on-going through the SESAR (Single European Sky ATM Research) programme. SESAR is the technological and operational pillar

of the Single European Sky (SES) framework. As elaborated in the European ATM master plan (EUROCONTROL, 2015), this ATM change is performance-driven, focusing on 4 key performance areas (KPAs): environment, cost-efficiency, safety, and capacity/quality of service. The change is expected to bring about 3-fold increase in air traffic movements (capacity), whilst reducing delays (quality of service); improvement of the safety performance by a factor 10; a reduction by 10% of the impact on the environment; and a reduction of service provision costs by a half.

Similar evolutions exist in the United States, within the NextGen (Next Generation Air Transportation System) programme led by the Federal Aviation Administration (FAA), which is aimed at the modernization of U.S. air transportation system. Its goal is to increase the safety, efficiency, capacity, predictability, and resiliency of aviation (US Department of Transportation, 2016b). According to the NextGen implementation plan (FAA, 2016), 6 programs have been recognized as the keys to reshape operations in the NAS, including Automatic Dependent Surveillance-Broadcast (ADS-B), data communications, en route automation modernization, terminal automation modernization and replacement, NAS voice system and System Wide Information Management (SWIM).

These new concepts of operations, proposed both in Europe and the United States, require a paradigm shift in the amalgamation of the flight planning and execution processes based on the flight trajectory management. Indeed, the flight trajectory is established as the fundamental element of a new set of operating procedures referred to as Trajectory Based Operations (TBO) (EUROCONTROL, 2015; FAA, 2016). The TBO concept has been the main focus of validation conducted in International Civil Aviation Organization (ICAO) Global Air Navigation Plan (International Civil Aviation Organization, 2016), as well as in multiple regional programmes such as the above SESAR (Europe) and NextGen (US), and also CARATS (Japan), OneSKY (Australia) and Sirius (Brazil). TBO require the ATM to introduce innovations in all parts of the system in order to enable the envisioned changes. Stakeholder involvement, better data sharing and usage, introduction of advanced decision support tools for human operators, both on ground and in the air, and improving management in all the facets of the air transportation, are just a few of the envisioned and needed changes.

TBO is based on the concept of business trajectory (EUROCONTROL, 2016), which is rather different from the current concept of a flight plan. The business trajectory is a full four dimensional (4D) trajectory of a flight, encompassing the geographical and location in time of the flight. What is more, the business trajectory is conceived as a contract between the airline, the ANSP, airports and the NM. Another difference from the current system is that the business trajectory should be designed and shared with other stakeholders already at the strategic level (six months and more from the time of departure). Today, the flight plans are submitted a few hours before the flight and the resource (air and airport capacity) planning is relying mainly on historical data. Furthermore, in the time-period from the inception of the business trajectory until the actual execution, the trajectory is to be updated with the new information, as it becomes available (i.e. actual aircraft to fly the trajectory, trajectory changes due to weather influences, etc.), which is not the case today. The updates are to be shared with all the stakeholders, thus easing the overall planning for the whole air transportation system.

I.1.2 Development of the business trajectory

Fig. I-1 shows the lifecycle of a business trajectory, where three different ATM planning temporal layers are foreseen: strategic (long term), pre-tactical (mid/short term), and tactical (execution).

In line with the latest SESAR 2020 concept of operations (EUROCONTROL, 2017), during the strategic design/planning of the trajectory the airlines compute their preferred trajectories resulting in the business development trajectory (BDT). Eventually, the BDT will become the shared business trajectory (SBT) and will be available to other stakeholders via the network operations

plan (NOP), which will coordinate the NM and ANSPs. Using these SBTs, the ANSP can assess airspace configurations and route structures and their allocation of resources. The NM, having visibility of all SBT and ANSP resources can identify possible capacity and demand imbalances and act accordingly by proposing trajectory changes and/or negotiating different configurations with the ANSPs (leading to different capacity distributions). This iterative and collaborative process of negotiations will end when an acceptable solution for all the stakeholders is found. At this point, the SBT becomes the reference business trajectory (RBT), which the airline agrees to fly and the ANSPs/airports agree to facilitate. Yet, during the trajectory execution, RBT might be impacted, e.g., by de-conflicting, real-time queuing, or weather hazards. Therefore, the RBT might be revised, negotiated, and updated in the meantime.

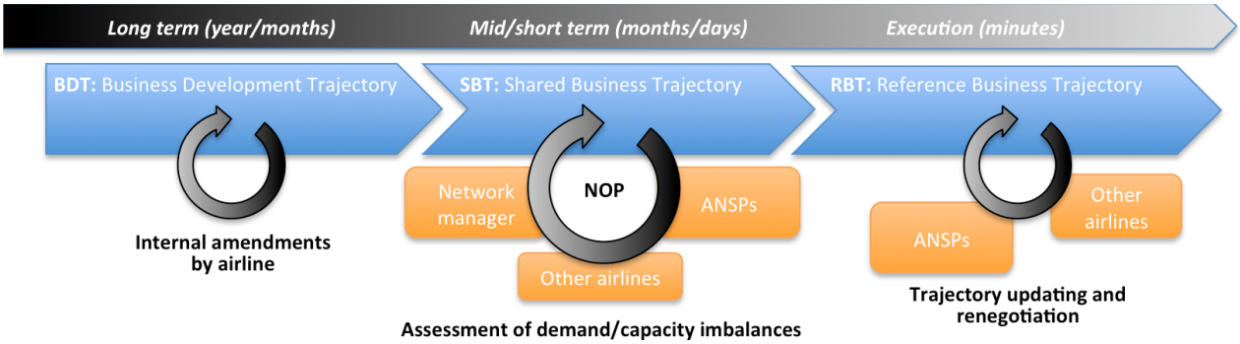

Figure I-1: *Development phases of the business trajectory under SESAR TBO concept of operations.*

Derived from the development of business trajectory discussed above, the following consequences emerge:

- The business trajectories are full four-dimensional trajectories that evolve over time.
- Accurate and robust trajectory prediction at all time becomes critical. Tackling different sources of uncertainty, in particular weather uncertainty, becomes paramount.
- Efficient, fair and adaptive demand and capacity balancing algorithms are needed when (airspace) resources are scarce.
- Effective negotiation mechanisms, among different stakeholders, on the achievement of agreed trajectories function as the key enabler of collaborative air traffic flow management.
- All necessary data regarding the trajectory needs to be shared for proper synchronization of airborne and ground systems.
- Higher levels of ATM automation of decision support tools for human operator are also required to handle larger number of trajectories and the associated negotiations in real time.

I.2 Motivation of this PhD thesis

The above TBO concept of operations envisions that the early information sharing and continuous updates will enable the early identification of potential problems (e.g., demand-capacity imbalances). In turn, this would invoke the collaborative decision-making processes for the problem resolution. As the trajectories evolve over time, such collaboration across different stakeholders

would range through all flight stages, including strategic (7 days or more before the day of operation), pre-tactical (1 day to 6 days before the day of operation), tactical or real-time (on the day of operation) and post-operational (after the day of operation).

Following this thought, this PhD thesis identifies several potential problems encompassing the ATFM initiatives under current operations and proposes some solutions aiming at the future TBO paradigm. The motivations to drive the work of this PhD thesis are elaborated as follows.

I.2.1 Maximize airborne delay at no extra fuel cost

In the majority of the situations, ATFM regulations are issued due to weather related capacity reductions. Considering the uncertainties in weather prediction and other unforeseen factors, ATFM decisions are typically conservative and the planned regulations may last longer than actually needed (Cook & Wood, 2010). At present, ground delay is more preferable than airborne delay (holding) from a safety, environmental and operating cost points of view. However, when regulations are canceled before their initial planned ending time, as occur often (Ball *et al.*, 2010b; Inniss & Ball, 2004), the already accomplished delay on ground cannot be recovered, or can be partially recovered by increasing speed, leading to extra fuel consumption.

In order to overcome this issue, a speed reduction strategy was proposed in (Prats & Hansen, 2011), which aimed at partially absorbing ATFM delays airborne. This strategy was further explored in (Delgado & Prats, 2012), where aircraft were allowed to cruise at the lowest possible speed in such a way the specific range (i.e. the distance flown per unit of fuel consumption) remained the same as initially planned. In this situation, if regulations were canceled, aircraft already airborne and flying slower, could increase their cruise speed to the initially planned speed and recover part of the delay without extra fuel consumption (Delgado *et al.*, 2013; Delgado & Prats, 2014). In this PhD thesis, the speed reduction strategy is further extended in such a way that not only the cruise phase is used to perform this linear holding, but also the climb and descent phases are subject to optimization to maximize the total amount of airborne delay that can be realized without incurring extra fuel consumption.

Following this thought, this PhD thesis will identify the maximum delay absorption that can be realized by linear holding (at no extra fuel cost). Performing linear holding lower than this maximum bound, it will be cheaper and possibly safer than typical airborne holding, and can be used as a complementary strategy to ground holding when airlines plan their delayed flights. In this situation, the departure time can remain as close to the original plan as possible, and thus a more smooth flight schedule will be guaranteed, if compared with the case in which the entire assigned delay is imposed on ground holding. Apart from these and the benefits previously analyzed in detail in (Delgado *et al.*, 2013; Delgado & Prats, 2014), more potential applicability can be expected, which will be presented hereafter in this PhD thesis.

I.2.2 Apply linear holding to AFPs in planning phase

Currently, once a flight is captured in an AFP, an Expected Departure Clearance Time (EDCT) will be assigned to that flight based on certain slot allocation algorithm (Pourtaklo & Ball, 2009), which aims at entirely absorbing all the assigned delay by means of ground holding at the origin airport. Nonetheless, with the paradigm shift from an airspace-based ATM to trajectory based operations, delays could eventually be assigned directly in form of Controlled Time of Arrival (CTA) or Over (CTO) at the FCA (Smedt *et al.*, 2013), instead of being wholly imposed on the pre-departure time by means of an EDCT. In such a way, as shown in Fig. I-2, a flight affected by an AFP delay could reduce its ground holding (i.e., take off earlier than the EDCT), and then perform the necessary linear holding to experience the rest of the delay airborne in order to meet the assigned CTA (or CTO) at the particular FCA.

Consider two scenarios for unexpected weather situations: turning better or worse than initially forecast. For the better case, obviously, with increased airspace capacities available there is no need to further regulate the controlled flights including those performing linear holding airborne. In some circumstances, ATC instructions such as short-cuts could be applied to those flights to take advantage of the advanced unoccupied slots, while the grounded aircraft (not performing linear holding) might be still holding in the departure airport. For the worse case, on the other hand, although the aircraft performing linear holding took off earlier than the nominal EDCT, the CTA/CTO at the border of FCA will be still the same as with ground holding, due to the airspeed reduction (see Fig. I-2). In other words, if the areas of (unforeseen) reduced capacity, close to or at the downstream of the FCA (as in most of the cases), require further movements such as holding patterns and diversions (under conventional operations), the same will happen to the aircraft performing linear holding as to those with only ground holding.

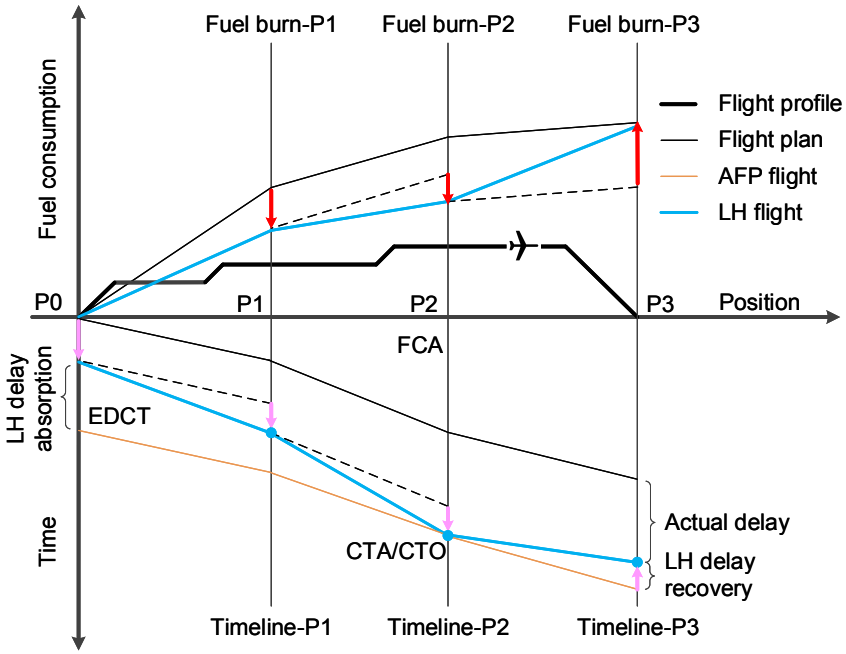

Figure I-2: *Schematic of linear holding (LH) applicability in an AFP.*

Motivated from such benefits, this PhD thesis addresses the potential applicability of linear holding to AFPs. In a GDP scenario, delay was only recovered in case the regulation was lifted before scheduled. Hence, the delay recovery was performed at the tactical phase of the flight (once it is known that the regulation is lifted). This generates some concerns regarding network effects and unforeseen conflicts or sector congestion downstream. In this AFP case, on the other hand, regulated aircraft can recover some arrival delay at the destination airport even if the AFP is kept as planned since delay absorption (before reaching the concerned airspace) and recovery (after overflying the concerned airspace) are both planned in the pre-tactical phase of the flight (i.e. at the flight planning stage). This is important since the speed adjustments could be integrated into the trajectory negotiation process with the ATFM authority in line with the TBO paradigm. In this way, potential conflicts and/or sector overloads could be detected in advance and mitigated before the agreed trajectories are tactically executed.

I.2.3 Replace ground holding by linear holding

Fig. I-3 illustrates some flight key events (blue rectangles) and respective time intervals. In (Bilimoria, 2016), historical flight operations from five airports, whose arrivals experienced the most pre-departure ground holding in 2015, were examined computing the variance between scheduled times and actual times. According to this study, each of the key events of Fig. I-3 can be associated with a possible additional delay event (red rectangles in the figure).

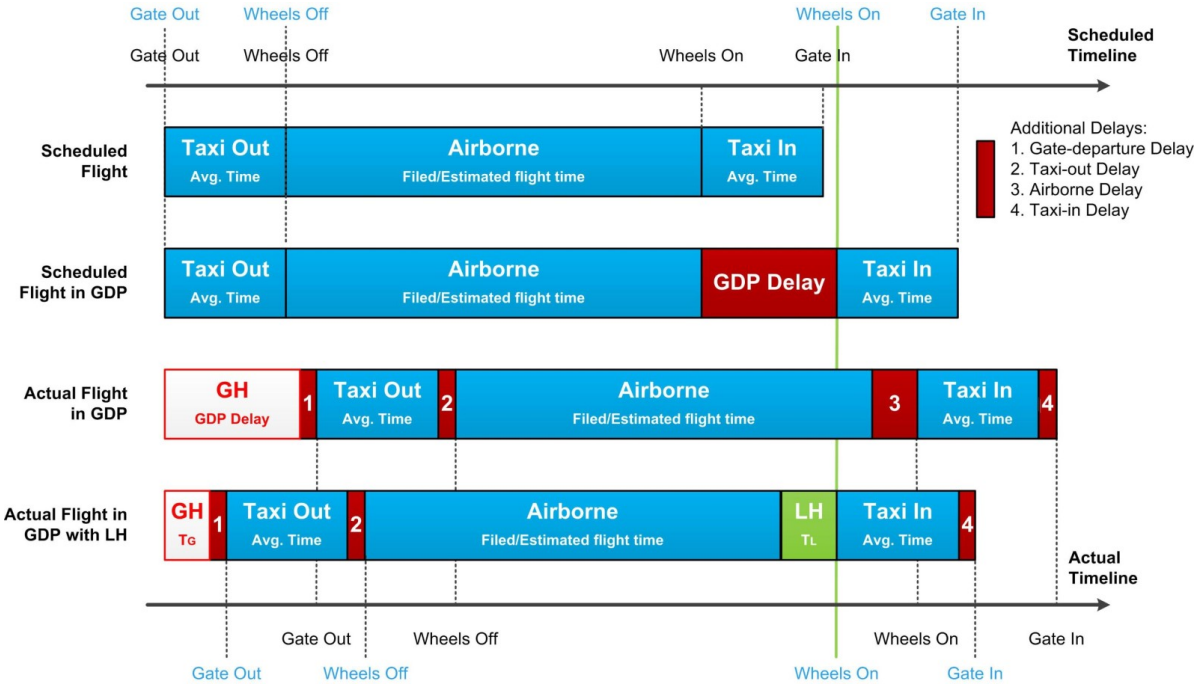

Figure I-3: *Schematic diagram of a GDP delayed flight, with a potential LH applicability, showing the differences between planned and actual flights, which might experience additional (unforeseen) delays.*

Consider a particular flight affected by a GDP. As mentioned previously, because of the capacity reduction at the destination airport, the arrival time becomes "controlled" and postponed by a certain GDP delay (from "Scheduled Flight" to "Scheduled Flight in GDP" in Fig. I-3). At present, time-of-arrival control is not enforced and a time-of-departure control is preferred. The reason is because a departure time is actually enforceable, being much more difficult to enforce the arrival time with current navigation and guidance technology. Thus, the assigned delay is entirely transferred from the arrival airport to the departure in the form of ground holding (GH) also to avoid (relatively) costly airborne holding, and to obtain a parallel shift on the scheduled arrival time (Wheels On in the figure).

Due to the likely additional (and unforeseen) delays, however, the already delayed time of Wheels On could be delayed again, as from "Scheduled Flight in GDP" to "Actual Flight in GDP". In such a situation, extra fuel has to be consumed by increasing flight speed if these unforeseen delays are to be recovered (as usually done nowadays by some airlines). Furthermore, it is also a common practice for some airlines to speed-up after departure to even recover part of the initially assigned GDP delay, since arrival times are not (yet) enforced.

In this PhD thesis, we propose to shorten the ground holding and absorb part of the assigned delay airborne by means of linear holding, i.e. by flying slower than initially planned. This is depicted in Fig. I-3 as "Actual Flight in GDP with linear holding (LH)" and at the same time the

scheduled arrival time in GDP is met (green line). Thanks to the flexibility of this method, every time an additional delay is encountered during the execution of the flight, the required linear holding can be updated through speed control. In this way the extra (unforeseen) delay can be neutralized adding only, in theory, taxi-in time uncertainties into the final gate-in time.

I.2.4 Potential of including linear holding in network ATFM

To see the potential applicability of linear holding in network ATFM, consider a flight assigned with a certain delay as a result of a GDP, as shown in Fig. I-4. In the near future, we could assume that CTA could be enforced at the destination airport, in order to guarantee the arrival slot allocation computed by the GDP (Jones *et al.*, 2015). Our flight could absorb all delay by means of ground holding, as currently done (orange line in Fig. I-4); or perform less ground holding but some linear holding in the air, such that the CTA is still met (blue solid line). If we assume that at some point the GDP is canceled, due to weather improvement for instance (purple line), airborne aircraft could stop the linear holding, accelerate to the nominal speed, and recover part of its delay (blue dash line). Obviously, if the CTA is not changed, aircraft will finally arrive at the destination airport with the same amount of delay as in the case where all delay is served on the ground.

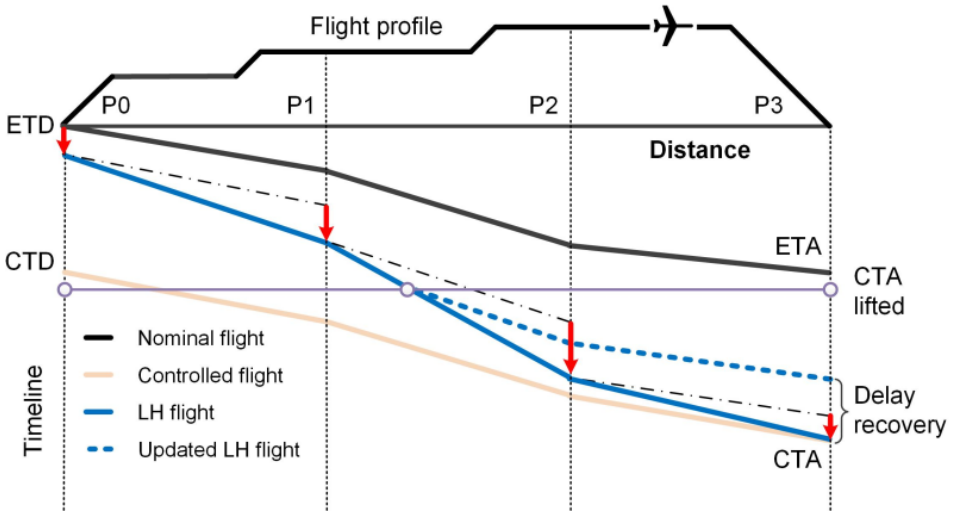

Figure I-4: *Schematic of a potential applicability of linear holding for network ATFM.*

Under the circumstance that more (every) aircraft fly slower (to perform linear holding) absorbing part of the delay that could have been realized by ground holding, the airborne traffic density will accordingly increase. This may in the long run cause heavier workloads to air traffic controllers who are responsible to guarantee aircraft separation. However, from the ATFM point of view, higher airborne density could instead contribute to better utilization of airspace sector capacities, and is what we expect to achieve by implementing linear holding. It is worth noting that the traffic density's growth does not necessarily increase traffic throughput since the latter is equal to density multiplied by flow speed (which has been reduced in this case).

I.2.5 Increase AUs' participation in ATFM planning

As mentioned above, re-routing flights out of the capacity constrained sectors would be also an option, in addition to undertaking the required delays (which could be in different ways although). Given the planned flight trajectories and airspace structures (and corresponding entity capacities), the initial demand and capacity balancing situations could be assessed, and subsequently the hotspot areas (where demand is greater than capacity) can be identified, as well as the associated flights. As both flight trajectory and airspace structure are time-dependent, it is clear that the hotspot areas would be also time-varying. Although there might be several hotspot sectors detected in the network for the same time period, the captured flights only need to bypass the sectors that they are scheduled to traverse, without taking into account the other hotspots.

However, re-routing could be too expensive to be adopted by the AUs, such that their incentives of participating in the Collaborative Decision-Making (CDM) process may be reduced. Thus, this PhD thesis considers, with the objective of incurring as few extra costs as possible, sharing additional hotspot-avoidance information to each of the captured flights. As airspace sectors are 3-Dimensional volumes, it is not only changing the flight path laterally, but also adjusting vertically the flight altitude (as well as their possible combinations). Consequently, the avoidance information should contain both the lateral and vertical cases, and so do the re-scheduled alternative trajectories. Eventually, this PhD thesis would incorporate all these potential options, and compute for the best trajectory selections and the optimal distribution of delay assignments, minimizing the deviation to the initial status, which is composed of all the user-preferred trajectories.

I.2.6 Further include ANSPs' involvement in ATFM collaboration

The airspace system nowadays is typically partitioned into sectors, each of which is handled by one or two air traffic controllers and is bonded with a limited capacity. However, as pointed out in (Kopardekar *et al.*, n.d.), some of these capacity resources might be under-utilized and lack of flexibility, and thus requires a better reorganization.

One implicit problem of previous motivations is that the given airspace structures (and corresponding capacities) are often designed to best accommodate the traffic flow patterns that are accumulated by the planned (or historical) flight trajectories. In other words, once these trajectories have been changed, either by imposing delays or diverting to the alternatives, the temporal-spatial flow patterns will change too, and thus the initial airspace structures may turn to be not optimal.

An illustrative example can be seen in Fig. I-5(c) and Fig. I-5(d) where the airspace structure is fixed and is subject to flexible adjustment respectively. For the original flight plans, more airline operators prefer to schedule a flight route, as colored in red, to fly from Rome (LIRF) to Amsterdam (EHAM). Accordingly, for the two areas labeled out in the map, as shown in Fig. I-5(c), the one crossed by the congested route is divided to 4 sectors (for instance) operating at the same time to provide more capacity, whilst the other area is run by only 1 sector as a whole. However, having been through the above-mentioned DCB algorithm, some flights could be diverted to the route colored in green (see Fig. I-5(d)), and some flights could be assigned with certain delays such that their CTAs at that area would be changed (and sequenced) as well. That is to say, the previous congested area could become less demanded of capacities.

Therefore, it would be beneficial to merge the former 4 sectors to 1 entire sector to reduce the extra ATC costs, and, meanwhile, to diverge the previously less-congested area from 1 sector to 2 smaller sectors to better handle the additional traffic. Following this thought, it would be an opportune to realize the synchronization of (collaborative) traffic flow management (as mentioned before) along with the (dynamic) airspace management, in order to achieve a better DCB performance.

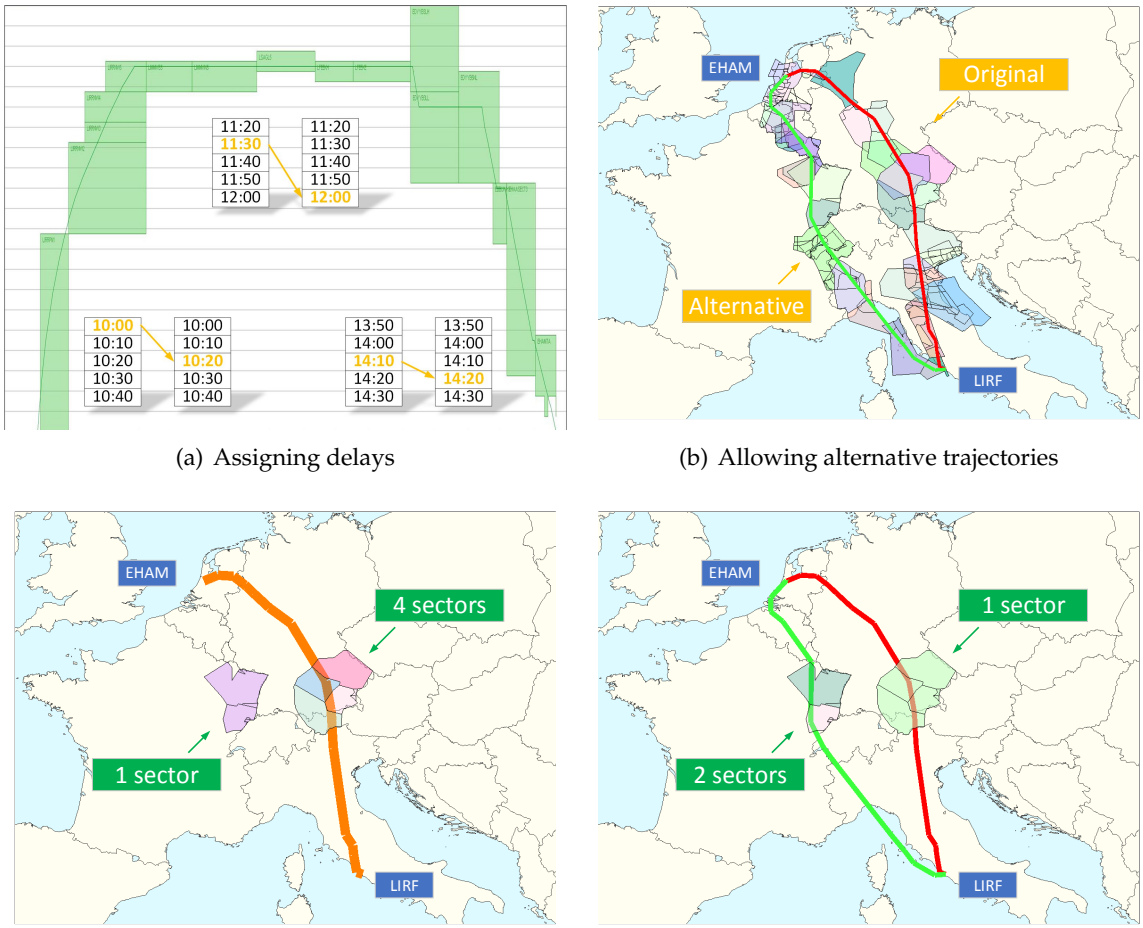

(a) Assigning delays

(b) Allowing alternative trajectories

(c) Fixed airspace structures

(d) Adjusting airspace structures

Figure I-5: *Illustrative examples of synchronization of traffic flow and airspace configurations for balancing demand and capacity.*

I.3 Objective of this PhD thesis

The overall concern of current ATFM is typically to reach a global optimum based on some unanimous fairness criteria (e.g., first scheduled, first served), being the specific preferences of one particular flight usually not taken into account. With the paradigm shift for the future ATM, the AUs have been expected to increasingly participate in ATM decisions, using, in particular, more CDM mechanisms.

The general goal of this PhD thesis, therefore, is to study and explore the way of enhancing the participation of AUs in the ATFM decision making under the TBO, and what is more, to improve the current ATFM performance by taking advantage of such enhanced collaboration. Concretely, the specific objectives for each of the sub problems to achieve the general goal of this PhD thesis are outlined below:

- Demonstrate the maximum range of airborne delay that aircraft can perform during all flight phases (including climb, cruise and descent), at no extra fuel cost and/or with certain amount of extra fuel allowance.
- Apply trajectory optimization techniques in AFPs for more flexible airborne delay absorption and delay recovery, in such a way to improve the cost-efficiency of AFP regulations.

- Give the benefits of reducing additional ATFM delays (due to fixed ground holding) by means of replacing (partly) ground holding with the proposed cost-based linear holding.
- Build a network ATFM model under the TBO to integrate various different delay management methods into a centralized optimal delay assignment algorithm, which is also subject to iterative re-executions in response to situation changes.
- Adapt the above network ATFM model to further incorporate the alternative trajectory options (with increased AUs' participation), in such a way that the traffic flow patterns can be managed in both time and space domains.
- Explore the possibility of synchronizing the traffic flow optimization and the sector opening scheduling, with the aim of achieving even more flexible demand and capacity balancing.

I.4 Scope and limitations of this PhD thesis

The work presented in this PhD thesis is mainly focused on the pre-tactical ATFM planning phase. In some cases, tactical trajectory updates (e.g., speed recovery) may be required, which may increase the ATC complexity, and thus deduct from the expected ATFM benefits. In other words, the results represent best-case outcomes assuming no traffic conflicts or other constraints specified by detailed airspace and airport (e.g., the runway usage) operations.

Furthermore, the aspect of collaboration in this work is limited within an (unique) ATFM authority, (various) AUs and ANSPs, without considering airports, air traffic controllers, or any inter negotiations between different AUs.

Besides, some specific simplifications and/or assumptions have been also taken in this PhD thesis as outlined below.

- The significant increase when linear holding is allowed in climb and descent indicates that it would be possible to have much delay absorbed airborne without changing the initial flight plan. It raises a question on how to properly implement the strategy whilst meeting the potential needs to such as handle traffic uncertainties, organize traffic flow, recover flight speed, and be compatible with terminal ATM procedures.
- While linear holding proves efficient in delay recovery, one premise must be noted, which is time-of-arrival control in the trajectory in order to enforce the full assigned delay at the destination, as conveyed in the concept of TBO. Otherwise, airlines may be prone to depart intentionally earlier in order to compete for the reduced (and not enforced) available arrival slots, somehow aggravating traffic congestions, as has been identified in (Evans & Lee, 2016), as one of the main contributors to double delays.
- Weather (atmosphere) conditions are assumed to be standard when conducting simulations for linear holding. A no-wind condition and the International Standard Atmosphere have been assumed as the generic scenario. Given that ATFM regulations are typically issued under severe weather conditions, the wind (which, as assessed in (Delgado & Prats, 2013), could have a positive impact to the realization of linear holding) and non-standard atmospheres will have a great effect on real flights, which should be taken into further consideration.
- For ATFM problem, only the aircraft entrance rate is considered as a (capacity) constraint, and thereby a controlled time at each airspace entity's entry position is imposed, while neglecting the specific movements inside the entity (and the airport). Nevertheless, in actual

operations not all aircraft flying along a route in an airspace entity are in line going to the same direction, such that a variety of aircraft (performing linear holding for instance) would invariably induce conflicts with the traffic flow along side.

- The costs of delay are simplified as being linear with respect to the growth of the amount of delay assigned to a flight, and the values are assumed to be the same for different flights and for different AUs.
- The proposed DCB algorithm aims at improving the (cost) efficiency of the whole system. Although some specific preferences of each particular flight can be taken into account, the overall fairness across different AUs (e.g., equilibrium concerns) have not been considered.
- It is assumed that AUs can and are willing to well participate in the collaborative ATFM decision making, and model accurately their cost structure (such as how much delay and fuel cost), as the DCB algorithm will optimize the overall cost for all the flights according to their provided information. Otherwise, the assigned solution to their flights might be unsuitable and could incur unnecessary environmental impact as well as vicious competition issues.
- Following the above point, detailed mechanisms of negotiations within the collaborative ATFM process are not considered and overly simplified, which however should be carefully designed such that key performances (such as fairness and effectiveness) can be maintained.
- When AUs generating alternative trajectories, only the hotspots that are identified based on the initial trajectories can be bypassed (through lateral re-routing or vertical avoidance), without taking into account the impact of the newly submitted alternative trajectories.
- Uncertainty factors (e.g., in trajectory and capacity) have not been considered. While the study is aimed at the pre-tactical phase, for the purpose of developing a robust model the uncertainty events will still be one of the critical issues.

I.5 Outline of this PhD thesis

The material in the present document is organized in eight Chapters and five Appendices which are summarized as follows:

- Chapter II presents the state of the art in flight trajectory management (including background on linear holding), ATFM programs and advances with the CDM, and methodologies in ATFM modeling and analysis.
- Chapter III elaborates in detail the cost-based linear holding practice enabled by proper aircraft trajectory optimization, which can generate a certain amount of airborne delay at no extra fuel cost than the initially scheduled.
- Chapter IV introduces a method to improve the AFP performance by means of using linear holding in delay absorption and recovery, where a two-stage trajectory optimization process is implemented for planning AFP-affected flights. Then, it also proposes an applicability for reducing additional ATFM delays that are subject to the fixed ground holding, where the amount of realizable airborne delay is adjusted through reactive trajectory planning in order to neutralize the potential tactical delays.
- Chapter V, as a milestone connecting two main topics of this PhD study (i.e., linear holding and ATFM) of this PhD study, builds a network ATFM model incorporating multiple types of delay to manage the traffic flow as a whole. The optimization model can be iteratively

executed following the changes of network constraints, such as the airspace capacity, and the required system delays can be flexibly handled thanks to the inclusion of linear holding.

- Chapter VI extends the previous network ATFM model with increased AUs' participation, allowing them to submit alternative trajectory options. In addition to the default initial trajectory, two types of alternative (i.e., lateral and vertical) trajectories are considered to route out of the identified (time-varying) hotspot airspace for each affected flight. The centralized optimization model computes for the best distribution of trajectory selections and delay assignments (with different possible types of delay).
- Chapter VII further extends the collaborative ATFM to eventually involve ANSPs' participation, in which a (limited) dynamic airspace sectorization method is enabled, such that the task of demand and capacity balancing can be conducted from the both sides (i.e., traffic flow and airspace configuration) in a more synchronized way.
- Chapter VIII summarizes the main contributions and remarks of this PhD thesis, and envisions some further work that could be considered based on the present research.
- Appendix A gives additional results derived from the simulation experiments conducted for validating the linear holding practice.
- Appendix B provides scalability tests for the network ATFM model, illustrating the effects of critical parameters with sensitivity analysis, and showing the computational performance with empirical studies.
- Appendix C discusses about more details for the Collaborative ATFM framework, including the possible fairness concerns across different AUs, iterative updates in this model context, and technical aspect of retrieving capacity information from a published database.
- Appendix D demonstrates the entire involvement procedures of an illustrative flight participating in the proposed Collaborative ATFM, which ranges from planning the initial trajectory, receiving hotspot information, rescheduling alternative trajectories, to finally adjusting the selected trajectory with assigned delays imposed.

If I have seen further than others, it is by standing upon the shoulders of giants.

— Isaac Newton

II

Background and state of the art

This chapter gives an overview of the background knowledge and state of the art, including flight trajectory management, commonly-seen air traffic flow management (ATFM) programs and the advances through using collaborative decision making (CDM) mechanisms, and more methodological studies in ATFM modeling and analysis. These are the three main aspects concerning with the work of this PhD thesis.

II.1 Flight trajectory management

Ground holding, the practice of delaying the take-off of a flight due to anticipated congestion at the destination airport (or at some airspace along the route), is motivated by the fact that it is less expensive and safer than holding in the air (Richetta, 1991). By less expensive, it means less fuel is consumed waiting at the apron with the engines off than delaying the aircraft in the air by means of holding stacks or path stretching instructions given by ATC. By safer, it means that the aircraft is not burning (reserve) fuel unnecessarily and by the fact that ATC workload is decreased in the airspace(s) where aircraft are required to lose time.

Waiting on ground, however, has the inconvenience that if the delay is no longer necessary and thus canceled before initially planned (due to the unexpected improving of congestion or weather for instance) (Inniss & Ball, 2004; Cook & Wood, 2010; Ball *et al.*, 2010b), the grounded aircraft are still at departure airports and the already delayed time on departure cannot be recovered (or can be partially recovered by increasing flight speed, leading to extra fuel consumption if compared with the initially planned flight).

II.1.1 Cost-based linear holding

To overcome the above issue, a linear holding strategy was proposed by (Delgado & Prats, 2012) where aircraft were allowed to cruise at the lowest possible speed in such a way that the fuel consumption remained exactly the same as initially planned. In this situation, if the delays are canceled ahead of schedule, aircraft already airborne and flying slower, can speed up to the initially planned and recover part of the delay without extra fuel consumption. Previously, this strategy was explored by (Prats & Hansen, 2011), aimed at partially incurring in the air, by flying slower, the assigned ground delays. In this study, ground delayed aircraft were enabled to fly at the minimum fuel consumption speed (typically slower than the nominal cruise speed initially chosen by the airline), performing in this way, some airborne delay at the same time fuel was saved with respect than the nominal flight. Thereafter, more related work to the strategy has been done discussing such as the impact to Ground Delay Programs (GDPs), the effects from en route wind and the potential applicability for handling air traffic flow (Delgado *et al.*, 2013; Delgado & Prats, 2013; Delgado & Prats, 2014).

In order to better explain the linear holding concept, it is appropriate to start with a short comparison between the two commonly seen holding practices in current ATM: ground and airborne holding, along with the proposed cost based linear holding, as shown in Fig. II-1.

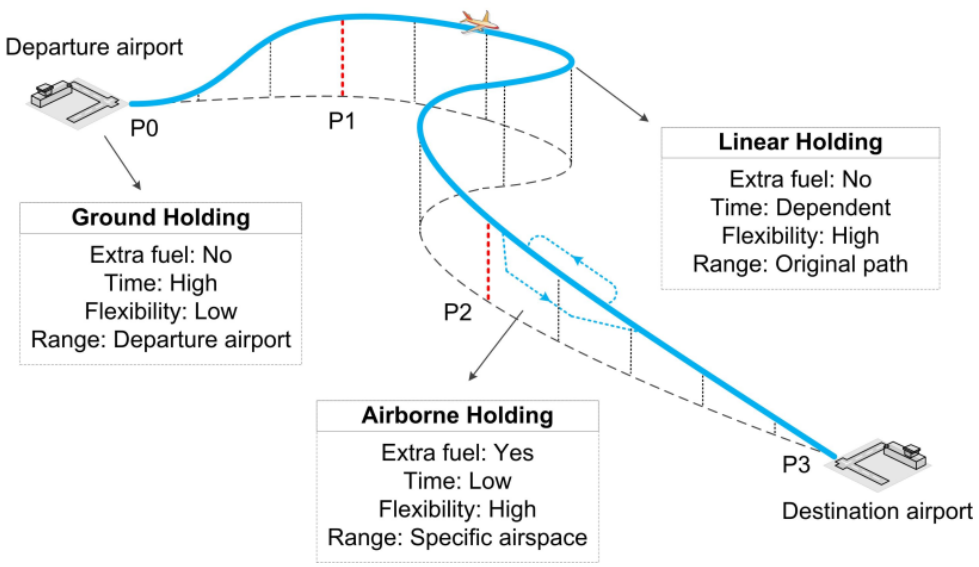

Figure II-1: *A comparison between ground holding, airborne holding and linear holding.*

In terms of fuel consumption, typical airborne holding would consume more fuel due to the extended flight track (the deviation of actual trajectory to the initially planned) (Belkoura *et al.*, 2016), whilst holding on the ground should make no difference with the planned fuel. For linear holding a trade-off is possible between fuel and time, depending on the speed adjustment strategy.

Due to the increased extra fuel, the airborne holding time is fairly limited if compared with ground holding, taking account that safety related issues may arise from a reduction of the onboard reserve fuel. On the other hand, the linear holding time should depend on several factors, such as aircraft type, flight distance, payload, cruise flight level, etc., and requires a detailed analysis.

Other than the typical airborne delay (holding pattern or path stretching), linear holding means that only speed is adjusted and the planned route remains the same. Furthermore, in

line with the implementation of CTA, linear holding could be seen as a complementary ATFM strategy, in addition to ground holding, pre-tactical re-routing or strategic deconfliction initiatives (Ruiz *et al.*, 2014). Then, through a dynamic speed management along the route, the arrival time at different waypoints could be tactically adjusted in response to uncertainties.

From the implementation point of view, ground holding can be only performed at departure airport, prior to take-off, while the airborne holding, technically, can be realized at any available airspace during the flight, but practically due to the constraints from ATM (FAA, 2015), it is typically performed in specific designated airspace, which differs from the linear holding that is done progressively along the original planned route.

Generally, the most promising feature of linear holding is that the amount of airborne delay absorption can be flexibly managed along the flight trajectory, and without incurring extra (safety related) on-board fuel than initially scheduled. With the paradigm shift of an airspace-based ATM to the TBO, the proposed linear holding could be integrated into the four dimensional aircraft trajectory for the purpose of dynamic delay management.

II.1.2 Speed control strategy

As the core method to perform linear holding, speed reduction is essentially one of the speed control methods that have proven successful for several ATM scenarios. For instance, (Jones *et al.*, 2013; Jones *et al.*, 2015) presented a speed control approach for transferring delay away from the terminal to the en route phase, from which significant fuel saving on a per flight basis was also yielded. In (Günther & Fricke, 2006), a pre-tactical speed control was applied en route to prevent aircraft from performing airborne holding patterns when arriving at a congested airspace, with both flight efficiency and controller workload reported improved. Similar but more at tactical level, aircraft were required to reduce their speed to avoid arriving at the airport before its opening time to reduce unnecessary holdings (Airservices Australia, 2007).

More widely, the applicability of speed control with regard to the conflict resolution problem has been discussed for decades, and typically it was implemented along with other approaches such as path changing (Tomlin *et al.*, 1998) or flight level assignment (Vela *et al.*, 2009). With metering operations under TBO, aircraft trajectories are tactically managed to their schedules across meter points, through speed control or path extension based on accurate trajectory predictions and modifications, which raises the critical need of concern about uncertainties (such as aircraft-specific parameters and predicted winds), as has been studied in (Kirkman *et al.*, 2014). Regarding terminal procedures (where aircraft are typically climbing or descending), however, speed control has been mainly used for (tactical) separation purposes. (see for instance in (Barmore, 2006; Xu *et al.*, 2016)).

II.1.3 Aircraft trajectory optimization

With the forthcoming TBO concept, a transition in ATM from control by tactical clearance to management by reference to a trajectory is expected. This emphasizes the importance of efficient trajectory planning (optimization) for airspace users (AUs), in order to realize, for instance, the above mentioned cost-based linear holding and the extensive speed control strategies.

The aircraft trajectory optimization problem can be modeled and solved using optimal control techniques (Betts & Cramer, 1995; Betts, 2010). Several studies in the last decades assessed the optimal flight profiles for commercial aircraft, focusing most of the time on continuous descent operations (CDO) or continuous climb operations (CCO) (Clarke *et al.*, 2004; Jin *et al.*, 2013; Zhao *et al.*, 2013). Optimal cruise operations were explored in (Dalmau & Prats, 2015; Dalmau & Prats, 2017), showing the qualitative advantages of suppressing the vertical constraints in cruise in terms

of fuel and time savings. Complete frameworks of aircraft trajectory optimization were also presented in (Soler *et al.*, 2012; Dalmau *et al.*, 2018), revealing comparisons between conventional and continuous operations. A recent study (Gardi *et al.*, 2016) provided a comprehensive review of the trajectory optimization techniques, with a special focus on the recent advances introduced in the ATM context.

II.1.4 Airspace users' operating costs

The cost of delay usually accounts for only one part of the operating costs for AUs (i.e., AUs in this PhD thesis), and there exist other major causes, such as the fuel consumption. The focus of previous studies of the operating costs has evolved with historical changes in the aviation industry. Early studies (Meyer & Oster, 1981; Morrison & Winston, 2010) explored the impacts of deregulation and the statistical relationships between operating cost variables and financial performance, with a focus on fuel and crew costs. Reference (Holloway, 2008) provided an overview of the different types of schemes established to categorize costs in the airline operations.

The flight cancellation decisions in GDP was studied in (Xiong & Hansen, 2009), revealing the value of a flight cancellation and airline preference structure in decision makings. (Ball *et al.*, 2010a) presented the economic impact of flight delay, where the cost of delay to AUs is estimated by modeling the relationship between airline total cost and operational performance metrics. Different charging zones are found within European airspace, and this study analyzed the routes submitted by AUs to be operated on a given day and compares the associated costs of operating those routes with the shortest available at the time, in terms of en-route charges and fuel consumption (Delgado, 2015). For the costs of delay that AUs might have to consider with respect to their operating flights, a series of reports, e.g., (Cook & Tanner, 2015), serve as reference for European delay costs, at both the strategic (planning) and tactical stages.

II.2 ATFM programs and CDM

With the paradigm shift for the future ATM, the AUs have been expected to increasingly participate in ATM decisions using, in particular, more CDM mechanisms. For example, the SESAR concept of reference business trajectory (RBT), as output of an ATFM negotiation, is the trajectory that the AUs agree to fly and the ANSPs and airports agree to facilitate.

II.2.1 Current ATFM Programs

Adverse weather is a major cause of congestion in the United States National Airspace System (NAS). In order to ensure that the traffic demand does not exceed the capacity under adverse weather conditions, the Federal Aviation Administration (FAA) typically issues air traffic flow management (ATFM) measures; such as miles-in-trail restrictions (Grabbe & Sridhar, 2003), aiming to keep a certain (reduced) demand level towards congested areas; or re-routings (Mukherjee & Hansen, 2009), which directly avoid them. Nevertheless, if the traffic volume reaches a point where these initiatives are not sufficient, the ATFM personnel may decide to issue more restrictive actions such as Ground Holdings or Ground Stops, in which certain flights are delayed from their scheduled departure times to mitigate the anticipated congestion at the concerned airspace (FAA, 2009). Among these ATFM initiatives, ground holding is the most common action to absorb the distributed delays and it is also widely used when congestion affects the destination airport.

In this context, the FAA started to introduce the Ground Delay Programs (GDPs) in the late 1990s. As elaborated in (FAA, 2009), for planning the GDPs, FAA uses software called Flight

Schedule Monitor (FSM) that compiles scheduled flight information and flight plans to determine when an overload of demand versus capacity exists for a specific airport. A GDP is then modeled through the FSM software and arrival slots are assigned to aircraft, based on the available capacity (i.e., Airport Acceptance Rate) and flight arrival times. Delays are then issued in sequential order, namely the Ration-By-Schedule (RBS) algorithm, until demand equals capacity for each hour of the program.

Marked as a significant milestone in en-route traffic management in the NAS, FAA further introduced the Airspace Flow Programs (AFPs) in June 2006, in which only those flights scheduled to traverse this concerned airspace are subject to pre-departure delays at their origin airport (Libby *et al.*, 2005). Compared with GDP, an AFP does not unnecessarily delay flights to an airport that do not pass through the en route region of reduced capacity (Robinson *et al.*, 2009). It identifies constraints in the en route system, develops a real-time list of flights that are filed into the Flow Constrained Area (FCA), and distributes Expected Departure Clearance Times (EDCTs) to meter the traffic demand through that area (Sherali *et al.*, 2011). An AFP might be used, for example, to reduce the rate of flights through an ATC center when that center has reduced en-route capacity due to severe weather, replacing miles-in-trail restrictions with a required re-routing, managing airport arrival fix demand or controlling multiple airports within a terminal area.

Similar initiatives exist in Europe, implemented by Eurocontrol's Central Flow Management Unit (CFMU) which is currently known as the Network Manager (NM). Prior to the tactical flight operations, AUs submit their preferred flight plans to the NM, while the regional ANSPs manage the capacity of their responsible airspace sectors and airports based on available resources. Then, the NM assesses the potential imbalances between traffic demand and capacity, and, if necessary, regulates the demand by means of imposing ground delays on certain flights (EUROCONTROL, 2017). The algorithm used for assigning these delays is named as the computer assisted slot allocation tool (CASA), which is a function within Eurocontrol's ETFMS (Enhanced Tactical Flow Management System) that follows the principle of RBS principle (Cook, 2007; EUROCONTROL, 2018a) to maintain the equilibrium across the different flights. Some efforts were also made based on the existing CASA algorithm including a function extension to handle the conflict resolution problems, in addition to the demand and capacity balancing (Barnier & Allignol, 2009).

II.2.2 CDM mechanisms

Collaborative Decision-Making (CDM) is more of a philosophy for better managing air traffic through information exchange, procedural improvements, tool development, and common situational awareness (Ball *et al.*, 2000). It allows decisions to be taken by those best positioned to make them based on the most comprehensive, up-to-date accurate information and ensuring that all concerned stakeholders are given the opportunity to influence the decision (EUROCONTROL, 2017). In general, under CDM, ATFM is conducted in a way that gives significant decision-making responsibilities to AUs (Vossen *et al.*, 2012).

CDM was first implemented in the United States within GDPs in the late 1990s (Chang *et al.*, 2001), and then incorporated tools such as flight substitution, cancellations, compression, and slot credit substitution (Ball *et al.*, 2005). Under current GDPs, one of the most sophisticated ATFM tools used in the United States, resources (i.e., arrival slots) are assigned to flights in accordance with a RBS mechanism (first-scheduled first-served prioritization). It is accompanied with CDM initiatives, such as flight substitution, cancellations, compression, or slot credit substitution, allowing AUs to manage their own flights in line with their specified policies (Ball *et al.*, 2005). Following this thought, one could envision that AUs would be willing to provide specific flight information to the ATFM authority, especially if potential benefits might exist (e.g., reducing flight delays) along with feasible negotiation mechanisms (e.g., the TBO paradigm).

II.2.3 ATFM progress with CDM

Researchers have explored different ways to incorporate the methodological advances with CDM mechanisms to further improve current ATFM performance. An efficient dual network flow formulation for the static-stochastic GDP was presented in (Ball *et al.*, 2003), showing how this formulation can be implemented under CDM with equity considerations. The integer programming formulation for the GDP was extended by (Vossen & Ball, 2006a), to approximate the CDM process where the slot compression step can be considered as a mediated bartering between AUs. The opportunities for slot trading in a single airport setting was, at the same time, studied under the condition that GDP offers are given to trade from various AUs (Vossen & Ball, 2006b). Similarly, slot exchange mechanisms in an AFP scenario through a mediated bargaining of assigned slots was discussed in (Sherali *et al.*, 2011), allowing AUs to improve flight efficiencies. The overall collaboration process was then simulated by (Molina *et al.*, 2014) using the agent-based approach, where different ATM stakeholders were modeled within the CDM framework such as the NM, AUs, airports and flight crews.

Besides, a mechanism for slot allocation was proposed in (Castelli *et al.*, 2011), which is based on market principles as it enables AUs to pay for delay reduction or receive compensation for delay increase. The mechanism fulfills the properties of individual rationality, budget balance, and it can be implemented through two alternative distributed approaches that do not require AUs to disclose confidential information. As stated in (Pilon *et al.*, 2016), ATFM slot swapping typically represents the first step towards the participation of AUs in the collaborative processes, and SESAR has been advancing this through development of the user driven prioritisation process (UDPP) to achieve additional flexibility for AUs to adapt their operations in a more cost-efficient manner. The expected benefits of UDPP to AUs arise from a reduction of delay and cost for important flights in presence of a hotspot. In general, the UDPP concept allows the AUs to redistribute the delay across its own fleet through prioritisation of flights. Besides redistributing the delays among different (prioritized) flights, it was also studied in (Castelli *et al.*, 2015) to induce AUs to better distribute their flights among different congested airspace sectors and their overloaded hours, by means of adopting a scheme of peak-load pricing when applying en-route charges.

In addition, as one current effort toward generating and sharing alternative trajectories to aid in CDM operations, the Collaborative Trajectory Options Program (CTOP) developed by the FAA and airlines has completed its testing and is being deployed, which has been aimed at balancing en route traffic demand with available capacity in the NAS (FAA, 2014; Miller & Hall, 2015). For the current version of CTOP, an RBS scheme is adopted, namely, flights are assigned the best available routes and slots available at the time flight operators submit their preference requests during the planning period, in a sequential manner (Miller & Hall, 2015). However, the rules of allocation in that algorithm have some obvious drawbacks, such as competitive responses from airlines, and (Kim & Hansen, 2015) investigated a game theoretic treatment of preference submission behavior within the First Submitted First Assigned allocation process. Recently, an alternative flight scheduling approach aligned with CDM, based on linear optimization instead of pure RBS has been studied, whilst using a Max-Min fairness rule to maintain the equity (Rodionova *et al.*, 2017).

II.2.4 Game theory in collaboration

Game Theory has been used as a mathematical theory for the modeling and analysis of strategies among multiple players in several fields (Morgenstern & Von Neumann, 1953). Since the use of airport runways (and relevant infrastructures) can be seen as a limited resource, the matching markets models can be associated to ATFM processes considering the demand and capacity of airport. Furthermore, such demand and capacity relations occur in airspace sectors as well, when taking account the network ATFM problems. Therefore, the allocation of slots, either for landing, take-off or controlled time of over one navigation point can be modeled as a “market”, and approaches

based on this assumption were presented in (Schummer & Vohra, 2013). However, it is indeed a challenge to exploit the potential of the matching approach for enhancement of the current CDM. Two solutions based on market models using Top Trading Cycle (TTC) and Vickrey-Clarke-Groves (VCG) were developed in (Balakrishnan, 2007).

For the purpose of delay reduction, (Swaroop *et al.*, 2012) analyzed the welfare effects of slot controls on major US airports, showing the effects of trade-off between queuing delay reduction and costs due to simultaneous schedule delay with increasing to passengers. With the implementation of reinforcement learning, (Cruciol *et al.*, 2013) developed reward functions related to the management of aircraft on the ground or in the air, for ground delay control, and for complexity analysis of airspace sectors.

Under the TBO, AUs could take advantage of the new flight plan filling system, attempting to gain advantage over their competitors using a variety of strategies. In this circumstances, (Wieland *et al.*, 2008) quantified the effects of such gaming on the NAS by determining the payoff to each AU as well as the benefit (or loss) to society as a whole, and also examined gaming strategies that could be used by the centralized authority to change the players' motivations such that the societal benefit is maximized.

II.3 ATFM modeling and analysis

ATFM refers to processes of a more strategic nature, involving taking a higher-level view of the overall air traffic network rather than controlling specific flights. It detects and resolves demand-capacity imbalances, smoothing aggregate traffic flows and keeping the workload of ATC under manageable levels. For practical reasons, the institution in charge of ATFM cannot take care of the specific preferences of one particular flight, since the overall objective of ATFM is typically to reach a global optimum (e.g., minimize total delay across all controlled flights) based on some unanimous fairness criteria (e.g., first scheduled, first served).

II.3.1 Ground holding problem

Following the pioneering work done in (Odoni, 1987), a number of researchers have focused their activity on the development of optimization models to minimize the congestion costs in response to airport capacity reduction. Delay assignment, such as ground holding, has been used as a common short-term measure for ATFM regulation for instance. The problem of assigning ground delays in the context of a single airport (the single-airport ground-holding problem) was studied in (Terrab & Odoni, 1993; Richetta & Odoni, 1993), while (Terrab & Paulose, 1992; Vranas *et al.*, 1994) extended the single-airport case to multiple airport setting, solving the multiairport ground-holding problem. According to (Hoffman & Ball, 2000), both the single-airport and multi-airport ground-holding problem can be extended by the inclusion of banking constraints to accommodate the hubbing operations of major AUs. These constraints enforce the desire of AUs to land certain groups of flights, called banks, within fixed time windows, thus preventing the propagation of delays throughout their entire operation.

Moreover, (Richetta & Odoni, 1994; Ball *et al.*, 2003) focused particularly on the dynamic solution concerning stochastic nature of the problem, and indicated cost advantages when compared with deterministic solutions under different weather scenarios. Detailed discussions were given in (Richetta, 1991), where the dynamic stochastic programming algorithm was proved being able to perform significantly better than the static. In addition, a dynamic stochastic integer programming (IP) model for the single airport ground holding problem was proposed in (Mukherjee & Hansen, 2007), in which ground delays assigned to flights can be revised during different decision

stages, based on weather forecasts. This work also presented a methodology that could enable intra flight substitutions by AUs after the model has been executed and scenario-specific slots have been assigned to all flights, and hence to the AUs that operate them.

II.3.2 Network flow optimization

Further taking into account the capacity constraints from airspace sectors, in addition to those of destination airports, the problem of controlling release times (i.e., ground holding) and speed adjustments as well as reroutings of aircraft while airborne for a network of airports and sectors was studied in (Bertsimas & Patterson, 1998; Bertsimas & Patterson, 2000). With the added complication of the problem, dynamical rerouting proved highly effective in the case of weather affected approaches around the airport which itself can operate at full capacity (Mukherjee & Hansen, 2009).

As indicated in (Lulli & Odoni, 2007), a critical practical difference between the current ATM systems in the United States and in Europe is that the capacity constraints in the former occur primarily at major airports or in the terminal airspace around them, whereas in the latter the en route airspace poses an equally important and frequent capacity constraint. In other words, the network flow model might fit better to the European ATFM setting than using the single- or multi-airport models that were well studied in the United States scenario.

Another way of modeling the network traffic flow is, instead of focusing on each individual aircraft, using the Eulerian modeling approach to spatially aggregate air traffic to generate models of air traffic flow in one-dimensional control volumes (Menon *et al.*, 2004). Consequently, the order of the airspace model depends only on the number of control volumes used to represent the air traffic environment and not on the number of aircraft operating in them. Relevant work include an Eulerian network model based on Lighthill-Whitham-Richards (LWR) partial differential equation (Bayen *et al.*, 2004), a modified 2-Dimensional computer-aided Eulerian air traffic flow model (Menon *et al.*, 2006), and a multi-commodity large scale cell transmission model for en route traffic (Sun & Bayen, 2008). A detailed comparison of these network flow models can be found in (Sun *et al.*, 2007) with respect to their performances for strategic ATM.

However, as mentioned in (Bertsimas & Gupta, 2015), it is important to highlight that network formulations present significant challenges in computational tractability, and so far, no network models have been able to incorporate equity considerations effectively. Specifically, these two barriers, the computational performance and the lack of an acceptable notion of fairness among AUs, are regarded as the main reasons preventing any network flow model to be transitioned into practice. In fact, there have been also much research effort exclusively targeting on these two issues, which are briefly introduced below.

II.3.3 Computational challenges

Aimed at a transition for realistic applications by the practitioners, the computational challenges were largely reduced by means of using different numerical computation methods such as the decomposition approaches in linear programming. For the network ATFM models based on the Bertsimas Stock-Patterson formulation (Bertsimas & Patterson, 1998), the Dantzig-Wolfe decomposition method was proved highly efficient to solve that block-angular form (Rios & Ross, 2010). As such, the overall traffic flow is decomposed flight by flight, with the master problem devised concentrating only on the coupling constraints, such as the network capacity constraints, and the sub problems focus only on flight-specific constraints. Furthermore, the effects of this parallel speedup were reported in (Rios & Ross, 2010) to have been significantly improved by implementation on Graphics Processing Units (GPUs), due to the large amount of cores that current GPUs would have if compared to those on the CPUs (Central Processing Units) of a typical computer.

On the other hand, for the network ATFM models, based on the Eulerian approach, the dual-decomposition method has been adopted, which decomposes the traffic flow path by path, and each flight path is solved (optimized) independently (Sun *et al.*, 2011). Accordingly, the dimension of the large-scale cell transmission model depends only on the number of identified flight paths, rather than the total amount of flights.

The problem associated with the above work, however, is that the ATFM problem is formulated using mixed integer linear programming (MILP) but solved with linear programming (LP) relaxation, whether using the Dantzig-Wolfe or the dual decomposition method. Some rounding heuristic must follow to obtain an integer solution, meaning that the optimality is not guaranteed (Cao & Sun, 2012). In response to this issue, (Wei *et al.*, 2013) explored the solution space structure of the problem and proved that there exists an optimal integral solution in the LP relaxation, which is also the optimal for the original integer program.

II.3.4 Fairness concerns

Under current operation protocols, arrival slots (and thus delays) are typically assigned to flights in accordance with their published schedules by a discipline of "first-scheduled, first-served" priority, namely the RBS principle (Ball *et al.*, 2001). Given the fact that the regulations are usually canceled ahead of planned, overly pessimistic forecasts usually lead to excessive ground delay. Hence, a new allocation principle, ration-by-distance (RBD) was proposed in (Ball *et al.*, 2010b), in which a greater proportion of delays are assigned to shorter-haul flights and ground delay decisions can be reactively adjusted. However, a subsequent issue is that AUs operating more short-haul flights would be treated unequally, while those running more long-haul flights could, on the contrary, avoid most of the delay assignments.

Despite the use of RBS has achieved a consensus recognition from AUs in terms of fairness, there have been so far no network ATFM models that satisfy the RBS principle. This is because applying RBS to each of the airports (or airspace sectors) individually might not lead to a schedule preserving time, sector, and connectivities, and might even have no feasible solution returned. Aiming at maintaining the equity in delay assignment, a two-stage approach for network ATFM that incorporates fairness and AU collaboration has been recently proposed in (Bertsimas & Gupta, 2015). The first stage attempts to distribute delays among AUs by controlling the number of reversals (i.e., flights switching their scheduled arrival time) and total amount of overtaking (i.e., time periods caused from the reversals), which is a natural generalization of RBS. Taking the assignment from the first stage as input, the second stage initiates a mediated (i.e., ATFM authority as the mediator) slot re-allocation process, allowing for intra-AU exchange of arrival slots, based on their submission of "at-most, at-least" (AMAL) slot trading offers.

The Max-Min rule could be also an option, which specifies that no single AU can increase its benefits (incurring less extra costs) without reducing the benefits of other AUs. The principle has been initially implemented in networking and telecommunication applications (Bertsekas & Gallager, 1992), and is recognized as one of the applicable fairness criteria in many similar areas (Prats *et al.*, 2011a; Prats *et al.*, 2011b). Some other potential metrics to achieve an acceptable fairness level, compensated by some loss of system efficiency, were proposed and discussed in (Barnhart *et al.*, 2012). Nevertheless, it must be noted that, as reported by (Bertsimas *et al.*, 2011), a pure fairness rule may result in a significant decrease in system efficiency.

Everything you can imagine is real.

— Pablo Picasso

III

Trajectory optimization for linear holding

This chapter extends the work done in (Delgado & Prats, 2012; Delgado *et al.*, 2013; Delgado & Prats, 2013; Delgado & Prats, 2014) by proposing a linear holding strategy that not only takes into account the cruise phase, but also considers climb and descent phases. Compared to previous work, the strategy can be realized more precisely through the use of aircraft trajectory optimization techniques. In this work, the differences of performing linear holding during each flight phase will be fully utilized, in such a way to generate the optimal trajectory realizing the maximum airborne delay. The inclusion of climb and descent will increase the overall capability of delay absorption and even make it appealing for short-haul flights. Since changes of flight trajectory have a direct effect to fuel consumption, which is one of the main safety and operating costs issues that airspace users (AUs) have concerns about (Cook & Tanner, 2011), this maximum airborne delay is computed with the pre-condition that the delayed flight must burn the same (or less) quantity of fuel than the original flight, as it was planned before receiving the ATFM regulation.

III.1 Different linear holding variants

Current on-board flight management systems enable AUs to optimize the aircraft trajectory in terms of DOC (Direct Operating Costs), including fuel and time related costs by means of the Cost Index (CI), which represents the ratio between time-based cost and the cost of fuel (Airbus, 1998; Roberson, 2007). According to the definition of CI, an increase of this parameter will give more

importance to the time-related costs, rather than the costs of fuel, which means higher speeds would be favored despite of the added fuel to be burned. In this chapter, optimal trajectories computed with a given $CI > 0$ would be regarded as the nominal flights, and labeled as Case-0. Based on Case-0, three additional Cases using the LH strategy will be analyzed in this chapter and explained in this section.

III.1.1 Case-1: LH only in the cruise phase maintaining the nominal flight level

Typical operating cruise speeds are higher than the MRC (Maximum Range Cruise) speed (i.e. the speed corresponding to CI=0). Accordingly, the cruise specific range (i.e., SR, the distance flown per unit of fuel consumed) is lower than the maximum for that altitude. In (Delgado & Prats, 2012; Delgado *et al.*, 2013; Delgado & Prats, 2013; Delgado & Prats, 2014) this Case was already explored and the authors defined an equivalent speed v_{eq} as the minimum speed yielding the same SR as flying at the nominal speed $V^{crz}_{nom} = V^{crz}_{ECON}$, as shown in Fig. III-1(a). Therefore, for all cruise speeds between V^{crz}_{eq} and V^{crz}_{nom}, the fuel consumption will be the same or lower than initially planned while LH can be performed when cruising. This case is repeated in this chapter for comparison purposes.

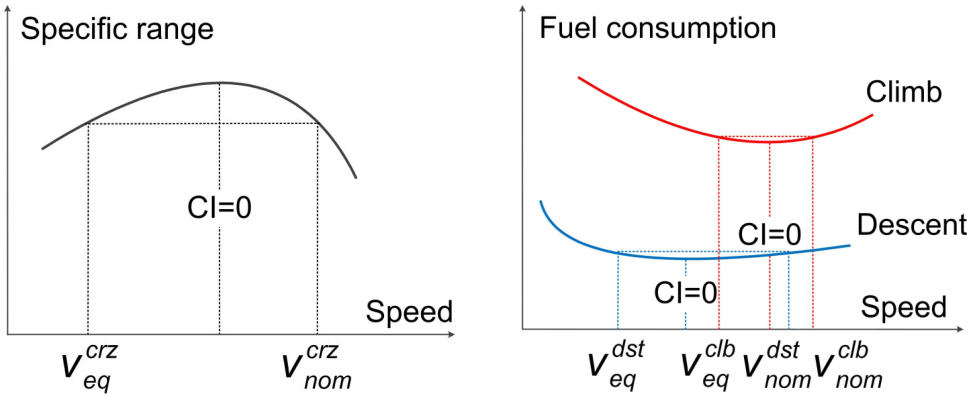

(a) Cruise (b) Climb and Descent

Figure III-1: *Definition of equivalent speeds (V_{eq}) in climb (clb), descent (dst) and cruise (crz) phases, as a function of the (given) nominal speeds (V_{nom}).*

The margin between V^{crz}_{eq} and V^{crz}_{nom} is a function of both the nominal CI and the shape of the SR curve, which in turn is aircraft, flight level and mass dependent. Moreover, it is still worth noting that V^{crz}_{eq} might be limited by the minimum operational speed of the aircraft at that given flight level and mass (including possible safety margins). For the LH strategy presented in this chapter, the Green Dot (GD) speed is adopted as the minimum bound, which depicts the best lift to drag ratio speed in clean configuration.

The lowest selectable speed V_{LS} (defined as the stalling speed plus a 30% safety margin) can be manually selected by the pilot and it is lower than the GD speed (Airbus, 1993). Yet, considering the operability of the LH strategy and aiming at automatic flight managed by the flight management system (FMS), it is more realistic to choose GD, which is the lowest speed the FMS can choose (Airbus, 1993).

III.1.2 Case-2: LH in climb, cruise and descent phases maintaining the nominal flight level

Not only is the cruise phase affected by CI, but also climb and descent profiles. The effects of different CI values within the climb and descent phases can be seen in Fig. III-1(b), which depicts a schematic of curves computed with the Performance Engineering Program (PEP) of Airbus for an A320 aircraft model at a typical mass. Seeing from the figure, there exists a minimum-fuel speed at the bottom of the function curve (for each flight level), and by accelerating or decelerating from that speed more fuel is consumed.

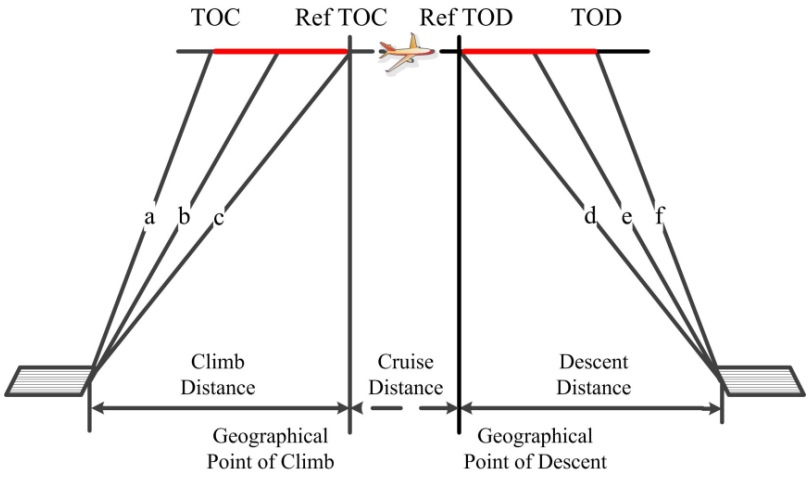

Figure III-2: *Effects of different climb/descent speeds (caused by different CIs) to the vertical flight profile.*

Thus, the LH strategy of Case-1 could be extended to the whole flight. A similar behavior than in cruise occurs for climb and descent phases when a CI higher than 0 is selected by the operator: the climb (descent) speed is faster than the minimum fuel speed, and there exists an equivalent speed yielding to the same fuel consumption as initially planned. Therefore, for all speeds within the dash line intervals of Fig. III-1(b), the fuel consumption will be the same or lower than the nominal case, while some LH will still be performed.

Moreover, since the angle of climb (descent) varies with speed, the climb (descent) distances will be different at different speeds, meaning that the location of the top of climb (TOC) and top of descent (TOD) will depend on these speeds. The vertical flight profiles will then change with the variation of the CI too. For instance, by flying higher speeds, the climb profile becomes shallower, while conversely the descent profile turns steeper, as shown in Fig. III-2 (Airbus, 1998).

In order to specify a common reference framework to define what are the climb and the descent phases, a reference (Ref.) TOC or Ref. TOD, fixed at a given geographical distance, is assumed as shown in Fig. III-2. In this figure, the red line denotes a short cruise segment whose length depends on the (speed dependent) distance between the original TOC (TOD) and the Ref. TOC (TOD).

According to (Airbus, 1998), this short cruise segment can be calculated as the difference between the "low cost index TOC/TOD" and the "high cost index TOC/TOD". By the same thought, the geographical point of the Ref. TOC (TOD) for a particular flight level is assumed, in this chapter, as the maximum distance flown with regard to all feasible speeds when ascending up to (or descending down from) that particular altitude (e.g., climb profile "c" and descent profile "d" in Fig. III-2, which corresponds to the longest climb and descent distance respectively.

Nonetheless, in real operations the climb/descent speed is not constant, due to operational or ATM constraints. Unlike in cruise, where flight is typically performed at a constant Mach number, the climb is divided into several speed segments. These normally include a speed limitation at low altitudes, typically 250kt CAS (calibrated airspeed) below FL100, followed by an acceleration to achieve a constant CAS climb, finally followed by a constant Mach climb above the crossover altitude. The same segments are for descent, but with the opposite order.

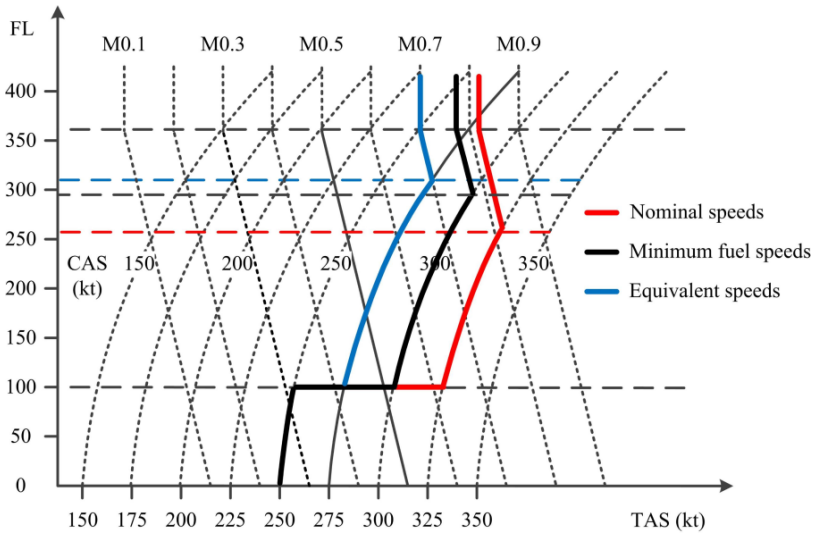

Figure III-3: *Typical operational climb and descent speed profiles.*

Fig. III-3 shows an example for such a climb/descent speed profiles (250kt /300kt /M0.78) with a solid black line. Nominal flights for CI greater than zero will lead to climb and descent speed profiles as shown by the red line, while the blue line denotes the equivalent climb/descent speed profile, which maximizes linear holding but might be limited by the lower speed bound (GD speed).

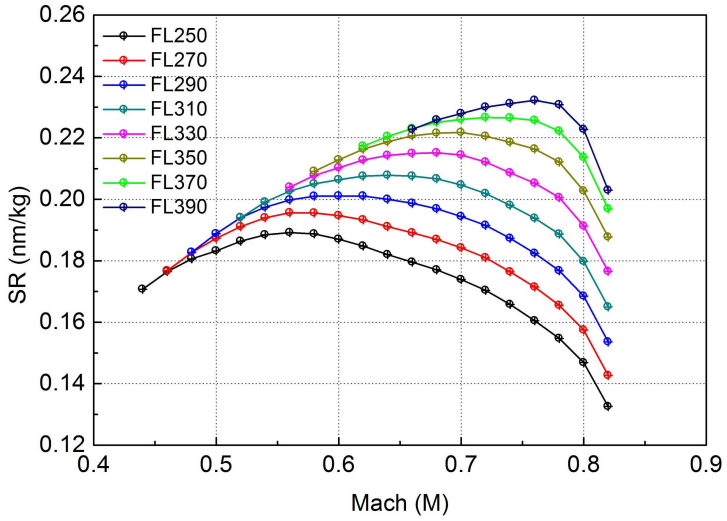

Figure III-4: *Cruise specific range vs. Mach for different cruise flight levels.*

III.1.3 Case-3: LH in climb, cruise and descent phases and optimizing for cruise flight level

In general, as the cruise speed reduces, the optimal flight level decreases. See how in Fig. III-4 the SR changes with different flight levels computed with PEP for an Airbus A320 at a typical mass. Since the equivalent cruise speed is lower than the nominal cruise speed, it is possible that the initial planned flight level is no longer the optimal one in the LH Cases. Thus this case allows freedom to the trajectory planning tool to choose the best cruising flight level(s) such that the linear holding is maximized, but as always, the total fuel consumption is equal or below the nominal fuel consumption (Case-0).

Recall the discussions about incorporating LH strategy to climb and descent phases in Sec. III.1.2. It can be understood that a lower cruise flight level may produce a lower LH time in climb and descent, as the interval between the nominal and equivalent speed that contributes to generating LH would last for a shorter period (see Fig. III-3 for instance). But at the same time save some fuel due to the lower climb and descent altitudes. Conversely, it can generate a higher LH time in the cruise phase but consume more fuel (which is also dependent on flight distance). Therefore, as discussed above, it is possible that taking the cruise flight level into the optimization it could bring better results in terms of larger LH.

III.2 Configuration of trajectory generation tool

This section introduces the main features of the tool used to generate the trajectories in this PhD thesis, which is an in-house software capable to optimize trajectories for any phase of flight, allowing to setup a wide range of operational constraints and taking into account different optimization criteria. The main architecture of this tool is shown in Fig. III-5. Given a set of inputs, the optimization of a trajectory is formulated as a multi-phase constrained optimal control problem, in which it is desired to determine the controls of the aircraft (typically thrust and flight path angle) such that a given cost function is minimized (or maximized) while satisfying a set of operational and ATM constraints.

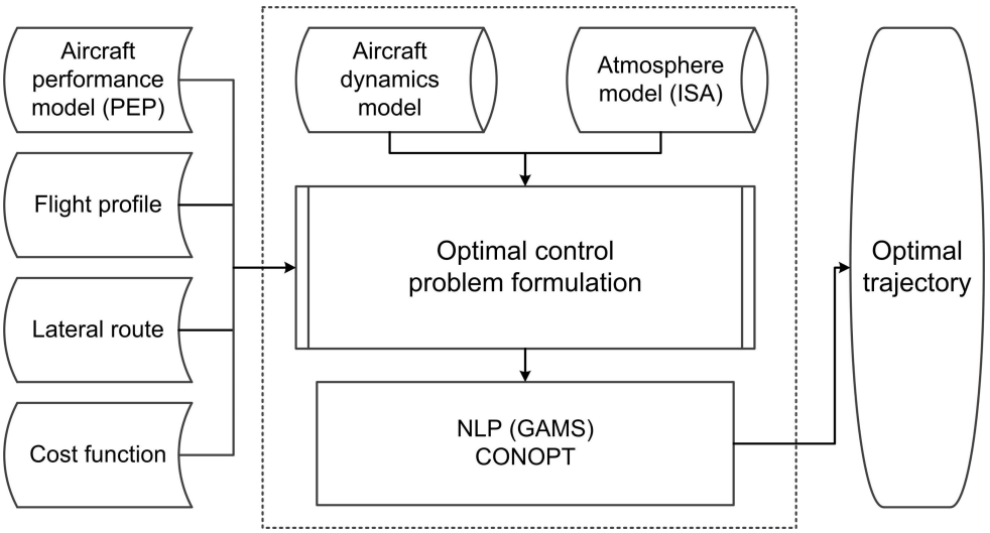

Figure III-5: *Main architecture of the trajectory optimization tool used in this thesis.*

The formulation of the optimal control problem requires mathematical models capturing aircraft dynamics and performances, along with a model for certain atmospheric variables. The equations of motion are derived for a point-mass aircraft model (three degrees of freedom) without winds and assuming continuous vertical equilibrium. On the other hand, the generated trajectories rely on propulsion and aerodynamics models developed with accurate aircraft performance data derived from PEP. For the atmosphere, the International Standard Atmosphere (ISA) model is used (International Civil Aviation Organization, 1994).

A generic aircraft trajectory can be divided into several segments $i \in [1, ..., N]$. For each segment defined over the time window $[t_0^{(i)}, t_f^{(i)}]$ the state vector $\boldsymbol{x}^{(i)} = [v\ s\ h\ m]^T$ is composed by the true airspeed (TAS), along path distance, altitude and mass of the aircraft, respectively; the control vector $\boldsymbol{u}^{(i)} = [T^r\ \gamma]$ includes the aircraft thrust and flight path angle; and a parameter $\boldsymbol{p}^{(i)}$ vector of variables that are not time depended is also defined.

For the nominal flight, the objective of trajectory optimization is to minimize a compound cost function J over the whole time window $[t_0^{(1)}, t_f^{(N)}]$ as follows:

$$J = \int_{t_0^{(1)}}^{t_f^{(N)}} (FF(t) + CI)\mathrm{d}t \tag{III.1}$$

where $FF(t)$ is the fuel flow and CI the Cost Index, combined as to reflect AUs' DOC.

The optimization constraints come from different aspects, while the first important set are the dynamics of the aircraft itself (point-mass dynamic model). Then, some algebraic event constraints fixing the initial $\boldsymbol{x}(t_0^{(1)})$ and final $\boldsymbol{x}(t_f^{(N)})$ state vector must be satisfied. In this chapter, the initial and final points are taken, respectively, at the moment the slats are retracted (after taking off) and extended (before landing). The remaining parts of take-off and approaching are not optimized due to the heavy constraints from operational procedures.

Some bounds (known as box constraints) on the control variables are specified as follows:

$$\gamma_{min} \leq \gamma \leq \gamma_{max} \tag{III.2}$$

where γ_{min} and γ_{max} are aircraft dependent scalars. However, the maximum T^r_{max} and minimum T^r_{min} thrust are not scalars but functions of the state variables. Therefore, this control is bounded by additional path constraints:

$$T^r_{min} \leq T^r \leq T^r_{max} \tag{III.3}$$

Similarly, box constraints for the state variables are not required, since they are bounded by generic path constraints on auxiliary variables such as the Mach number (M) and the CAS (V_{CAS}):

$$M_{GD} \leq M \leq MMO;\ V_{GD} \leq V_{CAS} \leq VMO \tag{III.4}$$

where MMO and VMO are the maximum operational Mach and CAS, respectively, and M_{GD} and V_{GD} are green dot speeds (Airbus, 1993), which approximate the best lift to drag ratio speed in clean configuration.

In order to ensure the continuity of the trajectory composed by different segments, link constraints must be defined at the final point and initial point of each segment, on all the state variables:

$$\boldsymbol{x}^{(i)}(t_f^{(i)}) = \boldsymbol{x}^{(i+1)}(t_0^{(i+1)});\ i = 1, ..., N-1 \tag{III.5}$$

Next, additional path and event constraints on the flight profile, which are flight segment dependent, must be considered in order to guarantee the optimized trajectory be consistent with typical ATM operations and regulations. Following a conventional operation concept, the flight profile is divided into several segments where different models and standard operational procedures apply. Fig. III-6 summarizes the flight segments in simulation and the corresponding path and event constraints, being m the step climb index.

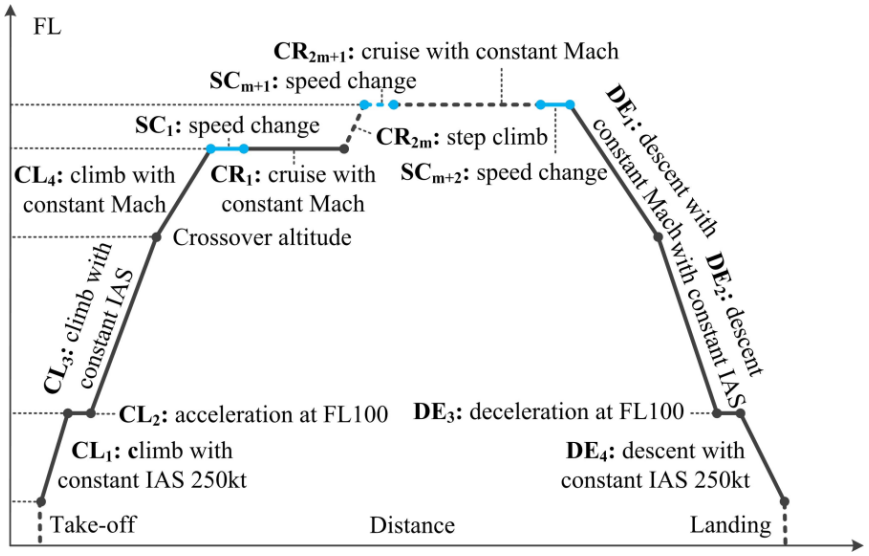

Figure III-6: *Model for the vertical profile used in the trajectory optimization tool.*

Note: the dash line in cruise phase means possible step climb cruise, which could be more than once. The subscript m is the ordinal number of the step climb cruise and equals to 0, 1, $\cdots$, n.

It should be noted that before each cruise flight level, a short cruise segment less than 1 min is added, allowing in this way proper speed adjustments (as shown with the blue lines in Fig. III-6). A similar segment is also added at the end of the last cruise segment. In addition to the flight vertical (and speed) profile, a flight route must be defined either in terms of Great Circle Distance (GCD) between city-pair airports, or by using air traffic services (ATS) route waypoints and published procedures (such as standard instrumental departures and arrivals).

To find the optimal solution of the formulated optimal control problem, direct collocation methods (Betts, 2010) are used in this chapter, which discretize the time histories of control and state variable at a set of nodal or collocation points, transforming the original continuous (infinite) optimal control problem into a (discrete and finite) nonlinear programming (NLP) optimization problem (Betts, 2010). The new finite variable NLP problem is then solved by using commercial off-the-shelf solvers: CONOPT (as NLP) and SBB as MINLP (mixed integer nonlinear programming), both bundled into the GAMS software suite (GAMS Development Corporation, 2013a; GAMS Development Corporation, 2013b). The whole process is briefly presented in Fig. III-5, and further mathematical details of this tool can be found in (Dalmau *et al.*, 2018).

III.2.1 Trajectory modeling for the different Cases of study

For the nominal flights, i.e., Case-0, the objective of the optimization is to minimize the compound cost function consisting of fuel F_i and time T_i for each flight segment i, weighted by the CI:

$$min(\sum_i F_i + CI \cdot T_i) \tag{III.6}$$

For the LH flights, (i.e., Case-1, -2 and -3), the optimization objective is changed to maximize the total flight time (Eq. III.7), while subject to the basic constraint on the fuel consumption, as depicted in Eq. III.8:

$$max \sum_i T_i \tag{III.7}$$

$$s.t. \sum_i F_i \leq F_{nom}, \tag{III.8}$$

where F_{nom} is the fuel consumption in nominal flight.

This makes it clear that the flight as a whole is optimized rather than the climb, cruise or descent phases separately. Although some trade-off between fuel consumption and time (speed) within each phase can be found, the trade-off between the three phases should be considered as well, which may contribute to better LH results.

Since in Case-1 the LH is implemented only in the cruise phase, the optimization process only considers segments between SC_1 and SC_{m+2} (inclusive) as shown in Fig. III-6. For this Case the climb and descent phases are fixed to those of the nominal flight. Therefore, only the speed in cruise is subject of optimization. In addition, the following constraints must be enforced at both initial and final points of each step climb segment CR_{2m} (if any), where H and D denote the flight level and distance respectively, in order to preserve the vertical profile of the nominal cruise phase:

$$H_{Case1}^{CR_{2m}} = H_{Case0}^{CR_{2m}}; \;\; D_{Case1}^{CR_{2m}} = D_{Case0}^{CR_{2m}} \tag{III.9}$$

In Case-2: the LH is extended to include climb and descent phases but keeping unchanged the nominal cruise flight level (or flight levels if $m > 0$). Accordingly, the whole flight (from CL_1 to DE_4 in Fig. III-6) is subject of optimization. Yet, the following constraint must be enforced so that the altitude of both TOC (final point of CL_4) and TOD (initial point of DE_1) remain unchanged:

$$H_{Case2}^{CL_4} = H_{Case0}^{CL_4}; \;\; H_{Case2}^{DE_1} = H_{Case0}^{DE_1}; \;\; H_{Case2}^{CR_{2m}} = H_{Case0}^{CR_{2m}} \tag{III.10}$$

Here, the distance at which each step climb (if any) is performed is no longer enforced, considering that possible changes in the TOC and/or TOD positions could impact on the length of the different cruise segments. In addition, it should be noted that an upper bound must be set for the aircraft mass at the initial point of CL_1, in such a way to stipulate the fuel consumption is not exceeding that initially scheduled.

Finally, for Case-3, the LH is implemented in the whole flight in the same manner as Case-2. In this case, however, only the constraint of fuel consumption (Eq. III.8) is enforced, allowing the solver to optimize also the cruise altitude(s). Taking the realistic limits of available altitudes into consideration, specific constraints on the range of flight levels could be enforced as well.

It is worth noting that the decision to perform LH is taken at dispatch level, when planning the flight before take-off. Thus, the new submitted flight plan might always be subject to ATM clearances, especially for Case-3, where changes in requested flight level(s) are involved. Recall the SESAR concept of Reference Business Trajectory (RBT), which the airspace user agrees to fly and ANSPs and airports agree to facilitate (Klooster *et al.*, 2010). Then, the three Cases will be able to provide alternative options for AUs to plan their flights. For instance, if Case-3 is eventually not

agreed, the operator can choose Case-2 where the flight level(s) is(are) fixed as initially scheduled (and agreed). Eventually, it might occur that heavy constraints in terminal airspace would not even allow Case-2, so in this instance the operator can still select Case-1 which performs LH only in the cruise phase. This chapter, therefore, presents the maximum delay absorption, by means of LH, for all the above three Cases.

III.3 Trade-offs of fuel and time

Some illustrative examples are given in this section (with additional results shown in Appendix A), analyzing the amount of LH that can be achieved for six routes representative of short/mid haul flights in Europe. Each route is further analyzed with different CI ranging from 5 to 150 kg/min with an Airbus A320, a common two-engine, narrow-body transport aircraft. The six flight routes studied are:

- DUB (Dublin, Ireland) - LHR (London Headrow, United Kingdom): 243 nm;
- FCO (Rome Fiumicino, Italy) - CDG (Paris Charles de Gaulle, France): 595 nm,
- FRA (Frankfurt, Germany) - MAD (Madrid, Spain): 769 nm;
- AMS (Amsterdam, The Netherlands) - SVQ (Seville, Spain): 1000 nm;
- STO (Stockholm, Sweden) -ATH (Athens, Greece): 1305 nm; and
- LIS (Lisboa, Portugal) - HEL (Helsinki, Finland): 1819 nm;

Some assumptions have been taken for all simulations: 1) The identification of flight phases is based on Ref. TOC/TOD (see Fig. III-2) instead of TOC/TOD; 2) Great Circle Distance (GCD) is considered between origin and destination airports, instead of considering air traffic services routes; 3) a passenger occupation (payload factor) of 81% is considered for all flights (Delgado & Prats, 2012); 4) alternate and reserve fuel are not modeled; 5) only even flight levels are used (FL260 as the lowest altitude); and 6) cruise step climbs are allowed with 2000ft steps and 5 minutes as minimum time for each flight level.

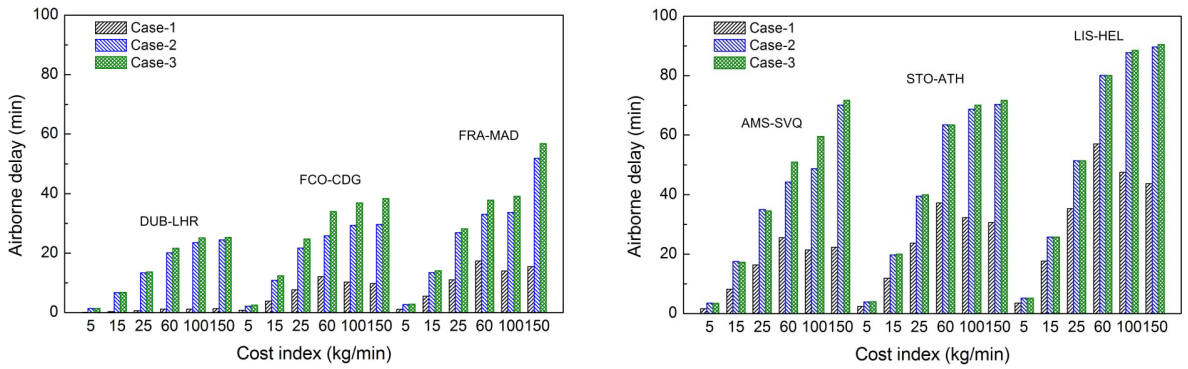

(a) Short-haul flights

(b) Mid-haul flights

Figure III-7: *Airborne delay generated for the simulated trajectories.*

As seen in Fig. III-7, the airborne delay for Case-2 is always greater than that of Case-1, since in the former LH is also allowed in the climb and descent phases. The benefits of this strategy are more noticeable for short flights, since the percentage of the climb/descent phases with respect to the whole flight is higher. It is worth noting, that in some flights (especially for higher CIs) the LH of Case-2 is more than 2-fold the LH of Case-1. This highlights the importance of including the climb and descent phases into the LH strategy.

Differentiating from Case-2 or Case-3, where the achievable airborne delay always grows with the increasing of CI, as can be noticed from Fig. III-7, there is, however, a peak value for each route of Case-1, appearing at the CI of 60 kg/min. Remember in Case-1, the cruise phase is the only flight segment that is subject to LH strategy. By selecting higher CI, more fuel will be consumed during the whole trip of the nominal flight (Case-0), and thus an increased amount of fuel will be allowed to perform LH, leading to a growth of airborne delay (as in Case-2 and Case-3). But as discussed previously in Fig. III-2, higher CI will also affect the vertical flight profile, typically with a flatter climb and a steeper descent. It happens that by selecting CI greater than 60 kg/min, the cruise distance of the nominal flight, which is then fixed in Case-1, becomes even shorter to realize the LH strategy, and thus contributes to less airborne delay. For detailed analysis about this Case, the readers may refer to (Delgado & Prats, 2012).

Regarding Case-3 (cruise flight level is also subject to optimization), the amount of airborne delay increases for some flights where the altitude change is feasible. Yet, this increase in LH is not so remarkable as from the comparison between Case-1 and Case-2. This is due to the fact that within the low cruise speeds the SR curves for different cruise flight levels are quite close (see Fig. III-4), such that the speed reduction from altitude changes, i.e., Case-2 vs. Case-3, will not be as large as the reduction from nominal speed to equivalent speed in the whole flight, i.e., Case-1 vs. Case-2.

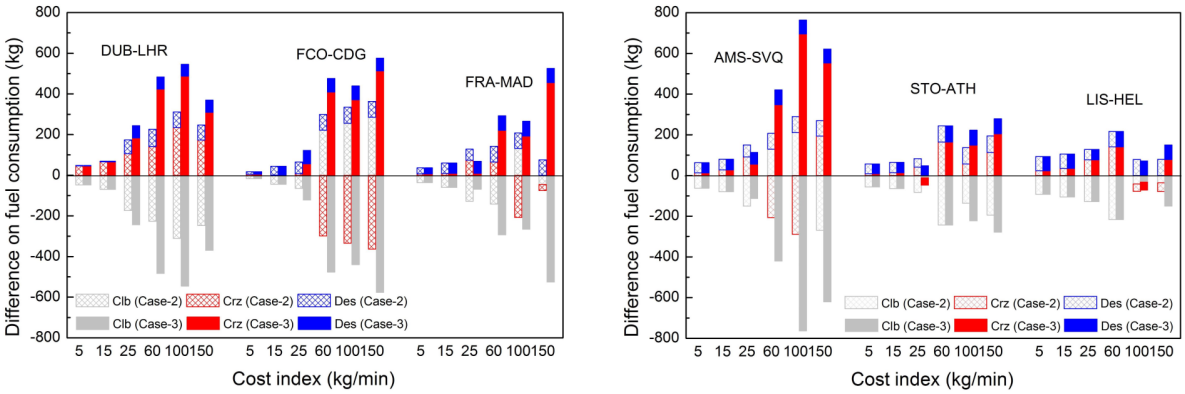

(a) Short-haul flights

(b) Mid-haul flights

Figure III-8: *The changes of fuel consumption in each flight phase (defined by TOC/TOD) compared to Case-0 for the simulated trajectories.*

On the other hand, Fig. III-8 presents the changes on trip fuel consumption of each LH Case for the different flight phases, with respect to the nominal flight (Case-0). In Case-1 only the cruise phase is subject to performing LH, with the allowable fuel consumption fixed at location of TOC and TOD (see Sec. III.2.1), such that there should be no difference in the regard of trip fuel if compared with Case-0. Accordingly, only Case-2 and Case-3 are shown in Fig. III-8, being their distributed fuel consumption (compared to those in Case-0) appreciated in the climb, cruise and descent flight phases.

It can be seen from the figure that different types of trade-off (among flight phases) of trip

fuel might apply for the simulated trajectories. For example, under the condition that the total fuel remains unchanged, there exist flights which save fuel during the climb, use extra fuel during the cruise and descent, or flights which use more fuel during climb and descent, save fuel during cruise, and etc. This suggests that the different efficiency of fuel consumption (to generate delays) in each flight phase could enable the optimizer to utilize these differences and produce the best allocation of trip fuel, in order to maximize the achievable airborne delay. Nevertheless, some general rules can also be noticed. For instance, all the trajectories in simulation are observed to consume more fuel in the descent phase, and (only) in Case-3 it seems that the fuel are all saved in the climb phase. A detailed analysis of the possible reasons will be discussed in the following section.

The specific trade-off of fuel and delay with respect to the nominal trajectory (Case-0) for each individual flight phase, i.e., climb, descent and cruise, can be seen from Fig. III-9. Furthermore, the detailed distribution of each type of trade-off are also as shown in the respective quadrant of the figure. As discussed in Sec. III.1, with different climb and descent profiles (i.e., CI), the distances when TOC and TOD are reached might vary. In order to have a representative comparison of the differences on fuel consumption and flight time, the Ref. TOC and Ref. TOD are used, which depict respectively the longest and shortest distance of the TOC and TOD appearing within the simulated flights for each route. In addition, to further understand the impacts from that short cruise segment produced by the variation of TOC/TOD, Fig. III-9 also presents, by the side of trip fuel and time, the distribution of changes on, such as the TOC, TOD and cruise distance, with regard to the nominal flight.

It can be noticed from the figure that, for almost all the simulated flights, the trip time are extended to achieve some airborne delay during each of the three flight phases (regardless of defining Ref. TOC/TOD or not), even with more fuel or less fuel consumed than the nominal. However, an exception occurs in the climb phase (see Fig. III-9(a)), where negative airborne delays are generated together with some fuel saved at the same time. Moreover, it applies only when considering the real TOC.

For Case-3, those negative values are mainly due to the reduction of the cruise flight level (which is changeable in this Case) that shortens both the climb altitude (i.e., TOC) and the climb distance (see Fig. III-9(b) in which all the flights are observed to have a shorter climb distance in Case-3 if compared to Case-0). On the other hand, the fewer exceptions in Case-2 (negative airborne delay and fuel consumption shown in Fig. III-9(a)) could be as well due to the shortened climb distance (see also Fig. III-9(b)), considering that a lower speed will contribute to less climb distance, leaving the climb time dependent on their quotient. Then, setting a common climb point, i.e., defining the Ref. TOC, would remove all these exceptions, as shown in Fig. III-9(a). It can be noticed that, in order to realize some airborne delay, part of the fuel could be saved or extra consumed before reaching that Ref. TOC.

In the descent phase, as shown in Fig. III-9(c), the difference on fuel is quite smaller than that in the climb phase (given that the overall fuel consumption of climb should be much larger than in descent), but the airborne delay that can be realized is still remarkable. This suggests that the efficiency of trade-off between trip fuel and time could be higher in descent than in climb, meaning that for the purpose of maximizing airborne delay it could be better to save more fuel in climb and allocate it in descent. This effect can be validated from the results of Case-2 and Case-3 (using TOD) in Fig. III-9(c). For all the flights more fuel are burned in descent, with 6 to 12 minutes of airborne delay generated at the same time, although some of such delay may be thanks to the extension of the descent distance (see Fig. III-9(d)).

Finally, Fig. III-9(e) presents the results of the cruise phase. A slightly difference on fuel can be observed even in Case-1 when using Ref. TOC/TOD, as it is the real TOC/TOD that are the points fixed for Case-1 in the simulation. Meanwhile, most of the flights in Case-2 and Case-3 consume more fuel, especially for those in Case-3 (for both using TOC/TOD and Ref. TOC/TOD),

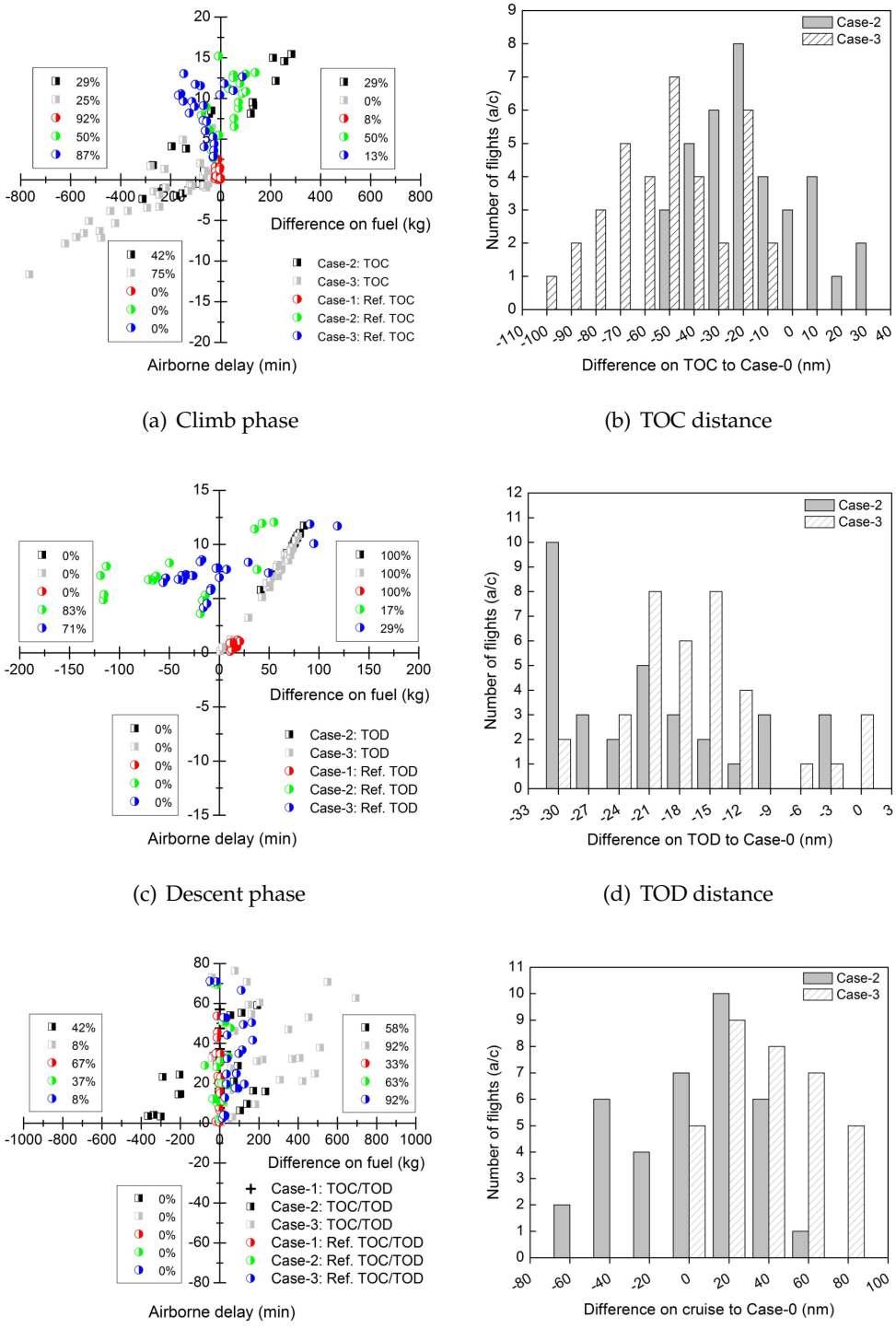

(a) Climb phase

(b) TOC distance

(c) Descent phase

(d) TOD distance

(e) Cruise phase

(f) Cruise distance

Figure III-9: *Airborne delay versus difference on fuel consumption of each flight phase (defined by TOC/TOD and Ref. TOC/TOD) with respect to the nominal flight (Case-0).*

which is due to the fact that lower cruise flight level typically brings lower SR (see Fig. III-4) that incurs more fuel consumption per unit of cruise distance. Nevertheless, there are several flights in Case-2 that can be seen with a relatively large amount of fuel saved instead, some of which only yield few minutes of airborne delay. This is because, resulted from the combined effect of the

movement of TOC and TOD, the real cruise distance could be reduced on some level, as shown in Fig. III-9(f). And in Case-3, however, the cruise distance is enlarged for all the flights, leading to even more fuel consumed (in addition to the factor that the SR decreases).

III.4 Impacts on aircraft trajectory

The vertical trajectories and the corresponding TAS profiles are plotted at the same figure, versus flight distances, as shown in Fig. III-10, where the set of flights are categorized with respect to the six flight routes studied and for two different CI (CI=25 and 100 are selected as examples, representing lower and higher CI respectively). Then, for illustrative purposes, the FRA-MAD flight with CI=60kg/min, is selected in Sec. III.4.2 and III.4.3 to further show the effects that the different LH strategies have on the aircraft trajectory (vertical and speed profiles).

III.4.1 Vertical trajectory profile

For the nominal Case-0, the optimal trajectories are as shown with the red circles in Fig. III-10, and due to the fuel burnt en route, step climbs in cruise are observed for long distance flights. It can be also noticed that the higher the CI is, the higher the optimal cruise TAS (red lines) will be.

Since only the cruise phase is subject of LH in Case-1, where climb and descent phases are fixed with the corresponding nominal ones, the trajectories of both Case-1 and Case-0 are exactly the same. The speed profile (black lines), however, differs in cruise as the equivalent speed is adopted instead of the nominal one, between which the gap shows the interval of the speed reduction which realizes LH.

In Case-2, with climb and descent phases included into the LH strategy (but cruise flight level fixed), the trajectories are slightly different from the nominal ones, since the TOC and TOD may move forward or backward as the case may be (blue diamonds). Furthermore, a much larger interval of the speed reduction occurs within the whole flight, compared with Case-1 (blue lines), which, in turn, will produce a remarkable increase on LH time.

With regards to Case-3, as the cruise flight levels are subject of optimization, a decrease on optimal cruise flight level is observed in some trajectories (green squares), which corresponds to the general fact that with speed reducing, the optimal cruise flight decreases simultaneously (see Fig. III-4). However, due to the flight level allocation scheme (only discrete flight levels at 2000 ft intervals are allowed), some of the trajectories just keep unchanged as those in Case-2. With CI increasing, an even larger speed reduction from the nominal speed occurs (green lines), compared with the one in Case-2.

III.4.2 Time and fuel trade-offs

A specific flight "FRA-MAD with CI=60" is studied in detail with numerical values for the resulting speed profiles for climb, cruise and descent, respectively. It should be noted that the total fuel consumption in each Case is always kept the same as consumed in the nominal flight, but could be different during each specific phase (i.e., climb, cruise and descent).

Aiming at showing the different tradeoffs between time and fuel as a function of the flight distance, Fig. III-11 displays, for each LH Case (Case-1, Case-2 and Case-3), the difference on flight time (i.e., airborne delay) and fuel consumption with respect to the nominal trajectory (Case-0) along with the execution of the flight. Meantime, Table III-1 summarizes from the figure, for each flight phase, the main trip parameters including the fuel, time, average TAS and LH (including specific range and altitude information for the cruise). Note that the identification of the

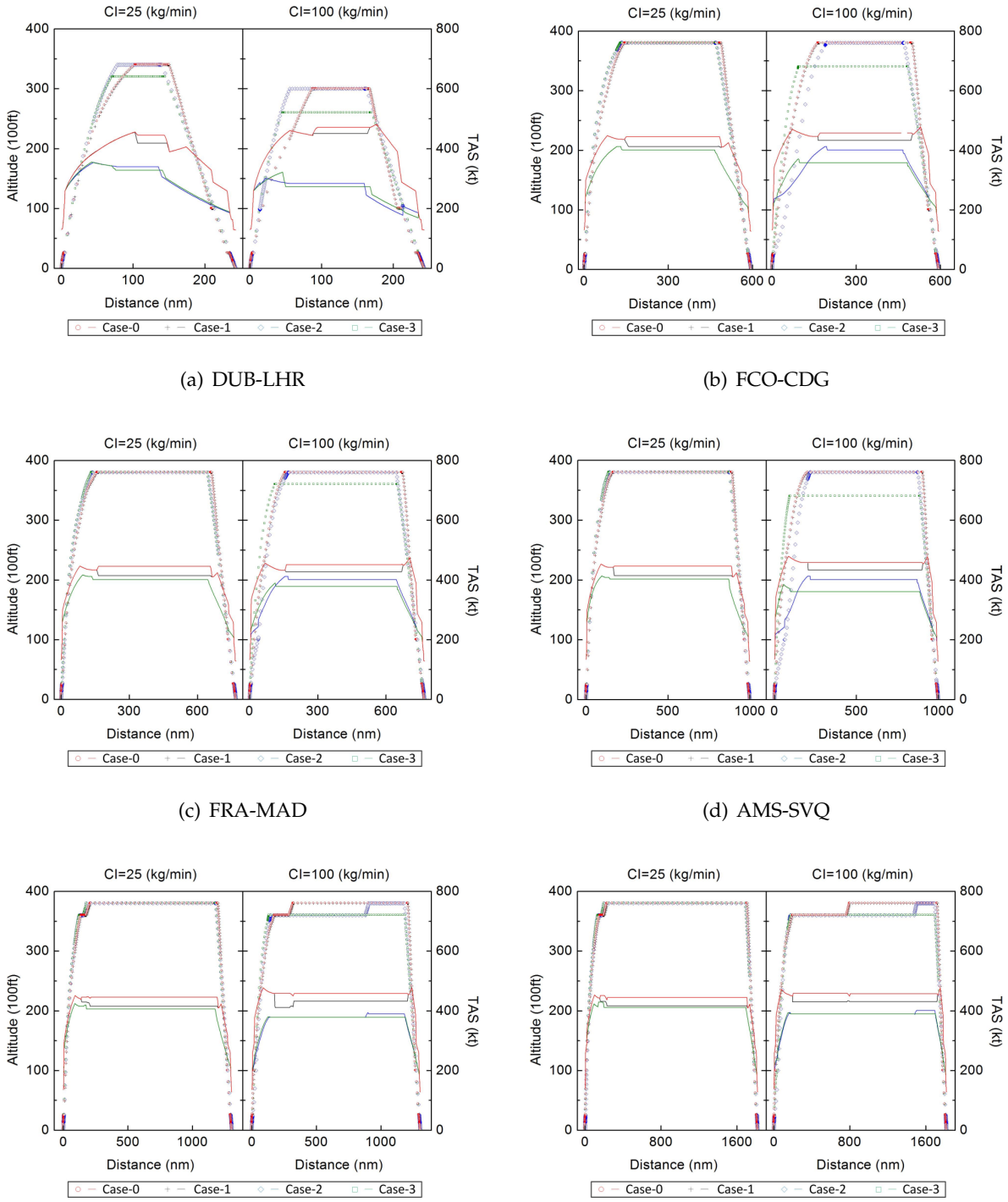

(a) DUB-LHR

(b) FCO-CDG

(c) FRA-MAD

(d) AMS-SVQ

(e) STO-ATH

(f) LIS-HEL

Figure III-10: *Vertical and true airspeed (TAS) profiles for the six flight rutes studied.*

climb/descent phases is based on Ref. TOC/TOD concept.

Compared with the nominal flight (Case-0), Case-1 consumes almost the same fuel in each phase, while the slightly difference (see Fig. III-11(b)) is due to the fact that speed is changing in the short cruise segment (Ref. TOC/TOD) to realize LH and to recover the nominal descent speed. Therefore, the avg. TAS of climb/descent reduces gradually, such that 0.6 and 1.2 minute of LH

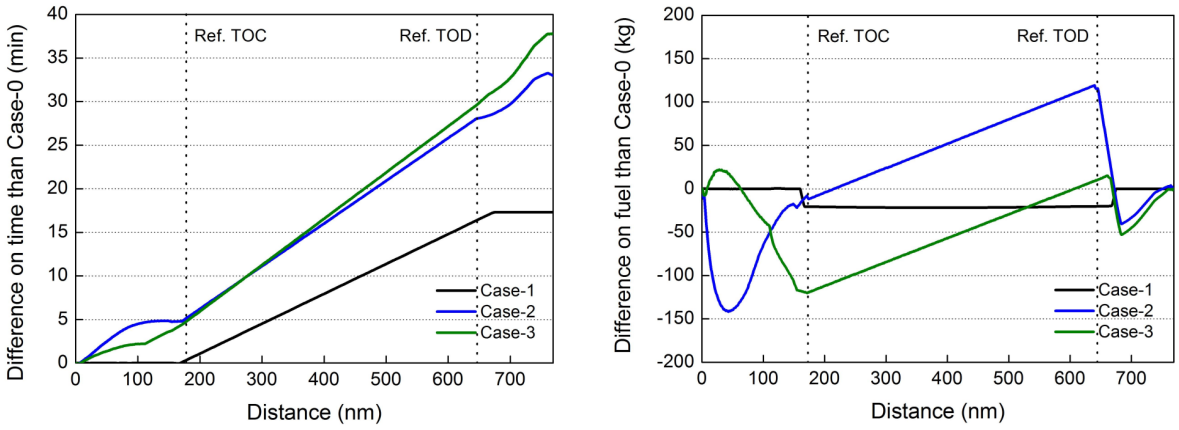

(a) Airborne delay

(b) Fuel consumption

Figure III-11: *Airborne delay and fuel difference change along flight distance with respect to the nominal trajectory (Case-0).*

Table III-1: *Main trip parameters for the FRA-MAD with CI=60kg/min.*

Cases	Climb (Ref TOC 171nm)					Descent (Ref TOD 124nm)				
	Fuel (kg)	Time (min)	Avg.TAS (kt)	Dif. Fuel (kg)	LH (min)	Fuel (kg)	Time (min)	Avg.TAS (kt)	Dif. Fuel (kg)	LH (min)
Case-0	1900	27,5	372	-	-	389	23,1	323		-
Case-1	1881	28,1	365	-19	0,6	375	24,3	307	-14	1,2
Case-2	1893	32,4	317	-7	4,8	275	28,1	265	-115	5,0
Case-3	1780	32,0	321	-120	4,4	380	31,4	237	-9	8,3

Cases	Cruise (Ref 474nm)							Whole flight (769nm)		
	Alt. (FL)	Fuel (kg)	Time (min)	SR (nm/kg)	Avg.TAS (kt)	Dif. Fuel (kg)	LH (min)	Fuel (kg)	Time (min)	LH (min)
Case-0	380	2200	59,5	0,2154	478	-	-	4490	110,1	-
Case-1	380	2234	75,0	0,2122	379	33	15,5	4490	127,4	17,3
Case-2	380	2323	82,7	0,2041	344	122	23,2	4490	143,2	33,0
Case-3	360	2330	84,7	0,2035	336	129	25,1	4490	148,0	37,8

time are observed in climb and descent, respectively. Then, as Table III-1 shows, by shifting to the equivalent cruise speed (99kt less than the nominal one in avg. TAS), 15.5 minutes of LH could be achieved, which accounts for the 21% of the cruise time and the 12% of the total time.

The fuel consumption of Case-2 reduces 115kg (29%) in descent and the LH time is almost 5 minutes in this phase, while another 4.8 minutes is realized in climb phase but only about 7kg (0.3%) of fuel is saved instead. As shown in Fig. III-11(b), since the total trip fuel keeps the same, this 115kg of fuel saved from descent plus 7kg from climb can be allocated to the cruise phase (122kg, 6% increase), which reduces the SR by 0.01133 nm/kg and thus further lower the equivalent cruise speed by 35kt, generating 7.7 minutes of extra LH, compared with Case-1. In general, as shown in Fig. III-11(a), the total LH in Case-2 reaches 33 minutes, which accounts for the 23% of total time, and which is 15.7 minutes more than the one in Case-1 (91% increase).

As for Case-3, with speed reducing in LH, the optimal cruise flight level for the lower cruise speeds decreases from FL380 to FL360 (see Table III-1), leading to 113kg (6%) of fuel saving in

climb while 105kg (39%) increasing in descent, if compared with Case-2. Although the LH time in climb becomes 0.4 minute less than Case-2, the relatively higher percent of fuel added in descent, however, produces 3.3 minutes more instead. Moreover, a slightly increase of fuel with only 7kg (0.0006 nm/kg lower in SR) in cruise helps to generate 1.9 minutes more of LH time than that in Case-2 (compare the curve slopes between Ref. TOC and Ref. TOD in Fig. III-11(a)), due to the lower cruise flight level, but its maximum is already approaching as the cruise speed (336kt) is constrained by the GD speed for that flight level. Generally, the total LH time grows 4.8 minutes more than the one in Case-2 (15% increase).

III.4.3 Speed profiles and fuel consumption

As shown in Fig. III-12(a), the climb speed profiles of all the Cases have similar structures, which mainly include a continuous acceleration process at low altitude, a constant CAS climb, followed by constant Mach climb at higher altitudes. At the end of the climb phase, a small deceleration is observed in each LH Case, which allows to reach the (slower) optimal cruise speed. Being Case-0 the baseline, the difference with Case-1 only lays on this deceleration process in cruise, such that the avg. TAS of Case-1 turns down slightly, leading a reduction on fuel consumption (see Table III-1).

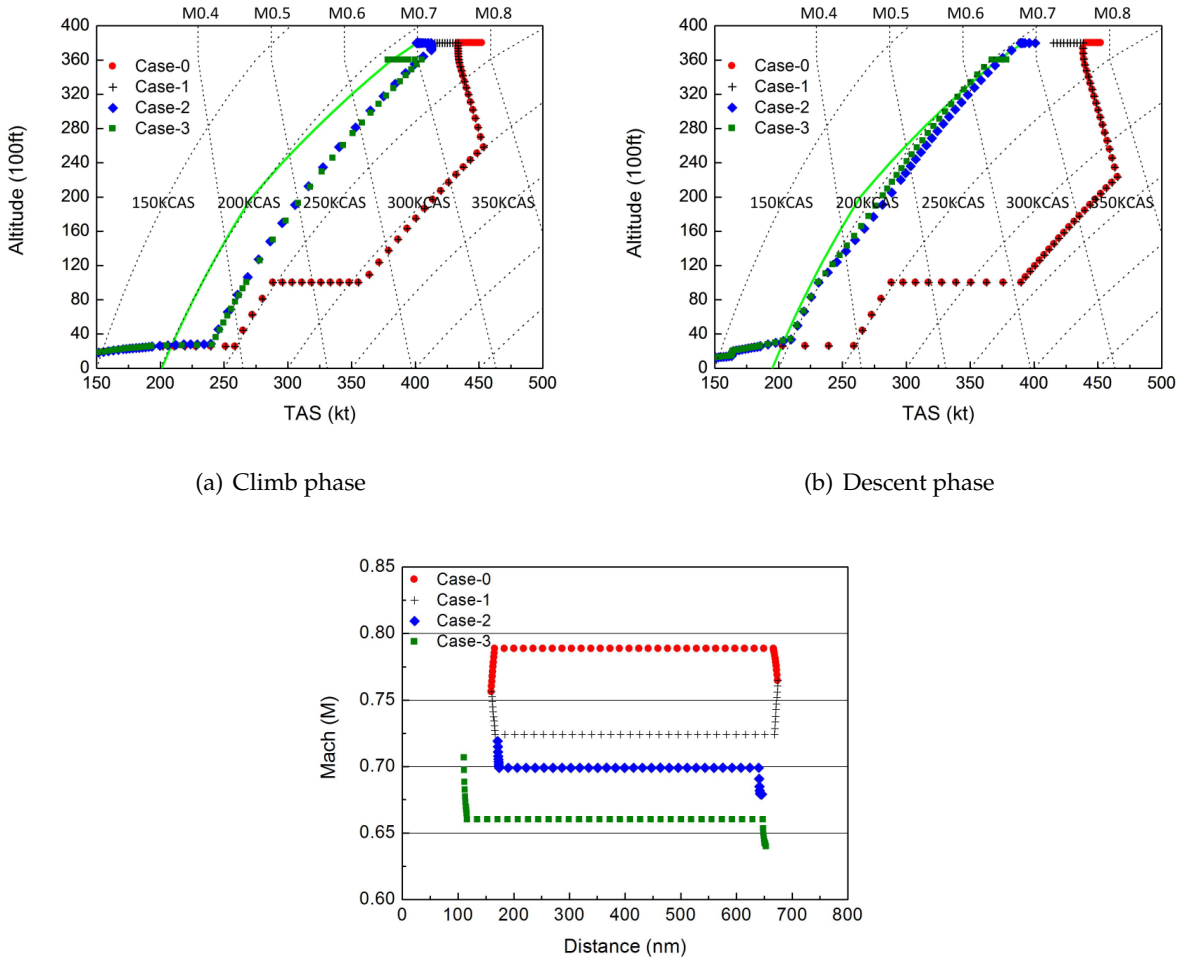

(a) Climb phase

(b) Descent phase

(c) Cruise phase

Figure III-12: *Climb, cruise and descent speed profiles for the FRA-MAD (CI = 60kg/min).*

In Case-2, the optimizer chooses a climb with CAS around 230kt (instead of the 300kt observed in Case-0). Due to this lower CAS climb, a higher crossover altitude (around FL360) is found, were climb resumes at constant Mach number (also lower than the nominal one).

Results in Case-3 show that the climb speed profile is the same with the one in Case-2, except for the constant Mach climb segment, as the crossover altitude for this flight is higher than its optimal cruise flight level (FL360). Due to this lower final altitude of climb, the fuel consumption decreases to 1780kg, corresponding to an avg. TAS of 321kt which, however, is higher than the 317kt in Case-2 (see Table III-1), so the LH time in climb will not be as much as that in Case-2.

As for the descent speed profiles shown in Fig. III-12(b), Case-2 and Case-3 have no deceleration process at FL100 (like in Case-0 and Case-1) because the descent speed is already below the ATC constraint of CAS lower than 250kt below FL100. Moreover, the segments of constant Mach descent are both missing too, since the crossover altitudes lay higher above the cruise flight levels due to the lower speeds in constant CAS descent.

Normally, the fuel consumption in descent phase accounts for the lowest of the three phases, but it still generates a high percentage of LH with regard to the total descent time in the above example. Similar situation as in climb, with a deceleration at the initial of descent, Case-1 has an avg. TAS of 307kt lower than the nominal one at 323kt, while in Case-2 with descent CAS declining to near the GD speed, the avg. TAS reduces further to 265kt and some fuel are saved (see Table III-1).

In Case-3, the descent CAS keeps decreasing and reaches the GD speed for this flight (see Fig. III-12(b)). Remember the GD speed is not the same in climb that in descent, since the aircraft mass is different (fuel has been burnt in cruise). It is worth noting that after the reduction of cruise flight level in Case-3, the fuel consumption of descent increases instead, compared with Case-2, which is on the contrary of the situation in climb. In this way, the avg. TAS further reduces to 237kt in order to produce a longer LH time (see Table III-1).

When it comes to the cruise phase, as shown in Fig. III-12(c), if LH is realized only in this phase as Case-1, then the cruise Mach decreases from M0.79 to M0.72, while after climb and descent phases are involved in LH, the cruise speed keeps decreasing to M0.7 and M0.66 in Case-2 and Case-3, respectively, resulted from the lower SR (extra fuel "allowance" due to savings in climb/descent), as also seen in Table III-1. If the curve of SR becomes flatter when speed is lower than the equivalent speed (see Fig. III-4), it happens that a slightly decrease in SR could bring a relative larger decrease in cruise speed, by which a remarkable amount of LH time can be produced, considering the long distance and time that cruise phase could take.

III.5 Chapter summary

A cost-based linear holding strategy was proposed on basis of previous work where linear holding was only allowed by reducing cruise speed. By analyzing the relationship between fuel consumption and speed in all phases of flight, the equivalent speed concept was extended to the climb and descent phases. Thus, the speed reduction proved to be feasible to be implemented along the whole flight to generate linear holding at no extra fuel cost. Through a detailed simulation on typical flights with the developed optimal trajectory generation tool, the effects of three subdivided cases of the strategy were thoroughly assessed, where a remarkable increase of the maximum airborne delay absorption was observed compared with previous studies.

Results suggest that the difference of trade-off between fuel and time in each flight phase (even in flight segments within a particular phase) contributes to the remarkable amounts of linear holding. For instance, all the trajectories in simulation are observed to consume more fuel in the descent phase to produce airborne delay, and (only) in Case-3 the fuel are all saved in the climb

phase with negative delay generated. Besides, a specific transition of fuel, e.g., from climb to cruise phase, may not be a general pattern that satisfies all the cases, but the reallocation of fuel among different flight phases does exist generally. Including climb and descent would make it possible for the optimizer to utilize these differences on trade-off to maximize the total airborne delay.

Note that although a reasonable amount of extra fuel allowance could bring a considerable increase of the maximum linear holding time, this option is out of the scope of this chapter and the pre-condition is that linear holding must be done at no extra fuel cost.

Knowing is not enough; we must apply. Wishing is not enough; we must do.

— Johann Wolfgang Von Goethe

IV

Linear holding applications for ATFM

This chapter introduces the potential applicability of the cost-based linear holding for air traffic flow management (ATFM). In previous work (Delgado *et al.*, 2013), an application for the Ground Delay Program (GDP) has been discussed. It demonstrates that, using the linear holding strategy, significant delay can be recovered (without extra fuel) if the GDP is canceled prior to the planned ending time. In this chapter, we first focus on another commonly-seen ATFM program, namely the Airspace Flow Program (AFP), and show the benefits of linear holding even without AFP's early cancellation.

Specifically, trajectories are optimized at the AFP planning stage in such a way that the program performance is improved in terms of delay absorption before the congested area, and delay recovery at the destination airport. This recovery process is studied by comparing the case where the same fuel consumption is fixed as the nominal flight, with several cases where some extra fuel allowances are considered during flight planning. The effects for AFP delayed flights are thoroughly discussed in a case study followed by a sensitivity analysis on possible influential factors.

Next, another approach is introduced to implement linear holding for flights initially subject to ground holding, in the context of Trajectory Based Operations (TBO). The aim is to neutralize additional delays raised from the lack of coordination between various traffic management initiatives (TMIs) and without incurring extra fuel consumption. Motivated from previous results on the features of linear holding to absorb delays airborne, an applicability to compensate part of the fixed ground holding is proposed. Then, its reactive adjustment in response to tactical delays is formulated as a multi-stage aircraft trajectory optimization problem, addressing both pre- and post-departure additional delays.

IV.1 Improve AFP performance

As stated in (FAA, 2009), AFPs are one of the initiatives associated with ATFM in the NAS, marked as a significant step in en route traffic management in the United States. It identifies constraints in the en route system, develops a real-time list of flights that are filed into the Flow Constrained Area (FCA), and distributes Expected Departure Clearance Times (EDCTs) to meter the traffic demand through the area. Compared with GDP, an AFP does not unnecessarily delay flights to an airport that do not pass through the en route region of reduced capacity (Libby *et al.*, 2005).

IV.1.1 Features of linear holding in AFP

Currently, once a flight is captured in an issued AFP, an EDCT will be assigned to that flight, which aims at entirely absorbing all the assigned delay by means of ground holding. This is similar than when delays are applied in GDP. Yet, options like re-routing may also help to get the flight out of the AFP list and thus avoid the delay assignment (Mukherjee & Hansen, 2009), but this is out of the scope of this chapter. Under current ATM paradigm this EDCT is enforced at the departure airport.

Nonetheless, a flight affected by an AFP delay could reduce its ground holding (i.e., take off earlier than the EDCT), and then perform the necessary linear holding (LH) to experience the rest of the delay airborne in order to meet the assigned CTA (or CTO) at the particular FCA. As discussed in Sec. II.1.1, this could be done at the same time some fuel is saved. After passing the FCA, it would be possible to take advantage of the saved fuel to accelerate along the rest of the trajectory to recover part of the delay at the destination airport. Different from a GDP, in which CTA is assigned at the arrival airport, the arrival time for a flight captured in an AFP is not enforced, making this delay recovery process feasible and legitimate.

Thus, if the aircraft operator chooses to fly with a nominal speed faster than the minimum fuel speed (i.e. at a Cost Index greater than zero), there will exist a range of slower speeds with a fuel consumption equal or lower than the fuel consumption attained when flying at the nominal speed (recall Fig. III-1). Consequently, this would allow to perform some LH at no extra fuel cost (or with some fuel savings). This is the key concept that motivates the applicability of trajectory optimization to enhance AFPs initiatives presented in this chapter.

Furthermore, convective weather may occur at multiple airspaces simultaneously, leading to more than one constrained areas identified (by different AFP) to meter the traffic demand through each corresponding area. Additionally, a flight could be eventually captured in both a GDP and an AFP at the same time, where the former has constraints closer to the airport and the latter specifies an FCA somewhere in the route. Under current operations, assigned delays will be transferred to the departure airport. In the United States a GDP has higher priority than an AFP, such that the EDCT arising from a GDP will override that one coming from an AFP. If in the future the EDCT enforcement is replaced by a CTA (or CTO) enforcement, this hierarchy principle may apply as well (but is out of the scope of this chapter). Since AFPs are aimed to identify constraints in the en-route domain of the NAS, this chapter will only take account the issued en route FCA as the constrained airspace.

It is also worth noting that AFPs are issued based on convective weather predictions which might be not correct as always and could be subject to timely updates, and in turn, would impact the AFP delayed flights. As such, the robustness of the method proposed in this chapter needs to be clarified given that the increased airborne traffic density (as ground holding is reduced via LH) will have more aircraft in the air potentially affected by any incorrect weather predictions.

IV.1.2 Two-stage trajectory optimization

Incorporating LH in an AFP is modeled in this section as a two-stage trajectory optimization process. During the first stage, the operator computes the optimal trajectory in terms of direct operating costs (DOC) for the nominal flight plan (denoted by *nom* flight in this chapter). Then, assume some delay is assigned to the *nom* flight due to an AFP (denoted by *AFP* flight). During the second stage, a new optimal trajectory is generated such that the delay recovery is maximized (denoted by *LH* flight).

IV.1.2.1 First stage: nominal flight generation

As mentioned in the previous chapter, the optimization of aircraft trajectory requires the definition of a mathematical model representing aircraft dynamics and flight performance, along with a model for certain atmospheric parameters. This PhD thesis considers a point-mass model, an enhanced performance model using manufacturer certified data and the International Standard Atmosphere (ISA) model. See Sec.III.2 for more details about the method of optimal trajectory generation for the nominal flight.

IV.1.2.2 Second stage: AFP delayed flights with no LH

Then, based on the 4-dimensional (4D) trajectory found for the *nom* flight, a capacity reduction is assumed en route, requiring to issue an AFP at a specific FCA located at a flight distance d from the departure airport ($D - d$ is the remaining distance to the arrival airport where D is the whole flight distance). Resulting from the AFP, the *nom* flight is captured in the program list with a Δt delay assigned. Then, the CTA for the *AFP* flight at the FCA will be $t_{FCA} = t_{FCA \cdot nom} + \Delta t$, where $t_{FCA \cdot nom}$ is the time at which the *nom* flight planned to arrive at the FCA.

Apparently, the only difference of the *AFP* flight, with respect to the *nom* flight, lies on the timeline which takes a parallel movement from the latter one, so as to transfer all the Δt on the EDCT, keeping the other 3D trajectory unchanged. Yet, as a consequence of enduring some delay on ground, the operator of the *AFP* flight may be inclined to increase the flight speed after the FCA even if more fuel than initially planned has to be burnt in order to recover part of the delay at the arrival airport. This is sometimes necessary for aircraft operators trying to guarantee, for instance, connecting passengers and/or to mitigate reactionary delays as much as possible.

In this context, it is considered in this chapter that the aircraft operator will plan (at dispatch level) for $\omega\%$ extra fuel than the total trip fuel as initially scheduled for the nominal flight. Then, not only the timeline but the whole 4D trajectory of the *AFP* flight will change if compared with the *nom* flight. It is worth noting that regarding this $AFP + \omega\%$ flight, an earlier arrival time at the FCA could be technically achieved provided that the CTA is not (currently) enforced. However, aimed at future TBO, it is more realistic to fix CTA at the FCA, only permitting delay recovery at the arrival airport where no capacity reduces.

For the $AFP + \omega\%$ flight, the trajectory optimization problem will maximize the delay recovery (i.e. minimizing the arrival time t_f), instead of minimizing the function written in Eq. III.1. Besides all optimization constraints already used when generating the *nom* flight (see Sec. IV.1.2.1), this new trajectory will consider as well the following restrictions:

$$t_0 = t_{0 \cdot nom} + \Delta t \tag{IV.1}$$

$$t_{FCA} = t_{FCA \cdot nom} + \Delta t \tag{IV.2}$$

$$s(t_{FCA}) = d \tag{IV.3}$$

$$\int_{t_0^{(1)}}^{t_f^{(N)}} FF(t)dt \leq [m(t^1_{0\cdot nom}) - m(t^N_{f\cdot nom})](1+\omega\%) \tag{IV.4}$$

Eq. IV.1 and IV.2 specify that the assigned delay Δt is fully realized in terms of the EDCT at origin airport, and the CTA at the FCA, respectively. Eq. IV.3 ensures the flight arrives at the FCA meeting the assigned CTA. Eq. IV.4 imposes the maximum fuel consumption allowed which equals to the total trip fuel burnt in the *nom* flight (difference between initial and final aircraft mass) plus the ω allowance.

IV.1.2.3 Second stage: AFP delayed flights with LH

As explained before, with the LH strategy the aircraft can experience less ground holding and depart earlier than the initially assigned EDCT, absorbing the remaining delay airborne and still meeting the CTA at the FCA (and with some eventual fuel savings due to the reduced speed). After passing the FCA, the *LH* flight is able to use this saved fuel to increase speed and recover as much delay as possible at the arrival airport. Like in the *AFP*+ω% flight previously presented the aim of the *LH* flight is also to maximize delay recovery.

Regarding the optimization constraints, however, the key difference compared with the *AFP* flight is that the EDCT for the *LH* flight is no longer enforced. Thus, besides all constraints listed in Sec. IV.1.2.1 for the *nom* flight, equations IV.2, IV.3, IV.4 are also enforced, while Eq. IV.1 is replaced by $t_0 \geq t_{0\cdot nom}$ just to ensure that the *LH* flight does not depart the origin airport before its initially scheduled time.

IV.2 Examples for an AFP delayed flight

In this section, the application of trajectory optimization in AFP is simulated by using the above mentioned method. Sec. IV.2 presents the numerical results for a given case study, representing a realistic AFP in the NAS.

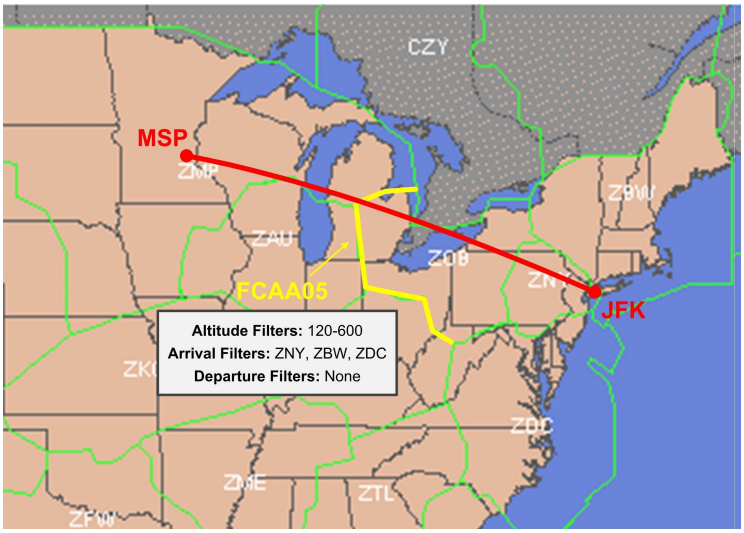

Figure IV-1: *A sketch of flight "MSP-JFK" passing the AFP flow constrained area FCAA05 (defined by the western boundary of ZOB and the eastern boundary of ZID air route traffic control centers).*

IV.2.1 Case study

The case study for this chapter is shown in Fig. IV-1, where a flight from MSP (Minneapolis-Saint Paul) to JFK (John F. Kennedy) airport is scheduled to fly through a pre-coordinated (known as "canned") AFP, passing an FCA frontier named FCAA05. From MSP to FCAA05, the flight (great circle) distance is 350 nm, and from FCAA05 to JFK it is 544 nm.

An Airbus A320 model is used in this study assuming a typical passenger load factor of 81% (Delgado & Prats, 2012) and a CI of 45 kg/min. The following additional assumptions have been considered in this case study: 1) a 20 min AFP delay is assigned at FCAA05; 2) no wind conditions are considered; 3) only even flight levels are used (FL260 as the lowest altitude); and 4) cruise step climbs are allowed (if any) with 2,000ft steps.

Results for the cases with no extra fuel included (i.e., the *AFP* and *LH* flights) are presented in Fig. IV-2, showing the true airspeed (TAS), flight timeline, vertical profile, and various representations of the fuel cost (including the unit, aggregate and difference) taking the *nom* flight as the baseline.

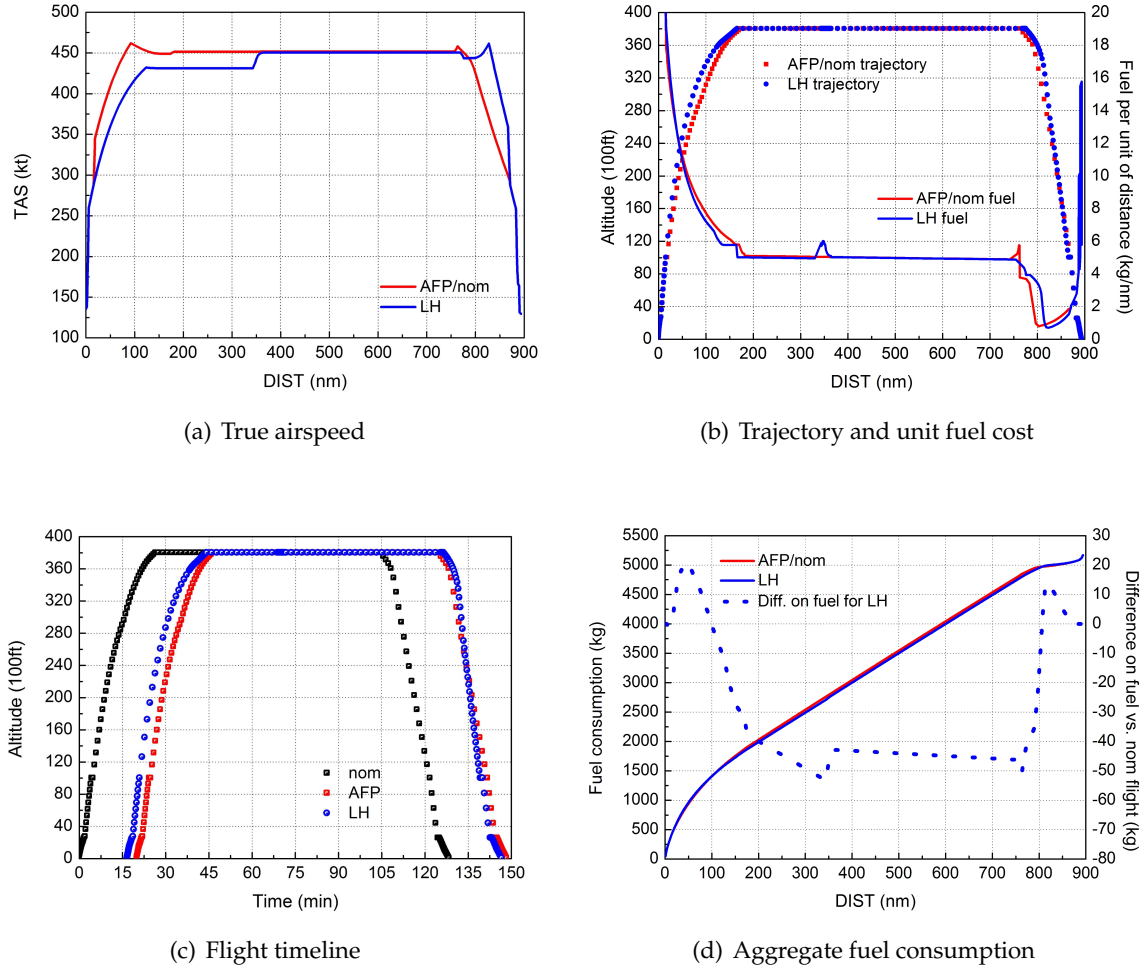

(a) True airspeed

(b) Trajectory and unit fuel cost

(c) Flight timeline

(d) Aggregate fuel consumption

Figure IV-2: *Comparison between the nom, AFP and LH trajectories (at no extra fuel cost)*

Due to the TAS variation (as shown in Fig. IV-2(a)), LH is realized and thus part of the delay is absorbed airborne before the FCA (at 350 nm), satisfying the CTA (at 70 min) with a shorter ground holding if compared with the *AFP* flight (see Fig. IV-2(c)). As discussed in Sec. IV.1.2.2, when extra fuel is not allowed, the AFP flight shares the same trajectory with the *nom* flight except

for the timeline, and thus, an anticipated parallel movement of 20 min on flight timeline can be observed as shown in Fig. IV-2(c).

In addition, some fuel is saved before arriving at the FCA (at around 70 min), as shown in Fig. IV-2(d), because of the lower selected climb and cruise speeds (leading to lower unit fuel consumption as shown in Fig. IV-2(b)). Afterwards, this fuel saved is burnt after the FCA till the final arrival (see the difference on fuel consumption versus the *nom* flight in Fig. IV-2(d)), contributing to a higher TAS for descent, a steeper vertical descent profile (leading to an extended cruise distance), and an earlier arrival time (see Fig. IV-2(c)).

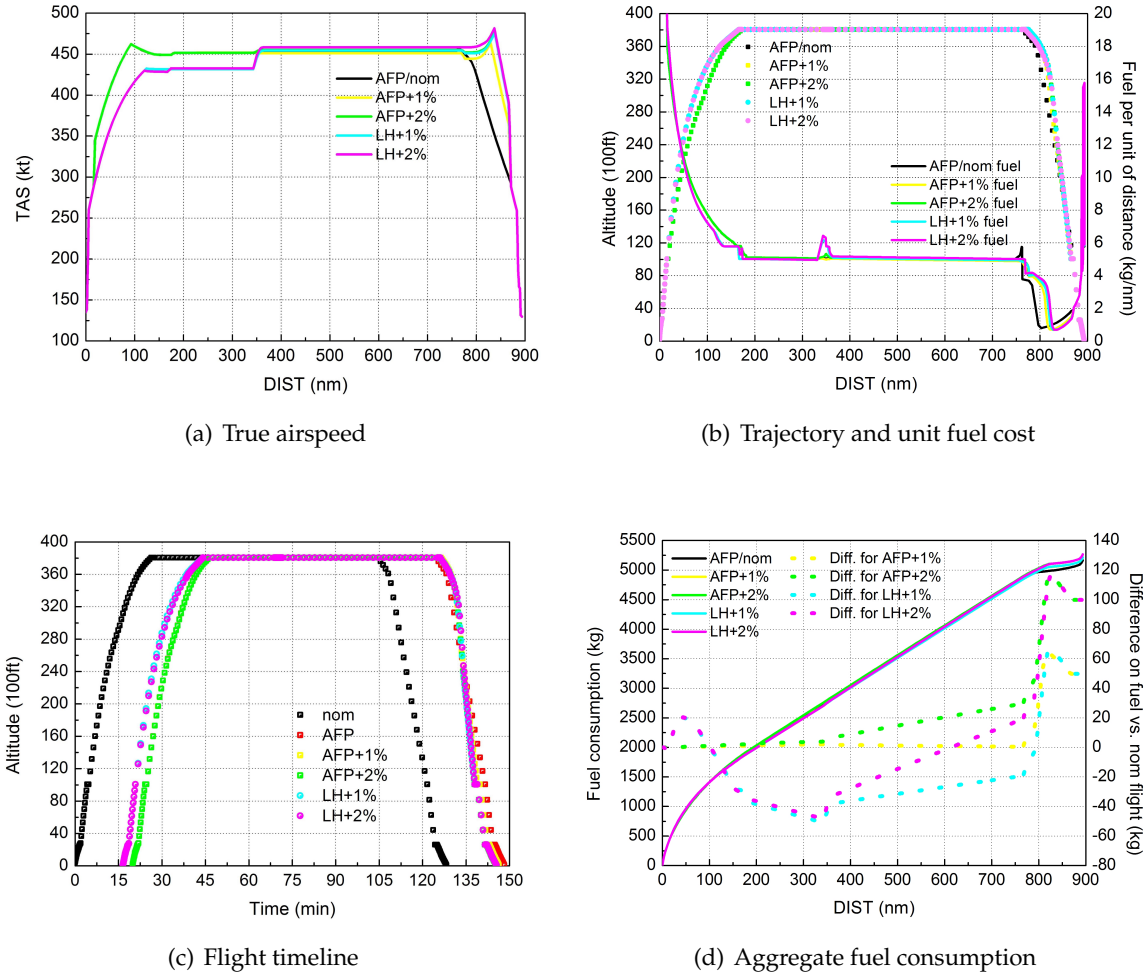

(a) True airspeed

(b) Trajectory and unit fuel cost

(c) Flight timeline

(d) Aggregate fuel consumption

Figure IV-3: *Comparison between the AFP and LH trajectories (with 1% and 2% of extra fuel allowances)*

Figure IV-3 shows the cases when 1% and 2% of the total trip fuel is added at dispatch level (i.e., the *AFP+1%*, *AFP+2%*, *LH+1%* and *LH+2%* cases). Here, the assigned delay is partially recovered for all of these flights, with the same CTA (at 70 min) satisfied at the FCA (see Fig. IV-3(c)). Next, if compared to the *AFP+1%* and *AFP+2%* flight, higher cruise speeds (and thus higher unit fuel consumption, see Fig. IV-3(b)) can be selected after the FCA for the *LH+1%* and *LH+2%* flights, respectively (see Fig. IV-3(a)), as a result of the fuel saved from LH before the FCA (see the difference on fuel consumption versus the *nom* flight in Fig. IV-3(d)). Therefore, more time can be recovered at the arrival airport. In other words, with the same amount of fuel included, the *LH* flight will still perform better for the *AFP* delayed flights than only increasing flight speed after the FCA.

Table IV-1: *Summary of results for each case study.*

Cases	Total			MSP		FCA		JFK	
	Dist (nm)	Fuel (kg)	Time (min)	ETD/EDCT (hh:mm:ss)	GH (min)	ETA/CTA (hh:mm:ss)	Delay abs. (min)	ETA (hh:mm:ss)	Delay rec. (min)
nom	894	5167	128,4	**0:00:00**	-	**0:49:50**	-	**2:08:24**	-
AFP	894	5167	128,4	**0:20:00**	20,0	**1:09:50**	0,0	**2:28:24**	0,0
LH	894	5167	130,0	**0:16:41**	16,7	**1:09:50**	3,3	**2:26:40**	1,7
AFP+1%	894	5217	126,5	**0:20:00**	20,0	**1:09:50**	0,0	**2:26:31**	1,9
LH+1%	894	5217	129,0	**0:16:41**	16,7	**1:09:50**	3,3	**2:25:39**	2,8
AFP+2%	894	5267	125,6	**0:20:00**	20,0	**1:09:50**	0,0	**2:25:33**	2,9
LH+2%	894	5267	128,3	**0:16:38**	16,6	**1:09:50**	3,4	**2:25:00**	3,4

Table. IV-1 summarizes the numerical results of the key parameters for all the flights of this case study. It can be noticed that, by performing LH, 1.7 min of the AFP delay can be recovered when arriving at JFK, at no extra fuel cost, which accounts for nearly 8.5% of the total delay assigned. Meanwhile, 3.3 min of the delay can be absorbed airborne by LH, saving 16.5% of the GH (ground holding) as supposed to perform at MSP. With 1% (50 kg) and 2% (100 kg) extra fuel allowed, 1.9 min and 2.7 min can be recovered respectively without LH, but all of the 20 min of AFP delay have to be fully realized on ground. On the other hand, with LH performed at a similar delay absorption (3.3 min and 3.4 min), the delay recovery can be extended to 2.9 min and 3.4 min, respectively, which makes an increase of 0.8 min and 0.5 min with respect to each of the above two cases where LH is not in effect.

It is worth noting that the amount of achievable delay recovery, along with the delay absorption, appears to be not such remarkable (for around several minutes) that could be expected to largely reduce the initially assigned AFP delay. Even so, it still proves to be always more efficient (at the same fuel cost) than the case where ground holding is fully experienced followed by burning more fuel to speed up (as commonly done nowadays). In other words, with the aim of recovering the same delay, implementing the LH strategy will contribute to some fuel saved. In fact, given the exponential relation between aircraft speed and fuel consumption (recall Fig. III-1), a relatively small increase of delay recovery could incur much more costs on fuel, as will be discussed in Sec. IV.2.3. Furthermore, considering the simple procedure (at the airline dispatch level) of the proposed strategy, it could be effectively realized in practical, and thus the accumulative delay recovery of various AFP delayed flights shall mount remarkably.

IV.2.2 Detailed trajectory analysis

In order to better understand the changes of trajectories for the above cases, a further discussion is presented in this section analyzing separately the climb, cruise and descent phases. Fig. IV-4 shows the different speed profiles. As expected, the *LH* flight (including *LH+1%* and *LH+2%* flight) selects the lowest CAS (250kt) during the constant CAS climb segment, while the *nom* flight, along with the *AFP* flight (including *AFP+1%* and *AFP+2%* flight) all choose 300kt (see Fig. IV-4(a)). During the descent phase, as shown in Fig. IV-4(b), the *nom* flight selects 250kt, while the *AFP+1%*, *LH+1%*, *AFP+2%* and *LH+2%* select speeds from 300kt to VMO, orderly. It is worth noting that the higher the climb/descent CAS, the lower the crossover altitude will be to change to/from the climb/descent Mach number.

As for the cruise phase, both the *LH* flight and *AFP+1%* flight select lower cruise Mach after the FCA than the *nom* flight, as shown in Fig. IV-4(c) and IV-4(d), respectively. Given that both of the flights have delay recovered at final arrival (see Table IV-1), the recovery process is actually realized only in the descent phase. The reason is due to the fact that the trade-off of fuel and

time, as presented in Fig. III-1, differs between each flight phase, and the descent is more fuel efficient than the cruise (see also the unit fuel consumption in Fig. IV-2(b) and Fig. IV-3(b)). In this way, increasing the descent speed incurs less fuel consumption than cruise speed, but keeping increasing will in turn lower its marginal efficiency.

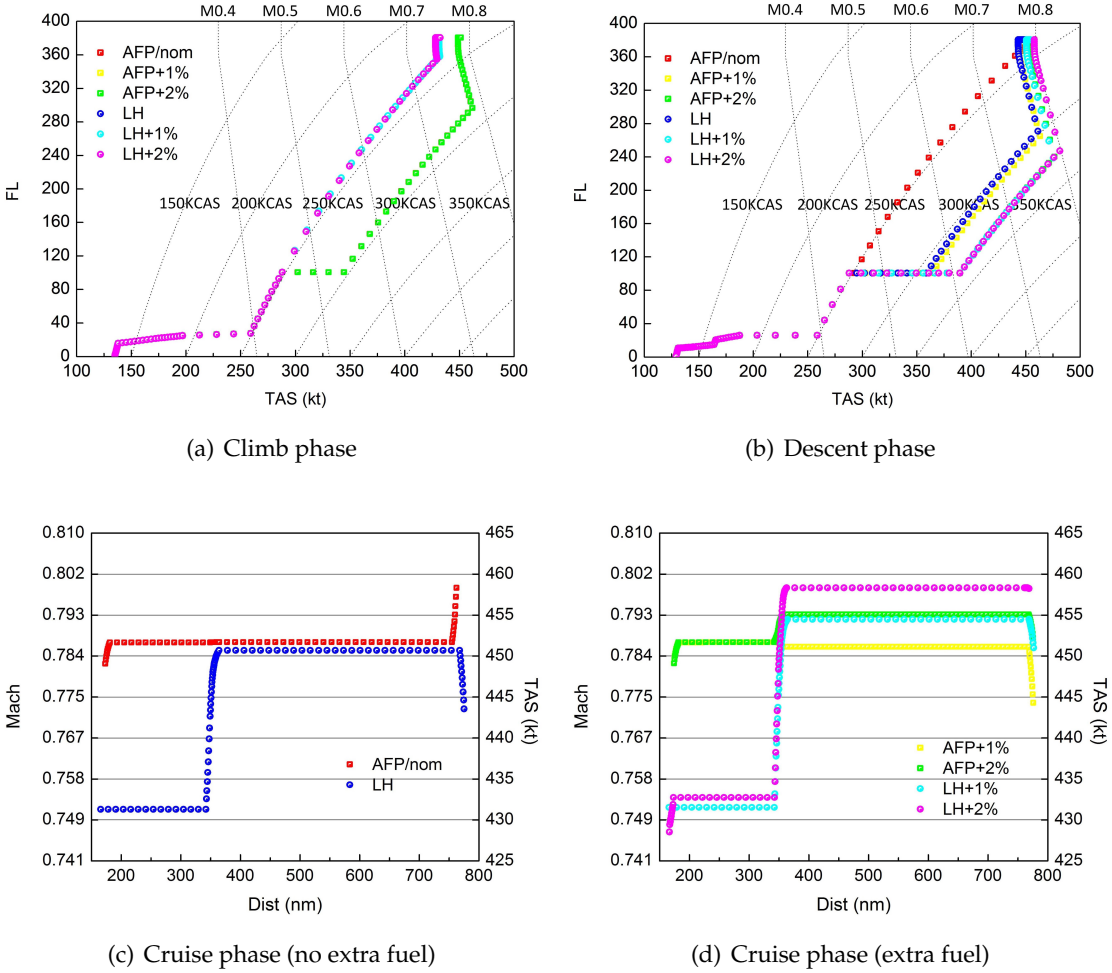

(a) Climb phase

(b) Descent phase

(c) Cruise phase (no extra fuel)

(d) Cruise phase (extra fuel)

Figure IV-4: *Speed profiles for the different flight phases*

Therefore, when less (or no) extra fuel is allowed, descent is prior than cruise for delay recovery, but when more fuel is appended, cruise phase is involved, as revealed by the *AFP+2%*, *LH+1%* and *LH+2%* flight in Fig. IV-4(d). It is also worth mentioning that the extended cruise distance caused by the steeper descent profile (due to higher descent speed) also accounts for delay recovery, as enlarging cruise phase will keep the flight flying at high altitude and high speed as much as possible.

Summing up, delays can be recovered by means of two contributions: enlarging the cruise phase (retarding the top of descent) and increasing speed in the descent. The specific changes within different flight phases before and after the FCA are summarized in Tables IV-2 and IV-3, respectively. Note that take-off and landing phases (out of the scope of optimization) are fixed in this study.

As presented in Table IV-2, for each of the *LH* flight, nearly 75 kg of fuel are saved during the climb phase, reducing climb distance by 8 nm. Among this saved fuel, 29 kg is allocated to the cruise phase to compensate with that extra 8 nm of cruise distance. In total, the fuel is saved for nearly 48 kg until the FCA, realizing 3 min of delay absorption. As for the rest of the

Table IV-2: *Main parameters for each flight phase before reaching FCAA05.*

Cases	Take-off			Climb				Cruise_1					Total	
	Dist (nm)	Fuel (kg)	Time (min)	Dist (nm)	Fuel (kg)	Time (min)	TAS (kt)	Dist (nm)	Fuel (kg)	Time (min)	TAS (kt)	SR (nm/kg)	Fuel (kg)	Time (min)
AFP/nom	4	176	2	170	1721	25	411	176	895	23	451	0,196	2793	50
LH	4	176	2	162	1646	26	375	184	924	26	431	0,199	2745	53
AFP+1%	4	176	2	171	1725	25	411	175	894	23	451	0,196	2795	50
LH+1%	4	176	2	163	1649	26	376	183	924	26	431	0,198	2749	53
AFP+2%	4	176	2	171	1728	25	411	175	894	23	451	0,196	2798	50
LH+2%	4	176	2	163	1651	26	375	183	926	25	431	0,197	2753	53

Table IV-3: *Main parameters for each flight phase after reaching FCAA05.*

Cases	Cruise_2					Descent				Landing			Total	
	Dist (nm)	Fuel (kg)	Time (min)	TAS (kt)	SR (nm/kg)	Dist (nm)	Fuel (kg)	Time (min)	TAS (kt)	Dist (nm)	Fuel (kg)	Time (min)	Fuel (kg)	Time (min)
AFP/nom	413	2058	55	452	0,201	122	237	20	360	8	80	3	2375	79
LH	426	2114	57	451	0,202	110	228	17	390	8	80	3	2422	77
AFP+1%	427	2114	57	451	0,202	109	229	17	392	8	80	3	2422	77
LH+1%	427	2144	56	454	0,199	108	244	16	403	8	80	3	2468	76
AFP+2%	426	2142	56	455	0,199	109	248	16	404	8	80	3	2469	76
LH+2%	419	2144	55	458	0,196	116	291	17	410	8	80	3	2514	75

trajectory, increases on descent speeds can be found in Table IV-3, if compared with the baseline (*AFP/nom* flight). However, due to the reduction of marginal efficiency, as discussed previously, these increases on descent speeds turn slower after more extra fuel appended, while cruise speeds start increasing, driving down the corresponding specific ranges (SR). It is also interesting to notice that, after the FCA, the *LH* flight (including *LH+1%*) is quite similar to the case of adding every 1% of extra fuel to the *AFP* flight, as shown in Table IV-3.

IV.2.3 Sensitivity of influential factors

The effects of some independent variables to the amount of delay absorption and delay recovery are presented in this section. Table IV-4 shows the relevant variables and their associated ranges considered for this sensitivity study. It can be noticed from Fig. IV-5 that with regards to delay absorption, the differences between various extra fuel are quite small when the allowances lower or equal than 10%. However, this does not imply that the LH time has no relation with the amount of extra fuel included (see the maximum LH that can be realized at certain fuel consumptions in Chapter III).

Table IV-4: *Independent variables in the sensitivity analysis.*

Category	Variables	Baseline	Min	Max	Step	Num
Scenario	City pair distance (nm)	1000	500	2000	20	76
	FCA position (%)	50	25	75	1	51
	AFP delay (min)	10	10	10	-	1
Aircraft	CI (kg/min)	30	5	100	1	96
	Aircraft payload (%)	80	0	100	1	101
	Extra fuel buffer (%)	all	0	unlimited	-	8

For the AFP case, LH is implemented aimed at saving fuel, not realizing the maximum airborne delay, before arriving at the FCA. Therefore, when large amounts of fuel appended, like in the unlimited case (i.e. removing Eq. IV.4 from the optimization), it can be seen that the as-

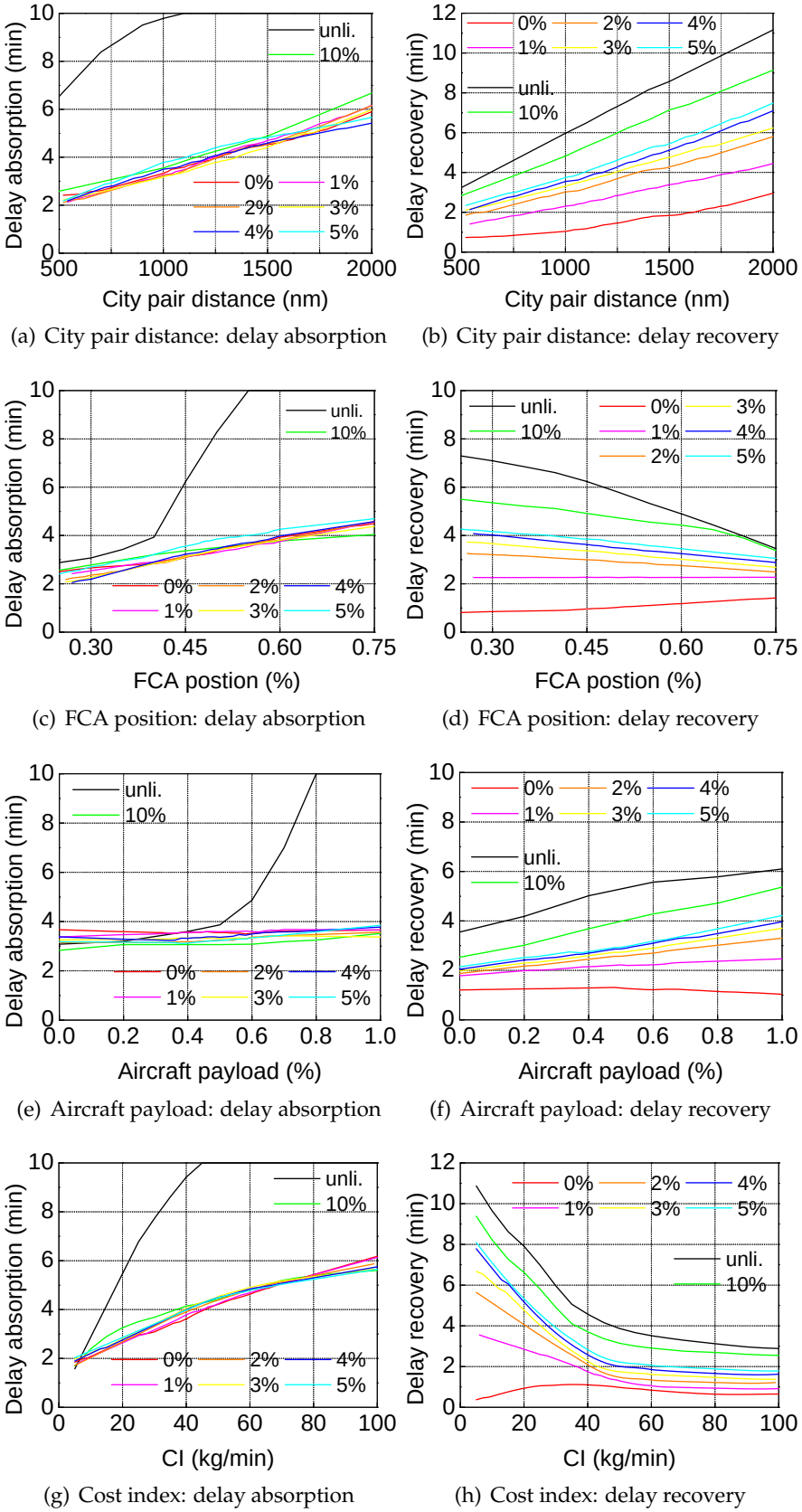

(a) City pair distance: delay absorption (b) City pair distance: delay recovery

(c) FCA position: delay absorption (d) FCA position: delay recovery

(e) Aircraft payload: delay absorption (f) Aircraft payload: delay recovery

(g) Cost index: delay absorption (h) Cost index: delay recovery

Figure IV-5: *Delay absorption and recovery sensitivity when performing LH for different extra fuel allowances*

signed AFP (10 min fixed in the experiments) would be entirely absorbed besides the objective of minimizing arrival time at the destination airport.

On the other hand, notable distinctions on the delay recovery can be observed from Fig. IV-5 as a function of the extra fuel allowed, especially for a remarkable change from 0% to 1%, which indicates the recovery time can be almost doubled (even more in some cases) with only 1% increase of the total fuel consumption. However, keeping adding extra fuel cannot bring always large increase on delay recovery as from 0% to 1% (see for instance the cases ranging from 10% to unlimited fuel allowance), because higher speeds tend to be more fuel-costly (see Fig. III-1), and the maximum operating speed (also dependent on the altitude) is enforced (see Eq. III.4).

Moreover, observing the cases with an extra fuel allowance greater than 10% it can be noticed that even with large amounts of fuel included, the delays that can be recovered are still quite small. Depending on the specific case, the actual extra fuel consumed when setting an unlimited allowance would range approximately from 20% to 30%. All this suggests that accelerating aircraft speed much higher than initially scheduled is not very efficient, in terms of fuel consumption, to recover delays airborne.

Specifically, for the case of 0% extra fuel, the amount of recovered delay (realized after the FCA) is lower than the delay absorbed before the FCA, meaning that the fuel savings from a certain minutes of delay absorption are lower than the extra fuel needed to recover the same amount of delay. Recall the relationships between fuel consumption and flight speed shown in Fig. III-1. As discussed previously, airlines would also consider time-related costs besides the cost of fuel (see Eq. III.1), and thus the initially planned speeds are typically higher than the minimal-fuel speed (see the extreme points in Fig. III-1). Therefore, on the same fuel consumption level, the interval of speed reduction should be much larger than that of increasing speed, which makes recovering delays more difficult than absorbing delays airborne.

- City pair distance

  As shown in Fig. IV-5(a) and IV-5(b), both delay absorption and recovery are positively correlated with the city pair distance. The longer the flight distance, the more time is available to perform LH, and thus the more delay can be absorbed and recovered after passing the FCA. Moreover, LH also proves to be appealing for short-haul flights, as with respect to 500nm distance, the flight can even take-off 2 min earlier with almost 1min delay recovered.

- FCA position

  According to Fig. IV-5(c), the FCA position and the delay absorption are positively correlated regardless of the extra fuel included. However, as the extra fuel increases, the relation with delay recovery turns from positive to negative. Fig. IV-5(d) suggests that if no extra fuel is allowed, a longer distance from departure airport to the FCA is better for delay recovery. On the contrary, when extra fuel included, that distance (with fuel saved) weighs less and less than the other distance that is from the FCA to arrival airport, in terms of delay recovery.

- Aircraft payload

  With aircraft payload increasing, the delay absorption (see Fig. IV-5(e)) remains constant, which is due to the fact that the optimal flight speed is barely affected by aircraft mass, but the fuel consumption is affected notably. Therefore, for each extra fuel allowance the actual amount of added fuel is increasing with payload, which is why the delay recovery is even higher for heavier aircraft (see Fig. IV-5(f)). However, at 0% extra fuel, a slightly decline can be observed. Since the aircraft mass is reducing with the fuel burned along flight distance, a higher payload will leave a heavier aircraft mass for the delay recovery process (after the FCA), consuming more fuel, in such a way the time can be recovered reduces on some level.

- Cost index

  According to the definition of CI (see Sec. II.1.1), the higher the CI, the more importance will be given to the trip time and the faster the optimal flight speed will be. As a result, for higher CI, more speed reduction can be achieved, and thus more delay can be absorbed, as shown in Fig. IV-5(g). Nevertheless, as for the delay recovery, an interesting change can be noticed at no extra fuel allowance, i.e., the maximum delay recovery occurs at CI around 40 kg/min, as shown in Fig. IV-5(h), but when extra fuel included, higher CI leads to even less delay recovered instead.

  When the fuel is limited (e.g., extra fuel at 0%), first increasing CI, from 5 to 40 kg/min, brings a growth on fuel consumption than initially planned, providing more fuel to be saved by LH before the FCA, leading to a higher delay recovery after the FCA. Then, with CI keeping increasing, the initially planned speed (nominal speed) continues increasing too, but the speed in the delay recovery process is approaching the upper bound of maximum operational speed, such that their interval will turn narrow, and thus the delay recovery will reduce. Meanwhile, if extra fuel appended (e.g., 1% to unlimited allowance), the recovery speed can reach up to the maximum no matter how the initial CI changes, such that the delay recovery will always decline following the growth of CI.

IV.3 Neutralize additional unforeseen delays

An analysis presented in (Bilimoria, 2016) raised the problem of additional delays experienced by flights subject to ground holding for GDPs or AFPs. Statistic results obtained from five airports of arrivals suffering the most pre-departure ground holding in 2015 were shown, suggesting that the additional delays of those EDCT (Expect Departure Clearance Time) affected flights were substantially larger in four of the five airports (about two to three times on average) than for arrivals that were not subject to ground holding. Meanwhile, a similar analysis of "double delay" (or "double penalty"), due to the interaction between GDPs and arrival metering (terminal scheduling delays), was given in (Evans & Lee, 2016), providing a deep dive into the underlying causes of those double delays and the circumstances in which they occur in real operations.

IV.3.1 Additional delays subject to ground holding

As seen in Fig. I-3, imagine a flight held on ground due to a GDP/AFP, before being rerouted around a thunderstorm, and then subject to the Miles-in-Trail (MIT) as it passes through a congested sector. The joint impact of all these initiatives together, however, may not be well coordinated and eventual inequities in their implementation may be perceived for the AUs. Under current operations, delays assigned by the GDP/AFP are normally transferred from the area of affected capacity to the departure airport, while imposed entirely on the EDCT, prior to take-off. As a consequence, it is possible that some unnecessary delays may have been performed through the ground holding, before the controlled flight encounters other initiatives yielding delays likewise, which again pushes back its final arrival time.

The above discussions might point to a drawback of ground holding, namely the low flexibility, especially in terms of integrating various Traffic Management Initiatives (TMIs), as reported by (Grabbe *et al.*, 2011; Rebollo & Brinton, 2015). This chapter therefore explores the potential of replacing ground holding with linear holding that is of high flexibility for delay absorption. In this situation, the fuel consumption would keep unchanged while some linear holding is performed in compensation with the reduced ground holding.

It should be noted, however, that this strategy requires an enforcement of arrival times and

therefore only makes sense in the near future scenario, where we could expect accurate 4D navigation and guidance equipment (in line with the TBO concept). Besides, some types of additional delays, such as those associated with gate-departure and taxi-out/in, are being targeted heavily by research and development efforts in (airport) surface management systems. See (Balakrishnan & Jung, 2007; Khadilkar & Balakrishnan, 2014) and the references therein. If one day these delays are well reduced as a result, then part of the motivation for this chapter might disappear. Nevertheless, despite of all the efforts devoted to reduce delays, there will always be uncertainties in the trajectories and this LH strategy shall help to absorb unplanned delays and thus enhance the predictability of flights.

IV.3.2 Reactive trajectory planning

In this section, the initially scheduled flight is regarded as the nominal flight. The Scheduled trajectory filed into a GDP with an EDCT assigned is firstly generated, which is in line with the method introduced for producing the optimal trajectory for the nominal flight, as presented in Sec. III.2. Then, the difference between nominal flight and the one performing entirely ground holding lies only on the timeline, maintaining the remaining 3D trajectory unchanged. Therefore the initially assigned GDP delay could be added directly on the flight's EDCT.

IV.3.2.1 Scheduled trajectory with LH meeting GDP delay at final arrival airport

Let $t^{(1)}_{0,(nom)}$ be the initial time of nominal flight. For the flight performing LH the objective function is switched from Eq. III.1 to Eq.IV.5, in order to minimize ground holding and to leave enough time to neutralize possible additional delays before departure.

$$J = t^{(1)}_0 - t^{(1)}_{0,(nom)} \tag{IV.5}$$

This new optimization problem is subject to the same constraints in generating nominal trajectory, along with the following restrictions:

$$t^{(1)}_0 - t^{(1)}_{0,(nom)} \geq 0 \tag{IV.6}$$

$$t^{(N)}_f = t^{(N)}_{f,(nom)} + \Delta t_{GDP} \tag{IV.7}$$

$$\int_{t^{(1)}_0}^{t^{(N)}_f} FF(t)dt \leq m(t^{(1)}_{0,(nom)}) - m(t^{(N)}_{f,(nom)}) \tag{IV.8}$$

Eq. IV.6 ensures the departure time not earlier than that initially scheduled. Eq. IV.7 specifies that the assigned GDP delay (Δt_{GDP}) is fully realized at the arrival. Eq. IV.8 imposes the maximum fuel consumption allowed, which equals to the amount consumed by the nominal flight, where $m(t^{(1)}_{0,(nom)})$ and $m(t^{(N)}_{f,(nom)})$ are, respectively, the initial and final mass of aircraft (whose difference is the fuel burned on trip).

In this case, the ideal scheduled trajectory performing LH will be generated. If none of the additional (unexpected) delay occurs later, the flight will endure less ground holding but still meet the same arrival slot at the GDP airport exactly as performing an entire ground holding, while consuming no extra fuel.

IV.3.2.2 Actual trajectory after pre-departure additional delays are experienced

After ready for gate-out, assume an additional delay Δt_1 arises in the gate-departure process (see Fig. I-3), followed by another one Δt_2 during taxi-out phase before departure. It should be noted that these delays can be negative, and an airborne holding may be needed if the scheduled LH has reached its maximum (recall Chapter III). However, considering the same situation applies in the context of ground holding only, and assessing the impact of these negative delays are out of the scope of this chapter and are left for future work.

Then, the initially scheduled trajectory can be updated with a new objective function, minimizing the difference between the arrival time and the final time of the ideal scheduled trajectory with LH ($t^{(N)}_{f,(LH)}$):

$$J = t^{(N)}_f - t^{(N)}_{f,(LH)} \tag{IV.9}$$

The same constraints for the nominal flight and Eq. IV.8 apply in such situation, along with the following additional restrictions:

$$t^{(N)}_f - t^{(N)}_{f,(LH)} \geq 0 \tag{IV.10}$$

$$t^{(1)}_0 = t^{(1)}_{0,(LH)} + \Delta t_1 + \Delta t_2 \tag{IV.11}$$

Eq. IV.10 ensures the final arrival time not earlier than the assigned slot at GDP airport, which is $t^{(N)}_{f,(nom)} + \Delta t_{GDP}$, as stated in Eq. IV.7. Eq. IV.11 updates the departure time with regards to the amount of additional delays experienced on ground.

IV.3.2.3 Actual trajectory after post-departure additional delays experienced

When airborne, additional delays Δt_3 may arise (see Fig. I-3); due to TMIs, such as speed instructions to meet MIT restrictions; or air traffic control (ATC) maneuvers, such as path stretching (radar vectoring) for separation purposes, or air holding patterns (usually in a shape of racetrack pattern, involving two turns and two legs, used to keep an aircraft within a prescribed airspace with respect to a geographic fix (FAA, 2016)) to tactically absorb large delays. The effects from each of them to aircraft trajectory may vary substantially, and because flights are typically under real-time control from these TMIs, there is rarely any space for trajectory optimization.

Accordingly, the short flight segment during this phase is regarded as a black box in this chapter, being only time and mass (fuel) discretized by fixed values, while keeping other variables continuous and unchanged.

In this case, the objective function is still as presented in Eq. IV.9, but the initial point of the optimization problem is moved to the phase where this airborne delay occurs (i.e., initial time is defined as $t^{(1)}_{AD}$). In addition, the flown trajectory must also be fixed, along with added constraints below:

$$t^{(1)}_{AD} = t^{(1)}_{AD,(LH,pre)} + \Delta t_3 \tag{IV.12}$$

$$m(t^{(1)}_{AD}) - m(t^{(1)}_{AD,(LH,pre)}) = -FF(t^{(1)}_{AD,(LH,pre)})\Delta t_3 \tag{IV.13}$$

$$\int_{t^{(1)}_{AD}}^{t^{(N)}_f} FF(t)dt \leq m(t^{(1)}_{AD,(LH,pre)}) - m(t^{(N)}_{f,(nom)}) \tag{IV.14}$$

where $t^{(1)}_{AD,(LH,pre)}$ denotes the time when the (unforeseen) airborne delay starts. Eq. IV.12 updates the initial time of optimization with the airborne delay added. Eq. IV.13 deducts the fuel consumed by using current fuel flow multiplied by the delayed time, while Eq. IV.14 specifies that this part of fuel caused from airborne delay is not taken account into the premise that no extra fuel is allowed.

IV.4 Examples to reduce GDP additional delays

In accordance with the flight process, as discussed in Sec. IV.3.2, the computational experiment has been conducted in five main steps:

- Nominal (nom): Initially scheduled flight minimizing direct operating costs (Eq. III.1);
- Step1: Scheduled trajectory filed into a GDP with an EDCT assigned;
- Step2: Scheduled trajectory with LH meeting GDP delay at final arrival;
- Step3: Actual trajectory after pre-departure additional delays experienced; and
- Step4: Actual trajectory after post-departure additional delays experienced.

IV.4.1 Effects for a specific flight

An illustrative example is shown in this section, with results obtained for a specific case study, where a scheduled flight, from ATL (Atlanta) to LGA (LaGuardia) airports with a great circle distance of 662 nm, is captured in a GDP list issued from LGA and assigned with a delay of 40 mins. An Airbus A320 is assumed to execute this flight mission. For the nominal trajectory (scheduled flight) generation, a typical passenger load factor of 81% has been considered (Delgado *et al.*, 2013), along with a CI of 30 kg/min in the FMS.

Some assumptions have been taken: 1) each type of additional delay, is set as a fixed number according to the average statistic value found in (Bilimoria, 2016), i.e., gate-departure: 9 mins, taxi-out: 9 mins, airborne: 7 mins; 2) airborne delay occurs at the middle of the flight distance, and ends at the same place (i.e., at place of 331 nm after departure); 3) no wind conditions are considered; 4) only even flight levels are used (FL260 as the lowest altitude); and 5) cruise step climbs are allowed (if any) with 2000ft steps.

Fig. IV-6(a) plots the vertical trajectory and true airspeed (TAS) versus flight distance for each Step. It can be observed that in order to realize the maximum LH, the best solution is to fly at a lower cruise flight level (FL) than the nominal flight (from FL380 to FL360). In general, as the cruise speed reduces to perform LH (see the TAS of Step2), the optimal flight level decreases, to achieve a higher specific range (lower fuel consumption). However, when pre-departure additional delays are experienced, the required LH is neutralized from the maximum, leading less speed reduction (see the TAS of Step3), and due to the discrete FL allocation scheme (increments of 2000ft), the actual trajectory remains at its initial altitude (FL380).

With regards to climb and descent phases, the lower the speed is, the steeper the climb and the flatter the descent will be, as can be noticed in Fig. IV-6(a). Climb and descent speeds, however, are not continuous in TAS (see Sec. IV.3.2). Instead, they are performed mainly from a continuous ac/deceleration process at low altitudes, a constant CAS climb/descent, followed by a constant Mach climb/descent over the crossover altitude, as shown in Fig. IV-6(b), with the opposite order for climb and descent (see Speed in Table. IV-5).

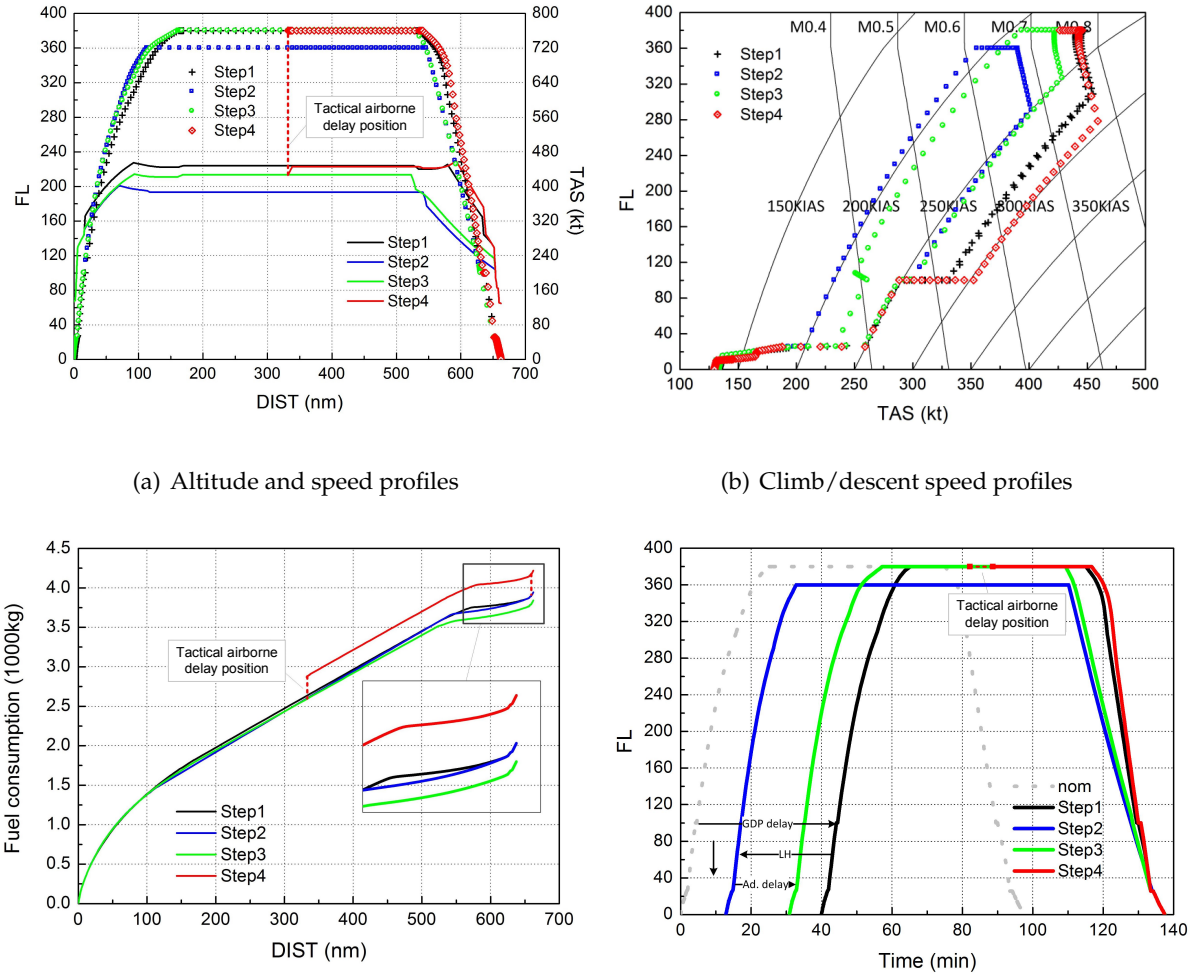

(a) Altitude and speed profiles

(b) Climb/descent speed profiles

(c) Fuel consumption

(d) Vertical trajectory vs. flight time

Figure IV-6: *Resulting aircraft trajectories for each step of the study.*

Through an airborne delay, the required LH continues to decrease, with a speed increase observed (see the TAS for Step4) compared to the Step3 for the remaining trajectory, which is even higher than the nominal, as seen also in Fig. IV-6(b), 305kt than 286kt in constant CAS descent. Nevertheless, recall that in Sec. IV.3 we emphasize that within the margin between the nominal speed and equivalent speed, no extra fuel is allowed (see Fig. III-1), and in Step4, the descent speed seems out of this margin, as shown with 3938 kg in Table. IV-5. This is because before the airborne delay, some fuel has been saved in Step3, and if nothing happens the total fuel consumption will be lower than initially scheduled (see Fig. IV-6(c)), such that it is feasible to have this part of saved fuel consumed for the rest of the flight to maintain a higher speed and still fulfill the total fuel basic constraint.

Fig. IV-6(d) illustrates the changes on flight timeline for the different optimization steps, where we can first observe a parallel shift from nominal flight to Step1 with a length of GDP delay (40 mins). It can be also observed that Step2 departs 27 mins earlier than Step1 (maximum LH) whilst keeping the same arrival time (i.e., the total flight time is extended by 27 mins). However, the total flight time shrinks in Step3 due to the additional pre-departure delays (18 mins). Finally, after an airborne delay lasting 7 mins (see Step4 in Table. IV-5), the arrival time still remains the same. That is to say, the additional delays (25 mins in total) in this case study are entirely recovered at final arrival, and at no extra fuel cost.

Table IV-5: *Summarized key parameters with respect to different flight phases.*

Cases	ATL	Climb				Descent			
	Slot (hh:mm:ss)	Dist (nm)	Speed (kt/kt/M)	Time (min)	Fuel (kg)	Dist (nm)	Speed (M/kt/kt)	Time (min)	Fuel (kg)
nom	**00:00:00**	162,2	250/288/0.77	25,2	1786	127,7	0.77/286/250	22,4	327
Step1	**00:40:00**	162,2	250/288/0.77	25,2	1786	127,7	0.77/286/250	22,4	327
Step2	**00:12:53**	112,7	250/259/0.68	19,9	1467	115,4	0.62/201/201	27,3	273
Step3	**00:30:53**	161,2	250/261/0.74	26,4	1751	132,4	0.69/214/225	28,2	310
Step4	**00:30:53**	161,2	250/261/0.74	26,4	1751	121,4	0.77/306/250	20,8	320

Cases	Criuse				LGA	Total		
	AD Slot (hh:mm:ss)	Dist (nm)	Speed (M)	Time (min)	Fuel (kg)	Slot (hh:mm:ss)	Dist (nm)	Fuel (kg)	Time (min)
nom	**00:47:56**	372,4	0,78	49,9	1831	**01:37:28**	662,2	3945	97,5
Step1	**01:27:56**	372,4	0,78	49,9	1831	**02:17:28**	662,2	3945	97,5
Step2	**00:59:24**	434,2	0,67	77,3	2205	**02:17:28**	662,2	3945	124,6
Step3	**01:21:26**	368,6	0,74	52,0	1779	**02:17:28**	662,2	3840	106,6
Step4	**01:28:26**	379,6	0,78	52,4	1867	**02:17:28**	662,2	3938	99,6

IV.4.2 Range of delay reduction

In order to see how much delay recovery can be realized when having different combinations of pre- and post-departure delays, more computational experiments have been performed in the same scenario, changing the value for each delay. Results are as shown in Fig. IV-7.

Two lengths of GDP delay are considered, 20 mins and 40 mins, where the former is lower than the maximum LH (27 mins) of this particular flight, while the latter higher. Fig. IV-7 shows the actual additional delays experienced at the arrival as a function of pre- and post-departure delays, both of which range from 0 to 20 mins with a step of 1 min. Each color strip represents an interval in 2 mins, and the shaded gray area highlights those combinations where no additional delay is realized (i.e., all recovered).

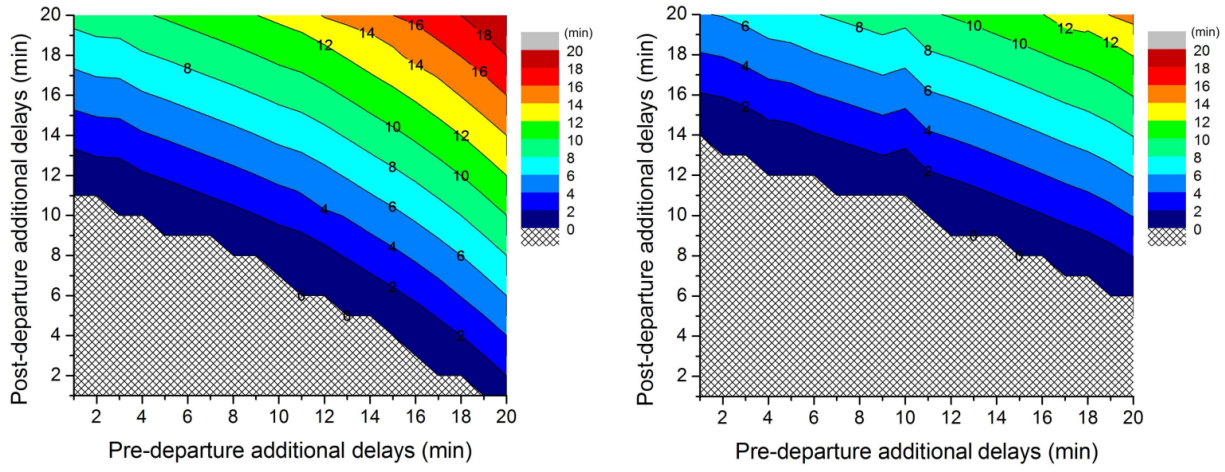

(a) GDP delay of 20 minutes

(b) GDP delay of 40 minutes

Figure IV-7: *Extent of arrival delay finally realized (shown with different color) in response to combinations of pre- and post-departure delays at no extra fuel cost.*

For the GDP delay of 20 mins, since the updated departure time cannot be prior to initially scheduled (see Eq. IV.6), which restrains the effect of an earlier departure time (Step2) enabled by LH to neutralize additional delays, we can see the delay recovery is limited to some extent compared with that in GDP delay of 40 mins (compare Fig. IV-7(a) and IV-7(b)).

In both of the cases, it seems that more delay recovery can be yielded with respect to pre-departure than post-departure delays, because there is obviously more space and time for LH (to adjust speed) during the whole flight, rather than partially after the unforeseen delays are found en route. For the same reason, the contour lines turn to be flatter in areas where high post-departure and low pre-departure delays occur, if compared to the opposite areas within the same stripe of additional delays.

Finally, it is worth noting some non-smooth segments on the contour lines, where the pre-departure delay equals to 3 mins and 10 mins in Figs. IV-7(a) and IV-7(b), respectively. Recall again the trade-offs between fuel consumption and flight time shown in Fig. III-1. Any LH lower than the maximum contributes to saving some fuel. Therefore, when a specific LH is performed at the same time having the minimum fuel consumed, the saved fuel can be burned at the most to increase flight speed after airborne delays, in such a way to trade for a higher delay recovery.

IV.5 Chapter summary

Aiming at the forthcoming TBO paradigm, a method was presented in this chapter to introduce linear holding to partially absorb ATFM delays due to AFPs. It is shown how some fuel can be saved before reaching the congested airspace, which can be allocated to recover delay once this constrained area is overflown. It is worth noting that the implementation is focused on the pre-tactical operations, enhancing the efficiency of each individual flight (trajectory) planning. Results suggest that using the proposed method could partially recover part of the AFP delay, even with no extra fuel allowances (e.g., reducing 3.3 min of ground delay and 1.7 min of arrival delay for a typical short-haul flight). When extra fuel is allowed, however, the maximum delay recovery increases up to 10 min for the studied case, which also proves to be more cost-efficient than current operations, when flight speed is increased after experiencing all delay on ground.

Fuel consumption accounts for the largest part of airline operating costs, and also generates greenhouse gas emissions bringing adverse environmental issues, which makes it one of the major drivers of current research efforts in air transportation. Results show that, without extra fuel consumption, the delay assigned in an AFP could be partially absorbed and, eventually, recovered. Even small amounts of them per flight will become significant when considering the cumulative effect for numerous AFP delayed flights: according to statistics data published in (FAA, 2017), there have been 79 AFPs at annual average issued in the NAS for the past 5 years, and the number is still growing, with 177 in 2015 year and 208 in 2016 year. Results also indicate that if some extra fuel consumption is allowed, performing linear holding still presents some cost-efficiency benefits than simply increasing flight speed after enduring all the delay on ground.

In addition, another potential applicability of linear holding was proposed to neutralize the additional delays due to uncertainty in the execution phase of the flight. Illustrative examples were given in a scenario of the NAS in the United States, particularly with the GDPs which are one of the most sophisticated ATFM protocols currently in use. But the usability of the proposed strategy should not be limited in the examples as such, given that the essentials of additional delays (i.e., uncertainties) might apply for any ATFM scenario and the linear holding could always help to enhance the traffic flow predictability and thus, lower the uncertainties.

In this application, through multiple stages of optimal trajectory generation, linear holding was enabled to be implemented along the whole flight phases, and adjusted flexibly in response

to different kinds of TMIs and the amounts of unforeseen delays they produce. Compared to the case where ground holding is fully endured followed by burning more fuel to increase flight speed to partially recover delays (as usually done nowadays for some airlines), the proposed strategy in this chapter can reduce the additional delays without consuming any extra fuel than initially scheduled. Results suggest that additional delays of 25 mins in a typical case study can be totally recovered at no extra fuel cost. A notable extent of delay reduction observed from the computational experiments further supports the benefits for reducing different combinations of additional delays without consuming extra fuel.

It is impossible to escape the impression that people commonly use false standards of measurement - that they seek power, success and wealth for themselves and admire them in others, and that they underestimate what is of true value in life.

— Sigmund Freud

V

Network ATFM model incorporating linear holding

This chapter introduces a strategy to include linear holding into air traffic flow management (ATFM) initiatives, together with the commonly-used ground holding and airborne holding measures. In this way, flow management performance can be improved when handling delay assignment with uncertainty events. Firstly, a trajectory generation method is adopted, aiming at computing, per flight, the maximum linear holding realizable using the same fuel as the original nominal flight. This information is assumed to be computed and shared by the different airspace users (AUs) and it is then used to build a network ATFM model to optimally assign delays, in the scope of trajectory based operations (TBO). Hence, the best distribution of delay is optimized at given positions along the flight trajectory (combining the three holding practices together) and taking into account the cost of delay, especially in the fuel consumption. The problem is formulated as a mixed integer linear program (MILP) and solved with a commercial off-the-shelf solver. An illustrative example is given, showing that under the circumstance of capacity recovered ahead of schedule, including linear holding contributes to a notable delay reduction compared to the case where only ground and airborne holding apply.

V.1 Network model and AUs participation

A network ATFM model is proposed in this section, which assigns delays at designed positions. Ground and airborne holdings remain the default measure for delay absorption, while linear holding is possible for those AUs willing to participate in the ATFM delay assignment, by generating

and sharing certain information with the Network Manager (NM) to aid in an outlined Collaborative Decision-Making (CDM) process.

V.1.1 Problem statement

Under existing ATFM network models (see (Bertsimas & Patterson, 1998) and the references therein), delays could be assigned to flights by means of ground or airborne holding. Airborne holding, however, tends to be less preferred (especially when a long-time delay occurs) because of its higher fuel costs (and potential safety issues) as has been discussed in Sec. II.1.1.

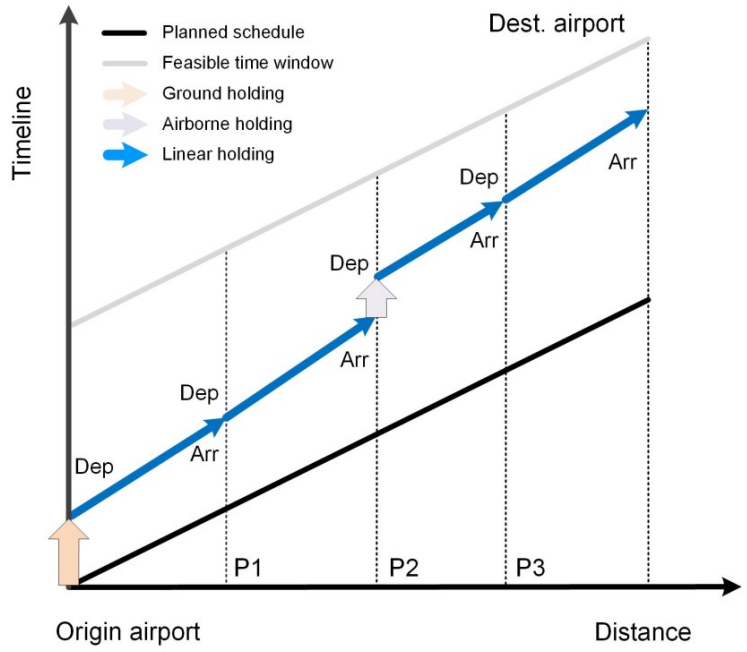

Figure V-1: *Characteristics of ground, airborne and linear holding in the ATFM network model proposed in terms of flight time versus distance.*

In the model proposed in this chapter, we maintain the above two holding practices, but add the linear holding (LH) option. Nevertheless, aiming at differentiating the proposed LH with typical airborne holding, the delay assignment is conducted at specific designed "positions" along the scheduled trajectory, by using the concept of Controlled Time of Arrival (CTA) and Controlled Time of Departure (CTD) at each position. Accordingly, the decision variables of the model are defined as follows:

$$x^j_{f,t} = \begin{cases} 1, & \text{if flight } f \text{ departs from the position } j \text{ by time } t \\ 0, & \text{otherwise} \end{cases}$$

$$y^j_{f,t} = \begin{cases} 1, & \text{if flight } f \text{ arrives at the position } j \text{ by time } t \\ 0, & \text{otherwise} \end{cases}$$

Note that the "by" time is used, rather than "at" as the decision variables in this chapter, which would enable a faster solution searching time according to (Bertsimas & Patterson, 1998), while the "at" time can be derived by $(x^j_{f,t} - x^j_{f,t-1})$ and $(y^j_{f,t} - y^j_{f,t-1})$ respectively. To enforce that only one time slot will be assigned to one flight at each designed position, within a prescribed feasible window T^j_f, it has to satisfy:

$$\sum_{t\in T_f^j}(x_{f,t}^j - x_{f,t-1}^j) = 1, \quad \sum_{t\in T_f^j}(y_{f,t}^j - y_{f,t-1}^j) = 1 \tag{V.1}$$

However, when using the "by" time, this constraint can be simplified as to $x_{f,\overline{T}_f^j} = 1$, $y_{f,\overline{T}_f^j} = 1$, and $x_{f,\underline{T}_f^j-1} = 0$, $y_{f,\underline{T}_f^j-1} = 0$, where $\underline{T}_f^j$ and $\overline{T}_f^j$ are respectively the lower and upper bound of the feasible solution, namely $[\underline{T}_f^j, \overline{T}_f^j] = T_f^j$.

Fig. V-1 shows schematically flight time versus distance and the three types of holding strategies: ground holding is performed only at the origin airport; airborne holding can only be performed "at" a given position (the difference between the "departure" and "arrival" time at that position equals to the holding time); and since LH is performed by flying slower, the slope of the lines is increased if compared with the planned schedule.

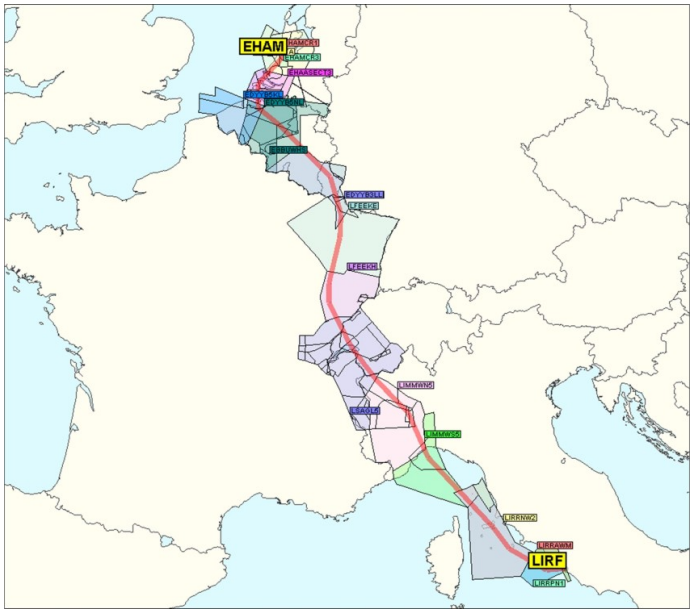

Figure V-2: *An example of a scheduled 3D trajectory from LIRF to EHAM airports, which traverses multiple contiguous sectors. (Source: Eurocontrol's NEST modelling tool)*

Recall that we distinguish the typical airborne holding from LH by the fact that when performing the former, the actual flight distance will be extended (either by vectoring or using holding patterns). This flight path "stretching", however, does not contribute to the execution of trajectory defined by each contiguous point. Thus, the typical airborne holding, on some level, can be seen as a "circling" at a particular position.

It is also worth noting that the "positions" referred here (such as P1, P2 and P3 in Fig. V-1) may not correspond to the actual geographical waypoints existing in current airspace. The model in this chapter defines entrance and exit positions at each elementary sector that the controlled flight is scheduled to traverse (as well as the two representing origin and destination airports respectively, as shown in Fig. V-2), in such a way that the traffic demand of each sector and airport (for departure and arrival) during different time periods can be managed under capacity constraints. In addition, the feasible time window shown in Fig. V-1 defines a solution space based on the flight schedule, which will largely reduce the number of variables taken into optimization, and that in turn can be further discretized to prescribed time steps.

Table V-1: *Flight route extracted from current planning information.*

Enter Time	Airport	Elementary Sector	Flight level	Crossed Duration	Exit Time
-	LIRF	-	0	0:00:00	7:59:00
8:00:36	-	LIRRPN1	35	0:06:42	8:07:18
8:08:10	-	LIRRNW2	208	0:06:08	8:14:18
8:14:18	-	LIRRNW3	284	0:01:50	8:16:08
8:16:08	-	LIRRNW4	304	0:03:01	8:19:09
8:19:09	-	LIRRNW5	334	0:05:48	8:24:57
8:24:57	-	LIMMWS5	360	0:08:47	8:33:44
8:33:44	-	LIMMWN5	360	0:14:14	8:47:58
8:47:58	-	LSAGL5	360	0:11:31	8:59:29
8:59:29	-	LFEEKH	360	0:07:21	9:06:50
9:06:50	-	LFEEKE	360	0:07:54	9:14:44
9:14:44	-	EDYYB3LH	360	0:09:03	9:23:47
9:23:47	-	EDYYB3LL	335	0:05:40	9:29:27
9:29:27	-	EDYYB5NL	300	0:08:41	9:38:08
9:39:47	-	EHAASECT3	230	0:07:23	9:47:10
9:47:10	-	EHAMTA	85	0:04:26	9:51:36
9:52:18	-	EHAMCR1	28	0:03:22	9:55:40
9:55:40	EHAM	-	0	0:00:00	-

V.1.2 Participation of AUs in the ATFM process

As indicated in Sec. III, the amount of delay absorption that LH can realize is constrained by the fuel consumption, which again is dependent on the aircraft type, take-off mass, flight distance, etc. Thus, from the ATFM perspective, considering all these data would be a daunting task. Moreover, some of the AUs' information is proprietary, such as aircraft mass and fuel consumption figures, which is normally not publicly accessible. From the AUs' perspective, however, they could have a clear view of all the information of their own flights, and thus have an intimate knowledge of the capability of each particular flight to absorb delays airborne.

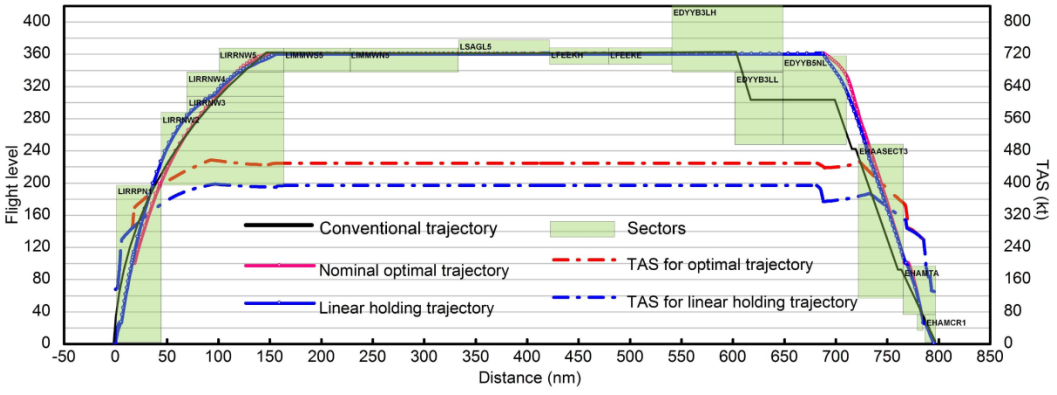

Figure V-3: *Vertical and speed profiles of the nominal and LH trajectories traversing the scheduled contiguous sectors.*

Consequently, aiming at including the proposed LH into delay assignment, the ATFM model in this chapter requires (only) one more input from AUs than those models found in the literature: the maximum LH bound per flight, along the planned trajectory. Given the procedure in practice,

as a matter of fact, the NM currently offers a high level of flexibility to AUs for flight planning (Bolić *et al.*, 2017). In addition, in case that no data for this input is provided, the model could still work by setting the default value for LH to zero.

Table V-2: *Nominal and LH trajectories flight planning information.*

Position	Nominal optimal trajectory							
	Enter Position		Exit Position		Crossed Segment			
	Dist (nm)	Time (h:m:s)	Dist (nm)	Time (h:m:s)	Len (nm)	Duration. (m:s)	Fuel (kg)	LH (min)
LIRF	-	-	0	7:59:00	-	-	-	-
LIRRPN1	2	7:59:50	46	8:07:53	44	08:03	778	-
LIRRNW2	48	8:08:28	80	8:13:06	32	04:38	333	-
LIRRNW3	80	8:13:06	98	8:15:14	18	02:08	136	-
LIRRNW4	98	8:15:14	115	8:17:34	17	02:20	135	-
LIRRNW5	115	8:17:34	165	8:24:26	50	06:52	311	-
LIMMWS5	165	8:24:26	229	8:32:43	64	08:17	322	-
LIMMWN5	229	8:32:43	334	8:46:54	105	14:11	549	-
LSAGL5	334	8:46:54	423	8:58:33	89	11:39	447	-
LFEEKH	423	8:58:33	479	9:05:46	56	07:13	276	-
LFEEKE	479	9:05:46	538	9:14:10	59	08:24	320	-
EDYYB3LH	538	9:14:10	649	9:28:36	111	14:26	546	-
EDYYB5NL	692	9:34:38	708	9:36:49	16	02:11	59	-
EHAASECT3	729	9:39:42	763	9:44:41	34	04:59	34	-
EHAMTA	774	9:46:25	786	9:51:44	12	05:19	35	-
EHAMCR1	786	9:51:44	796	9:55:28	10	03:44	85	-
EHAM	796	9:55:28	-	-	-	-	4366	-
Position	**Linear holding trajectory**							
	Enter Position		Exit Position		Crossed Segment			
	Dist (nm)	Time (h:m:s)	Dist (nm)	Time (h:m:s)	Len (nm)	Duration. (m:s)	Fuel (kg)	LH (min)
LIRF	-	-	0	7:59:00	-	-	-	-
LIRRPN1	2	7:59:50	44	8:08:01	42	08:11	760	0,13
LIRRNW2	48	8:08:42	70	8:12:53	22	04:11	258	-0,45
LIRRNW3	70	8:12:53	87	8:14:59	17	02:06	105	-0,03
LIRRNW4	87	8:14:59	115	8:19:26	28	04:27	208	2,12
LIRRNW5	115	8:19:26	165	8:27:03	50	07:37	311	0,75
LIMMWS5	165	8:27:03	229	8:37:45	64	10:42	322	2,42
LIMMWN5	229	8:37:45	334	8:56:05	105	18:20	549	4,15
LSAGL5	334	8:56:05	423	9:12:21	89	16:16	493	4,62
LFEEKH	423	9:12:21	479	9:21:29	56	09:08	276	1,92
LFEEKE	479	9:21:29	538	9:30:37	59	09:08	275	0,73
EDYYB3LH	538	9:30:37	649	9:50:23	111	19:46	567	5,33
EDYYB5NL	684	9:56:48	708	10:00:39	24	03:51	71	1,67
EHAASECT3	727	10:03:50	763	10:10:13	36	06:23	46	1,40
EHAMTA	773	10:11:26	786	10:17:09	13	05:43	39	0,40
EHAMCR1	786	10:17:09	796	10:20:52	10	03:43	85	-0,02
EHAM	796	10:20:52	-	-	-	-	4366	25,13

Let us first take a look at what could be found from current flight planning information, as provided by the demand data repository v2 (DDR2) published by Eurocontrol. Table V-1 presents the detailed information obtained for a specific flight scheduled from Rome Fiumicino Airport (LIRF) to Amsterdam Schiphol Airport (EHAM) shown in Fig. V-2. These data include "enter time", "exit time", "crossed duration" and "altitude" at each of the sectors (and airports) the aircraft is scheduled to fly, which correspond to the designed "positions" (sector boundaries and airports) used in our model.

Based on the planned vertical profile found in DDR2, the nominal optimal trajectory has been reconstructed, on one hand, using the trajectory optimization methodology described in Sec. III.2 (see the red line in Fig. V-3). On the other hand, the blue line in the figure represents the same flight when performing the maximum amount of LH (recall Chapter III), while incurring the same

fuel consumption, during every single flight segment (i.e., each discretized flight phase, as shown in Fig. III-6, in accordance with typical ATM regulations) in the trajectory optimization. Fig. V-3 also shows the true airspeed (TAS) of both trajectories, where the airborne delay generation by means of LH can be easily seen.

Table V-2 summarizes the trajectories of Fig. V-3 in form of the current flight planning information (as Table V-1), but is added with a "LH time" bound (see the rightmost column), which equals to the difference of crossed duration between the nominal trajectory and the LH trajectory (negative values appear in climb/descent because of the slight differences on the trajectory caused from speed changes), and that is the one that should be provided (by AUs) to the NM. It is worth noting that, the crossed segment shown in Table V-2 represents the distance flown between the entry and exit of a particular sector, which differs from the flight segment mentioned above incurring the same fuel between the nominal and LH trajectories, and thus there appear some slight differences in fuel. Still, they should be similar and at the end of the trajectory always be the same with respect to the total fuel burns.

V.1.3 Model formulation

The network ATFM model with the above presented AU-enabled LH is formulated in the following section. As mentioned before, the overall framework of the model is based on the widely-studied Bertsimas and Stock-Patterson model (Bertsimas & Patterson, 1998).

V.1.3.1 Objective function

In this model, the cost of the total delay (TD) is minimized including the costs consequence of ground holding (GH), airborne holding (AH) and linear holding (LH):

$$\min(cost_{TD}) = \min(GH + \alpha AH + \beta LH), \tag{V.2}$$

where α and β are the cost weighting factors. Since $TD = GH + AH + LH$, we can substitute LH in (V.2), yielding to:

$$\min(cost_{TD}) = \min[\beta TD + (\alpha - \beta)AH + (1 - \beta)GH)]. \tag{V.3}$$

Taking into account the fairness of delay assignment, as discussed in (Bertsimas & Gupta, 2015), the total delay can be multiplied by a coefficient $c_f = (t - r_f^a)^{1+\epsilon}, \epsilon > 0$ in (V.3). In this way, delays will be assigned moderately across all the flights, instead of unevenly to one particular flight. Accordingly, the objective function can be arranged as:

$$\min \sum_{f \in F} [\beta c_f h_f + (\alpha - \beta) a_f + (1 - \beta) g_f],$$

$$c_f h_f = \sum_{t \in T_f^a, P(f, n_f) = a} (t - r_f^a)^{1+\epsilon} (y_{f,t}^a - y_{f,t-1}^a),$$

$$a_f = \sum_{t \in T_f^w, w \in P(f,i): 1 < i < n_f} t(x_{f,t}^w - x_{f,t-1}^w - y_{f,t}^w + y_{f,t-1}^w),$$

$$g_f = \sum_{t \in T_f^a, P(f,1) = a} (t - r_f^a)(x_{f,t}^a - x_{f,t-1}^a). \tag{V.4}$$

The constraints of this model can be grouped into flight operations, network capacities, decision variables and delay updates, as presented in each subsection below. It is worth noting that, for updating the delay (assignment), different from state-of-the-art stochastic dynamic models (see for instance (Mukherjee & Hansen, 2007)), full deterministic information (e.g., weather forecast) is assumed in this chapter, such that it is feasible to realize the dynamic updating by re-executing the model (by means of further including specific constraints, i.e., Constraints V.15, V.16, V.17 and V.18).

V.1.3.2 Flight operations constraints

$$x^j_{f,t} - x^j_{f,t-1} \geq 0 \quad \forall f \in F, \forall j \in P_f, \forall t \in T^j_f, \tag{V.5}$$

$$y^j_{f,t} - y^j_{f,t-1} \geq 0 \quad \forall f \in F, \forall j \in P_f, \forall t \in T^j_f, \tag{V.6}$$

$$x^j_{f,t} - y^j_{f,t} \leq 0 \quad \forall f \in F, \forall w \in W, \forall t \in T^w_f, \tag{V.7}$$

$$y^{j'}_{f,t'} - x^j_{f,t} \leq 0 \quad \forall f \in F, \forall i \in [1, n_f - 1], P(f,i) = j, P(f,i+1) = j', \\ \forall t \in T^j_f, t' = t + z^{j,j'}_f, \tag{V.8}$$

$$y^{j'}_{f,t'} - x^j_{f,t} \geq 0 \quad \forall f \in F, \forall i \in [1, n_f - 1], P(f,i) = j, P(f,i+1) = j', \\ \forall t \in T^j_f, \forall t' \in T^{j'}_f, t' = t + z^{j,j'}_f + v^{j,j'}_f. \tag{V.9}$$

Constraints (V.5) and (V.6) ensure that each flight f is assigned with only one slot, from the predefined feasible time window T^j_f (see Sec. V.1.1), for departing and arriving, respectively, at position j. Constraint (V.7) imposes a maximum airborne holding time u^w at each designed position. Constraint (V.8) enforces that LH to be non-negative (i.e., flying faster than initially planned is not considered for delay assignment in this model). This is because, as discussed in Sec. III, the on-board flight management system could help AUs to optimize the aircraft trajectories by setting the CI input, which reflects AUs preferences (or trade-offs) on speed and fuel burns when planning their flights, and thus these initially scheduled speeds, should already be the highest that are favored by AUs. Constraint (V.9) stipulate that the LH performed between two contiguous positions of flight f should not exceed the maximum LH bound $v^{j,j'}_f$, which is provided by AUs and that is set by 0 as default if such information is not provided.

V.1.3.3 Network capacity constraints

$$\sum_{f \in F: P(f,1) = a} \sum_{t \in T^a_f \cap T(\tau)} (x^a_{f,t} - x^a_{f,t-1}) \leq C^a_{dep}(\tau) \quad \forall a \in A, \forall \tau \in \mathcal{T}, \tag{V.10}$$

$$\sum_{f \in F: P(f,n_f) = a} \sum_{t \in T^a_f \cap T(\tau)} (y^a_{f,t} - y^a_{f,t-1}) \leq C^a_{arr}(\tau) \quad \forall a \in A, \forall \tau \in \mathcal{T}, \tag{V.11}$$

$$\sum_{f\in F:P(f,i)=w,i\in[1,n_f-1]}\ \sum_{t\in T_f^w\cap T(\tau)}(x_{f,t}^w-x_{f,t-1}^w)\le C_{sec}^s(\tau)\quad\forall w\in s\subset S,\forall\tau\in\mathcal{T}. \tag{V.12}$$

Constraints (V.10), (V.11) and (V.12) ensure that the traffic demand would not exceed the capacity of departure airport, arrival airport and en route sectors, respectively. It is worth noting that the flight performing airborne holding in this model is counted within the boundary of its current sector (i.e., before departing the position). Since the capacity values are all defined within a period of time window, they are capable of being modified following the changes of the network environment, such as the improvement of weather conditions or traffic situations.

V.1.3.4 Constraints on decision variables

$$x_{f,t}^j\in 0,1\quad\forall f\in F,\forall j\in P_f,\forall t\in T_f^j, \tag{V.13}$$

$$y_{f,t}^j\in 0,1\quad\forall f\in F,\forall j\in P_f,\forall t\in T_f^j. \tag{V.14}$$

Constraints (V.13) and (V.14) state that the decision variables of the model are binary.

Above all, the model can be modified to perform the iterative delay assignment. Assume at the start of the $(\tau+1)$ th time period, i.e., $t_{(\tau+1)}$, the capacity changes from current status of the time period of $T(\tau')$, and requires for another round of delay assignment. We could simply fix part of the decision variables based on the current results, and optimize the rest of them in the next round of delay assignment. However, as previously mentioned, full deterministic information is assumed in this study with respect to capacity updates, for specifically tactical ATFM scenario, which may cause the model to run the risk of failure as the uncertainty grows if applied to a strategic stage.

V.1.3.5 Constraints from updating assignment

$$x_{f,t}^j(\tau+1)=y_{f,t}^j(\tau+1)=1\quad\forall f\in F,\forall j\in P_f,CTD_f^j(\tau)<t_{(\tau+1)},t=CTD_f^j(\tau), \tag{V.15}$$

$$x_{f,t}^j(\tau+1)=y_{f,t}^j(\tau+1)=0\quad\forall f\in F,\forall j\in P_f,CTD_f^j(\tau)<t_{(\tau+1)},t=CTD_f^j(\tau)-1, \tag{V.16}$$

$$\begin{aligned}x_{f,t}^j(\tau+1)=y_{f,t}^j(\tau+1)=1\quad\forall f\in F,\forall j\in P_f,\forall i\in[1,n_f-1],P(f,i)=j,\\ P(f,i+1)=j',CTD_f^j(\tau)\ge t_{(\tau+1)},CTD_f^{j'}(\tau)<t_{(\tau+1)},t=CTD_f^j(\tau),\end{aligned} \tag{V.17}$$

$$\begin{aligned}x_{f,t}^j(\tau+1)=y_{f,t}^j(\tau+1)=0\quad\forall f\in F,\forall j\in P_f,\forall i\in[1,n_f-1],P(f,i)=j,\\ P(f,i+1)=j',CTD_f^j(\tau)\ge t_{(\tau+1)},CTD_f^{j'}(\tau)<t_{(\tau+1)},t=CTD_f^j(\tau)-1.\end{aligned} \tag{V.18}$$

Constraints (V.15) and (V.16) enforce that values, prior to time $t_{(\tau+1)}$, of the decision variables ($x_{f,t}^j(\tau')$ and $y_{f,t}^j(\tau')$) derived from the first round of optimization should be assigned to those new

decision variables ($x^j_{f,t}(\tau'+1)$ and $y^j_{f,t}(\tau'+1)$) defined in the same domains (f, j and t). t_1 means the initial time of T, while $t_{(\tau+1)}$ represents the initial time defined in the $(\tau+1)$th time period $T(\tau'+1)$.

Constraints (V.17) and (V.18) stipulate that for specifically the flights in the air at time $t_{(\tau+1)}$, the new decision variables subject to the second round of optimization must start from the next position after finishing their current flight segment linked by (j, j'). This is because the remaining distance within the segment might be not long enough to realize the amount of LH previously provided by AUs, which, however, is based on the calculation by en entire segment. $t^j_f(\tau')$ and $t^{j'}_f(\tau')$ are the last assigned departure times for flight f.

V.2 Case study in single-airport setting

An illustrative example of the methodology introduced in this chapter is presented in this section. As stated in (Bertsimas & Gupta, 2015), network formulations present significant challenges in computational tractability, while some studies have focused exclusively on addressing the computational challenges of the network problem (see (Rios & Ross, 2010) for instance). Yet, given the fact that the main objective of this chapter is to primarily reveal the effects of including the linear holding practice in ATFM delay assignment, more than improving the model computational performance, we have taken firstly a small sample from the experiments to illustrate the collaborative delay handling process introduced in Sec. V.1. Some additional experimental materials to assess the computational complexity of the problem are provided in Appendix B. GAMS has been used as the modeling tool and Xpress v23.01 optimizer bundled into the GAMS suite has been used as the solver.

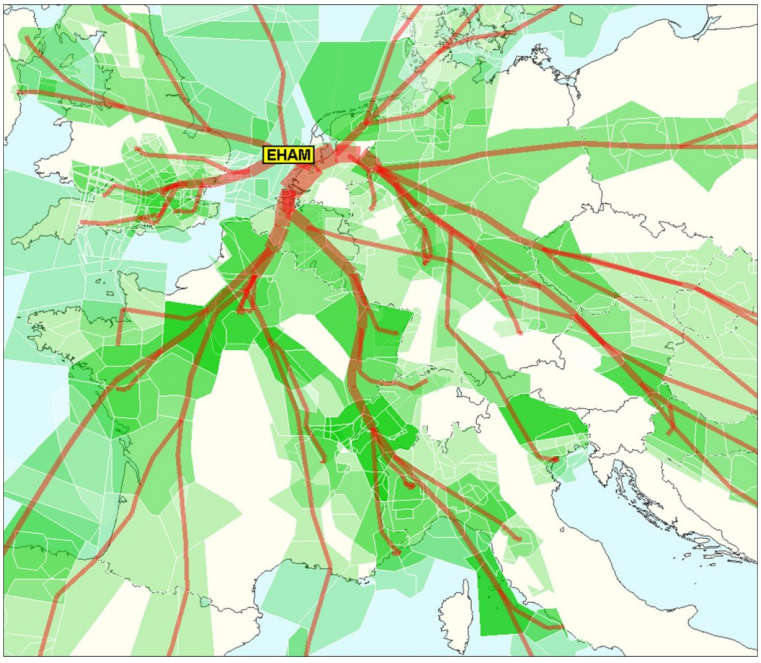

Figure V-4: *Network ATFM scenario in the computational experiments with single-airport setting. (Source: Eurocontrol's NEST modelling tool).*

V.2.1 Case of study setup

As shown in Fig. V-4, the data sample chosen for this illustrative example involve 156 flights (red lines) heading towards EHAM airport (yellow label) traversing 1121 elementary sectors (green polygons), with both Estimated Times of Arrival and Estimated Times of Off Block scheduled within the period from 6 AM to 12 AM on October 24, 2016. Initial flight schedules and elementary sector crossings have been taken from the DDR2.

The sectors considered in this chapter to define the control "positions" are elementary sectors, which could be combined in realistic operations with other elementary sector(s) and become a collapsed sector during different time period. Therefore, it is needed to obtain a table capturing, for each time period, the traversed sector's detailed form (i.e., elementary sector itself or collapsed sector it constructs) and the particular form's associated capacity in that time. Specifically, if it is a collapsed sector that contains several elementary sectors, then only the first entered elementary sector (where a control position is defined) for the flight will be counted as one traffic demand of that collapsed sector, and the remaining entires (in the same collapsed sector) will be regarded as internal movement. A general procedure of obtaining this information about sectors' opening scheme and associated capacity is attached in the Appendix C, and some examples can be seen in Table V-3.

Table V-3: *Examples of sector opening scheme and capacity values.*

Elementary sector	Initial time	End time	Sector configuration	Capacity
LFMMLE	10:00	10:20	LFMMMALY	38
LFEEYR	10:00	10:20	LFEEHYR	38
LFMMLS	10:00	10:20	LFMMMALY	38
Elementary sector	**Initial time**	**End time**	**Sector configuration**	**Capacity**
LFMMLE	10:20	10:40	LFMMLYO	44
LFEEYR	10:20	10:40	LFEEHYR	38
LFMMLS	10:20	10:40	LFMMLYO	44
Elementary sector	**Initial time**	**End time**	**Sector configuration**	**Capacity**
LFMMLE	10:40	11:00	LFMMLYO	44
LFEEYR	10:40	11:00	LFEE5R	42
LFMMLS	10:40	11:00	LFMMLYO	44

For the initial delay assignment, we assume four hot spots: EHAM airport and sectors EDDDALL1, LFEEKHRZIU and LFEEEUXE; where the demand exceeds the capacity during the studied period. Furthermore, we have also considered a situation where an early capacity recovery occurs at 9 AM, well before scheduled (12 AM), for the above four hot spots, which leads to an update of the delay assignment. It is assumed that updating can be initiated at once while flights can receive and immediately executed the latest delay assignment.

Some other key assumptions have been taken in the computation: 1) the discrete time interval is set to 1 min; 2) $\epsilon = 0.05$ is selected as the fairness factor; 3) the cost weights for airborne holding and linear holding are, respectively, $\alpha = 1.2$ and $\beta = 0.8$ with regards to the ground holding; 4) the LH time bound is approximated as 20% of the planned total trip time based on the statistical average value derived from previous work in Chapter III, if not otherwise specified, and are all shared by AUs to the NM; and 5) there are no separation violations or constraints due to other aircraft in the traffic flow.

V.2.2 Results of the delay assignment

Figures V-5(a) and V-5(b) show how in the initial process of delay assignment (i.e., the results generated in the first round of the model execution), part of the ground holding (and airborne holding) is replaced by LH. Referring to Table V-4, we can see the total delay has a reduction of 120 minutes after this replacement. This is because, including LH means that more space and periods can be used to absorb delays, rather than only at the departure airports prior to take-off. As a consequence, if multiple node constraints occur at the same time, separating delays at different places and periods would contribute to reducing the minimum delay required from multiple constraints. Moreover, we can also notice that more flights are included to share the reduced total delay, leading to an even lower average delay for each flight (see Table V-4).

In this particular example, four cases of the study are considered, as listed below:

- Case-A: Initial delay assignment with no LH
- Case-B: Initial delay assignment by using LH
- Case-C: Updated delay assignment with no LH
- Case-D: Updated delay assignment by using LH

Table V-4: *Summarized results for the four cases of study.*

Cases	Total delay (min)	Delayed flights (a/c)	Av. total delay (min)	Total AH (min)	Total GH (min)
Case-A	2421	86	28,15	3	2418
Case-B	2301	97	23,72	1	1681
Case-C	1369	66	20,74	2	1367
Case-D	499	38	13,13	0	370
Cases	**GH flights (a/c)**	**Av. GH (min)**	**Total LH (min)**	**LH flights (a/c)**	**Av.LH (min)**
Case-A	86	28,12	0	0	-
Case-B	72	23,35	619	96	6,45
Case-C	66	20,71	0	0	-
Case-D	27	13,70	129	24	5,38

Figures V-5(c) and V-5(d) illustrate the case when the early capacity recovery occurs (i.e., results yielded in the second round of model execution), assuming that the new round of ATFM delay assignment starts immediately after this recovery. It is also assumed that, the flights that have not been serving the ground holding, or have been holding on the ground partway, can request for an immediate departure, and thus, have their delays (partially) recovered, as revealed by results shown in Fig. V-5(c).

When implementing LH, however, the remaining total delay reduces remarkably once the delay assignment is updated (see Fig. V-5(d)). There are two main reasons that could account for these promising results. First, benefiting from the shortening of ground holding, the departure time of one flight can be advanced. Once the delay is updated, less ground holding, and thus less total delay will be realized, as exactly is the case shown in Fig. V-5(c). Since most of the flights are observed to substitute part of the ground holding by LH (see Table V-4), the effects can be enlarged notably. The second reason is because the flexibility of LH compared to the ground holding in terms of delay absorption, as mentioned previously in Sec. II.1.1. Regarding this feature, a detailed analysis is given in next section V.2.3.

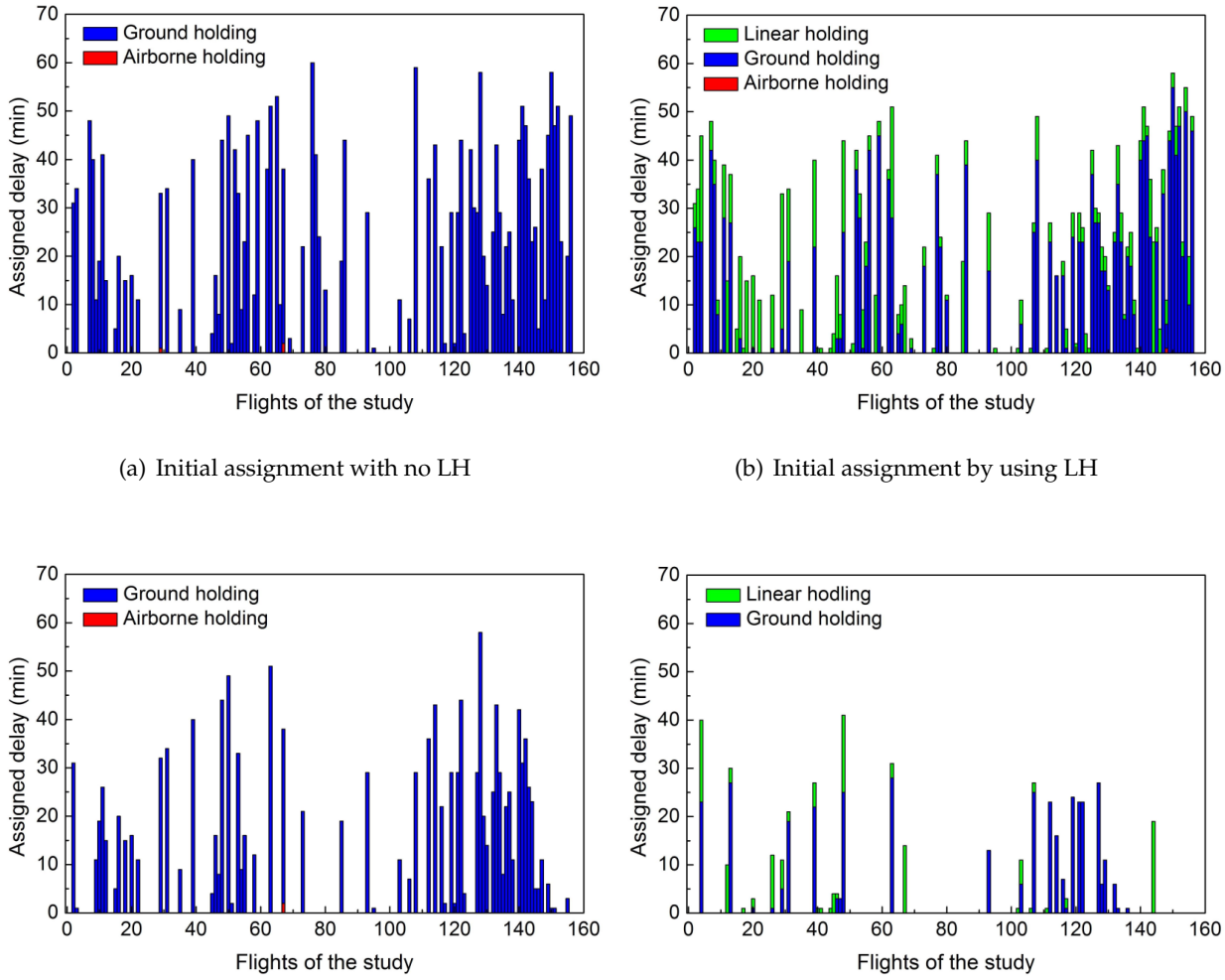

(a) Initial assignment with no LH

(b) Initial assignment by using LH

(c) Updated assignment with no LH

(d) Updated assignment by using LH

Figure V-5: *Amount of delay assignment in form of ground holding, airborne holding and linear holding with regards to the four cases of study.*

V.2.3 Delay recovery for a specific airborne flight performing LH

In this section, the same flight (LIRF-EHAM) introduced in Sec. V.1.2 is analyzed in detail. During the initial process of delay assignment, this particular flight is allocated with 41 min of delay in total (imposed on the arrival slot), while allowed to wait on the ground for 22 min (i.e., ground holding) but flying slower to absorb the rest of the delay, i.e., 19 min, by means of LH in the air (assuming no update occurs).

After serving 22 min of ground holding followed by encountering the update of delay assignment, at 9 AM, as shown in Fig. V-6(a), the flight starts to recover its nominal trajectory. The process is initiated when passing the next designated position (229 nm) compared to the flight's current geographical position. Afterwards, the updated timeline (the red line) deviates from the actual one performing an amount of LH (19 min, the blue line) which is lower than its maximum LH (25 min, the grey line) shared to the NM. It can be noticed that the slope of the red curve becomes flatter as to be exactly parallel to the nominal timeline (the black line) during the remaining distance. At the end, there are 14 min of delay saved, reducing the total delay from 41 min to 27 min.

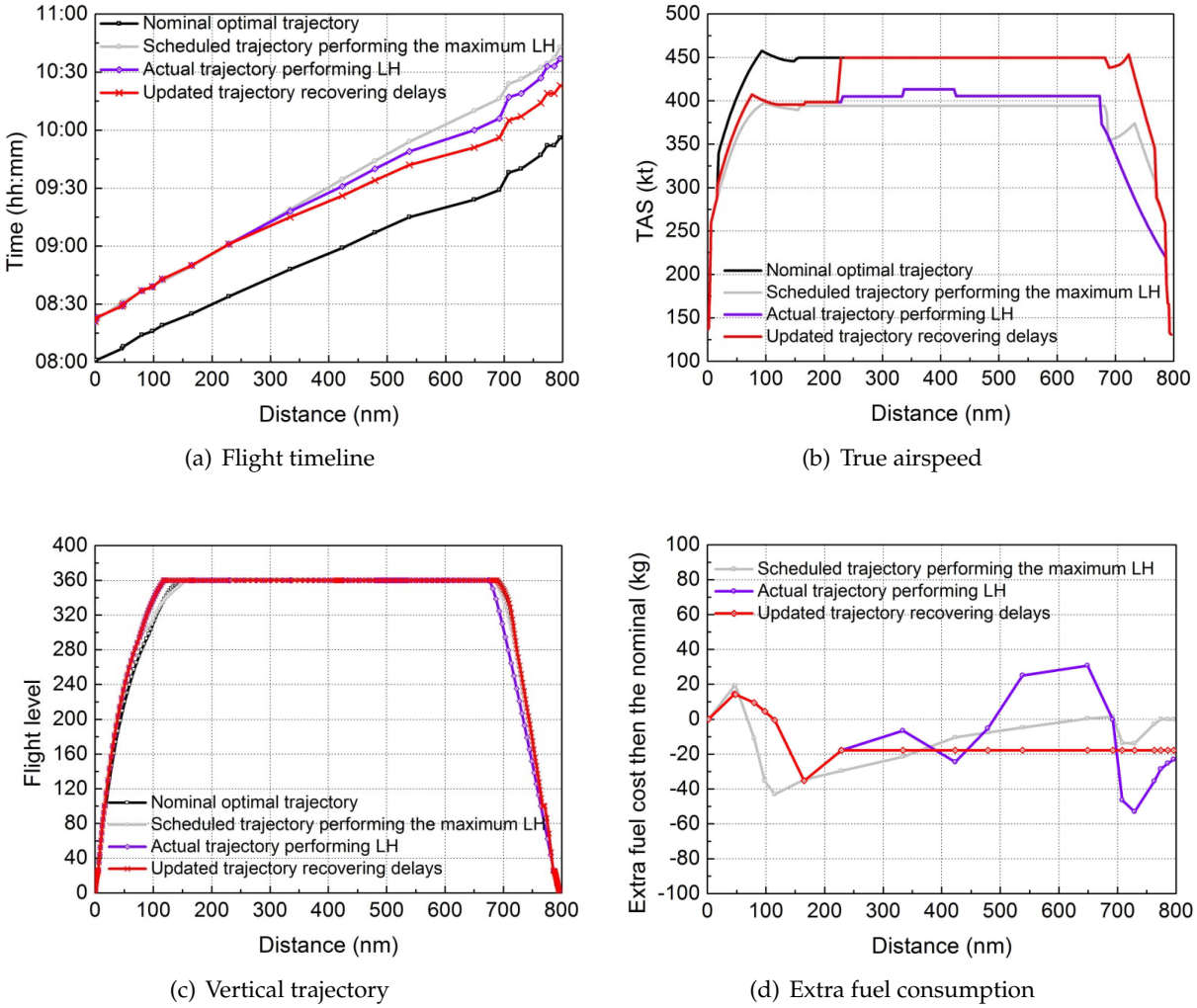

(a) Flight timeline

(b) True airspeed

(c) Vertical trajectory

(d) Extra fuel consumption

Figure V-6: *Effects of delay recovery for the flight (LIRF-EHAM) performing LH partway in the air when encountering the update of delay assignment.*

As we can see from Fig. V-6(b), the TAS of the actual trajectory performing 19 min of LH lies between the nominal TAS and the one having the maximum LH. Interestingly, since delays are not assigned evenly along the trajectory, we may notice that the actual speed (the blue line) changes progressively during the cruise phase (due to the discrete time step of 1 min assumed in this chapter), which may result in an increase in flight crew workload. However, given the Required Time of Arrival (RTA) featured in modern on-board Flight Management System (FMS), and aimed at autopilot when performing LH, it might not raise too much concerns on the procedures. As for the vertical trajectory illustrated in Fig. V-6(c), caused from the changes of climb and descent speeds seen in Fig. V-6(b), the geographical positions of TOC and TOD vary from the nominal trajectory.

At last, as shown in Fig. V-6(d), recall again that the difference of LH with respect to typical airborne holding is located at whether the extra fuel needs to be consumed. Obviously, without this premise, LH might not be favored by AUs, given a safer and cheaper ground holding is always there. As a consequence, by restricting the fuel along the whole trajectory when optimizing it for LH, the fuel consumption can be constrained to the nominal one. Note, however, that due to limitations of the model (fuel constraint is enforced for each discrete flight segment), the fuel consumption will not be exactly the same as the nominal one and small differences can be appre-

ciated. Consequently, as the trajectory updating (red line) occurs at the position where less fuel has been burnt (i.e., 229 nm) than the nominal, and keeps the same unit fuel consumed (or specific range, because the initially scheduled airspeed is recovered) for the remaining distance, such that the final difference in fuel is exactly the same as that observed at the distance of 229 nm.

V.3 Case study in multi-airport setting

In this case study, a multi-airport setting is adopted for validating the network ATFM model. Computational experiments with this setting have been performed using the initial flight schedules derived from the DDR2 database. Three cases of the study are considered where the changes of capacity apply, namely the initial delay assignment, delay updating of an improved and a reduced capacity. For each of these cases, results are further compared by whether or not the proposed LH is included (ground and airborne holding).

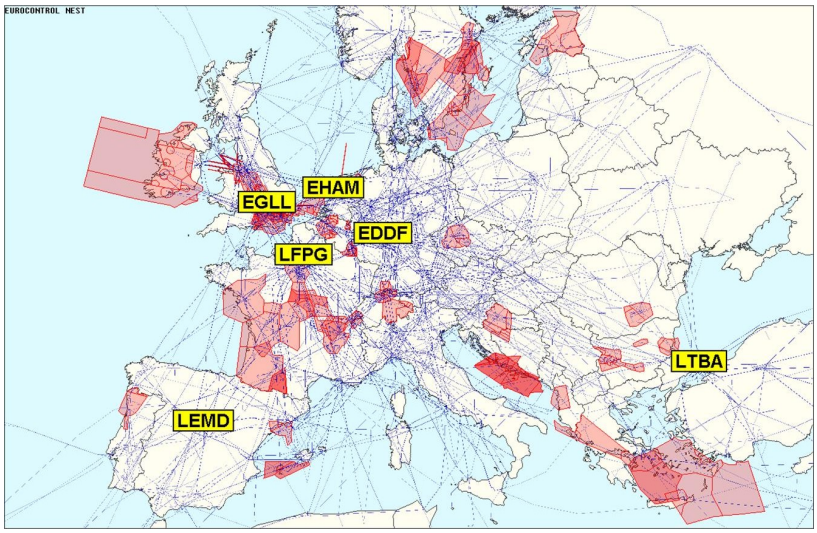

Figure V-7: *Network ATFM scenario in the computational experiments with multi-airport setting. (Source: Eurocontrol's NEST modelling tool)*

The sample data involve the flights scheduled to appear in the European airspace with Estimated Time of Arrival (ETA) and Estimated Take Off Time (ETOT) both located between 06:00 and 10:00 AM on Oct 24, 2016. As shown in Fig. V-7, the blue dash lines denote the 2938 scheduled trajectories across the overall 227 airports. In line with the schedules, there are 2639 elementary sectors that these flights were to traverse en route, among which 78 sectors (as colored in red in Fig. V-7) had reduced capacities.

Moreover, further decreases ranging from 10% to 30% were randomly applied with respect to their published capacities (with time scale in form of 20 mins) during the entire 4-hours time period (after which all recovered to the published) in the experiments. Besides the sectors of reduced capacity, there are 6 selected European airports (as shown with yellow labels in Fig. V-7) which, as assumed, had operation capacity reductions by 30% to 50% (equally for departure and arrival) during the same period and then recovered at once at 10:00 AM.

Following the initial delay assignment to handle the 4-hours capacity reductions, a situation where prior changes occurred at 08:00 AM has been considered. Under the circumstance, either the affected areas (including sectors and airports) recovered to their normal (published)

capacities, or further decreased by a certain number (10% in this experiment and only for the 78 en route sectors) on basis of their already reduced capacities, both requiring an updating of the delay assignment, namely, three Cases in summary as follows:

Case-1: Initial delay assignment with limited capacity;

Case-2: Delay updating if capacity improves; and

Case-3: Delay updating if capacity reduces further more.

Additionally, aiming at demonstrating the benefits of incorporating the LH, along with current ground holding and airborne holding, two sub case studies have been considered for each of the above three Cases, i.e., with and without LH, which are denoted respectively as:

Case-i: GA and *Case-i: GAL*, being i equal to 1, 2 or 3.

Some other key assumptions have been also taken in the computation: 1) the discrete time interval was set to 1 min; 2) $\epsilon = 0.05$ was selected as the fairness factor; 3) the cost weights for airborne holding and LH were, respectively, 1.2 and 0.8 with regard to the ground holding; 4) the LH time bound was approximated as 20% of the planned total trip time III, if no otherwise specified, and are all shared by AUs to the NM; and 5) the delay updating can be initiated at once while flights can receive and execute immediately the latest delay assignment.

V.3.1 Results of delay assignment and updating

The overall results of the delay assignment can be appreciated from Table V-5 with regard to the six Cases of the study. For the initial delay assignment, Case-1 (GA) and Case-1 (GAL), the total time of delay (2252 mins) and the amount of delayed flights (238 a/c) are exactly the same for both Cases, incurring, however, different delay costs as part of the delay (384 mins) is absorbed by LH in the latter Case.

Table V-5: *Overall delay assignment for all Cases of the study.*

Cases	Comput.	GH		AH		LH		Total		
	Time (sec)	Time (min)	Flight (a/c)	Time (min)	Flight (a/c)	Time (min)	Flight (a/c)	Time (min)	Flight (a/c)	Cost (GH)
Case-1 (GA)	40	2252	238	0	0	-	-	2252	238	2252
Case-1 (GAL)	328	1868	183	0	0	384	114	2252	238	2232,8
Case-2 (GA)	50	1584	200	0	0	-	-	1584	200	1584
Case-2 (GAL)	14	1189	155	0	0	258	88	1447	192	1434,1
Case-3 (GA)	18	2659	260	121	16	-	-	2780	274	2804,2
Case-3 (GAL)	26	2184	200	34	4	560	143	2778	273	2756,8

The benefits of partially performing LH can be noticed by comparing Case-2 (GA) and Case-2 (GAL). When the capacity recovers ahead of schedule, the aircraft already airborne are enabled to terminate LH and accelerate immediately to meet a (potential) advanced arrival time (i.e., delay updating), such that the total delay of Case-2 (GAL) is observed in Table V-5 to further reduce by 137 mins more than that of Case-2 (GA). An analysis on the effects of this behavior is presented in Sec. V.3.2 by a specific flight.

As for the situation where capacity turns worse, airborne holding appears in both Case-3 (GA) and Case-3 (GAL) which does not exist within the four Cases mentioned previously. It is

because the flights already in the air, obviously, cannot perform any ground holding, while at the same time the extra delay (required by the updated capacity) is out of the LH bound, and thus airborne holding remains the only option (for reducing the instant sector demand). Worth noting that most of the costly airborne holding are substituted by LH (87 mins, 72%) if comparing Case-3 (GA) and Case-3 (GAL) in Table V-5, leading to a reduction on the total delay costs, which could again reveal the benefits of including the proposed cost-based LH practice.

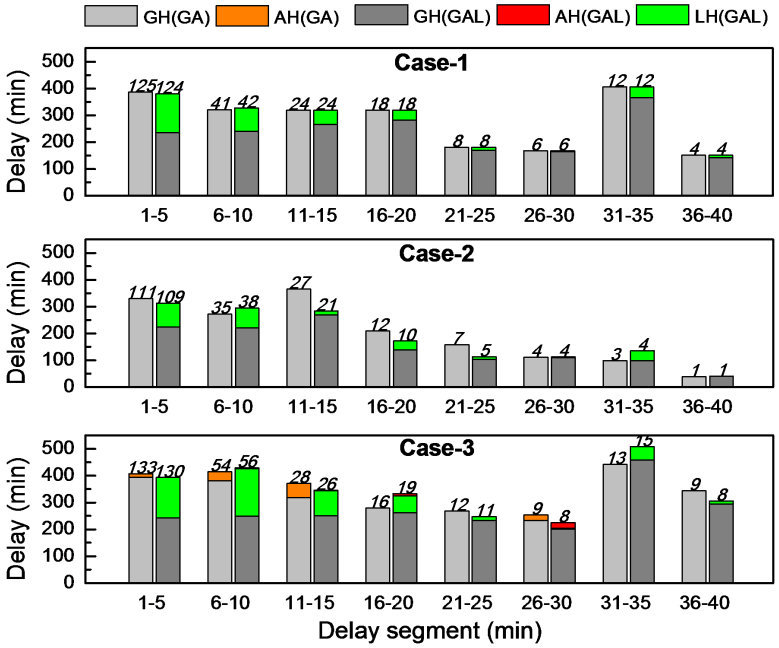

Figure V-8: *Distribution of aggregate delays and the amount of delayed flights.*

Concretely, the distribution of delays in a step length of 5-mins is as shown in Fig. V-8, where the number of respective delayed flights is labeled aside each column. Resulted from the fairness coefficient considered in the objective function (see Eq. V.4), most of the individual delays can be seen less than 5 mins in every Case of the study, which are randomly alloted to almost half of the total delayed flights. Nonetheless, the aggregate delays mounted by this large number of flights only contribute to an average total delay absorption, while a relatively small number of flights (e.g., assigned by 31-35 mins of delay) are to take the highest proportion (see Case-1 and -3 in Fig. V-8).

As mentioned previously, potential benefits can be achieved from implementing LH, on the condition of a prior capacity updating, regardless of an increasing or decreasing, which is due to the fact that performing LH is of high flexibility and at no extra fuel cost (recall Sec. II.1.1). These effects can be further appreciated in Fig. V-8. Seeing from Case-1 to -2, and from Case-1 to -3, the individual ground holding has little change on each column (specifically for lower delays), given the realization of ground holding is only applicable on the ground before departure, whilst the individual LH varies remarkably.

Fig. V-9 shows the capacity load (or utilization), i.e., the ratio of traffic demand over the instant capacity for that time period (defined by per-20-mins), across the entire 4-hours affected period for the six Cases, as well as a Case-0 representing the initial flight schedules.

It should be noted that both the demand and capacity are calculated using the total number with respect to the same group of areas of capacity changes, namely, 6 selected European airports for *Arrival* and *Departure*, and 78 constrained en route airspace for *Sector* as shown in Fig. V-9.

This also accounts for the reason why the capacity load is always lower than 100% even for those initial schedules (i.e., Case-0). It can be noticed from the figure that the arrival capacity load keeps increasing while the departure decreasing along with the time elapsed, because of the experiment scope that stipulates both the ETA and ETOT of flights within the 4-hours time period. In other words, during the initial periods, the captured flights for delay assignment are just to depart from their origin airports, such that the traffic demands are higher for the departure than for the arrival, and vice versa for the ending periods.

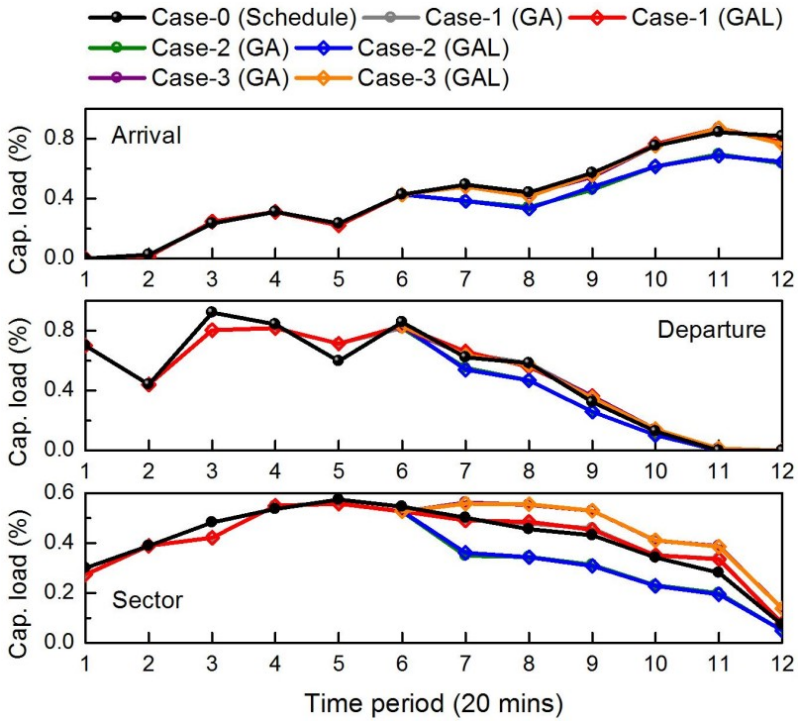

Figure V-9: *Capacity load changes with time elapsed for specific areas.*

It is worth noting that there is hardly any difference between the Cases with and without LH, i.e., Case-i (GA) and Case-i (GAL), as shown in Fig. V-9. One may suspect the reduced ground holding resulted from performing the proposed LH may lead to an increase of the airborne flights, somehow, aggravating traffic congestions. This conclusion drawn from Fig. V-9, however, means that the inclusion of LH does not unnecessarily increase the capacity load (and thus the air traffic controllers' workload), if compared with the current protocol (i.e., Case-i (GA)).

V.3.2 Illustrative example for a specific flight

A specific flight captured in the previous delay assignment is analyzed in detail in this section. The flight was scheduled to depart from ESSA (Stockholm Arlanda airport), with ETOT at 06:55 AM, and to arrive at EGLL (London Heathrow airport), with ETA at 09:03 AM. The total trip distance was planned as 829 nm and the cruise flight levels were at FL360/380. An Airbus A320 was scheduled to execute the flight.

The optimal vertical trajectory of this flight is generated in line with its initial flight schedule, as shown with the black dots in Fig. V-10(a), being the total trip fuel 4719 kg. However, due to the initial delay assignment (i.e., Case-1), the flight is imposed with 13 mins of arrival delay at the destination airport, meaning the CTA is at 09:16 AM.

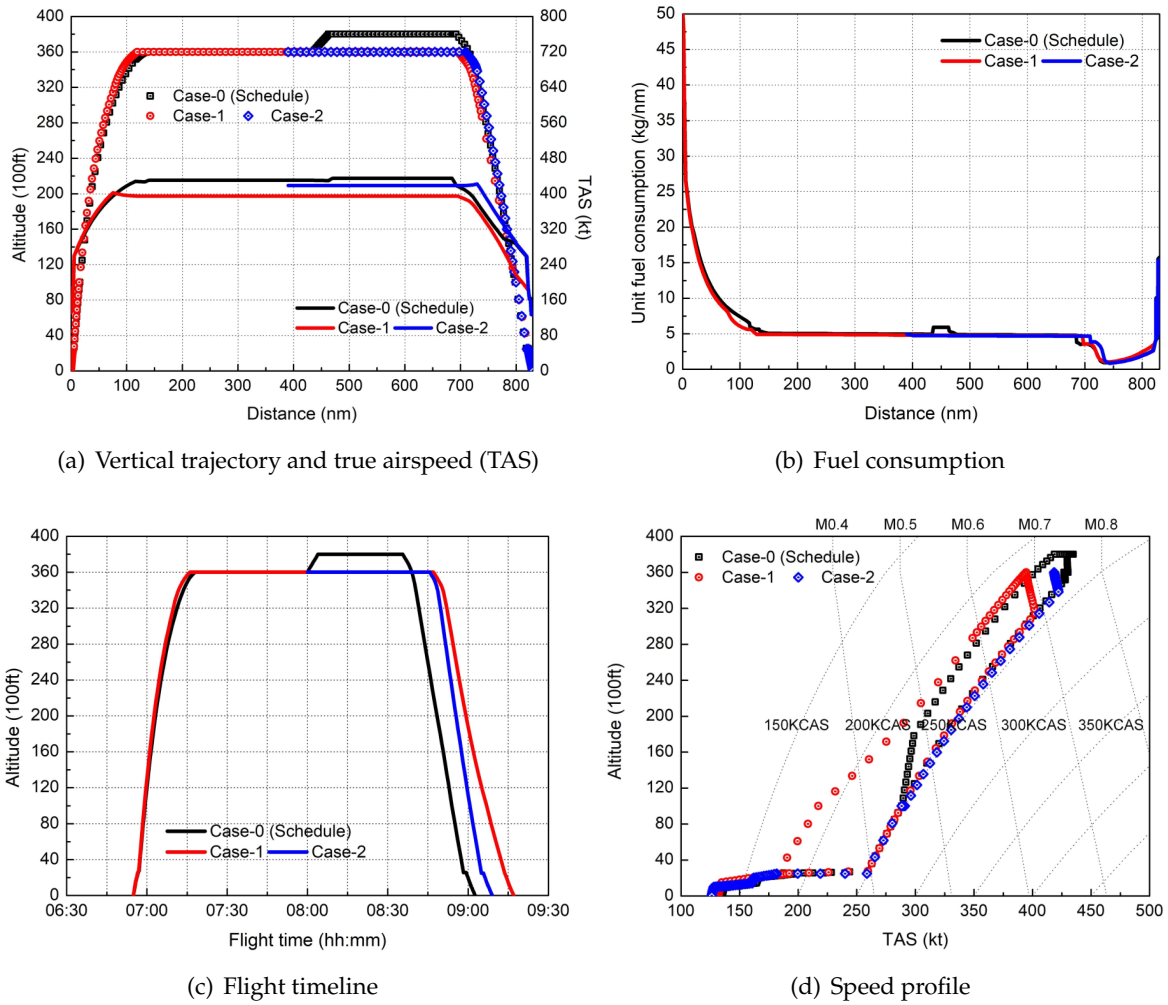

(a) Vertical trajectory and true airspeed (TAS)

(b) Fuel consumption

(c) Flight timeline

(d) Speed profile

Figure V-10: *Effects of the cost-based LH for delay recovery in Case-1 and delay absorption in Case-2 for a specific flight.*

Instead of enduring all the assigned delay on the ground by means of ground holding, the flight is enabled to take off earlier and absorb the necessary delays airborne through performing LH. As shown in Fig. V-10(c), it turns out that the flight can depart at 06:55 AM as initially scheduled, but has to fly slower (see the speed profile of Case-1 in Fig. V-10(d)) to absorb the entire 13 mins of delay en route, in such a way that the CTA (i.e., 09:16 AM) at the destination airport is still satisfied. Meanwhile, the fuel consumed from the optimal trajectory of Case-1 with LH integrated (see the red line in Fig. V-10(b)) is observed to reduce by 146 kg due to the speed reduction from which it can be understood for any speeds between the nominal speed and the equivalent speed, the amount of fuel consumption will not exceed than initially scheduled).

At the time when a prior capacity recovery occurs, i.e., 08:00 AM as in Case-2, the flight performing LH has flown 390 nm away from ESSA. Due to the released arrival capacity, an updated CTA at 09:11 AM is then assigned to the flight (see the blue line in Fig. V-10(c)), meaning that for the remaining 437 nm, it is applicable to accelerate (see the blue line in Fig. V-10(d)) to meet the advanced arrival time. Since the updated speed does not exceed the nominal speed, the fuel consumption (4602 kg) at the end is still lower than initially scheduled.

To sum up, through substituting ground holding by means of the LH, the specific flight is capable of reducing 5 mins of the assigned delay, at the same time, saving 117 kg of the total trip fuel once a prior capacity recovery occurs (as in Case-2). Moreover, if no such updating appears

eventually (as in Case-1), the total fuel consumption will be saved by 146 kg, with 13 mins of the delay entirely absorbed in the air (meaning that waiting on ground is then not needed).

V.4 Chapter summary

In this chapter, the cost-based linear holding was merged into a network ATFM model for delay absorption, together with the commonly seen ground and airborne holdings. In the light of trajectory based operations, AUs' sharing of maximum linear holding bounds derived from their own optimal aircraft trajectory generation, could be effectively utilized by the NM as one of the optimization factors considered for delay assignment.

Incorporating the LH means that more space and periods in the network can be used to absorb delays. Provided multiple node constraints occur at the same time, splitting delays at different places and times could contribute to reducing the minimum system delay needed to satisfy multiple constraints. Results suggest that once the delay updated due to the improvement of network situation, less ground holding, and thus less total delay would be eventually realized.

Moreover, if the delays are canceled ahead of schedule, aircraft already airborne and performing LH, could accelerate to the speed as initially planned and recover part of the delay at no extra fuel cost. Moreover, potential benefits can be also achieved when the capacity turns even worse than before, if compared with the case where only ground and airborne holding apply.

The person who reads too much and uses his brain too little will fall into lazy habits of thinking.

— Albert Einstein

VI

Collaborative ATFM with increased AUs participation

This chapter proposes a Collaborative Air Traffic Flow Management (ATFM) framework in the scope of trajectory based operations (TBO), which largely improves the cost-efficiency of ATFM. The framework consists of four modules. The first one involves airspace users (AUs) initially scheduling the preferred trajectories for their operational flights. The second module introduces a collaborative trajectory design process. Given the submitted initial trajectories, time-varying hotspot airspaces are first detected by the Network Manager (NM), who then generates the accurate hotspot-avoidance information for the affected flights. It is then shared, on basis of individual flight, to the relevant AUs, enabling them to precisely schedule alternative trajectories to avoid entering those volumes, with as few as possible extra costs incurred. Such avoidance, as discussed in the third module, can be performed by lateral or vertical maneuvers, or simply by adjusting the arrival time. AUs assess their costs and eventually submit the alternative trajectories and delay measure preferences that they believe are most beneficial. Incorporating all these potential combined options, the last module computes the best trajectory selections and the optimal distribution of delay assignments, minimizing the deviation to the initial status, which is composed of all the user-preferred trajectories.

VI.1 Overall framework structure

The structure of the proposed Collaborative ATFM framework is presented in Fig. VI-1. It is composed of four modules, each representing the job done by either the AUs or the ATFM authority

(e.g., NM in this chapter). The arrow direction denotes the task sequence, labeled with the information exchanged among different modules. The whole procedure is mainly focused on the pre-tactical ATFM planning phase (i.e., typically 1 day to 6 days before the day of operations). An outline of each module is as follows:

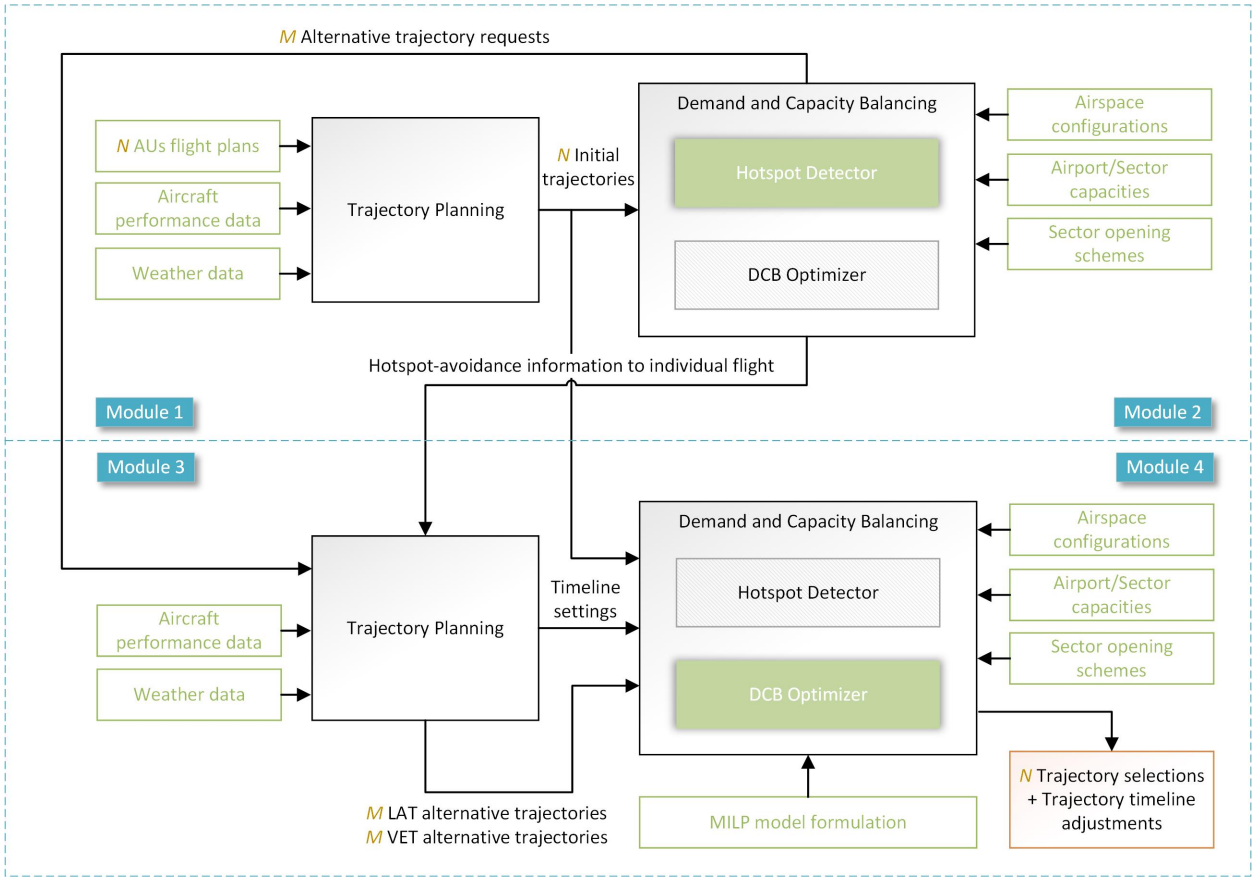

Figure VI-1: *An overview of the collaborative demand and capacity balancing framework.*

- **Initial planning of user-preferred trajectories**

  This module refers to the planing of trajectories by the AUs, taking into account forecast weather conditions and strategic ATM constraints, such as route availability restrictions or flight level allocation and orientation schemes (see Sec. VI.2.1). The optimization module has been reported in (Dalmau *et al.*, 2018). According to the SESAR concept of operations (ConOps), these trajectories would correspond to the Business Development Trajectories (BDT).

- **Detection of demand and capacity imbalance**

  Based on the trajectories computed in the previous module (i.e. initial traffic demand), a primary detection of imbalances between traffic demand and airspace capacity is conducted in this module (see Sec. VI.2.2). Time-varying hotspot volumes are thereby identified. Combined with airspace geometric descriptions, the specific hotspot avoidance information is shared to all AUs with one or more concerned flights, i.e., flights traversing at least one hotspot (see Sec. VI.2.3).

- **Submission of trajectory options and delay management**

  With the hotspot avoidance information received, concerned AUs compute alternative trajectories for their captured flights to avoid entering these hotspot volumes, using the same

trajectory optimization techniques implemented for initial trajectory planning (see Sec. VI.2.4). Different types of delay measures are also enabled (see Sec. VI.2.5). According to the SESAR ConOps, these trajectories would correspond to the Shared Business Trajectories (SBT).

- **System-wide optimization to balance demand and capacity**

  The module of system-wide optimization is then initiated by the NM to balance the demand and capacity, yielding eventually the best combinations of trajectory selections and delay assignments among all regulated flights (see Sec. VI.3). The objective considered in this chapter minimizes the overall deviation with respect to the status where all trajectories remain unchanged from their initial plan. These trajectories would correspond to the Reference Business Trajectories (RBT).

VI.2 Collaborative trajectory design

This section introduces a coordinated trajectory design process, aligned with the Collaborative Decision-Making (CDM). Specific avoidance information is generated by the NM and is shared to concerned AUs for each affected flight. Precisely-designed alternative trajectories, along with preferences on delay management measures, are produced by AUs and eventually submitted back to the NM.

VI.2.1 Initial schedule of user-preferred trajectory

In the European ATFM system, AUs have been offered a high level of flexibility in regard to flight planning (Bolić *et al.*, 2017), which enables the scheduling of initial trajectory to well reflect their preferences. For day-to-day operations, these preferences are generally focused on the aircraft direct operating cost encompassing a weighted sum of fuel consumption, route charges and time-related costs (Airbus, 1998; Roberson, 2007), as follows:

$$J = \int_{s_0}^{s_f} \left(\underbrace{\frac{c_t}{\dot{s}(s)}}_{\text{Time}} + \underbrace{\frac{c_f f(s)}{\dot{s}(s)}}_{\text{Fuel}} + \underbrace{\frac{\mathrm{d}c_r(s)}{\mathrm{d}s}}_{\substack{\text{Route} \\ \text{charges}}} \right) \mathrm{d}s = \int_{s_0}^{s_f} \left(c_f \frac{\mathrm{CI} + f(s)}{\dot{s}(s)} + \frac{\mathrm{d}c_r(s)}{\mathrm{d}s} \right) \mathrm{d}s \tag{VI.1}$$

where s represents the along path distance; f is the fuel flow; $\dot{s}$ is the ground speed; c_f and c_t are the unit costs of fuel and time, respectively; $\mathrm{CI} = \frac{c_f}{c_t}$ is the cost index, a parameter chosen by the operator that reflects the relative importance of the time and fuel costs; and c_r is the cost of the route charges.

Aiming at minimizing the total operating cost per flight, this chapter performs both lateral route planning and vertical profile optimization to generate an optimal 4D trajectory so as to represent the user-preferred trajectory. Nevertheless, as the main topic of this chapter is targeted on the demand and capacity balancing (DCB) problem of pre-tactical ATFM initiatives, the details of producing this initial traffic demand (as typically done prior to ATFM regulations) are out of the scope of the chapter. Here below presents a brief introduction to the relevant methods, but for more techniques implemented in this regard, the reader may direct to (Dalmau & Prats, 2017; Dalmau *et al.*, 2018)

To reduce the computational complexity of the optimization problem, this chapter decouples the generation of the optimal lateral route and the vertical profile for one trajectory. The

lateral route is determined in two different modes: structured route (SR), where aircraft must fly along the published Air Traffic Services (ATS) flight segments; and free route (FR), via intermediate (published or unpublished) waypoints, without being required to follow these ATS flight segments mandatorily. The airspace is represented by a graph, in which the edges and nodes are dependent on the activated route mode. Based on this graph, the optimal lateral route minimizing the direct operating cost is computed by using the A* algorithm (Hart *et al.*, 1968).

In addition, realistic weather conditions, especially the wind fields that have great impacts on the lateral route, are also considered, using GRIdded Binary (GRIB) formatted files (World Meteorological Organization, 1994), a concise data format in meteorology to store historical and forecast weather data. The effects can be seen clearly from Fig. VI-2(a), in which GCD (Great Circle Distance) represents the shortest distance, whereas the actual optimal route follows the green line's path.

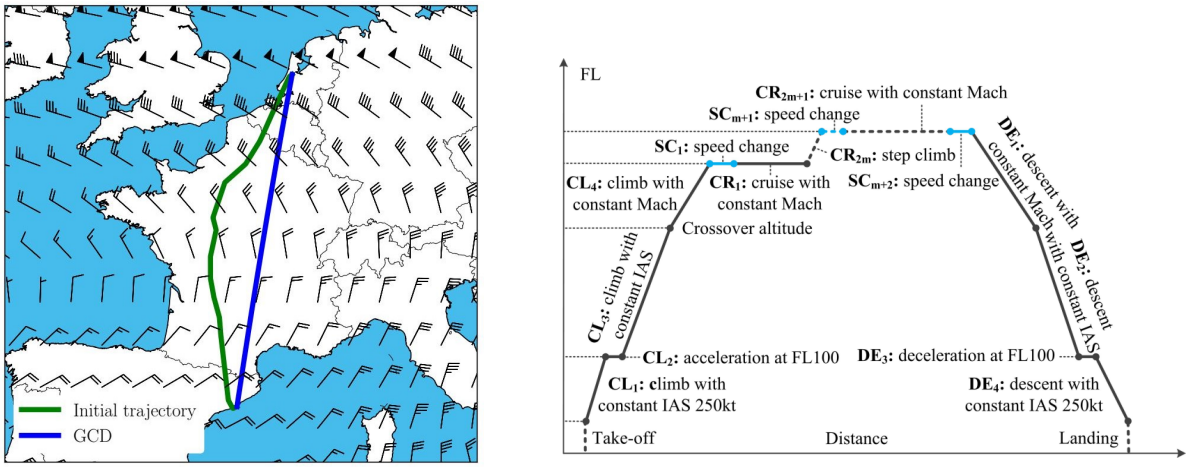

(a) Optimal trajectory taking into account weather conditions (green). GCD: Great Circle Distance

(b) Vertical profile with ATM restrictions

Figure VI-2: *Initial trajectory planning decoupled to lateral route and vertical profile.*

The vertical profile is composed by a given sequence of parametrized flight phases. Each phase within the flight profile contains information about the aerodynamic configuration and throttle setting, and may also include various constraints representing AUs' operations and ATM restrictions, as shown in Fig. VI-2(b). To obtain accurate fuel consumption and time figures, aircraft performance data from the Base Of Aircraft Data (BADA) v4 (Nuic & Mouillet, 2014) published by Eurocontrol are used, along with the above mentioned weather data (e.g., temperature and wind field at the different coordinates and pressure levels).

VI.2.2 Detection of time-varying hotspot airspaces

On basis of the initially planned trajectories, a primary detection on the imbalances of traffic demand and airspace capacity is conducted by the NM, identifying the hotspot volumes. Under the trajectory based operations, it is clear that not only airspace capacities vary with time, due to sectorization schemes or weather changes for instance, but also traffic demand, which depend on the scheduled flights for that day and the particular realization of 4D trajectories for each flight. Thus, the detected hotspot airspaces are also time-varying.

Multiple ways of defining traffic demand may apply for different scenarios, such as runway's take-off/landing number, occupied time and terminal entry/exit rate, when considering airport

capacity. Besides, in terms of sector's operational capacity, the traffic demand could be counted by means of aircraft entry rate, occupancy, density and complexity for instance (Sridhar *et al.*, 1998). On the other hand, the capacity of airport/sector can be evaluated (and quantified) in different ways as well, and might be affected by various factors (e.g., physical dimensions, facility equipments, regular traffic patterns and even air traffic controllers' abilities) (Janić & Tošić, 1982).

There have been much research in this regard for the last decades, see for instance (Delahaye & Puechmorel, 2000; Majumdar *et al.*, 2002; Xu *et al.*, 2016; Yang *et al.*, 2017). Nevertheless, discussing on the most suitable method is out of the scope of this chapter and for convenience, the entry rate is adopted as the criterion to count demand, which is also commonly used in current operations. Capacity values are directly retrieved from the Demand and Data Repository v2 (DDR2) database published by Eurocontrol (EUROCONTROL, 2018b). It is worth noting that the approach proposed in this chapter would also be applicable to other definitions of demand and capacity via certain adjustments (if needed).

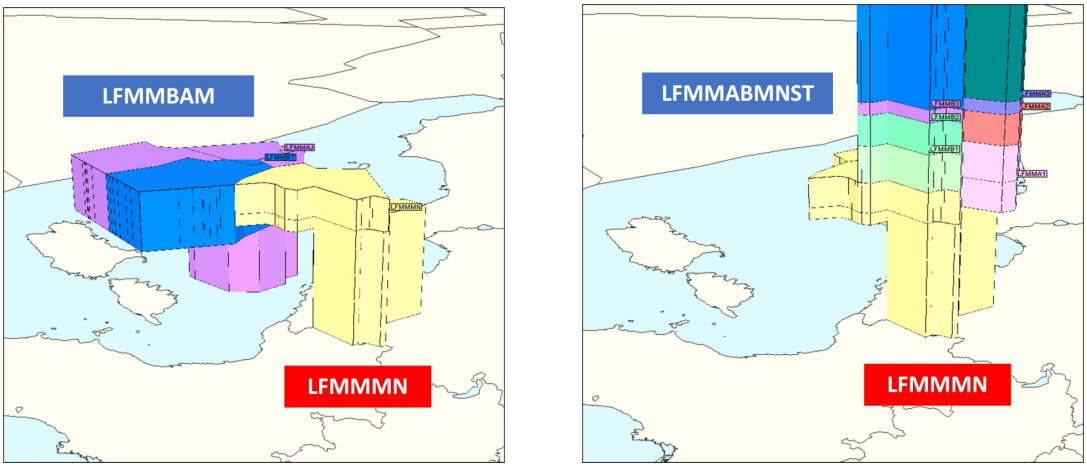

(a) Collapsed sector LFMMBAM (b) Collapsed sector LFMMABMNSR

Figure VI-3: *Elementary sector LFMMMN collapsed to different operating sectors during different time periods of the same day.*

Specifically, as for counting the entry rates, the (flight) entry points (into any airspace volume) are defined at the boundary of elementary sectors, as their geographical dimensions normally remain stable during a relatively long period, e.g., an AIRAC (Aeronautical Information Regulation And Control) circle of 28 days. However, an elementary sector could be collapsed with its adjacent elementary sector(s) in a much shorter time scale, acting as operating sector as a whole. For example, as illustrated by Fig. VI-3, an elementary sector LFMMMN (colored in yellow) is merged into two different collapsed sectors (LFMMBAM and LFMMABMNSR) in two different hours of the same day, along with other elementary sectors. Obviously, the two newly-formed operating sectors have quite different physical dimensions, and in many cases, they would have different operating capacities.

This difference between the airspace entity of defining entry point (i.e., elementary sector) and that of realistic operating capacity (i.e., collapsed sector) requires a specific judgement about whether a flight entry should be regarded as traffic demand. If a flight enters a collapsed sector, being its intersection with one of the elementary sectors which belong to the collapsed sector (e.g., LFRRJVKNG in Fig. VI-4(a)), then, according to the above discussion, the intersection is always seen as a flight entry (and is also subject to a control point as will be discussed in Sec. VI.3). However, as shown in Fig. VI-4(b), for exactly the same entry point (labeled with a red

star), assume that the intersected elementary sector belongs to another collapsed sector (e.g., LFRRJVKWS) at another time when the flight actually enters (because the flight has been delayed). In this case, the particular flight entry should not be counted as an extra traffic demand of that operating sector, which is, instead, treated as an internal movement inside the sector.

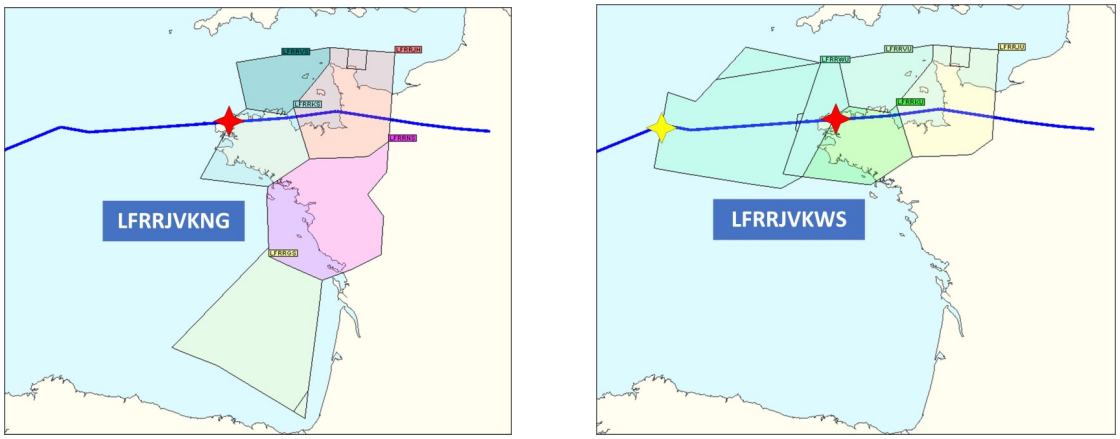

(a) Aircraft entry (red) counted (b) Aircraft entry (red) not counted

Figure VI-4: *Criteria of whether an aircraft entry into an elementary sector is counted as a traffic demand for different collapsed (operating) sectors.*

Following this thought, only the first entry to the collapsed sector, e.g., the red label in Fig. VI-4(a) or the yellow label in Fig. VI-4(b), is the one that will be counted as a demand (within a certain time period) among all the flight entries defined at various belonged elementary sectors. The above principle is given in Algorithm VI.1, where ETA and CTA represent, respectively, the Estimated and Controlled Time of Arrival at the entry point.

As can be seen from the 4th and 6th lines of Algorithm VI.1, there is an implicit relationship between the elementary sector (e), collapsed sector (c) and time variable (t). Namely, an elementary sector will belong to a specific collapsed sector at a certain time. As presented with Algorithm C.1 in Appendix C, an additional procedure is conducted to establish such (static) scheme from the published DDR2 database.

Algorithm VI.1: *Count traffic demand for collapsed sectors*

```
1: for c in collapsed_sector_list do
2:     for t in time_period_list do
3:         if c in operating_sector_list[t] then
4:             for e in elementary_sector_list[c][t] do
5:                 for f in flight_list[e] do
6:                     if ETA[f][e] == min(ETA_list[f][c][e]) then
7:                         initial_traffic_demand[c][t] += 1
8:                         if CTA[f][e] in t then
9:                             regulated_traffic_demand[c][t] += 1
```

Finally, based on one hand on the counted initial traffic demand and, on the other hand, on the retrieved airspace capacity, hotspot sectors are detected as a function of the time. Typically, the time scale for capacity evaluation is 20 min or 60 min, so the time-varying hotspot positions may evolve among the entire airspace network after every 20 min or 60 min. This list of predicted hotspots is the basis of the avoidance information provided to each individual concerned flight, as discussed in the next section.

VI.2.3 Hotspot avoidance information to individual flight

With the time-varying hotspots detected, all specific flights that planned to traverse those airspace volumes during the corresponding time period will be captured. Concerned AUs will be inquired to submit alternative trajectories (avoiding hotspots) for each of their affected flights. It must be noted that this submission is not mandatory for the AUs, who could decide that for some (or all) of their flights the initial trajectory is the only option, which will be likely subject to (significant) delay. Hence, AUs will have to consider the extra costs incurred if flying alternative trajectories (possibly subject to less or no delay) and decide whether the submission of alternatives is worthwhile based on the cost-breakdown particularities of each concerned flight.

As shown in Fig. VI-5, there could be multiple hotspot areas identified across the entire network of airport and sectors, but it is not necessary to require a single flight to evade all of them, whereas only the one(s) that the flight's initially scheduled trajectory traverses should be considered. This is because, as discussed in Sec. VI.2.2, the hotspots are time-varying (compare Fig. VI-5(a) and VI-5(b)) and, meanwhile, the entry time for the alternative trajectory is still unknown (which will be thereafter provided by the AUs). It is possible that when the alternative trajectory is scheduled to enter the specific airspace, there is no capacity overload at that particular time. Accordingly, only the already-known hotspot area(s) associated with the initial trajectory has/have to be avoided for the flight when planning alternative trajectories.

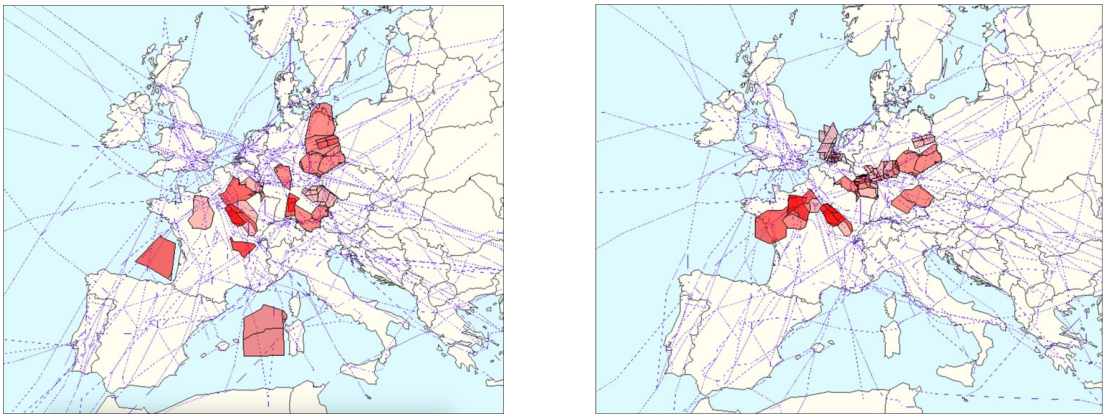

(a) 10:00 AM - 10:20 AM (b) 10:20 AM - 10:40 AM

Figure VI-5: *Time-varying hotspot volumes identified across the regulated airspace network.*

Given that airspace sectors are designed in 3 Dimensional, including lateral coordinates of boundary points and vertical altitudes of lower and upper bounds, a flight, in theory, should be able to avoid a sector in both lateral and vertical directions (except that the sector is close to the departure or arrival airport). For convenience, they are entitled hereafter as lateral-avoidance and vertical-avoidance alternative trajectory respectively.

To assist AUs design their lateral- and vertical-avoidance trajectories, some specific information can be shared to them with respect to each affected individual flight. An example can be seen from Table VI-1, where this flight is captured in a hotspot sector LFEEKDF. It is a collapsed sector and merged by two elementary sectors, LFEEKF and LFEELD, which in turn are constructed by a set of airblocks (e.g., 200LF).

For lateral-avoidance, the boundary coordinates of each airblock are given in such a way that a specific polygon graph can be formed on the horizontal plane to represent the entire hotspot area. For vertical-avoidance, based on the initial trajectory, it informs the flight at which distance

(to the destination airport, e.g., -234 nm) it should start to change the original altitude and at which distance (e.g., -196 nm) to recover that altitude (if desired), as well as the non-selectable flight levels (e.g., from FL345 to FL375) between the two distances, for each sector that the flight needs to avoid.

Table VI-1: *Precise avoidance information shared to an individual flight for scheduling lateral and vertical alternative trajectories.*

	Airblock code	Boundary No.	Boundary 1		Boundary 2		Boundary n	
Lateral avoidance			Lat. (min)	Long. (min)	Lat. (min)	Long. (min)	Lat. (min)	Long. (min)
	200LF	27	2920	187	2922	210	...	...
	202LF	35	2920	187	2922	210	...	...
	203LF	36	2920	187	2922	210	...	...
	204LF	16	2895	344	2879	360	...	...
Vertical avoidance	Sector code	Entry dist. (nm)	Exit dist. (nm)	Lower alt. (100 ft)	Upper alt. (100 ft)			
	LFEEKF	-196	-117	345	999			
	LFEELD	-234	-196	345	375			

This hotspot-avoidance information could be eventually taken into account by AUs, and the next section will introduce how to make use of it effectively from their perspective. In addition, it is worth noting that the reason of providing such set of accurate data is for reducing, as much as possible, the extra costs yielded from diverting a flight to its alternative trajectory, which accounts for a key performance of the system-wide optimization model as discussed below in Sec. VI.3.

VI.2.4 Lateral- and vertical-avoidance alternative trajectories

Once receiving the detailed hotspot-avoidance information, AUs could generate the alternative trajectories for their affected flights, with the same tools used for planning the initial trajectories (refer to Sec. VI.2.1), whilst adding additional constraints (as specified within the avoidance information) to the trajectory optimization/planning process.

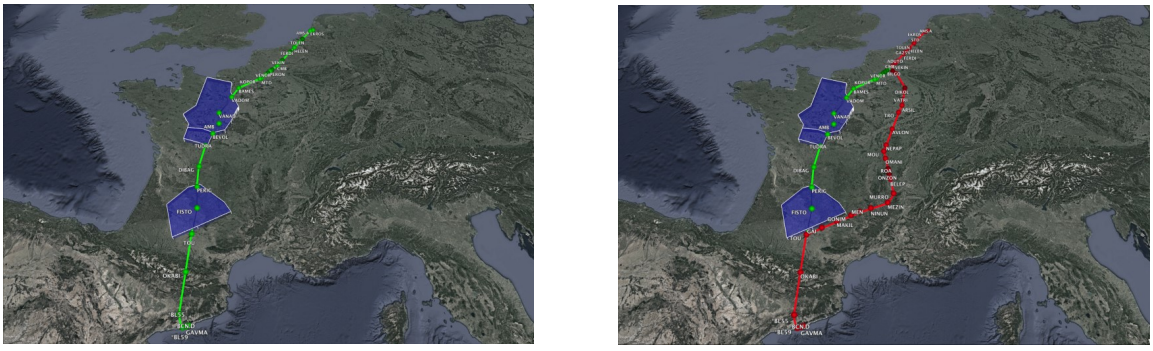

(a) Initial optimal lateral route

(b) Lateral-avoidance alternative trajectory

Figure VI-6: *Lateral route planning of the 4D trajectory optimization capable of producing the accurate lateral hotspot-avoidance alternative trajectory.*

As shown in Fig. VI-6(a), for the same flight (Barcelona El Prat - Amsterdam Schiphol) introduced in Fig. VI-2(a), the initial trajectory (green line) has been captured as it is scheduled to

traverse two hotspot sectors. Then, its lateral-avoidance trajectory is thereby computed, by means of removing from the graph those edges crossing any of the boundaries of the sectors (recall Table VI-1). It is then followed by re-computing the vertical profile on basis of the new lateral route (see red line in Fig. VI-6(b)). Note that if either the origin or destination airport is inside or close to any hotspot volume, the lateral-avoidance trajectory may not exist.

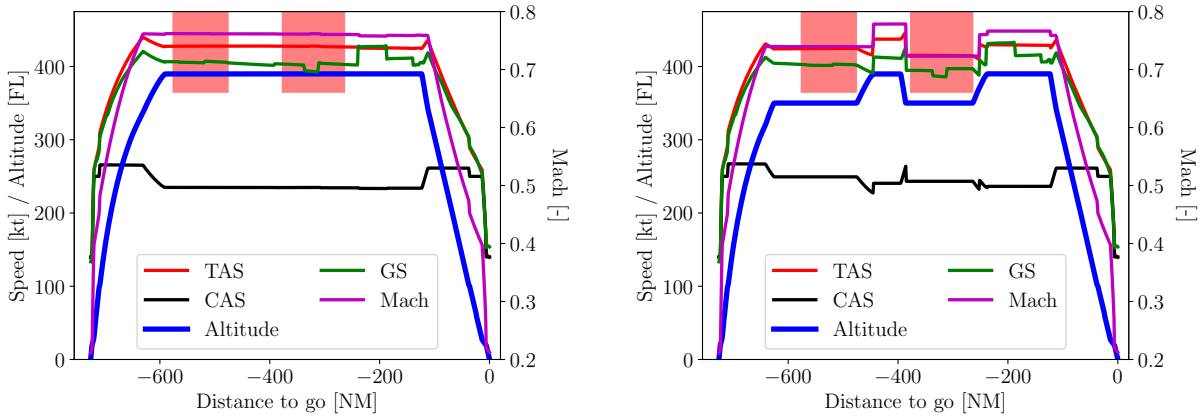

(a) Initial optimal vertical profile

(b) Vertical-avoidance alternative trajectory

Figure VI-7: *Vertical profile optimization based on the planned lateral route capable of producing the accurate vertical hotspot-avoidance alternative trajectory.*

For the vertical-avoidance alternative trajectory, the lateral route is firstly fixed to that initially scheduled, and, recall Sec. VI.2.3, the along path distance of the entry and exit points at each hotspot sector $i \in \mathcal{C}^f$ will be given by the NM (i.e., s_e^i and s_x^i respectively), in addition to the lower and upper non-selectable flight levels within the two distances (i.e., h_L^i and h_U^i), as shown with the red square in Fig. VI-7(a).

During the numerical integration of the climb phase, if current along path distance is included into any of the segments $\left[s_e^i,\, s_x^i\right]$, being $i \in \mathcal{C}^f$, it is checked whether the aircraft would cross h_L^i from below at the next integration step. If so, a level off at constant altitude and CAS (or Mach if h_L^i is above the cross-over altitude) would be performed until reaching s_x^i. Then, the climb is resumed until reaching the Top of Climb (TOC) at the optimal cruise altitude (compare the TOC positions in Fig. VI-7(a) and in Fig. VI-7(b)). The same principle applies for the integration of the descent phase.

When generating the cruise phase, from the TOC to the TOD (Top of Descent), the flight levels in the range $\left[h_L^i,\, h_U^i\right]$ are removed from the candidate set of flight levels in the segments $\left[s_e^i,\, s_x^i\right], \forall i \in \mathcal{C}^f$. At each integration step, the optimal cruise altitude (in terms of the direct operating cost) is computed to decide whether a step climb (see Fig. VI-7(b)) should be performed or not. The solving algorithm follows an iterative process similar to those implemented in state-of-the-art on-board Flight Management System (FMS), which systematically evaluates all potential sequences of decision parameters and selects the optimal one.

VI.2.5 Trajectory timeline adjustments for delay management

In addition to alternative trajectory options, assigning delays can be also used (and is even more commonly seen nowadays) to manage the traffic flow. However, different types of measures may apply to absorb (or recover) the assigned delays, and their costs, limitations and implementations are not necessarily the same. In this chapter, four specific measures are considered including

ground holding, airborne holding, linear holding (as already done in Chapter V) and delay recovery. As these measures will change the Controlled Times Over (CTOs) at the corresponding positions, they can be regarded all together as the adjustment of the 4D trajectory's timeline.

It should be noted that in this chapter delay recovery is foreseen at the flight planning stage, while obeying all the controlled times of arrival distributed along the trajectory. This must be differentiated from tactical delay recovery procedures typically performed in current operations, in which only the Controlled Time of Departure (CTD) is enforced, instead of the Controlled Time of Arrival (CTA) that is actually needed. Moreover, as time-related costs have been already considered for trajectory scheduling (recall Sec. VI.2.1), the initial speed profile should be the one that is most preferred by AUs. Hence, during the delay assignment process (as will be discussed in Sec. VI.3), the delay recovery is allowed only if some delay is imposed at the forepart of a trajectory (e.g., ground holding at the origin airport).

VI.3 Demand and capacity balancing

In this section, a linear optimization model is presented. It incorporates all potential options, such as alternative trajectories and delay management, coming from the collaborative trajectory design process (recall Sec. VI.2), as the measures to balance the traffic demand with capacity. The mathematical formulation is based on the well-studied Bertsimas Stock-Patterson model which has shown excellent computational performance to handle this type of problems (Bertsimas & Patterson, 1998).

VI.3.1 Problem statement

One possibility to balance traffic demand and airspace capacity consists in adjusting the system capacity via, e.g., dynamic sectorization based on the characteristics of traffic flow pattern (Zelinski & Lai, 2011). This is, nevertheless, out of the scope of this chapter. The DCB problem presented here can be simplified as to manage the demand under a set of fixed capacity (using a static scheme of sector configurations through the entire airspace network).

To manage the demand in a more user-friendly and cost-efficient way, the different solutions resulted from the above-mentioned collaboration process are integrated into a single optimization model, selecting eventually the best distribution of trajectory options and delay assignments. This means that the possible combinations to be taken for each flight would equal to $N_k^f(2^{N_d^k}-1)$, where N_k^f represents the number of trajectory options submitted for flight f, and N_d^k is the delay measures preferred by the concerned AUs. Meanwhile, it is forced that $N_d^k \geq 1$ in order to ensure that ground holding must be always applicable for every flight. The scalar -1 is to eliminate the situation that the flight has no delay executed beforehand but performs any delay recovery.

The model is formulated as mixed integer linear programming (MILP), and the corresponding decision variables are defined as follows:

- Decision variables for trajectory options:

$$w_k^f = \begin{cases} 1, & \text{if trajectory } k \text{ is chosen for flight } f \\ 0, & \text{otherwise} \end{cases}$$

- Decision variables for delay management:

$$x_{k,t}^j = \begin{cases} 1, & \text{if trajectory } k \text{ departs from position } j \text{ by time } t \\ 0, & \text{otherwise} \end{cases}$$

$$y_{k,t}^{j} = \begin{cases} 1, & \text{if trajectory } k \text{ arrives at position } j \text{ by time } t \\ 0, & \text{otherwise} \end{cases}$$

Fig. VI-8 presents the trajectory timeline versus designed positions (i.e., intersections with elementary sectors, along with origin and destination airports), where the four types of delay measures are implemented. Note that an alternative trajectory implies a new set of intermediate designed positions (e.g., P-1, P-2 and P-3 in Fig. VI-8).

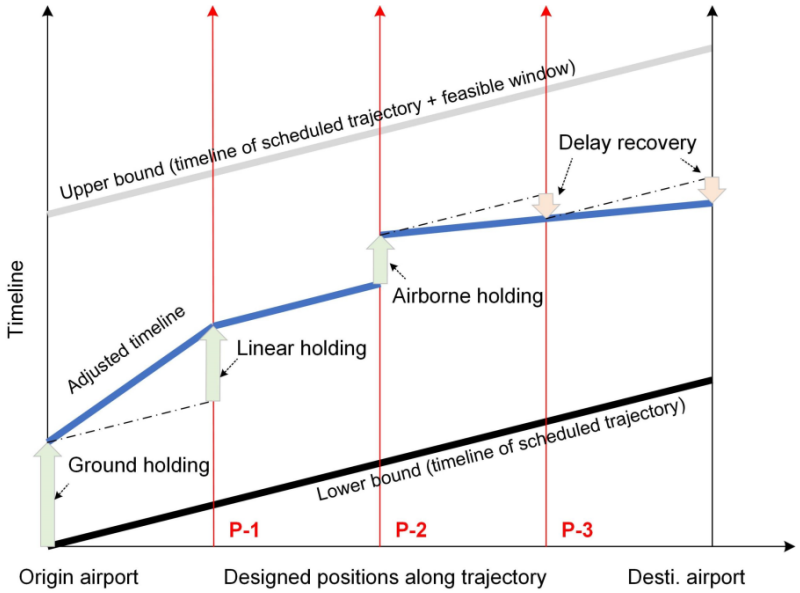

Figure VI-8: *Schematic of trajectory timeline versus designed positions.*

Then, at each designed position, ground holding is experienced only at the origin airport; airborne holding can only be performed "at" a given position (the difference between the "departure" and "arrival" time at that position equals to the holding time); and since linear holding and delay recovery are realized by speed control, the slope of the lines is increased or decreased compared with the initially planned schedule. It should be noted that all these are subject to the same principle adopted in Chapter V.

VI.3.2 Objective function

In light with the discussions in Sec. VI.2.1, the initially scheduled trajectory should represent the most preferred trajectory for a specific flight from the AUs' point of view (i.e. individual optimum). In this way, if every single initial trajectory were maintained as it is in the final execution of flights, a global optimum at system level would be achieved, which equals to the combination of all individual flight optima. Nevertheless, some regulations on those trajectories might be enforced due to certain reasons (e.g., a DCB problem), meaning that not all the individual optima can be attained.

The objective function used in the model presented in this chapter, therefore, aims to minimize such deviations[1]. Specifically, the extra fuel consumption, extra route charges, and the extra

[1]It is worth noting that for the reason of respecting the fairness principle, the objective function could be adjusted to minimize the maximum deviation of each flight, namely the Max-Min rule, in which no single flight can increase its benefits without reducing the benefits of other flights.

time related costs between the initial trajectory and that trajectory resulted from the DCB process:

$$\min J = \min(C_{\Delta F} + C_{\Delta R} + C_{\Delta T}) \tag{VI.2}$$

The summed three items correspond to those considered for the scheduling of initial trajectories (recall Sec. VI.2.1), which in turn are treated as the baseline for computing the extra costs. Accordingly, the extra fuel consumption $C_{\Delta F}$ are denoted as in Eq. VI.3.

$$C_{\Delta F} = \sum_{f \in F} \sum_{k \in K_f} \alpha_k (TJ_k^f - TJ_0^f) w_k^f \tag{VI.3}$$

where TJ_k^f and TJ_0^f are respectively the total fuel consumed with trajectory k and with the initial trajectory of flight f. Note that $k \in K_f$, where k is one of the trajectory options K_f submitted by flight f. In this case, if the initial trajectory is eventually selected, then the extra cost incurred from the fuel consumption for flight f would equal to zero. Similarly, the extra route charges $C_{\Delta R}$ are computed by Eq. VI.4, where RC_k^f and RC_0^f are the total ATS fees charged with trajectory k and with the initial trajectory of flight f. α_k and β_k are respectively the weighting cost of extra fuel and extra route charges, which in turn could be specified by AUs on a trajectory basis.

$$C_{\Delta R} = \sum_{f \in F} \sum_{k \in K_f} \beta_k (RC_k^f - RC_0^f) w_k^f \tag{VI.4}$$

It should be noted that, due to practical reasons, the route charges are nowadays paid based on the GCD between the entry and exit positions within the (different) charging zones based on the planned (initially scheduled) trajectory. They are not re-charged for the added and/or reduced distances caused from tactically altering the trajectories (Delgado, 2015). However, this may not reflect well the real air traffic services that they use. Therefore, aiming at future TBO concept of precise operations, this chapter calculates the route charges, for each flight, using the absolute distances along the flown trajectory inside the charging zones. Moreover, this is the most generic formulation of the model presented in this chapter and $C_{\Delta R}$ could always be set to zero if applying the current charging policy.

Eq. VI.5 defines the time-related costs discussed in Sec. VI.2.5, which are composed of those incurred from the different delay management measures, including ground holding GH_k, air holding AH_k (i.e., standard airborne holding and linear holding), and delay recovery DR_k. It can be noticed from Eq. (VI.5) that the cost weights (i.e., γ_k, δ_k and ζ_k) of each delay measure are trajectory-specific too, which means that the values could be also specified by the AUs[2], e.g., one particular trajectory might be given higher priority through setting a greater ζ_k enabling more delays to be recovered.

$$C_{\Delta T} = \sum_{f \in F} \sum_{k \in K_f} [\gamma_k GH_k + \delta_k AH_k - \zeta_k DR_k] \tag{VI.5}$$

Since delay recovery $DR_k = GH_k + AH_k - AD_k$, where AD_k denotes the arrival delay at the destination airport, Eq. (VI.5) can be organized as follows:

$$C_{\Delta T} = \sum_{f \in F} \sum_{k \in K_f} [(\gamma_k - \zeta_k) GH_k + (\delta_k - \zeta_k) AH_k + \zeta_k AD_k] \tag{VI.6}$$

Specifically, depending on the holding positions, GH_k, AH_k, and AD_k are formulated by the respective decision variables as depicted from Eqs. (VI.7)-(VI.9):

[2]This function may raise issues of unfair competition, such as gaming, which is still under development.

$$GH_k = \sum_{t \in T_f^j, P(f,1)=j} (t - r_k^j)(x_{k,t}^j - x_{k,t-1}^j), \tag{VI.7}$$

$$AH_k = \sum_{t \in T_k^j, j \in P(k,i):1<i<n_k} t(x_{k,t}^j - x_{k,t-1}^j - y_{k,t}^j + y_{k,t-1}^j), \tag{VI.8}$$

$$AD_k = \sum_{t \in T_k^j, P(k,n_k)=j} (t - r_k^j)^{1+\epsilon}(y_{k,t}^j - y_{k,t-1}^j). \tag{VI.9}$$

Taking into account the fairness factor of delay assignment, the total delay is multiplied by a coefficient $(t - r_f^k)^{1+\epsilon}$, with $\epsilon > 0$ in Eq. (VI.9), in such a way that the delays would be assigned moderately across all the flights (Bertsimas & Patterson, 1998), instead of unevenly to one particular flight.

VI.3.3 Constraints

The constraints concerned with the model are categorized into four groups, including aircraft operations, user-specified limits, network capacities, and decision variables.

VI.3.3.1 Aircraft operations

$$\sum_{k \in K_f} w_k^f = 1 \quad \forall f \in F, \tag{VI.10}$$

$$x_{k,\underline{T}_k^j - 1}^j = y_{k,\underline{T}_k^j - 1}^j = 0 \quad \forall f \in F, \forall k \in K_f, \forall j \in P_k, \tag{VI.11}$$

$$x_{k,\overline{T}_k^j}^j = y_{k,\overline{T}_k^j}^j = w_k^f \quad \forall f \in F, \forall k \in K_f, \forall j \in P_k, \tag{VI.12}$$

$$x_{k,t}^j - x_{k,t-1}^j \geq 0 \quad \forall f \in F, \forall k \in K_f, \forall j \in P_k, \forall t \in T_k^j, \tag{VI.13}$$

$$y_{k,t}^j - y_{k,t-1}^j \geq 0 \quad \forall f \in F, \forall k \in K_f, \forall j \in P_k, \forall t \in T_k^j, \tag{VI.14}$$

$$x_{k,t}^j - y_{k,t}^j \leq 0 \quad \forall f \in F, \forall k \in K_f, \forall j \in P_k, \forall t \in T_k^j. \tag{VI.15}$$

Constraint (VI.10) enforces that only one trajectory of all submitted options (including the initial and alternatives) is eventually selected for each flight. Constraints (VI.11)-(VI.12) guarantee that each selected trajectory k, (i.e., under the condition of $w_k^f = 1$, otherwise if $w_k^f = 0$ then all decision variables associated with the unselected trajectory are equal to 0), is assigned with only one time slot for departing and arriving respectively at position j within the prescribed time window T_k^j. Constraints (VI.13) and (VI.14) ensure the timeline's continuity, namely if an aircraft arrived/departed at time $t-1$ then it must have arrived/departed at time t. Constraint (VI.15) specifies that the departure time is not earlier than the arrival time for any aircraft at any position.

VI.3.3.2 User-specified limits

$$y^{j'}_{k,t+u^{j,j'}_k z^{j,j'}_k} - x^j_{k,t} \leq 0 \quad \forall f \in F, \forall k \in K_f, \forall i \in [1, n_k - 1] : P(k,i) = j, \\ P(k,i+1) = j', \forall t \in T^j_k \cap (T^{j'}_k - u^{j,j'}_k z^{j,j'}_k), \tag{VI.16}$$

$$x^j_{k,t+v^{j,j'}_k z^{j,j'}_k} - y^j_{k,t} \geq 0 \quad \forall f \in F, \forall k \in K_f, \forall i \in [1, n_k - 1] : P(k,i) = j, \\ P(k,i+1) = j', \forall t \in T^j_k \cap (T^j_k - v^{j,j'}_k z^{j,j'}_k). \tag{VI.17}$$

Constraints (VI.16) and (VI.17) present the user-specified limits, which stipulate the time bounds of delay recovery and linear holding respectively, i.e., the segment flight time allowed in comparison with the initially scheduled one. This information is to be shared by AUs (see Chapter V for details on how to compute the time bounds, per flight, under certain operating costs), and they are set to zero as default if such information is not provided.

VI.3.3.3 Network capacities

$$\sum_{f \in F} \sum_{k \in K_f : P(k,1) = j} \sum_{t \in T^j_k \cap T(\tau)} (x^j_{k,t} - x^j_{k,t-1}) \leq C^D_j(\tau) \quad \forall j \in P_{ap}, \forall \tau \in \mathcal{T}, \tag{VI.18}$$

$$\sum_{f \in F} \sum_{k \in K_f : P(k,n_k) = j} \sum_{t \in T^j_k \cap T(\tau)} (y^j_{k,t} - y^j_{k,t-1}) \leq C^A_j(\tau) \quad \forall j \in P_{ap}, \forall \tau \in \mathcal{T}, \tag{VI.19}$$

$$\sum_{f \in F} \sum_{k \in K_f : P(k,i) = S(k,l,\tau), i \in [1,n_k]} \sum_{t \in T^j_k \cap T(\tau)} (x^j_{k,t} - x^j_{k,t-1}) \leq C^S_l(\tau) \\ \forall l \in P_{sc}(\tau), \forall \tau \in \mathcal{T}. \tag{VI.20}$$

Constraints (VI.18), (VI.19) and (VI.20) ensure that the traffic demand does not exceed the capacity of departure airport, arrival airport and airspace sector, respectively. As discussed in Sec. VI.2.2, the situation for airport is relatively clear, while in the case of airspace sector, the opening scheme $S(l, \tau)$ has to be taken into account (recall Algorithm C.1). Accordingly, operating sectors l are used for matching the demand and capacity, instead of elementary sectors j at which the control points are defined in this chapter. Meanwhile, as shown with Algorithm VI.1, only the first aircraft entry into an operating sector among all the entered elementary sectors (if any) that belong to the operating sector during the certain time period τ, i.e., $P(k,i) = S(k,l,\tau)$ in Constraint (VI.20), is counted as a valid demand.

VI.3.3.4 Decision variables constraints

$$w^f_k \in 0, 1 \quad \forall f \in F, \forall k \in K_f, \tag{VI.21}$$

$$x^j_{k,t}, y^j_{k,t} \in 0, 1 \quad \forall f \in F, \forall k \in K_f, \forall j \in P_k, \forall t \in T^j_k. \tag{VI.22}$$

Constraints (VI.21) and (VI.22) declare the binary (0-1) decision variables and the associated domains of the problem. In addition, the model is also capable of iterative executions in response

to possible updates of the forecast information, such as the capacity changes due to improvements of weather conditions. In this case, additional constraints need to be imposed on certain decision variables, while a further discussion is included in Appendix C.

VI.4 Numerical experiments

This section presents the numerical experiments conducted under the proposed framework, with a real-world case study. The French airspace is considered along with 24h of traffic gathered from historical demand on February 20th 2017. All source data used in the experiments are based on the DDR2 database. Two case studies are considered, corresponding to two different operational modes in the route planning: following the ATS structured route (SR) network (see Fig. VI-9(a)) and full free route (FR) from origin to destination airports (see Fig. VI-9(b)). These case studies are labeled as Case-SR and Case-FR, respectively.

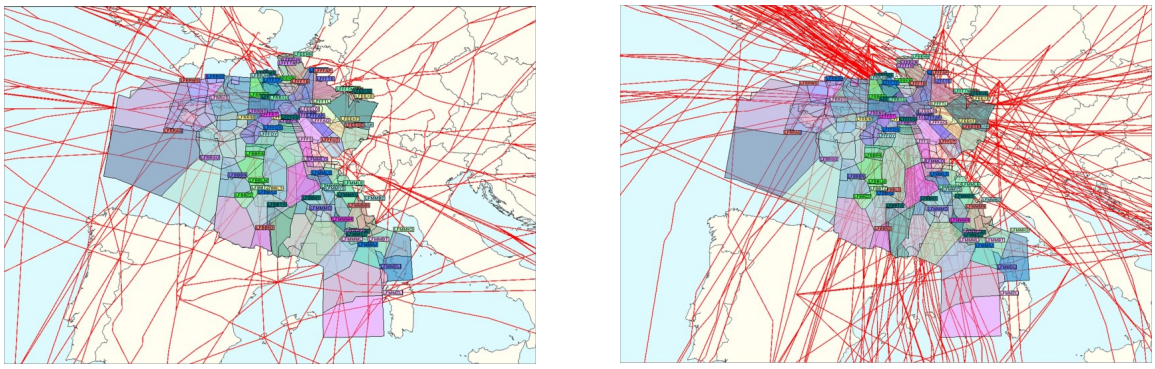

(a) Case-SR: structured route mode (b) Case-FR: free route mode

Figure VI-9: *Initial trajectories of 24 hours' scheduled flights traversing the French airspace (Source: Eurocontrol's NEST modelling tool).*

VI.4.1 Experimental setup

The original sample data involve 6,593 planned flights in total, but there appear some cases that their initial trajectories only form a small part of intersection with the airspace sectors. Due to operational limits, this temporal intersection is typically not counted as an independent flight entry. In this study, 60 sec is regarded as the minimal time spent in a sector. After removing those intersections less than 60 sec, there are 6,255 and 6,387 flights left for respectively Case-SR and Case-FR, which in turn, might be subject to regulations. On the other hand, The total number of elementary sectors are 164 for that day, which are merged into 224 different collapsed sectors through the 24 h period.

In addition, some important assumptions have been taken in this case study: 1) the unit time slot in the experiments is set to 1 min, while the time scale for matching demand and capacity is 20 min; 2) the costs of delay are linear, and apply the same across all the flights (i.e., 15 euro/min for ground holding and 20 euro/min for air holding including the standard airborne holding and linear holding); 3) the upper bound for performing linear holding is 20% of the segment flight time, and for delay recovery this bound is set to 10%, both of which are rounded to the greatest integer that is less than or equal to; 4) the cost of delay recovery is -5 euro/min, meaning that

all the flights would be in favor of increasing certain speed (burning some extra fuel) to recover part of their previously experienced delays[3]; 5) the price of fuel is 0.4 euro/liter, i.e., nearly 0.5 euro/kg; and 6) the route charges are calculated based on the absolute distance flown inside the charging zones.

VI.4.2 Benchmark indicators

Table VI-2 presents a set of benchmark results, namely, implementing CASA (Computer Assisted Slot Allocation) and Collaborative ATFM (with GH mode) to solve exactly the same problems in Case-SR and Case-FR. Note that the collaborative trajectory design process (as introduced in Sec. VI.2) is not allowed here. CASA is a function within Eurocontrol's Enhanced Tactical Flow Management System that follows the principle of Ration-By-Schedule (RBS) and matches traffic demand and airspace capacity by delaying flights' departure times (Cook, 2007). On the other hand, Collaborative ATFM (with GH mode) means that all the possible measures mentioned in Sec. VI.2.4 and Sec. VI.2.5 are disabled, except for ground holding, so that it seems quite similar to CASA. The key difference, however, is that the RBS "constraint" is not respected for Collaborative ATFM (GH mode).

Table VI-2: *Benchmark results for CASA and Collaborative ATFM (GH mode).*

Cases	Total delayed flights (a/c)	Total delay (min)
Case-SR (CASA)	2,510	406,042
Case-SR (GH mode)	1,840	219,862
Case-FR (GH mode)	1,798	207,506

As Table VI-2 shows, only about half of the delays are required by Collaborative ATFM (GH mode) with respect to those needed by CASA. This reveals, on some level, the trade-off between efficiency (i.e., minimizing the total delay cost in Collaborative ATFM - GH mode) and fairness (i.e., obeying the "first-come, first-served" principle in CASA). In other words, Collaborative ATFM (GH mode) gives the minimum delay (since it optimizes the delay assignment), while CASA always assigns slots according to that fairness rule. Note that the trade-off effects could be further enlarged for a greater network, as there will be even larger amount of nodes (airports and/or sectors) where the RBS rule should apply.

Worth noting that, a certain amount of capacity overloads are usually allowed in reality (and in some cases the allowance can be quite large). This could be due to several reasons, such as the lack of initial schedules for pop-up flights, the conservative method for capacity evaluation, and the current way of counting traffic demand (i.e., flight entry rate) without considering the factors of occupancy, traffic pattern and complexity. Nevertheless, for the illustrative purpose, any capacity allowance is not allowed in this study, which also accounts for the huge delays (see Table VI-2) assigned in these benchmark experiments that should not occur in real-world operations.

VI.4.3 Hotspot detection and trajectory options

The results using Collaborative ATFM, with full-functional mode, are presented hereafter. Through the hotspot detection process (recall Sec. VI.2.2), there are 86 (in Case-SR) and 115 (in Case-FR) time-varying hotspots identified. Then, the captured flights (1,464 and 1,813) are required to provide alternative trajectories making use of the sector avoidance information shared to each of them (see Sec. VI.2.3). In Case-SR, 1,305 lateral and 1,379 vertical alternative trajectories

[3]It should be noted that the delay recovery is only allowed when a flight is assigned with delays at its trajectory forepart, such as ground holding at the origin airport.

are generated by AUs and thereby all returned to the NM, while in Case-FR the numbers are 1,628 and 1,727 respectively. The missing ones are due to the fact that some hotspot volumes may be located close to origin/destination airports and/or restricted areas and consequently can not be avoided either with lateral and/or vertical trajectory alternatives. Generally, there are 8,939 (6,255 initial + 1,305 lateral + 1,379 vertical) trajectories scheduled for 6,255 flights in Case-SR, and in Case-FR, those are 9,742 (6,387 initial + 1,628 lateral + 1,727 vertical) trajectories for 6,387 flights.

Table VI-3: *Problem size and computational time.*

Summary	Case-SR	Case-FR
Variables	4,822,740	5,546,029
Equations	11,307,028	13,045,946
Non-zero elements	27,543,864	28,646,435
Generation time (min)	2	2
Solution time (min)	150	240
Objective value	129,027	240,768
Relative gap	0,05%	0,10%

Finally, with all these trajectory options taken as input to the system-wide optimization model (presented in Sec. VI.3), the problem dimensions for each of the two cases are summarized in Table VI-3. As the mathematical formulation is based on the Bertsimas Stock-Patterson Model, see (Bertsimas & Patterson, 1998) for the insights from the polyhedral structure and computational performance of this type of model. In the numerical experiments, GAMS v.24.2 software suite has been used as the modeling tool and Gurobi v.5.6 MIP optimizer has been used as the solver. The computations have been run on a 64 bit Intel i7-4790 @ 3.60 GHz quad core CPU computer with 16 GB of RAM memory and Linux OS.

VI.4.4 Overall demand and capacity situations

Figs. VI-10(a) and VI-10(b) present firstly the initial (i.e., pre-regulation) demand for each considered operating sector during each time period. The sequence has been ordered in accordance with the operating sectors' activation time in that day (but is arbitrary within each 20 min period). It can be also noticed that there are more sectors opened from 6 AM to 18 PM than the reverse, which is also roughly in line with the distribution of traffic occurrence.

Seeing from Figs. VI-11(a) and VI-11(b), indeed, large numbers of capacity overloads (i.e., demand higher than capacity) can be found, while in some cases it could be as high as twice the capacity value that the sector can provide. Moreover, the situation tends to be even worse for the free route case (i.e., Case-FR), if comparing Fig. VI-11(b) with Fig. VI-11(a). This is because, in the free route mode, different flights yet with the same origins and destinations may always find similar (or the same) lateral routes and/or vertical profiles to be their most cost-efficient trajectories. In such case, the (spatial) distribution of those initially scheduled trajectories would be less proportional, and thus yields more capacity overloads in some particular areas.

In addition, to further understand the balance between demand and capacity, their ratios are sorted (based on the initial demand) and presented in Fig. VI-12(a) and VI-12(b). Obviously, the curves representing pre-regulation (i.e., initial) are steeper with some parts growing higher than 1 (i.e., demand higher than capacity). On the contrary, the curves turn to be level and average with respect to the post-regulation cases, which means that more airspace capacities are well utilized. It is also worth noting that in Case-FR more exceeded demands are shifted to the place where the initial demand/capacity ratios are relatively low (see the area within 0-1500 operating sectors in Fig. VI-12(a) and VI-12(b)). Besides the higher traffic demand itself in Case-FR, this is also due to the fact that the free route mode enables flights to traverse some sectors that are not connected

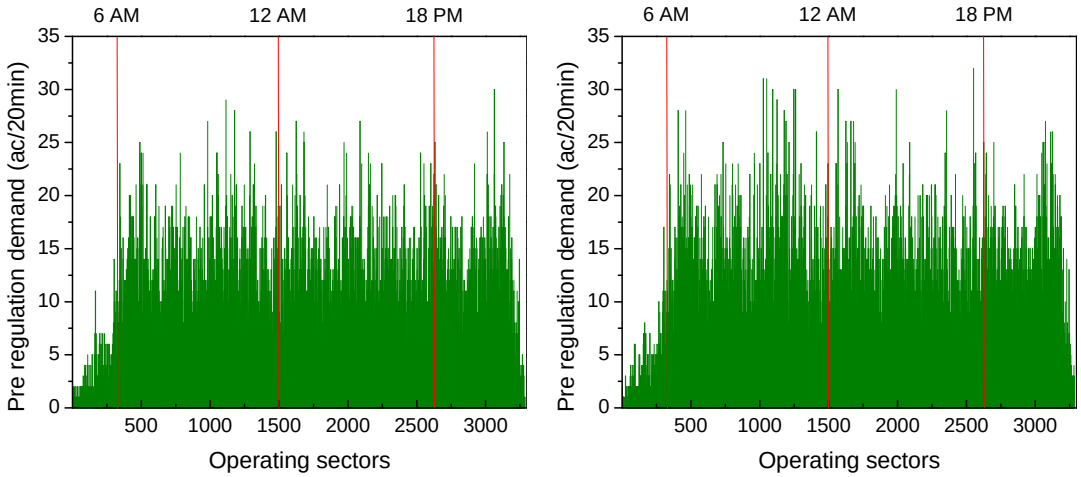

(a) Initial demand in Case-SR (b) Initial demand in Case-FR

Figure VI-10: *Initial traffic demand for each operating sector during each time period.*

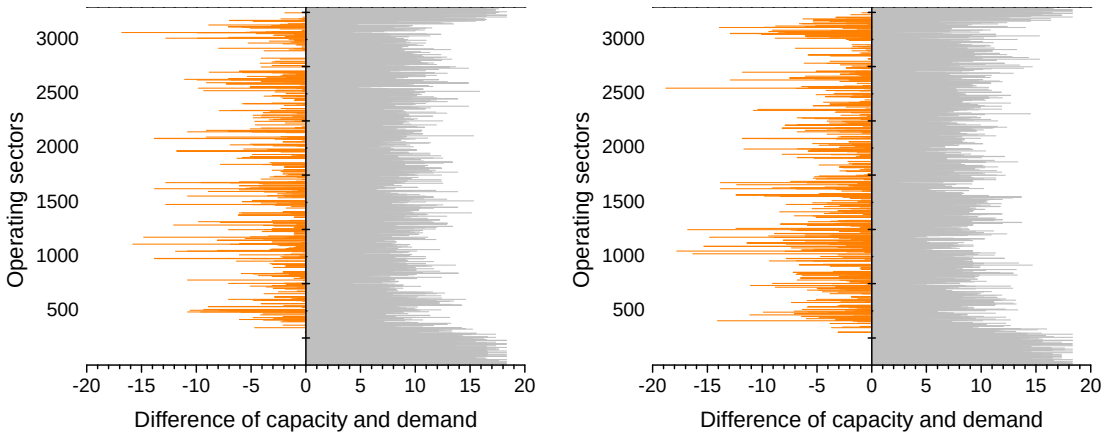

(a) Imbalance in Case-SR (b) Imbalance in Case-FR

Figure VI-11: *Imbalances between capacity and demand in the operating sectors.*

under the structured route mode.

VI.4.5 Trajectory selections and delay assignments

As mentioned previously, any of the measures proposed in Sec. VI.2.4 and Sec. VI.2.5 can be integrated together and imposed on a particular flight. In other words, for this case study there should be in theory $3 * (2^4 - 1) = 45$ (recall formula $N_k^f(2^{N_d^k} - 1)$ in Sec. VI.3.1) maximal different types of combinations in total, where 3 is the different trajectory options (initial trajectory or lateral/vertical alternatives), 4 corresponds to the different ways to manage delay (ground holding, airborne holding, linear holding and delay recovery). For example, an aircraft might be asked to experience some ground holding at the origin airport, fly its lateral alternative trajectory, undertake a small amount of airborne or linear holding en route, whilst being allowed to partially recover those delays along the remaining trajectory.

For the full version of Collaborative ATFM, the detailed results of trajectory selections and delay assignments can be appreciated from Table VI-4 through Table VI-7. The most promising result would be that the total (arrival) delay is reduced respectively to 4,691 min for Case-SR (see

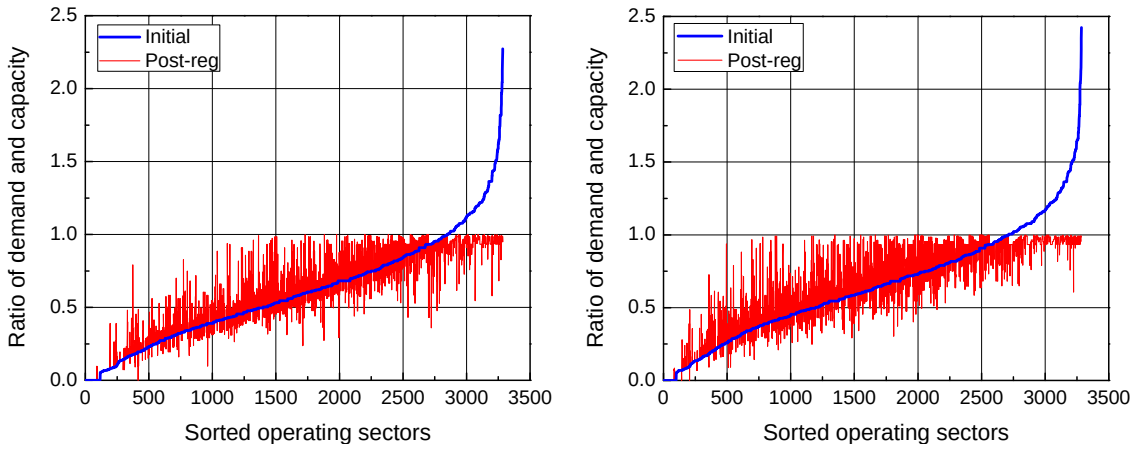

(a) Case-SR (b) Case-FR

Figure VI-12: *Sorted ratios of demand and capacity for initial and post-regulation situations.*

Table VI-4: *Summary of trajectory selections and delay assignments in Case-SR.*

Options	Initial		Lateral alter.		Vertical alter.		Total	
	5,546		388		321		6,255	
	Flight (a/c)	Time (min)	Flight (a/c)	Time (min)	Flight (a/c)	Time (min)	Flight (a/c)	Time (min)
GH	1,052	5,269	58	253	72	357	1,182	5,879
Non-GH	4,494	-	330	-	249	-	5,073	-
AH	34	249	1	1	4	34	39	284
Non-AH	5,512	-	387	-	317	-	6,216	-
LH	58	148	1	3	8	18	67	169
Non-LH	5,488	-	387	-	313	-	6,188	-
DR	765	-1,443	52	-106	55	-92	872	-1,641
Non-DR	4,781	-	336	-	266	-	5,383	-
AD	751	4,223	38	151	59	317	848	4,691
Non-AD	4,795	-	350	-	262	-	5,407	-

* GH-ground holding; AH-airborne holding; LH-linear holding; DR-delay recovery; AD-arrival delay

Table VI-4) and 5,836 min for Case-FR (see Table VI-5). Remember when using Collaborative ATFM with GH mode, the numbers are both greater than 200,000 min (see Table VI-2), which means that the delay reduction (by using the full version) is nearly 97%. Nevertheless, in compensation with the remarkable reduced delays, there are respectively 709 (388 lat. + 321 ver.) and 953 (376 lat. + 577 ver.) flights diverted to their alternative trajectories in Case-SR and Case-FR, respectively.

Furthermore, if comparing the total number of regulated flights, the difference between the GH mode and full mode is relatively small. For the GH mode, the only available measure is ground holding, and the flights captured to execute it are 1,840 and 1,798 (see Table VI-2). For the full version, the regulated flights (i.e., performing any of the available measures) are at least 1,768 (i.e., 6,255 - 4,487) and 2,140 (i.e., 6,387 - 4,247) as shown in Table VI-6 and Table VI-7. They are derived by the total number of flights deducting the ones keeping initial trajectory whilst having neither departure delay nor arrival delay. However, the reason of "at least" is because there may exist some flights meeting this criteria but also having some airborne and/or linear holding en route, along with the same amount of delay recovery. In other words, part of their initial trajectory has been revised (on the timeline), and thus they should be regarded as regulated flights as well.

Table VI-5: *Summary of trajectory selections and delay assignments in Case-FR.*

Options	Initial		Lateral alter.		Vertical alter.		Total	
	5,434		376		577		6,387	
	Flight (a/c)	Time (min)	Flight (a/c)	Time (min)	Flight (a/c)	Time (min)	Flight (a/c)	Time (min)
GH	1,173	6,362	89	278	149	467	1,411	7,107
Non-GH	4,261	-	287	-	428	-	4,976	-
AH	54	308	4	9	7	10	65	327
Non-AH	5,380	-	372	-	570	-	6,322	-
LH	87	189	6	14	8	13	101	216
Non-LH	5,347	-	370	-	569	-	6,286	-
DR	837	-1,516	69	-140	107	-158	1,013	-1,814
Non-DR	4,597	-	307	-	470	-	5,374	-
AD	890	5,343	54	161	110	332	1,054	5,836
Non-AD	4,544	-	322	-	467	-	5,333	-

Table VI-6: *Mixed types of delay assignments in Case-SR.*

Mixed options	Initial			Lateral alter.		
	Flight (a/c)	GH (min)	AD (min)	Flight (a/c)	GH (min)	AD (min)
GH + AD	744	4,678	4,187	38	214	151
GH + Non-AD	308	591	-	20	39	-
Non-GH + AD	7	-	36	0	-	0
Non-GH + Non-AD	4,487	-	-	330	-	-

Mixed options	Vertical alter.			Total		
	Flight (a/c)	GH (min)	AD (min)	Flight (a/c)	GH (min)	AD (min)
GH + AD	57	330	314	839	5,222	4,652
GH + Non-AD	15	27	-	343	657	-
Non-GH + AD	2	-	3	9	-	39
Non-GH + Non-AD	247	-	-	5,064	-	-

As for the difference between Case-SR and Case-FR, it can be seen that more flights are assigned to their alternative trajectories (recall that there are more capacity overloads appearing in Case-FR as shown in Fig. VI-11(a) and VI-11(b)). Delays imposed on the regulated flights are also higher in Case-FR than in Case-SR. Among the different ways, ground holding is obviously the most-commonly used, absorbing almost all the required system delays, but it appears in both Cases (see Table VI-4 and VI-5) that a small amount of airborne holding (284 min and 327 min) and linear holding (169 min and 216 min) could contribute to minimizing the total cost even if their unit cost of 20 euro/min is higher (than 15 euro/min the cost of ground holding). This is due to the fact that if any delay must be transferred from the capacity-affected area to the origin airport by executing ground holding, then it is the largest delay that will be issued once delays are actually required for (different) sectors, within the network, that the flight traverses. In addition, the way of delay recovery has the same effects as well, because some available capacity (or empty slot), caused from delaying a flight, can be taken by the other flight that is able to advance its arrival time to the certain place, which is similar to an intermediate slot swapping process.

Table VI-7: *Mixed types of delay assignments in Case-FR.*

Mixed options	Initial			Lateral alter.		
	Flight (a/c)	GH (min)	AD (min)	Flight (a/c)	GH (min)	AD (min)
GH + AD	876	5,882	5,260	51	201	148
GH + Non-AD	297	480	-	38	77	-
Non-GH + AD	14	-	83	3	-	13
Non-GH + Non-AD	4,247	-	-	284	-	-

Mixed options	Vertical alter.			Total		
	Flight (a/c)	GH (min)	AD (min)	Flight (a/c)	GH (min)	AD (min)
GH + AD	106	408	327	1,033	6,491	5,735
GH + Non-AD	43	59	-	378	616	-
Non-GH + AD	4	-	5	21	-	101
Non-GH + Non-AD	424	-	-	4,955	-	-

VI.4.6 Extra fuel consumption and extra route charges

Benefiting from the accurate avoidance information for individual flight (see Sec. VI.2.3), the alternative trajectory that is precisely re-scheduled by AUs may incur as less extra costs (compared to the initially scheduled) as possible. The distributions of extra fuel consumption and extra route charges for the respective lateral and vertical alternative trajectories are presented in Fig. VI-13. The overall alternatives are labeled with Lat and Ver, while the eventually selected, after regulation, are distinguished with Lat-S and Ver-S (which usually yield even less costs than the overall situation). In addition, the detailed costs (e.g., total trip fuel and total charged fees) are given in Appendix D using a specific flight as an illustrative example.

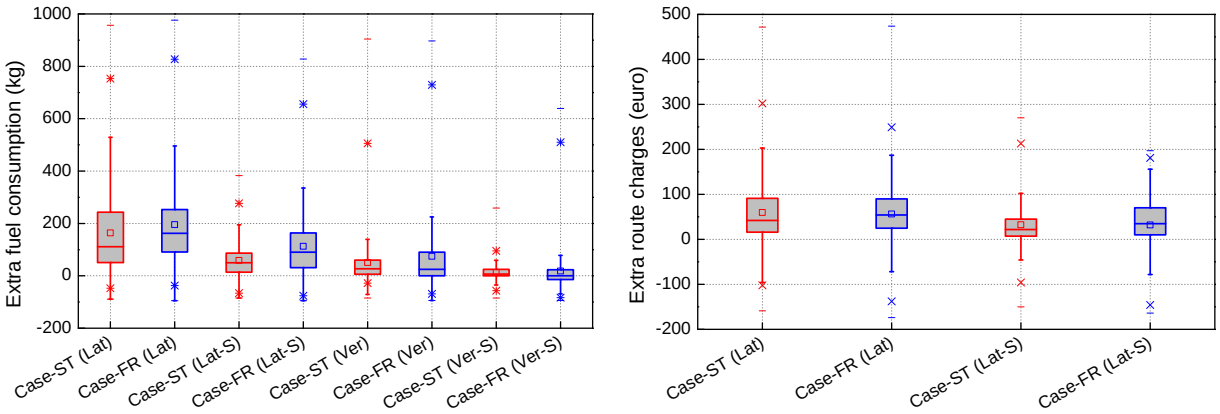

(a) Extra fuel consumption (b) Extra route charges

Figure VI-13: *The distribution of extra fuel consumption and extra route charges for the lateral and vertical alternative trajectories with respect to the initial trajectory.*

As can be seen in Fig. VI-13(a), an average of less than 100 kg extra fuel consumption, per flight choosing the alternative trajectory, is burned. The average cost of route charges, on the other hand, increases by only 50 Euro per diverted flight, as shown in Fig. VI-13(b). The extra fuel is higher in Case-FR than in Case-SR among most trajectories for the lateral alternative, while being similar for the vertical. This is because when producing the lateral trajectory in free route mode, a grid graph is used to replace the structured routes, and the grid might be too coarse that even

more distance is required to avoid a sector in lateral. It can be noticed from Table VI-4 and Table VI-5 that the percentage of selecting vertical alternative trajectories is higher in Case-FR than in Case-SR, and this can be one of the reasons. Another reason could be that, as shown in Fig. VI-13(b), there is no extra route charges for the vertical as typically needed by the lateral alternative trajectory.

VI.5 Chapter summary

A coordinated trajectory design process between AUs and the NM aligned with the CDM principle was presented in this chapter. During the process, based on the user-preferred trajectories initially planned by the AUs, some time-varying hotspot airspaces are detected, with which the NM shares detailed avoidance information to each concerned flight. In such a way, accurate alternative trajectories can be produced to avoid the corresponding hotspot areas, incurring as few extra costs as possible. AUs are then allowed to submit the newly scheduled alternative trajectories (in addition to the initial trajectory) as options for each of their affected flights, and are also allowed to specify preferences with regard to different types of delay. To manage the traffic flow in a more flexible way, a linear optimization model was established to incorporate all these options (i.e., different trajectories plus delays), while minimizing the overall deviation to the initial status that is user-preferred.

Real-world operational data were collected and processed in a case study to provide a realistic assessment of the framework for a typical operational day in the French airspace. Results show a significant delay reduction of 97% under the proposed framework, compared to the system delay that is required using the current ATFM tool in Europe, which is mainly contributed by the 10%-15% rerouting flights. Due to the precise scheduling of alternative trajectories (based on the hotspot-oriented avoidance information), their selection only incurs an average of less than 100 kg extra fuel consumptions plus 50 euro extra route charges per diverted flight. Besides, when ground holding remains the only option, delay reduction is lowered to 46% , which highlights the importance of the proposed trajectory design process.

It had long since come to my attention that people of accomplishment rarely sat back and let things happen to them. They went out and happened to things.

— Leonardo Da Vinci

VII

Enhanced Collaborative ATFM with AUs and ANSPs involvement

This chapter proposes a strategy to further incorporate the involvement of Air Navigation Service Providers (ANSPs) into the previously-presented Collaborative Air Traffic Flow Management (ATFM) model, synchronizing traffic flow optimization and sector opening scheduling, with the aim of achieving an even more flexible demand and capacity balancing (DCB). A mixed integer linear programming (MILP) model is built to combine the delay assignment, alternative trajectory options and sector opening adjustment all together, in such a way to manage the traffic flow and sector opening at the same time. For better illustrating the effects of such synchronization process, the two DCB models presented in Chapter V and Chapter VI are briefly reviewed and simplified appropriately, which are then used to generate the respective baseline and benchmark results for the new model introduced in this chapter.

VII.1 Simplify ATFM models in previous chapters

This section briefly reviews the ATFM models presented in the two previous chapters, and performs certain simplification upon them respectively. This will help to clarify the synchronization explained in the next section. Concretely, the first model in this section uses only delay assignment, which serves as the baseline of this chapter. Based on it, the second model includes alternative trajectory options, and provides key benchmark results. To distinguish the terminology from their full versions, here they are labeled with Model DCB and Model C-DCB as follows, along with the new model proposed as Model SC-DCB.

- **Model DCB**: assigning delays;
- **Model C-DCB**: assigning delays, and allowing alternative trajectory options;
- **Model SC-DCB**: assigning delays, allowing alternative trajectory options, and adjusting sector opening schemes.

It should be noted that, Model DCB and Model C-DCB correspond to respectively the network ATFM model introduced in Chapter V and the collaborative ATFM model in Chapter VI, but they are both simplified, being ground holding used as the only initiative for delay absorption.

VII.1.1 Baseline model for network ATFM: Model DCB

Model DCB aims at balancing traffic demand under capacity through assigning ground delays to certain flights. The demand is counted according to the 4-Dimensional (4D) trajectories initially scheduled by the airspace users (AUs). Meantime, the capacity is considered in form of aircraft entry rate. It is determined by the fixed airspace structures and the airspace sectors' unit capacity values, which, in turn, were planned and evaluated well in advance based on the historical data.

VII.1.1.1 Decision variables

Aiming at future trajectory based operations (TBO), delays are imposed in this chapter at each control point along the planned trajectory, with the Controlled Time of Arrival (CTA) concept, which is defined at each entrance position of elementary sector that the trajectory is scheduled to traverse. Subsequently, in order to assign the CTAs, we consider a set of decision variables as follows:

$$x^j_{f,t} = \begin{cases} 1, & \text{if flight } f \text{ arrives at elementary sector } j\text{'s entrance by time } t \\ 0, & \text{otherwise} \end{cases}$$

Other than the model presented in Chapter V, where various cost-based delay initiatives were adopted, this chapter considers only ground holding. The reason is because ground holding is still the cheapest and commonly-used way to absorb delays nowadays. Furthermore, the inclusion of other types of delay will not essentially change the DCB synchronization process, and thus is simplified in this particular chapter.

VII.1.1.2 Model formulation

The objective function (VII.1) of Model DCB is simply to minimize the total amount of delay assignments. Fairness issues could be partially taken into account by adding a small super-linear factor ϵ ($\epsilon > 0$) to the cost of delay for each flight, namely $(t - r^j_f) \rightarrow (t - r^j_f)^{1+\epsilon}$, as mentioned previously. However, as the equilibrium criteria is relatively subjective and also proves to have notable trade-offs with the system efficiency (Bertsimas *et al.*, 2011), it deserves another separate discussion. For convenience, we set ϵ to 0 for all the three model variants in this chapter, focusing only on the overall costs.

$$\min \sum_{f \in F} \sum_{j=J_f(1)} \sum_{t \in T^j_f} (t - r^j_f)(x^j_{f,t} - x^j_{f,t-1}), \tag{VII.1}$$

$$\text{s.t.} \quad x^j_{f,\underline{T}^j_f - 1} = 0,\ x^j_{f,\overline{T}^j_f} = 1 \quad \forall f \in F, \forall j \in J_f, \tag{VII.2}$$

$$x^j_{f,t} - x^j_{f,t-1} \geq 0 \quad \forall f \in F, \forall j \in J_f, \forall t \in T^j_f, \tag{VII.3}$$

$$x^{j'}_{f,t+\hat{t}^{jj'}_f} - x^j_{f,t} = 0 \quad \forall f \in F, \forall t \in T^j_f, j = J_f(i), j' = J_f(i+1) : \forall i \in [1, n_f), \tag{VII.4}$$

$$\sum_{f \in F} \sum_{j = J^\tau_{f,l}} \sum_{t \in T^j_f \cap \tau} x^j_{f,t} - x^j_{f,t-1} \leq c^\tau_l \quad \forall l \in L_\tau, \forall \tau \in \mathcal{T}, \tag{VII.5}$$

$$x^j_{f,t} \in 0, 1 \quad \forall f \in F, \forall j \in J_f, \forall t \in T^j_f. \tag{VII.6}$$

Constraint (VII.2) specifies the boundary of CTA at each control point for each flight, i.e., T^j_f, which depends on the corresponding Estimated Time of Arrival (ETA) added with an allowable maximal amount of delay. Constraint (VII.3) guarantees the timeline continuity of the decision variables. Since this model allows ground delay only, Constraint (VII.4) ensures that the airborne (segment) flight time for the controlled flight assigned with CTAs will still remain the same as the initially scheduled. Then, the airspace capacity constraints are enforced in (VII.5), where we may notice an inconsistence between the capacity entity (i.e., operating sector l) and the control point (i.e., elementary sector j). To solve this issue, we follow the commonly-used rule that, for each flight, only the first entry (control point) into an operating sector is counted, namely $j = J^\tau_{f,l}$. The remaining entries (if any) inside this operating sector during the same period will be regarded as internal activities, not another traffic demand. Finally, all decision variables are subject to Constraint (VII.6).

VII.1.2 Benchmark model for Collaborative ATFM: Model C-DCB

Model C-DCB is based on the previous Model DCB but requires more contributions from the AUs. Besides the submission of the initially planned trajectories, AUs are allowed in this model to submit a number of alternative trajectories for their affected flights in order to route out of the detected hotspot areas. The model will then decide which is the best distribution of trajectory selections and delay assignments for all the flights based on a centralized global optimization.

VII.1.2.1 Trajectory options

The key difference of Model C-DCB compared to Model DCB is that it allows more trajectory options for every single flight, rather than only having the initially planned one. In the previous Chapter VI, we have introduced a way of sharing the hotspot-avoidance information, aiming to assist AUs to schedule their alternative trajectories with as few extra costs as possible. Nevertheless, it must be noted that the submission of any alternative is not mandatory, and should be subject to the AUs' independent decisions. The operators could always keep the original one only, if for example the extra costs of all the feasible alternatives are relatively high.

On the other hand, if the extra costs are quite small, the flight simply needs to change its cruise flight level slightly such that two hotspot sectors can be avoided, then it might be worthwhile to submit it because in this way its potential delays might be avoided. In addition, if there exist some other flight who can bypass the two hotspots with even less extra costs required, then the model would more often decide to divert that flight, which means that this flight could probably still use its initial trajectory even though it has submitted the alternatives.

Besides, not only the above hotspot-avoidance trajectories, but also some others of specific purposes can be submitted as alternatives as well. For example, as time elapsed the weather forecast usually turns more accurate, and therefore it would be appropriate to schedule a new trajectory taking advantage of the latest predictions such as the wind field condition.

To sum up, no matter for what reasons, AUs are allowed to freely submit a set of preferred trajectories in this model (see Table VII-1), and are also required to label out the corresponding costs with respect to their initial trajectories. However, how to model these costs in an effective way is still under our assessment, as in most cases the AUs' cost information is still proprietary, and misusing of this information may also lead to competition issues in realistic operations.

Table VII-1: *Possible trajectory options submitted for one flight.*

Trajectory options	Extra costs	Comments
Trajectory 0	0	Initial trajectory
Trajectory 1	Cost 1	Lateral hotspot avoidance
Trajectory 2	Cost 2	Vertical hotspot avoidance
Trajectory 3	Cost 3	Updated wind field prediction
Trajectory 4	Cost 4	Experienced congestion areas
⋮	⋮	⋮
Trajectory n	Cost n	Any specific preferences

VII.1.2.2 Decision variables

Similar to the time-related decision variables $x^j_{f,t}$ defined previously in Model DCB, we include an extra domain k representing the trajectory options in this model, as follows:

$$x^{k,j}_{f,t} = \begin{cases} 1, & \text{if flight } f\text{'s } k\text{th trajectory arrives at elementary sector } j\text{'s entrance by time } t \\ 0, & \text{otherwise} \end{cases}$$

In this case, all the control points and associated CTAs are bonded to the kth trajectory, instead of the flight itself. Therefore, in order to connect between them, this model considers an additional set of decision variables z^k_f to tell if the kth trajectory is eventually selected for that flight f, namely:

$$z^k_f = \begin{cases} 1, & \text{if flight } f\text{'s } k\text{th trajectory is selected} \\ 0, & \text{otherwise} \end{cases}$$

The two sets of variables are linked together by a following constraint, in such a way that delays are still imposed on each particular flight, rather than any of its unselected trajectories.

VII.1.2.3 Model formulation

The objective function (VII.7) of Model C-DCB is to minimize the total delay costs and the extra costs incurred from altering trajectories. we consider the fuel consumption (d^k_f) and route charges (e^k_f) in this chapter as the main trajectory-related costs, but in realities more detailed costs could be further taken account and thus specified by AUs.

$$\min \sum_{f\in F}\sum_{k\in K_f}\sum_{j=J_f^k(1)}\sum_{t\in T_f^{k,j}} \alpha(t-r_f^{k,j})(x_{f,t}^{k,j}-x_{f,t-1}^{k,j}) + \sum_{f\in F}\sum_{k\in K_f}(\gamma d_f^k + e_f^k)z_f^k, \tag{VII.7}$$

$$\text{s.t.} \quad \sum_{k\in K_f} z_f^k = 1 \quad \forall f \in F, \tag{VII.8}$$

$$x_{f,\underline{T}_f^{k,j}-1}^{k,j} = 0,\ x_{f,\overline{T}_f^{k,j}}^{k,j} = z_f^k \quad \forall f \in F, \forall k \in K_f, \forall j \in J_f^k, \tag{VII.9}$$

$$x_{f,t}^{k,j} - x_{f,t-1}^{k,j} \geq 0 \quad \forall f \in F, \forall k \in K_f, \forall j \in J_f^k, \forall t \in T_f^{k,j}, \tag{VII.10}$$

$$x_{f,t+\hat{t}_f^{k,jj'}}^{k,j'} - x_{f,t}^{k,j} = 0 \quad \forall f \in F, \forall k \in K_f, \forall t \in T_f^{k,j}, j = J_f^k(i), j' = J_f^k(i+1) : \forall i \in [1, n_f^k), \tag{VII.11}$$

$$\sum_{f\in F}\sum_{k\in K_f}\sum_{j=J_{f,l}^{k,\tau}}\sum_{t\in T_f^{k,j}\cap\tau} x_{f,t}^{k,j} - x_{f,t-1}^{k,j} \leq c_l^\tau \quad \forall l \in L_\tau, \forall \tau \in \mathcal{T}, \tag{VII.12}$$

$$x_{f,t}^{k,j} \in 0,1 \quad \forall f \in F, \forall k \in K_f, \forall j \in J_f^k, \forall t \in T_f^{k,j}, \tag{VII.13}$$

$$z_f^k \in 0,1 \quad \forall f \in F, \forall k \in K_f. \tag{VII.14}$$

Constraint (VII.8) ensures that only one trajectory is selected for each flight from the set of its submitted trajectory options (K_f). Constraint (VII.9) and (VII.10) seem similar to those in Model DCB, but the difference is that the value at the upper bound of feasible time window ($\overline{T}_f^{k,j}$) is dependent on trajectory selection (z_f^k). The two constraints further enforce that if a trajectory is not selected, i.e., $z_f^k = 0$, then all its associated time variables are equal to 0, meaning that no CTA would be assigned to any of the control points along that trajectory. Constraints (VII.11) and (VII.12) remain the same functions as Constraints (VII.4) and (VII.5), which respectively guarantees the segment flight time and stipulates demand not to exceed the planned capacity provisions. Finally, Constraints (VII.13) and (VII.14) specify the set domains and state that all decision variables are binary.

VII.2 Enhanced Collaborative ATFM model

Model SC-DCB is to relax the hard constraint of airspace structures fixed in both Model DCB and Model C-DCB. As mentioned before, delays and alternative trajectories are used to regulate the 4-D traffic flow, which may lead to severe unfitness to the initially planned airspace structures. This model maintains all previous traffic management initiatives but also adjusts (if needed) the sector opening schemes, trying to balance the traffic demand and airspace capacity in a synchronized way.

VII.2.1 Airspace structure and capacity

According to the European airspace structure, as shown in Fig. VII-1, a large piece of airspace typically consists of several Area Control Centers (ACCs). Under current operations, each ACC normally runs independently, and has its own limited amount of configurations and the corresponding opening schemes. Next, each specified configuration is composed of several elementary sectors and/or collapsed sectors, and each collapsed sector is in turn merged by several smaller elementary sectors. In addition, the small elementary sector is further defined by a certain number of basic airblock volumes, as well as the specific bottom and top flight levels.

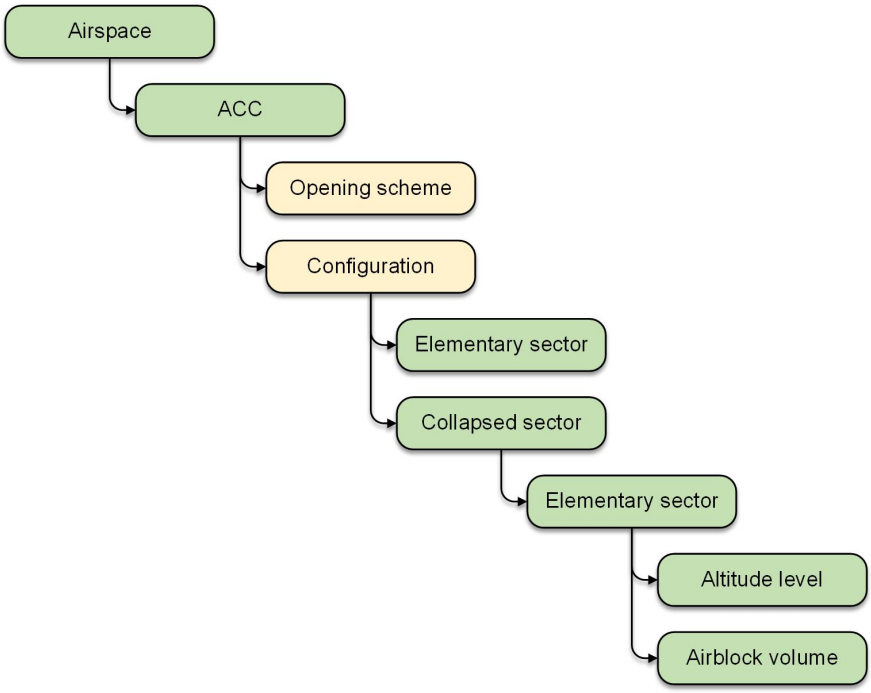

Figure VII-1: *Schematic of airspace structure implemented in the Eurocontrol area.*

However, given the basic airblock volumes typically remain stable in a relatively long period (and this chapter is focused on the pre-tactical phase), we consider elementary sectors being the smallest entities in this model. Consequently, we can imagine an entire 3-D block of airspace filled by a network of non-overlapping elementary sectors (see Fig. VII-2). With the timeline added in a 4-D scenario, sometimes a small elementary sector itself functions as an operating sector, and at another time it is merged into a larger collapsed sector that acts as another operating sector. Moreover, each operating sector is bonded with a certain operating capacity, which in turn could be associated with several Traffic Volumes. Yet, only one of them should be activated at a time.

VII.2.2 Flexible sector opening

Let us recall the overall airspace structure shown in Fig. VII-1. There could be several ways to realize dynamic airspace reconfiguration (on different levels). For example, change the opening scheme of each elementary sector, and allow any adjacent elementary sectors to collapse, which then act as a whole as an operating sector (see Fig. VII-2). In this case, some unknown collapsed sectors might be created. More concretely, it is also possible to modify the physical dimension of the elementary sector (along with its opening scheme). Namely, design new elementary sectors based on the basic airblock volumes. Furthermore, even the smallest airblock volumes could be reshaped as well, according to the traffic flow pattern or complexity appearing in that specific area for instance.

In general, the above methods could provide a precise insight into the dynamic sectorization problem, and thus result in efficient airspace reconfiguration. On the other hand, however, incorporating such complicated approaches, i.e., creating unknown collapsed/elementary sectors or airblocks, into the original model presented in this chapter may largely increase its computational burden. Note that the model is aimed to optimize not only the sectorization but also trajectory selection and delay assignment in the meantime.

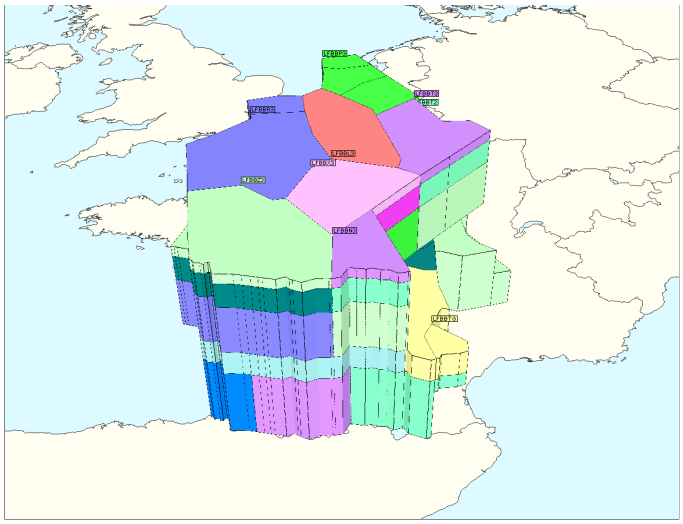

Figure VII-2: *Airspace filled with non-overlapping elementary sectors, some of which can be merged and operated as a whole during certain time periods depending on the traffic situation.*

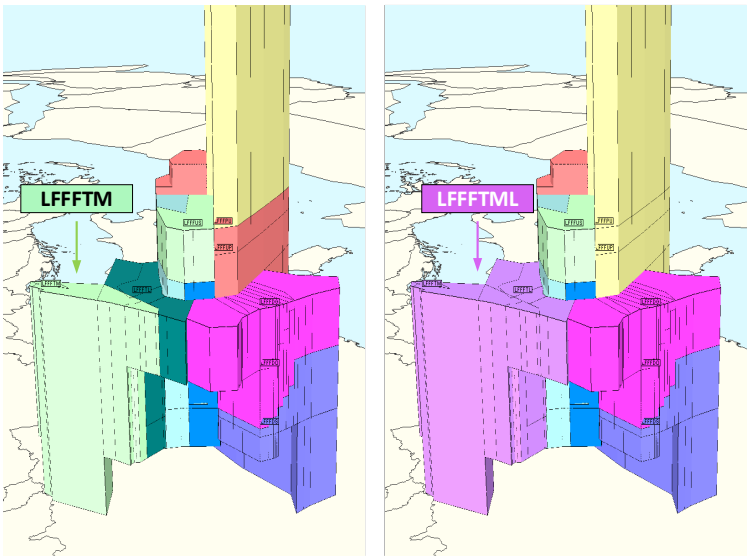

(a) LFFFCTAE: Conf. 10B (b) LFFFCTAE: Conf. 10F

Figure VII-3: *Operating sectors consisted in two different configurations 10B and 10F for ACC LFFFCTAE.*

Therefore, in this chapter we explore a less ambitious dynamic sectorization method, scheduling the opening schemes for the already existing operating sectors, without changing the shape of any collapsed and/or elementary sectors. To further reduce the computational com-

plexity, we specify that the opening schemes of sectors are subject to the existing airspace configurations. we can see an example in Fig. VII-3, where elementary sector LFFFTM acts as an independent operating sector (light green block in Fig. VII-3(a)) in configuration "10B" of ACC LFFFCTAE, while it is merged into a collapsed sector LFFFTML (purple block in Fig. VII-3(b)) when configuration "10F" is activated.

The effects of this limited dynamic sectorization are three folded:

- it enables flexible capacity provision, which means that capacities can be re-allocated from free areas to the newly-emerging congested areas (caused by traffic flow regulation);
- it allows the adjustment of collapsing architecture of the elementary sectors, which can affect the traffic demand counting for operating sectors (recall Constraint (VII.5) and relevant statements); and
- it takes the number of opening sectors into account, which is related with ATC system costs.

VII.2.3 Decision variables

Following the above discussion, we define an additional set of decision variables as follows, along with $(x_{f,t}^{k,j})$ and (z_f^k) that have been already introduced in Model C-DCB.

$$u_s^\tau = \begin{cases} 1, & \text{if configuration } s \text{ is activated in time period } \tau \\ 0, & \text{otherwise} \end{cases}$$

Note that once an airspace configuration (s) is settled, the status of its associated operating sectors (l) should be also determined. In other words, the following set of variables (w_l^τ) representing each individual sector's opening:

$$w_l^\tau = \begin{cases} 1, & \text{if sector } l \text{ is open during time period } \tau \\ 0, & \text{otherwise} \end{cases}$$

which can be replaced by $(w_l^\tau = \sum_{s \in S_l} u_s^\tau)$ for all sectors and time periods, where (S_l) is the configurations constructed (partially) by sector (l). In this case, if any of the airspace configurations related with sector (l) is activated (i.e., $\sum_{s \in S_l} u_s^\tau = 1$), then this sector must be open; On the contrary, if the sector is not open (i.e., $w_l^\tau = 0$), then it means that all the configurations (S_l) constructed by this sector cannot be activated.

For convenience, the time period (τ) is defined with the same length as the unit time scale used for demand counting and capacity provision. A smaller scale may also apply, but requires an equivalent capacity value to match with it.

VII.2.4 Model formulation

The multi-objective function (VII.15) minimizes three groups of costs, including the costs of total delays, the extra costs of using alternative trajectories (e.g., fuel consumption and route charges), and the ATC operating costs which are dependent on the total number of opened sectors.

$$\min \sum_{f \in F} \sum_{k \in K_f} \sum_{j = J_f^k(1)} \sum_{t \in T_f^{k,j}} \alpha (t - r_f^{k,j})(x_{f,t}^{k,j} - x_{f,t-1}^{k,j}) + \sum_{f \in F} \sum_{k \in K_f} (\gamma d_f^k + e_f^k) z_f^k + \sum_{l \in L} \sum_{s \in S_l} \sum_{\tau \in \mathcal{T}} \delta u_s^\tau \tag{VII.15}$$

s.t. (VII.8)-(VII.11) and (VII.13)-(VII.14)

$$\sum_{s\in S_a} u_s^\tau = 1 \quad \forall a \in A, \forall \tau \in \mathcal{T} \tag{VII.16}$$

$$\sum_{s\in S_l} u_s^\tau \leq 1 \quad \forall l \in L, \forall \tau \in \mathcal{T} \tag{VII.17}$$

$$\sum_{l\in L_j} \sum_{s\in S_l} u_s^\tau = 1 \quad \forall j \in J, \forall \tau \in \mathcal{T} \tag{VII.18}$$

$$\sum_{f\in F} \sum_{k\in K_f} \sum_{j=J_{f,l}^{k,\tau}} \sum_{t\in T_f^{k,j}\cap\tau} x_{f,t}^{k,j} - x_{f,t-1}^{k,j} \leq \sum_{s\in S_l} c_l^\tau u_s^\tau + (1 - \sum_{s\in S_l} u_s^\tau)M \quad \forall l \in L, \forall \tau \in \mathcal{T} \tag{VII.19}$$

$$u_s^\tau \in 0, 1 \quad \forall s \in S, \forall \tau \in \mathcal{T} \tag{VII.20}$$

Since Model SC-DCB maintains all the traffic management initiatives used in Model C-DCB, the corresponding Constraints (VII.8)-(VII.11) and (VII.13)-(VII.14) are also required in this model. Besides, Constraint (VII.16) guarantees that for each ACC there must be one configuration (among all the selectable configurations (S_a) associated with the specific ACC) activated in each time period. Constraint (VII.17) ensures that each operating sector can function in only one particular configuration for the maximal during one time period. Next, Constraint (VII.18) stipulates that all the elementary sectors in airspace should be "in use" (i.e., providing services) no matter how they are collapsed in different ways (recall Fig. VII-2).

In Constraint (VII.19) concerning the capacities, the left-hand term looks just the same as that appearing in Constraint (VII.12). For the right-hand term, since we have no idea which sector will be open before executing the model, we should consider the capacity for all the possible operating sectors (L), rather than a subset (L_τ) that are known and fixed in previous models. However, if one specific sector is not open, we will not expect it to become the reason of assigning delays for instance. Therefore, a large positive value (M) is added to the right-hand term. By doing this, if it is not open (i.e., $1 - w_l^\tau = 1$), the inequality of Constraint (VII.19) is still satisfied and there is no need to regulate the traffic flow. Finally, Constraints (VII.20) states that the additional set of decision variables are binary.

VII.3 Computational experiments

Computational experiments have been performed with the three model variants presented in this chapter. Real-world data are used for the experiments. Results are compared among the three variants, which illustrates the proposed synchronization process and show its significant effects on improving the DCB performances using the proposed strategy.

VII.3.1 Experimental setup

The experiment is focused on the French airspace with 24 hours' traffic traversing this area. Specifically, it includes 6,255 planned flights, 15 ACCs, 1,511 configurations, 164 elementary sectors and the associated 431 existing operating sectors. In this study, we consider 1 min as the unit time step, and 60 min as the time scale for demand counting. All this information is retrieved from the

Demand Data Repository version 2 (DDR2) published by Eurocontrol for a typical day in February in 2017. The flight trajectories, on the other hand, are generated according to their flight plans by an in-house trajectory planning tool (see Sec. III.2).

Table VII-2: *Problem size and computational time.*

Summary	Model DCB	Model C-DCB	Model SC-DCB
Time win. (min)	360	120	20
Variables	12,392,347	6,413,940	1,520,268
Equations	22,459,267	11,685,916	2,413,425
Non-zeros	47,518,810	24,718,752	6,169,484
Generation (min)	2	1	1
Solution (min)	4	2	51

The above statement presents the generic setup for all case studies in this chapter. However, for Model DCB, since the sector opening schemes are known (according to the DDR2 database) and fixed, the number of possible operating sectors decreases to 224 in total across the day. Next, for Model C-DCB, the airspace settings are the same as those for Model DCB. In addition, with 86 time-varying hotspot areas identified, there are 1,305 lateral and 1,379 vertical alternative trajectories further scheduled and submitted (see Sec. VII.1.2.1). Therefore, we have 8,939 trajectories in total for the planned 6,255 flights. Finally, for Model SC-DCB, it remains the generic airspace setup and also takes all the submitted trajectories from Model C-DCB into account.

Some key assumptions and parameters have been taken: 1) the unit cost of delay (α) keeps constant (i.e., 5 euro/min arbitrary value) and applies the same for different flights; 2) the unit cost of fuel consumption (γ) is 0.5 euro/kg; 3) the route charges are calculated according to the absolute distance flown; 4) AUs are willing to share the detailed costs of their alternative trajectories; 5) the unit cost of opening a sector (δ) for 60 min is 100 euro; 6) the time scale (τ) for demand counting and capacity is 60 min; and 7) the maximal allowance of capacity overload is set to 10%.

In addition, since the amount of delays required are quite different, we set different feasible time windows ($T_f^{k,j}$) in the three models, which in turn affects notably the problem dimensions, as listed in Table VII-2. In the numerical experiments, GAMS v.25.0 software suite has been used as the modeling tool and Gurobi v.7.5 optimizer has been used as the solver. The numerical experiments have been run on a 64 bit Intel i7-4790 @ 3.60 GHz quad core CPU computer with 16 GB of RAM memory and Linux OS.

The model generation time and solution time are presented in Table VII-2 as well. The integrity relative gap is set to 0%. we can notice that even though Model SC-DCB is much smaller than the other two models (because of the smaller time window), it is more challenging for the solver to search for the optimal solution. Concretely, most of its computing time is used to prove the solution's optimality. This means that if a sub optimal solution, with an integrity gap, is acceptable, then the required solution time could be much less.

VII.3.2 Overall results comparison

The main indices of the results are summarized in Table VII-3. For Model DCB, we can see that using only ground holding to balance demand with capacity needs huge amount of delays. Moreover, due to some long delays, many demands are actually moved to the next day (i.e., 27,654 - 26,371) which we assume has unlimited capacities. If they are further imposed, along with the next day's traffic, the required delays could be even higher. Nevertheless, it is worth noting that in realities there will never be such an amount of delays because in many cases some capacity

overloads will be allowed. and sometimes the allowance could be quite large. In this study, we consider a relatively conservative situation, with only 10% maximal capacity allowance, for the illustrative purpose.

Table VII-3: *Overall results comparison between the three models.*

Index	Model DCB	Model C-DCB	Model SC-DCB
Delays (min)	185,263	3,402	381
Delayed flights	1,353	417	167
Initial trajectory	6,255	5,741	5,755
Lateral altern.	0	265	246
Vertical altern.	0	249	254
Total capacity	45,708	45,708	33,545
Total # sectors	1,098	1,098	773
Pre demand	27,654	27,654	27,654
Post demand	26,371	27,242	24,840
Post D/C ratio	57.7%	59.6%	74.0%

For Model C-DCB, a promising finding is that delays are reduced significantly to 3,402 mins in total (see Table VII-3), because of using the alternative trajectory options. But we can notice from the table that most of the flights still keep their initially scheduled trajectories (5,741) which accounts for 92% of the total flights. In other words, only 8% of flights diverted to their (preferred) alternative trajectories could contribute to a reduction of 98% of total delays. This is because only assigning delays in a network scenario will normally cause inefficient usage (57.7%) of some airspace capacities, while allowing alternatives could take advantage of the capacities in those less-congested areas.

However, the most notable finding is for Model SC-DCB, in which delays are further reduced, more flights can use initial trajectories, and, moreover, less sectors are opened and less amount of total capacity provisions are needed. This reveals the obvious effects of adjusting sector opening schemes synchronously along with the changes of traffic flow.

Specifically, as shown in Table VII-3, a small number of delays (and delayed flights) exist in this model, being 381 min (and 167 flights) in total, which accounts for only around 11% of that assigned in model C-DCB. Besides, the number of flights using alternative trajectories also decreases by 14 flights.

Then, in terms of capacity, it is typically known that the more capacities we can make use of, the less delays there will be, but in this particularity case, the total capacity even reduces by 19%. Meanwhile, the number of opened sectors reduces too by around 30% from 1,098 to 773.

On the other hand, as mentioned previously, the adjustment of sector collapsing affects traffic demand counting, such that the more elementary sectors are merged into one operating sector, the less traffic demand (i.e., flight entry) will be counted. This is also observed in Table VII-3 where the traffic demand reduces by 10% to 24,840. Nevertheless, the average capacity usage increases to 74%, much higher than the numbers for the previous two models, which turns to be the main reason that causes less traffic flow regulations in this model.

VII.3.3 Demand and capacity

The demand and capacity situations are shown in Fig. VII-4 with respect to the original and those after executing the three models. we can see from Fig. VII-4(a) that, across the 1,098 operating sectors in total, a certain amount of capacity overloads occur for some sectors. Moreover, in some

cases, the traffic demand could be more than double of the capacity. That is to say, for the purpose of balancing demand with capacity in Model DCB (see Fig. VII-4(b)), we have to delay half of the flights traversing this sector, and the delayed flights will often incur new delays in other (near) congested sectors. This accumulative effect may easily evolve to large amount of total delays which we have seen in Table VII-3 for Model DCB.

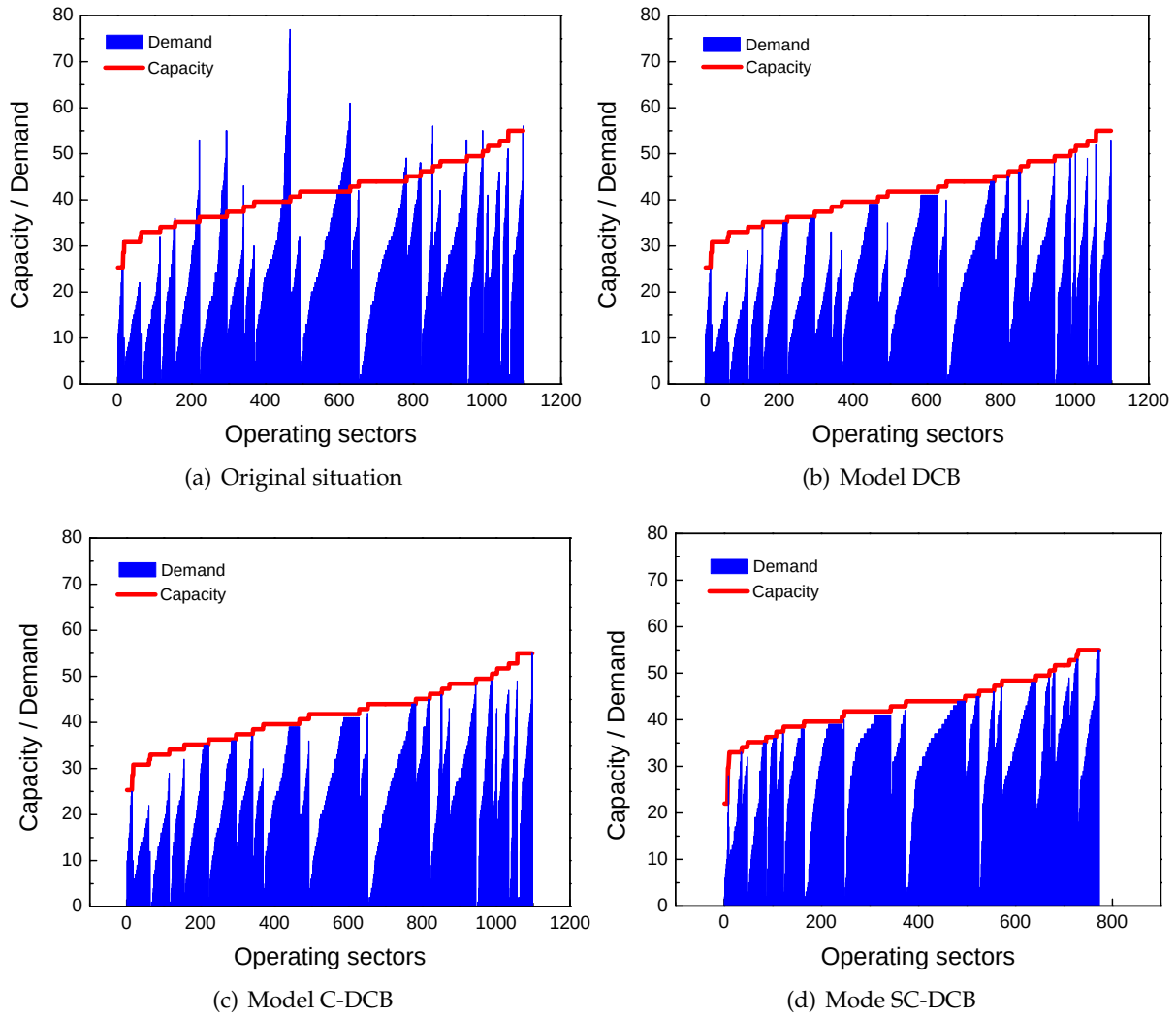

(a) Original situation

(b) Model DCB

(c) Model C-DCB

(d) Mode SC-DCB

Figure VII-4: *Demand and capacity situations in the original and the three models.*

Allowing alternative trajectories in Model C-DCB is obviously one way to leverage the above delay accumulation, because diverting flights to some less-congested sectors does not necessarily generate new delays. As shown in Fig. VII-4(c), some free sectors with low traffic demand in Fig. VII-4(b) is now filled with relatively high traffic demand. This can be seen more clearly by the demand and capacity ratio shown in Fig. VII-5(a), namely the blue line versus the red line. It is worth noting that even with this slight improvement, the delays can be reduced remarkably (recall Table VII-3). Nevertheless, we may still see may blank areas in Fig. VII-4(c) underneath the capacity line, meaning that many capacities are not well utilized.

The last Model SC-DCB solves this issue quite well, as proved by the results in Fig. VII-4(d). The number of opened sectors are reduced to 773, and all the traffic demand is compacted to the lessen area, which in turn leaves less blanks left. Meanwhile, Fig. VII-5(a) presents a large improvement of the capacity load for Model SC-DCB (green line) if compared to the other two models.

Finally, we can notice that not only the average value increases, but also most of the sectors (75%) have their capacity loads greater than 60%. This number for Model DCB and C-DCB is only around 40%. On the other side, there are almost 100 sectors in both Model DCB and C-DCB that have a capacity load less than 10% (with some 0% cases), which is quite low and not an expected situation even from the safety aspect. But in Model SC-DCB, we can see only quite few sectors having such low capacity loads.

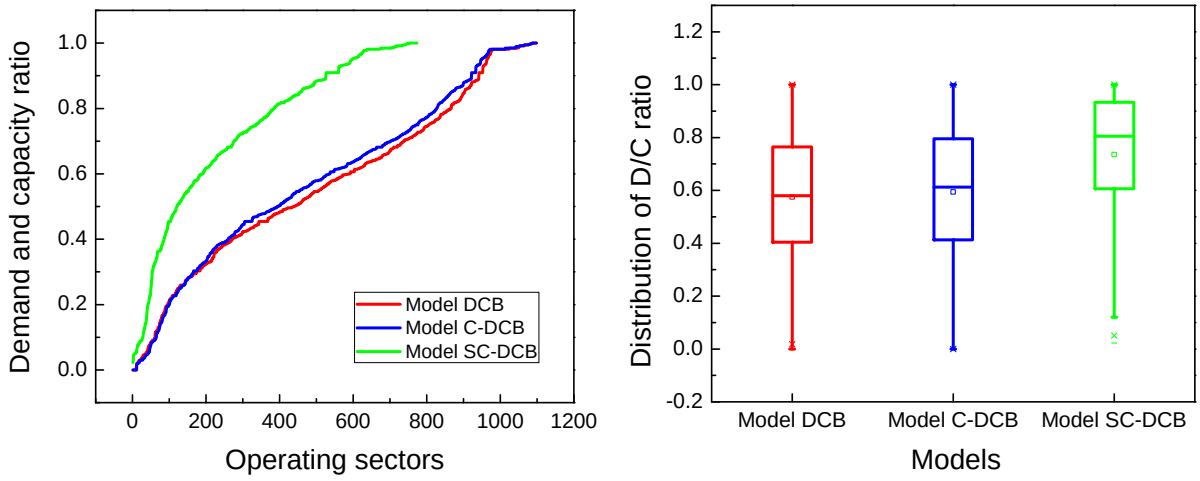

(a) Sorted capacity load

(b) Distribution of capacity load

Figure VII-5: *Final capacity load (i.e., demand and capacity ratio) in three models.*

VII.3.4 Sector opening scheme

In the previous Sec. VII.3.3, we have demonstrated that Model SC-DCB enables a notable improvement on the utilization of capacity resources. This is realized by optimizing sector opening schemes and traffic flow (including trajectory selections and delay assignments) in a synchronized way.

Fig. VII-6(a) shows the changes of number of opened sectors during each time period of the day, and we can observe the number reduction for every time period in Model SC-DCB. In the objective function (VII.15) of this model, we minimize the total number of opened sectors (as one of the multi objectives). This is because: 1) it is directly related to the ATC system costs, and 2) less number of sectors means larger size to each of them which means the traffic demand could be further compacted (recall Fig. VII-4(d)) to reduce the percentage of "idle" capacity. However, the number of opened sectors cannot be reduced unlimitedly, as more traffic in less sectors will soon cause the capacities to be fully taken or even overloaded.

Following the reduced amount of operating sectors, the total capacity provisions are lowered down as well, as shown in Fig. VII-6(b). Given most of the sectors' capacities are usually not varied too much, the changes of capacity provisions are basically in line with the number of opened sectors.

For the average capacity provision per opened sector (see Fig. VII-6(c)), the changes are worth noting. we can see that during the periods when there are less traffic (typically from 0-6 hour and 23-24 hour in a day), the original setting provides a higher average capacity, but during the congested periods, it somehow gives a relatively lower average value (see the gray line in Fig. VII-6(c)). This is because the original setting relies on cutting airspace into smaller pieces of sectors (each with lower capacity) to better manage the traffic flow.

On the contrary, Model SC-DCB provides an average capacity almost in consistent with the number of sectors and the capacity provisions (see the red line), meaning that the opened sectors in this model share similar unit capacities. Moreover, the unit capacities are also higher than those of the smaller sectors used in the original setting, and thus more demand can be accommodated per sector, as shown in Fig. VII-6(d).

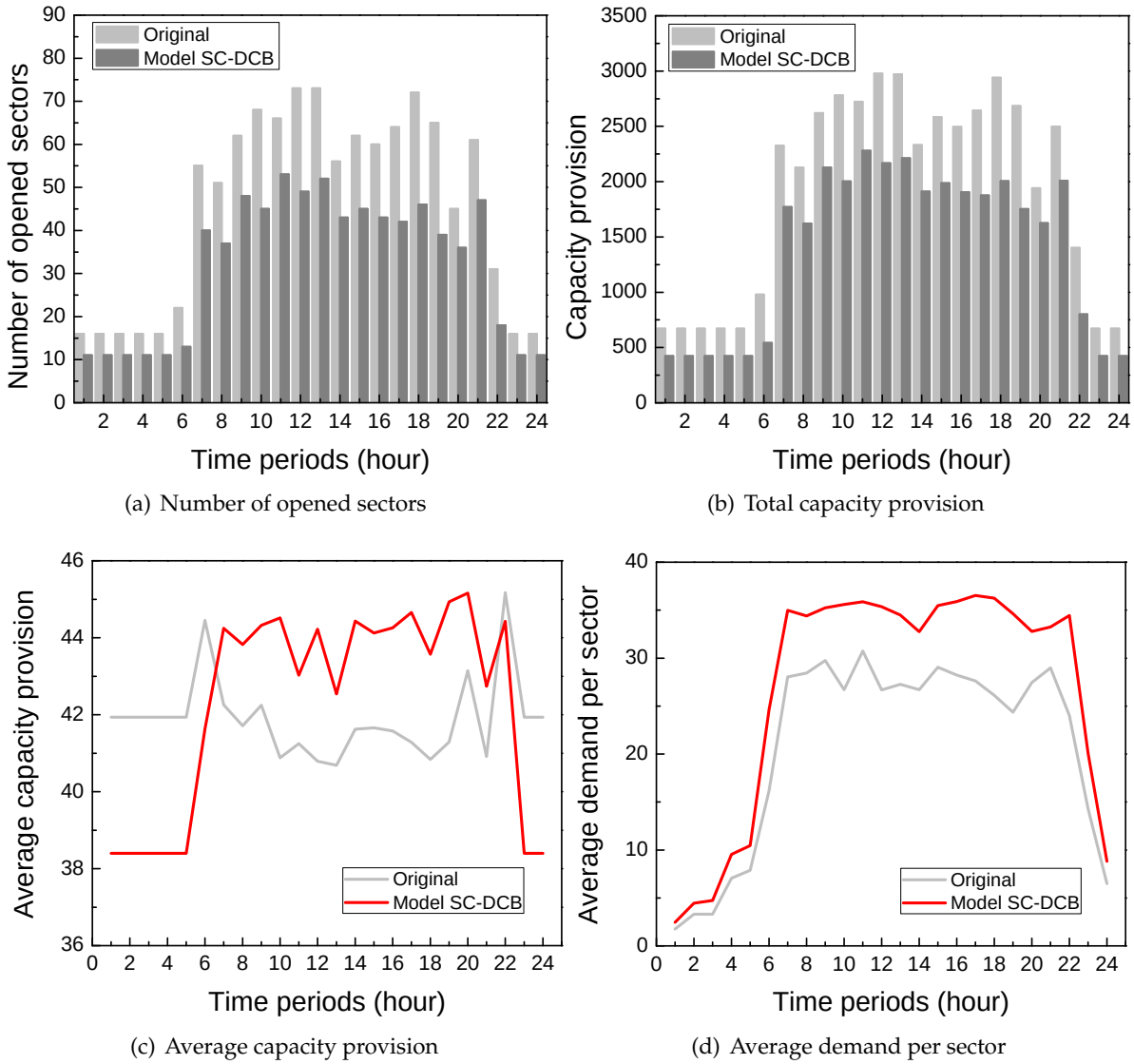

(a) Number of opened sectors

(b) Total capacity provision

(c) Average capacity provision

(d) Average demand per sector

Figure VII-6: *Changes of sector opening schemes in Model SC-DCB.*

The final configuration for each ACC of the study is presented in Table VII-4. We can notice that the choice of configuration, for some ACCs, evolves during different time periods of the day. Nevertheless, as mentioned in VII.2.2, we consider in this chapter a limited dynamic sectorization which is subject to the existing airspace configurations. This means that both the collapsing architecture of elementary sectors and the opening schemes of operating sectors must follow certain groups of rules.

Table VII-4: *Airspace configurations activated in Model SC-DCB for each ACC during each time period of the day.*

Time	LFBBCTA	LFEECTAC	LFEECTAE	LFEECTAN	LFFFCTAA	LFFFCTAE	LFFFCTAW	LFMLTMA	LFMMCTAE	LFMMCTAW	LFMMXCTA	LFRRCTAE	LFRRCTAN	LFRRCTAS	LFSBTMA
1	1.A	1CA	1EB	1NB	1	1A	1A	C1A	E1A	W1A	CF1	C01EA	C01NA	C01SFS	ALL
2	1.S	1CC	1EB	1NB	1	1A	1A	C1A	E1A	W1A	CF1	C01EFS	C01NFS	C01SA	ALL
3	1.A	1CA	1EA	1NA	1	1A	1A	C1A	E1A	W1A	CF1	C01EFS	C01NA	C01SA	ALL
4	1.S	1CB	1EA	1NA	1	1A	1A	C1A	E1A	W1A	CF1	C01EA	C01NA	C01SA	ALL
5	1.A	1CB	1EC	1NA	1	1A	1A	C1A	E1A	W1A	CF1	C01EA	C01NA	C01SFS	ALL
6	3.1AN	1CC	1EC	1NA	1	1A	1A	C1A	E1A	W1A	CF1	C01EA	C01NFS	C01SA	ALL
7	9.1A	3CA	2EB	4NC	1	5C	2A	C1A	E4A	W2A2A	CF1	CO5EZZ	C01NFS	C01SA	ALL
8	7.1D	2CA	2EB	5NA	1	3A	4C	C1A	E2B	W2B1A	CF1	C04EX	C03NC	C02SA	ALL
9	14.1P	2CA	2EB	4NC	1	5C	3A	C1A	E4A	W3B2A	CF1	CO5EZZ	C02NA	C02SFS	ALL
10	9.1D	3CA	2EB	5NA	1	4C	4A	C1A	E4A	W2A2A	CF1	C05EY	C03NC	C02SFS	ALL
11	12.1G	3CA	2EB	4NC	1	5C	3A	C1A	E4B1A	W4A1A	CF1	C07EK	C04NA	C03SC	ALL
12	12.1G	2CA	2EB	4NB	1	5F	3A	C1A	E4B1A	W3B1A	CF1	CO5EZZ	C04NA	C03SA	ALL
13	12.1G	3CA	2EB	7NA	1	5F	4A	C1A	E4A	W2A1A	CF1	C07EG	C03NC	C02SA	ALL
14	12.1G	2CA	2EB	5NN	1	3A	2A	C1A	E3C	W3A1A	CF1	C04EX	C04NC	C02SFS	ALL
15	10.1E	3CA	2EB	5NA	1	5F	2A	C1A	E4E	W3B2A	CF1	C04EA	C02NFS	C03SA	ALL
16	12.1G	2CA	2EB	5ND	1	4A	3A	C1A	E3C	W2A1A	CF1	CO5EZZ	C02NA	C02SA	ALL
17	12.1G	2CA	2EB	4NC	1	3A	2A	C1A	E4A	W3B1A	CF1	C04EA	C02NA	C03SA	ALL
18	14.1K	2CA	2EB	4NH	1	3A	2A	C1A	E3C	W2A2A	CF1	C07EE	C02NA	C03SC	ALL
19	10.1E	2CA	2EB	4NH	1	4C	3B	C1A	E3C	W2A1A	CF1	C04EX	C02NA	C02SFS	ALL
20	12.1G	2CA	1EB	4NB	1	3A	2A	C1A	E2B	W2A2A	CF1	C03EF	C01NFS	C02SFS	ALL
21	12.1G	3CA	4EK	5NA	1	5F	4A	C1A	E2B	W2A1A	CF1	C05EX	C02NA	C02SA	ALL
22	5.1D	1CC	1EB	1NB	1	1A	1A	C1A	E2B	W2A1A	CF1	C01EA	C01NA	C01SA	ALL
23	1.A	1CC	1EA	1NB	1	1A	1A	C1A	E1A	W1A	CF1	C01EA	C01NA	C01SFS	ALL
24	1.S	1CB	1EC	1NA	1	1A	1A	C1A	E1A	W1A	CF1	C01EFS	C01NA	C01SFS	ALL

VII.4 Chapter summary

This chapter presented a preliminary method of synchronizing the planning of traffic flow regulations and sector opening schemes. Through combining different traffic management initiatives - such as assigning ground delays and diverting flights to alternative trajectories - along with the dynamic sectorization into an integrated optimization model, the performance of demand and capacity balancing can be improved remarkably. Results show that not only the system delays can be largely reduced, but also the ATC operational costs and the required total capacity provisions.

Results suggest that large amount of delay reduction can be achieved by switching from Model DCB (i.e., baseline model) to Model C-DCB (i.e., benchmark model), and only 8% of flights diverted to their (preferred) alternative trajectories could contribute to a reduction of 98% of total delays. Moreover, the most notable finding is for Model SC-DCB, in which delays are further reduced, more flights can use initial trajectories, and, moreover, less sectors are opened and less amount of total capacity provisions are needed. This reveals the obvious effects of adjusting sector opening schemes synchronously along with the traffic flow regulation.

The greatest benevolence is like water. The highest virtue tolerates all.

— I Ching

VIII

Concluding remarks

The gradually saturated airspace and the subsequent growing of flight delays require a better air traffic flow management (ATFM) for the current air transportation system. To achieve this goal, airspace users (AUs) have been expected to get increasingly involved in the ATFM decision making, especially under the forthcoming concept of trajectory based operations (TBO). This PhD thesis, accordingly, studies how AUs could improve their flight (trajectory) planning process, such as using a cost-based linear holding practice, and in the meantime proposes a Collaborative ATFM model taking advantage of AUs' substantial participations, as well as presents a primary enhanced collaborative framework with further involvement of air navigation service providers (ANSPs). A brief summary of contributions and results achieved in this PhD thesis is presented below, as well as some future work that could be conduced based on the present research.

VIII.1 Summary of contributions

The main contributions of this PhD thesis are summarized as follows:

- A cost-based linear holding strategy was proposed in Chapter III, on basis of previous work where linear holding was only allowed by reducing cruise speed (Delgado & Prats, 2012). By analyzing the relationship between fuel consumption and speed in each flight phase, the equivalent speed concept was extended to the climb and descent phases, and thus the speed reduction proved to be feasible to be implemented along the whole flight to generate linear holding at no extra fuel cost (or allowing a configurable extra fuel consumption if desired). Through a detailed simulation on typical flights with the developed optimal trajectory gen-

eration tool, the effects of three subdivided cases of the strategy were thoroughly assessed, where a remarkable increase of the maximum airborne delay absorption was observed compared with previous studies.

- An aircraft trajectory optimization technique was adopted in Chapter IV in order to introduce linear holding to partially absorb delays due to Airspace Flow Programs during the ATFM planning stage. It is shown how some fuel can be saved before reaching the congested airspace, which can be allocated to recover delay once this constrained area is overflown. Besides, another potential applicability of the proposed linear holding was presented to neutralize the additional delays at no extra fuel consumption. Through multiple stages of optimal trajectory generation, linear holding was enabled to be implemented along the whole flight phases, and adjusted flexibly in response to different kinds of unexpected traffic management initiatives and the unforeseen delays they might produce. Compared to the case where ground holding is fully endured followed by burning more fuel to increase flight speed to partially recover delays (as usually done nowadays for some AUs), the proposed strategy can reduce the additional delays without consuming any extra fuel than initially scheduled.

- In Chapter V, the cost-based linear holding was merged into a network ATFM model for delay absorption, together with the commonly-seen ground and airborne holdings. In the light of TBO, AUs' sharing of maximum linear holding bounds derived from their own optimal aircraft trajectory generation, could be effectively utilized by the ATFM side as one of the optimization factors considered for delay assignment. Replacing ground holding with linear holding enables aircraft to depart earlier, with less ground holding. This provides more flexibility in responses to changes in capacity, and thus less total delay would be realized. Moreover, if the delays are canceled ahead of schedule, aircraft already airborne and performing linear holding, could accelerate to the speed as initially planned and recover part of the delay at no extra fuel cost.

- Chapter VI presented an innovative Collaborative ATFM framework in the scope of future full TBO. The collaborative trajectory design process was the key enabler of the framework for a series of downstream performance enhancements. The accurate provision of the identified time-varying hotspot airspaces contributed to assisting AUs to schedule alternative trajectories with as less extra costs as possible. Combining different measures, resulted from the collaborative process, as a whole to manage the imbalances of demand and capacity could improve the ATFM cost-efficiency. The centralized linear optimization model, taking fully advantage of the trajectory design solutions, incorporated potential traffic management initiatives (i.e., multiple trajectory options mixed with different types of delay measures) to balance the traffic demand with airspace capacity, trying to minimize the deviation to the initial set of user-preferred trajectories.

- Finally, an enhanced Collaborative ATFM model was introduced in Chapter VII, focusing on synchronizing the planning of traffic flow regulations and sector opening schemes. The preliminary method was intended to include not only AUs, but also ANSPs into the ATFM decision making process, aiming to achieve even higher level of collaboration than what was allowed in the models introduced in previous chapters. Through combining different traffic management initiatives - such as assigning ground delays and diverting flights to alternative trajectories - along with the dynamic sectorization measures into a single integrated optimization model, the performance of demand and capacity balancing (DCB) were proved to improve significantly.

VIII.2 Future work

In line with the scope and limitations of this PhD thesis as presented in Chapter I, the following future work are proposed based on the above contributions conducted during the thesis.

- The implicit characteristics of trade-offs between fuel and time still require a further analysis by performing more simulation experiments to have statistically meaningful data set of results, as they might have direct effects on the speed recovery process which contributes to one of the main advantages of the linear holding practice.
- In addition to the constraints of fuel consumption, more factors could be taken into account for realizing linear holding, such as the slots allocation in particular designated waypoints and the separations of passing specific positions.
- Since the GDP/AFP is typically issued under severe weather conditions, the wind and non-standard atmospheres (which always have a great effect on real flights) should be taken into consideration too.
- After suffering long delays, the operators may be inclined to burn extra fuel than initially scheduled to expect more delay recovered. Thus, further defining a relation between the amount of extra fuel and the extent of delay recovery would be helpful for airlines in decision making.
- Current version of the proposed collaborative ATFM framework is simply used for prototype testing, while a detailed set of negotiation mechanisms (including the effects of gaming) between different stakeholders does deserve a further discussion.
- A limited dynamic sectorization method was considered, which is subject to the existing airspace configurations. In future work, a more flexible sectorization method with such constraints relaxed should be taken into account, in line with the DAC (dynamic aisrpace configuration) concept, which is one of the SESAR 2020 solutions.
- The computational performance of the model needs more empirical studies, and requires further improvement, which can be done using certain meta-heuristics or decomposition methods, such as the classical Dantzig-Wolfe and Benders decomposition for linear programming problems.
- Uncertainty factors (e.g., trajectory execution errors and weather condition changes) should be further considered, in order that the proposed methods could be more robust for implementation in the future.

Keep your face to the sunshine and you can never see the shadow.

— Helen Keller

A

Additional examples of linear holding

This appendix presents some more experiments about linear holding (LH) simulations, in addition to those given in Chapter III. Results are analyzed in terms of trajectory variants and speed profiles due to the execution of LH in different cases (strategies), followed by a comparison of airborne delay that can be achieved in climb, cruise and descent phases.

A.1 Trajectories variants for a specific flight

The vertical trajectories corresponding to the four Cases of the flight AMS-SVQ: CI=150 flight are as shown in Fig. A-1. The changes when LH is implemented in climb and descent phases can be appreciated in the profile, while the optimal flight level for Case-3 decreases from FL340 to FL320. Comparing the blue dots (Case-2) with the red ones (Case-0), we find the aircraft is climbing steeper (recall that the cruise flight level keeps unchanged for this Case), saving some fuel in the climb phase while also delaying the flight. Conversely, the descent is performed more gradually and flying slower, but burning some extra fuel if compared with Case-0. As for the green squares (Case-3), a decrease in cruise flight level generates even steeper climb and shallower descent trajectories. Table A-1 illustrates clearly these changes for all Cases of study.

Compared with the nominal flight (Case-0), Case-1 consumes the same amount of fuel in each phase and achieves 22 minutes of airborne delay when cruising, which accounts for the 22% of the cruise time and the 17% of the total time.

In Case-2, the fuel consumption reduces 270kg (16%) in climb and the airborne delay is almost 2 minutes in this phase. Since the total fuel consumption is the same for the flight, the 270kg of

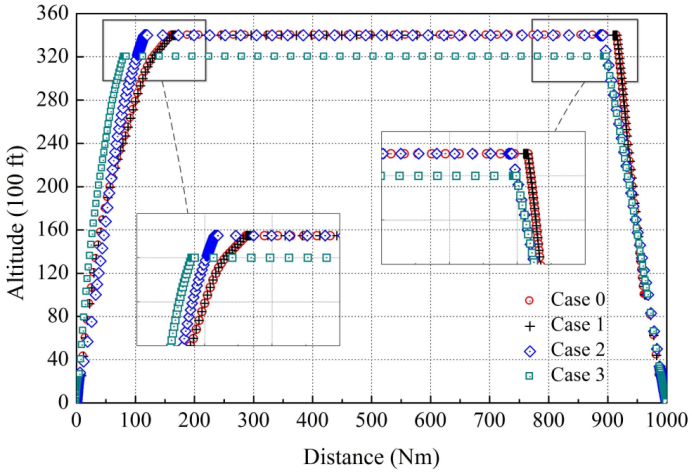

Figure A-1: *Optimal trajectories generated for each Case.*

Table A-1: *Details of a specific flight in climb, cruise and descent phases.*

Cases	Climb phase				Descent phase			
	Fuel (kg)	Time (min)	Dist (nm)	Avg V (kt)	Fuel (kg)	Time (min)	Dist (nm)	Avg V (kt)
Case 0	1685,4	21,5	157,3	438,0	107,2	12,6	75,6	359,7
Case 1	1685,4	21,5	157,3	438,0	107,2	12,6	75,6	359,7
Case 2	1415,8	23,3	110,7	285,1	183,5	22,8	99,5	261,4
Case 3	1064,4	13,7	76,4	335,3	176,0	21,5	92,8	258,5

Cases	Cruise phase						Total	
	FL (100ft)	Fuel (kg)	Time (min)	Dist (nm)	LH (nm/kg)	Avg V (kt)	Fuel (kg)	Time (min)
Case 0	340	4006,5	97,8	754,3	0,1883	462,6	5799,1	132,0
Case 1	340	4006,5	120,2	754,3	0,1883	376,6	5799,1	154,3
Case 2	340	4199,8	156,8	777,1	0,1850	297,4	5799,1	202,9
Case 3	320	4558,8	168,5	818,1	0,1795	291,3	5799,1	203,7

fuel saved in climb can actually be allocated in cruise (193kg, 5% of cruise) and descent (77kg, 71% of descent), which, in fact, allows to largely increase the time delayed in both phases: 59 minutes (60% of cruise) and 10 minutes (77% of descent), respectively. As a result, if we compare Case-2 with Case-1, it seems that a 193kg (5%) increase of fuel consumption in cruise could exchange for 37 minutes (31%) more time delayed.

Regarding Case-3, when cruise flight level is allowed to change, the new optimal altitude (FL320) allows the aircraft to perform more airborne delay with the same fuel consumption than in Case-0 (nominal Case). Compared to Case-2, 351kg (25%) of fuel are saved during the climb phase, 8kg (4%) of fuel during the descent phase, and 359kg (9%) of fuel are added to the cruise phase, lowering the specific range by 0.006 nm/kg, and further reducing the equivalent cruise speed to produce an even longer (12 minutes) air delay in cruise. Although the flight time in both climb and descent are shorter, the total flight time increases (by 1 minute) due to this extended cruise flight time.

A.2 Climb, cruise and descent speed profiles

As we can tell from Fig. A-2(a), the climb speed profiles of all the Cases have quite similar structures, which mainly include a continuous acceleration process at low altitude, a constant IAS climb, followed by constant Mach climb at higher altitudes. At the end of the climb a small deceleration is observed in order to reach the (reduced) optimal cruise speed. Making Case-0 as the baseline, the difference with Case-1 only lies on the deceleration process at cruise flight level, so they share exactly the same climb speed (see Table A-1).

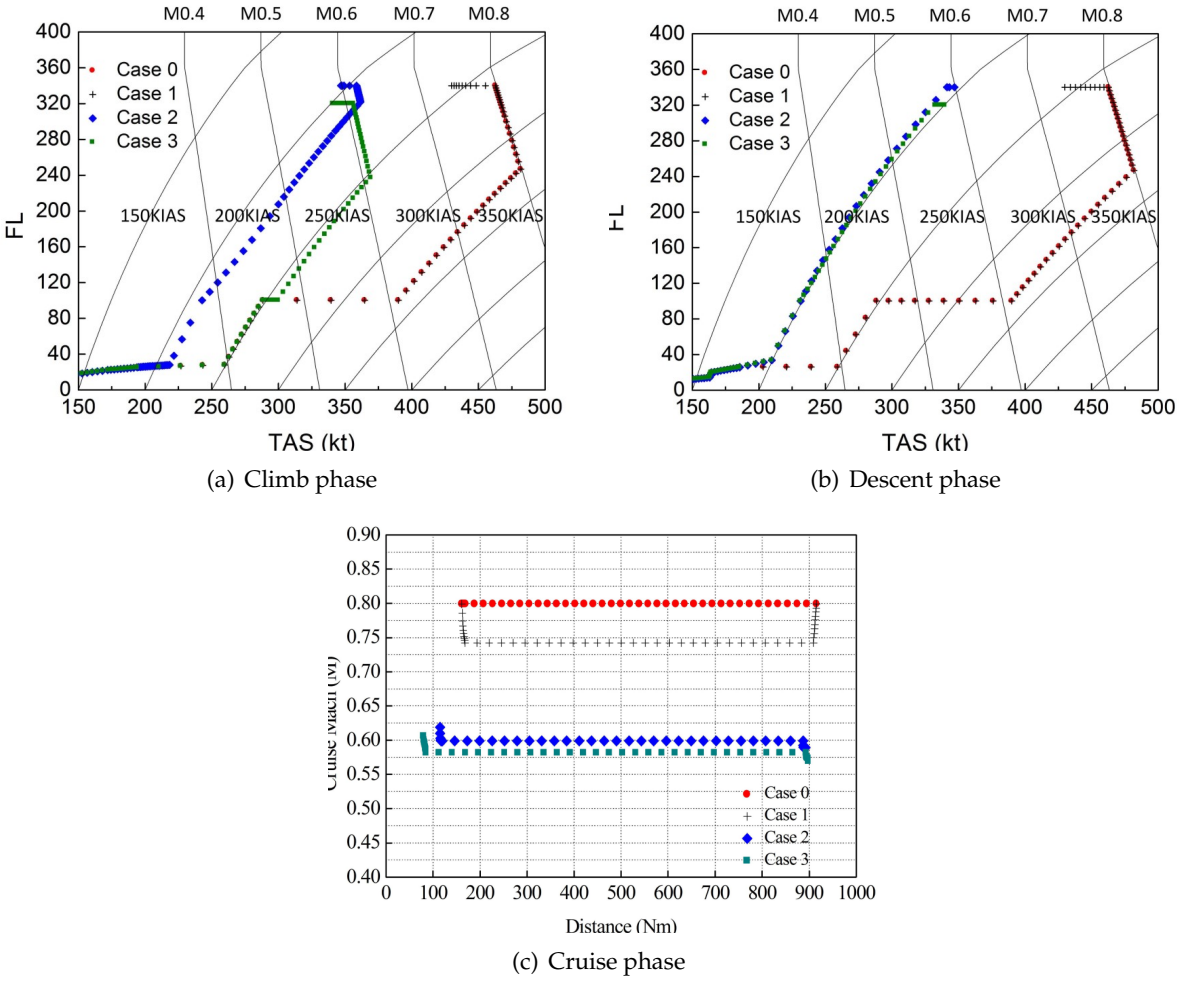

(a) Climb phase

(b) Descent phase

(c) Cruise phase

Figure A-2: *Changes of speed profiles in all the Cases of study.*

In Case-2 when LH is allowed in climb (and descent), the optimizer chooses a climb speed around 210kt (instead of the 330kt observed in Case-0), as is the minimum speed allowed (GD speed). Due to this lower IAS climb, a higher crossover altitude (around FL320) is obtained to switch to the climb Mach number, which is also lower than the nominal one.

Results show that the climb speed in Case-3 is higher than the GD speed used in Case-2 (see Fig. A-2(a)), but the gained fuel (saved from climb) makes a longer delay time in cruise and descent phases since the total flight time is longer than Case-2 (see Table A-1). That means, in this case, part of the delay time of climb is trade in exchange for saving more fuel.

When it comes to the cruise phase, if the fuel consumption is fixed in this phase in Case-1, then the cruise Mach decreases from M0.80 to M0.74, while the specific range keeps the same (both 0.188 nm/kg). Unlikely, in Case-2 and Case-3, the cruise Mach both reduce directly to the

GD speed for each flight level, M0.60 and M0.58 respectively (see Fig. A-2(c)).

As for the descent phase, we can see from Fig. A-2(b) that Case-2 and Case-3 have no deceleration below FL100 (like in Case-0 and Case-1) simply because the descent speed (around 200kt) is already below the ATC constraint of IAS lower than 250kt below FL100. Meantime, the segments of constant Mach descent are both missing too, since the crossover altitudes lie higher above the cruise flight level due to the lower speed in the constant IAS descent in Case-2 and Case-3.

Normally, the fuel consumed in descent phase accounts for the lowest of the three phases, but the trade-off still generates almost double the descent time in our example (see Table A-1). In Case-2, the fuel consumption grows from 107kg to 184kg, reducing the descent speed to the GD speed in descent. Remember that the GD speed is not the same in climb that in descent, since the weight of the aircraft is different (fuel has been burned in cruise).

A.3 Comparison of maximum airborne delay

More specific routes are further included to have a comparison on the amount of maximum airborne delay generated from different LH Cases, including FCO-CDG: 595 nm, FRA-MAD: 769 nm, AMS-SVQ: 1000 nm and STO-ATH: 1305 nm, all of which are representative of short and mid haul flights in Europe, and each is further analyzed with CI ranging from 25 to 500 kg/min. Results are summarized in Table A-2.

Table A-2: *Analyzed flights for airborne delay comparison.*

Flight Routes	Case-0										Case-1		Case-2		Case-3		
(Comp. time)	CI	FL	Time	Fuel	Clb D	Clb T	Crz D	Crz T	Dst D	Dst T	AD	AD	AD	AD	FL	AD	AD
	(kg/min)	(100 ft)	(min)	(kg)	(nm)	(min)	(nm)	(min)	(nm)	(min)	(min)	(%)	(min)	(%)	(100 ft)	(min)	(%)
FCO-CDG 595 Nm (10-15 Sec)	25	380	89	3464	140	21	346	47	97	17	8	16%	22	24%	380	22	24%
	60	380	86	3575	152	22	345	46	86	14	12	26%	26	30%	340	34	39%
	100	380	85	3641	160	22	338	44	85	14	10	23%	29	34%	340	37	43%
	150	380	85	3654	159	22	339	44	85	14	10	22%	30	35%	320	38	45%
	300	300	83	3991	137	19	378	48	68	12	12	24%	53	63%	260	55	66%
	500	260	83	4302	98	14	425	53	61	11	23	43%	60	73%	260	60	73%
FRA-MAD 769 Nm (10-15 Sec)	25	380	113	4334	153	23	506	68	97	17	11	16%	27	24%	380	27	24%
	60	380	110	4440	156	23	514	68	86	14	17	25%	33	30%	360	38	34%
	100	380	110	4464	152	22	519	69	86	14	14	20%	34	31%	360	39	36%
	150	340	107	4731	151	21	530	69	76	13	15	22%	52	48%	320	57	53%
	300	300	106	5030	142	19	547	70	68	12	17	25%	69	65%	280	71	68%
	500	260	104	5470	100	14	596	75	61	11	32	43%	78	75%	260	78	75%
AMS-SVQ 1000 Nm (15-20 Sec)	25	380	144	5482	161	24	729	98	97	17	16	17%	35	24%	380	35	24%
	60	380	140	5640	175	25	727	96	86	14	24	25%	44	32%	360	51	36%
	100	380	138	5768	200	27	702	92	85	14	21	23%	49	35%	340	60	43%
	150	340	137	5974	157	22	754	98	76	13	22	23%	71	52%	320	72	52%
	300	300	135	6389	147	20	772	98	68	12	25	25%	90	66%	280	90	67%
	500	260	133	6998	102	14	824	103	61	11	44	43%	104	78%	260	104	78%
STO-ATH 1305 Nm (20-30 Sec)	25	360	185	7054	133	20	40	5	98	17	0	9%	42	23%	360	42	23%
		380					991	133			23	17%			380		
	60	360	180	7242	148	21	40	5	86	14	1	24%	62	35%	360	62	35%
		380					988	131			37	28%			380		
	100	380	178	7360	210	29	997	131	85	14	31	24%	61	34%	360	71	40%
	150	340	177	7467	166	23	1050	136	76	13	51	38%	83	47%	320	86	48%
	300	300	174	7830	155	21	1069	136	68	12	59	43%	110	63%	280	110	63%
	500	260	172	9159	106	15	1126	141	61	11	59	42%	126	74%	260	126	74%

Seeing from the results of Case-0 in Table A-2, with the growth of CI, the climb distance increases from CI of 25 to 100 kg/min, and then decreases gradually after greater than 150 kg/min. However, remember that the higher the CI is, the longer the climb distance it should be. This is due to the fact the cases here in the table are resulted from a global optimization for the trajectory as a whole, while the situation in the previous figure is based on a single climb phase. The trade-

off of fuel and time among different flight phases (as illustrated by the specific flight in Sec. A.1) accounts for the partial inconsistent of these results.

In Case-1, it is obvious that the achievable airborne delay increases with the growth of flight route distance (i.e., the cruise distance in this case, as climb and descent phases are fixed in Case-1 in line with the nominal flight). Specifically, for each flight route, the higher CI the nominal flight chooses, the more airborne delay the flight will achieve (through the LH strategy) in general. However, we may also notice a reduction trend within the CI scope of 100 and 150 kg/min. It is because for those CIs, extra fuel is consumed in climb and descent to obtain higher speeds during the two phases, such that less fuel is left (given the total fuel kept constant) for the cruise phase, and thus a reduced amount of delay is generated.

As for Case-2, the airborne delay increases significantly only after climb and descent phases are included. If we compare the percentage that climb and descent normally account for in a flight, with the percentage that cruise has, we may find that for those short-haul flights, the distances of climb and descent may account for up to 50% while time nearly 50% too, but for the mid/long-haul flights, both distance and time percentages could reduce to about 20%. Nevertheless, most of the airborne delay in Case-2 increase to almost 3-fold of the ones in Case-1, which, as discussed in Sec. A.1, is due to the fact that adding climb and descent makes it possible to re-allocate the fuel consumption in each phase, as long as the total fuel consumption remains unchanged.

When the cruise flight level is allowed to change, as Case-3, the airborne delay further increase but not so remarkable as from Case-1 to Case-2 (see Table A-2). The main reason is that the specific range curves for different cruise flight levels are quite close within the low cruise speeds. As a result, the speed reduction from altitude changes, i.e., Case-2 to Case-3, will not be as large as the reduction from nominal speed to equivalent speed, i.e., Case-1 to Case-2. Typically, the new flight level would be lower than the original, but since the step interval is 2000ft, which is a discrete change due to operation constraints, some flights just keep unchanged as Case-2.

Life is made of ever so many partings welded together.

— Charles Dickens

B

Scalability tests for network ATFM model

This Appendix provides a supplement of scalability tests for the network ATFM model introduced in Chapter V. The tests are mainly focused on the sensitivity for certain model parameters and the computational performance of executing model with state of the art commercial solvers.

B.1 Sensitivity of critical parameters

With the aim to demonstrate how some of the key parameters affect ground holding and airborne holding as well as linear holding, more computational experiments have been conducted, with a sensitivity analysis presented in this section. Table B-1 shows the relevant independent parameters and their associated ranges considered for the design trade-offs. Tests of computational scalability have been also performed under three typical ATFM scenarios given different problem sizes. These numerical experiments have been run on a 64 bit Intel i7-4790 @ 3.60 GHz quad core CPU computer with 16 GB of RAM memory and Linux OS. GAMS v.24.02 software suite has been used as the modeling tool and Gurobi v.7.02 optimizer has been used as the solver.

A benchmark scenario taken for the sensitivity analysis involves 1131 flights traversing across 164 elementary sectors in the French airspace between 10 AM to 12 AM, July 28, 2016, as shown in Fig. B-1. The unit period of capacity is set to per 20 mins for all the (active) collapsed sectors (123 in total in the case). As mentioned in Sec. V.2.1, the elementary sectors might be combined to different collapsed sectors during each time period. Initial trajectory information and capacity data are processed in the same way as done for the previous case study. Parameters' baseline

values are as shown in Table B-1, and the sensitivity experiments are conducted by varying each individual parameter within its predefined range whilst fixing the rest by their baseline values.

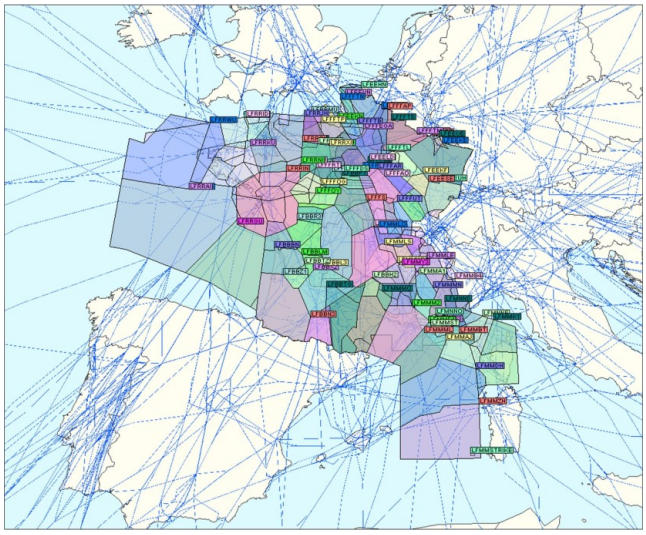

Figure B-1: *Flights and associated sectors used in the computational experiments.*

Changes of parameters ϵ, α and β would affect both the initial delay assignment and its subsequent (potential) update. Results of their sensitivity study are presented in Fig. B-2. The amount of imposed delays and the number of affected flights are considered, for each parameter, with respect to four indicators including total delay and individual delay realized by ground holding, airborne holding and linear holding respectively.

Table B-1: *Values of independent parameters in the sensitivity study.*

Parameters	Baseline	Min	Max	Step	Comment
ϵ	0,05	0	0,5	0,05	fairness factor of delay assignment
α	1,2	1,2	3	0,2	cost weight of airborne holding to ground holding
β	0,8	0,1	1,1	0,1	cost weight of linear holding holding to ground holding
τ	4	1	7	1	time period when capacity updated
$C^s(\tau)$	120%	80%	200%	10%	updated capacity with regard to the initial

The effects of increasing fairness factor (ϵ) can be appreciated from Figs. B-2(a) and B-2(b). Given an improved equality in the delay assignment process, the total delay that is required as a whole grows gradually, and it is the increased amount of airborne and linear holding that contributes to this growth as ground holding on the contrary decreases slightly. On the other hand, more flights are involved in the regulation as expected, in terms of all the three holding practices, to share the higher amount of delay.

Figs. B-2(c) and B-2(d) show the cases when varying the weighted cost of airborne holding. It is worth noting that the updated amount of airborne holding turns even higher than that resulted from the initial delay assignment when the parameter's value is relatively low (e.g., $\alpha = 1.2$). This is due to the fact that if performing airborne holding is only slightly expensive than ground holding (and linear holding), then it could be better to impose delays directly at certain sectors of reduced capacity (by means of air holding), rather than transferring the overall delay through multiple sectors (which may again yield extra delays) until the origin airports to execute ground holding which though is cheaper.

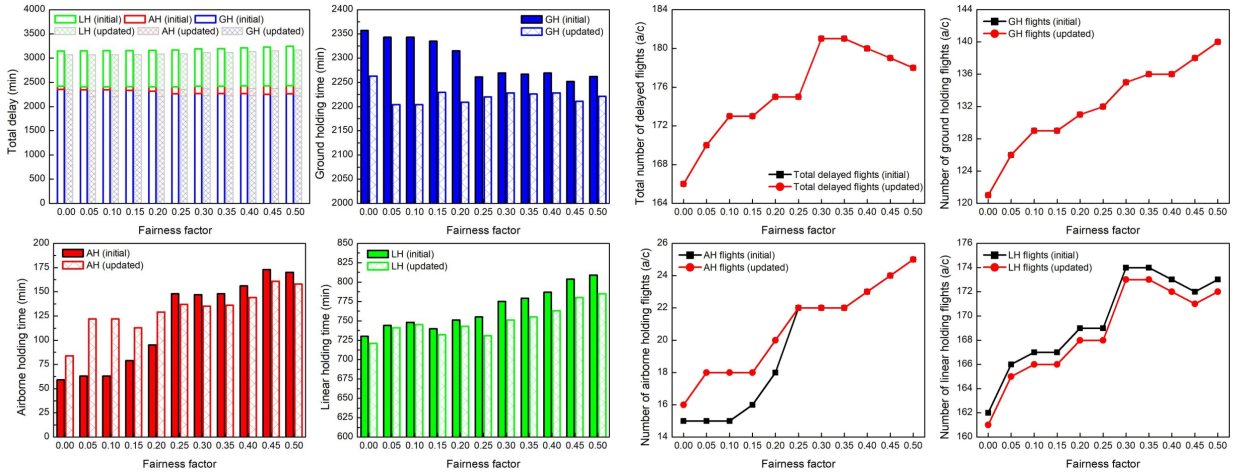

(a) Fairness factor - Amount of delay assignment

(b) Fairness factor - Number of affected flights

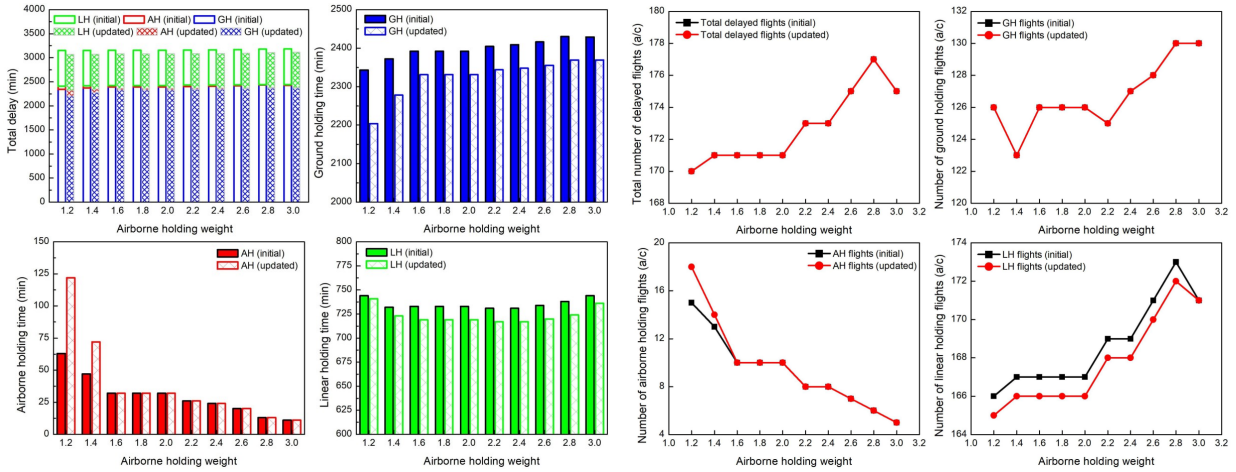

(c) Airborne holding cost - Amount of delay assignment

(d) Airborne holding cost - Number of affected flights

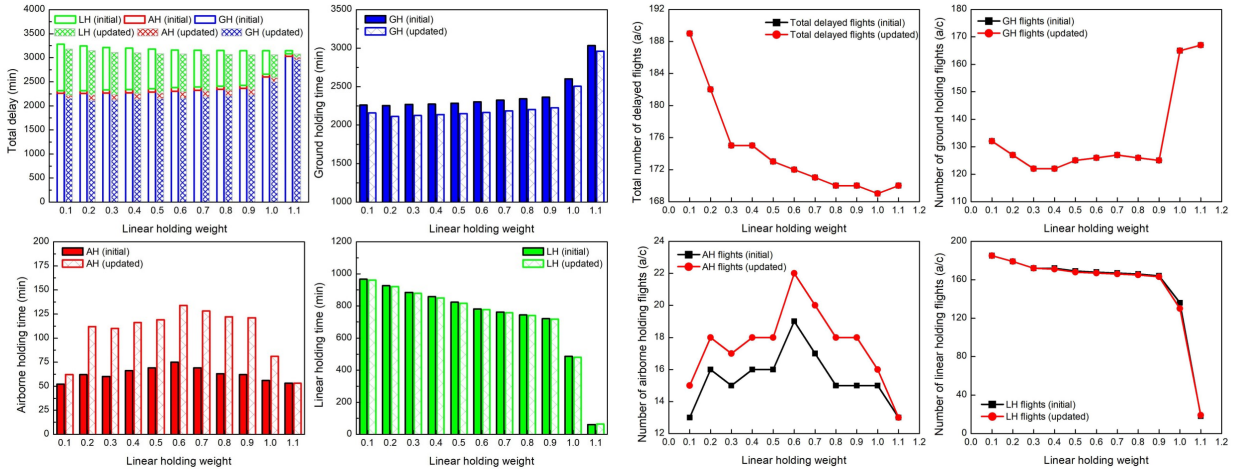

(e) Linear holding cost - Amount of delay assignment

(f) Linear holding cost - Number of affected flights

Figure B-2: *Sensitivity analysis on key parameters of model formulation with respect to the amount of delay assignment and the number of affected flights for each holding practice.*

The sensitivity results for linear holding's weighted cost are as shown in Figs. B-2(e) and B-2(f), from which it can be noticed that when its value is greater than 1 (i.e., higher than the cost

of ground holding), the assigned delays decrease remarkably while the reduced part is instead realized by ground holding. However, although the total delay keeps almost unchanged, the number of delayed flights reduces largely, meaning that the average delay for those affected flights would increase as well. In other words, with greater preference on the linear holding, more flights would be captured in the regulation to share a constant total delay.

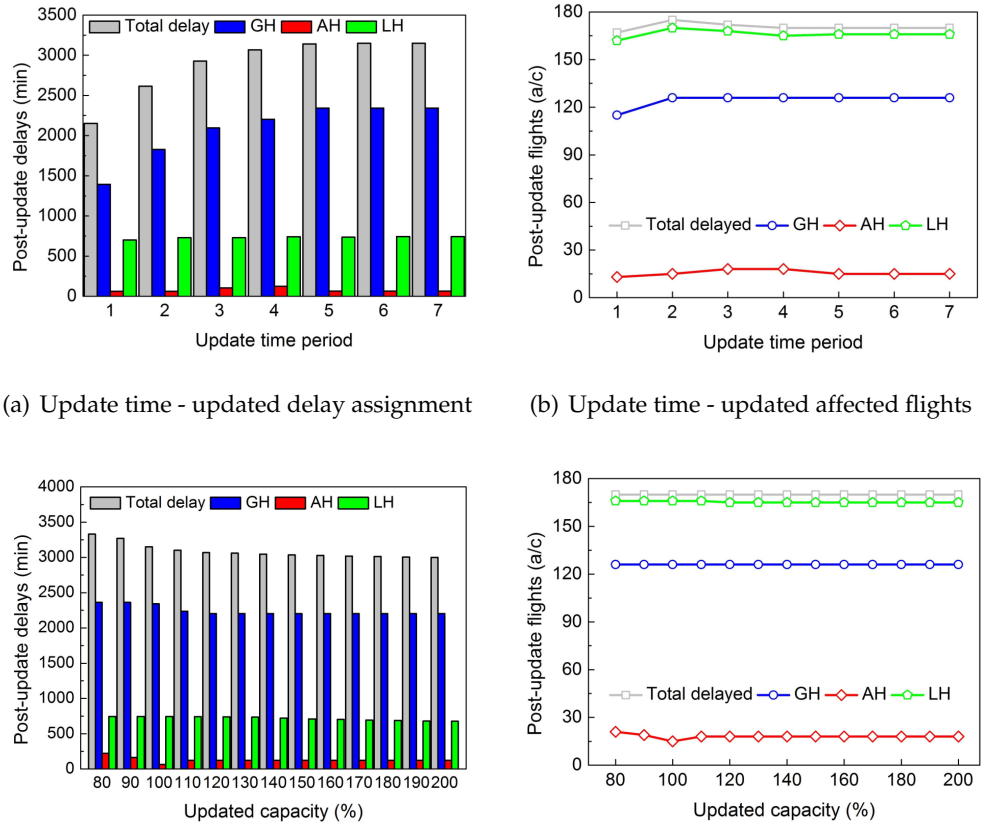

(a) Update time - updated delay assignment (b) Update time - updated affected flights

(c) Update capacity - updated delay assignment (d) Update capacity - updated affected flights

Figure B-3: *Sensitivity analysis on capacity updating parameters with respect to the post-update delay assignment and the number of affected flights for each holding practice.*

Meanwhile, the parameters τ and $C^s(\tau)$, other than ϵ, α and β, would only affect the delay updating process, and their results are summarized in Fig. B-3. Generally, the earlier the capacities start to recover and the higher the updated capacities turn to, the less delays are required in the updating process. However, after the 5th time period (i.e., 11:20 AM) the delays that can be saved keep almost constant, which is due to the fact that most of the flights have departed before that time, and therefore the already realized ground holding, in prior to take off, cannot be recovered even with the increased capacities.

B.2 Problem dimensions and computational time

Moreover, in order to understand what problem size can be handled, by executing the model of this paper, within a reasonable time given current optimization tools, two additional scenarios have been further considered (in addition to the benchmark scenario of the sensitivity experiment, which is labeled as S1) in the scalability tests. Namely, 2 hours' traffic across the ECAC (European

Civil Aviation Conference) area, labeled as S2, and 24 hours' traffic across the French airspace, labeled as S3. Scenario configurations are summarized in Table B-2, including the number of flights, time periods, elementary and collapsed sectors for instance. Tests of the initial delay assignment and the subsequent updating are conducted respectively for each scenario. Finally, the discrete time interval and the unit period of capacity are still set to 1 min and 20 min respectively, while the maximum delay allowed to each flight (i.e., solution search space) is limited to 180 min for the sake of reducing the total number of decision variables.

Table B-2: *Scenario setup for the scalability tests.*

Scenarios	Duration	Scope	Flights	Ele. Sectors	Col. Sectors	Time periods	Upd. time
S1	2 hour	France	1131	164	123	6	4
S2	2 hour	ECAC	3835	1626	1059	6	4
S3	24 hour	France	6089	164	205	72	37

Table B-3: *Problem size and computational time for each test of the study.*

Scenarios	Variables	Constraints	Non-zero elements	Generation time (s)	Comput. time (s)
S1_initial	575.101	1.193.063	3.605.217	308	238
S1_update	569.965	1.183.343	3.577.328	311	94
S2_initial	2,623,501	5,507,530	13,648,395	2184	665
S2_update	2,611,629	5,487,453	13,586,808	2168	34
S3_initial	2,743,201	5,825,900	14,483,261	1723	2566
S3_update	2,733,569	5,809,513	14,432,863	1519	171

Table B-4: *Results of delay assignment realized by the three holding practices.*

Scenarios	Ground holding		Airborne holding		Linear holding		Total delay	
	Time (min)	Flights (a/c)	Time (min)	Flights (a/c)	Time (min)	Flights (a/c)	Time (min)	Flights (a/c)
S1_initial	5155	308	338	39	898	268	6391	384
S1_update	4353	286	240	31	878	276	5471	361
S2_initial	13192	655	168	25	2063	400	15423	791
S2_update	12237	613	126	18	1929	376	14292	738
S3_initial	31456	1044	412	25	2440	835	34308	1157
S3_update	8604	650	45	10	1647	570	10296	796

The size of the problem and the computational time, for each scenario taken into the model, are summarized in Table B-3, while detailed results of the delay assignment can be found in Table B-4. Note that the generation time shown in the table includes the compilation time (for reading input files), execution time (for numerical calculations on existing data) and generation time (for constructing the equations and calling the solver), and this particular time could be saved remarkably for a second round of generation where only a few parameters change, such as the delay updating process, by means of using the save and restart option of GAMS. The solver's computational times recorded in Table B-3 show that the optimal solution of each scenario could be found within a reasonable time. Nevertheless, as there are numerous factors that may have effects on an MILP model's computational performance, such as the problem size (e.g., variables and constraints), the tightness of the formulation and the heuristic method used in the solver, it is quite difficult to only select a limited number of analytical indicators to predict the corresponding computational time. Empirical studies would be instead an appropriate way to quantify the actual scale that is tractable for this model, and deserve a further work in future.

Have no fear of perfection, you'll never reach it.

— Salvador Dalí

C

More about Collaborative ATFM model

This Appendix extends the original Collaborative ATFM model presented in Chapter VI, with more discussions on the details of the model, including the potential fairness criteria, model re-execution to tackle situation changes and/or possible trajectory errors, and the way of retrieving airspace capacity values from a published database. It should be noted that these branches can be further modified for different purposes, without affecting the original model's implementation.

C.1 Fairness concerns

As a complementary to the objective function discussed in Sec. VI.3.2, the following Eq. (C.1) further takes the fairness concern, across different airspace users, into account.

$$\min J = \min(\sum_{f \in F} \kappa c_f + \sum_{u \in U} \rho m_u) \tag{C.1}$$

where κ and ρ are the weighting factors for efficiency (i.e., extra direct operating costs) and fairness (i.e., maximal costs for airspace users) respectively. The extra direct operating costs c_f for each individual flight is the same as presented by Eqs. (VI.3), (VI.4) and (VI.5), and organized as below:

$$
\begin{aligned}
c_f = & \sum_{k\in K_f}[\alpha_k(TJ_k^f - TJ_0^f) + \beta_k(RC_k^f - RC_0^f)]w_k^f \\
& + \sum_{k\in K_f}\sum_{t\in T_f^j, P(f,1)=j}(\gamma_k - \zeta_k)(t - r_k^j)(x_{k,t}^j - x_{k,t-1}^j) \\
& + \sum_{k\in K_f}\sum_{t\in T_k^j, j\in P(k,i):1<i<n_k} t(\delta_k - \zeta_k)(x_{k,t}^j - x_{k,t-1}^j - y_{k,t}^j + y_{k,t-1}^j) \\
& + \sum_{k\in K_f}\sum_{t\in T_k^j, P(k,n_k)=j}\zeta_k(t - r_k^j)(y_{k,t}^j - y_{k,t-1}^j)\}
\end{aligned} \tag{C.2}
$$

whilst the maximal costs m_u for each airspace user ($u \in U$) is subject to:

$$
\sum_{u\in U} m_u \geq \sum_{u\in U}\sum_{f\in F_u} c_f \tag{C.3}
$$

where $f \in F_u$ represents all the regulated flights belonging to the airspace user u. In other words, the perfect equity appears when $m_1 = m_2 = \cdots = m_u$, i.e., $\overline{m}_u = \sum_{u\in U}\sum_{f\in F_u} c_f / \sum_{u\in U} 1$. This Max-Min rule specifies that no single airspace user can increase its benefits (incurring less extra costs) without reducing the benefits of other airspace users. The principle has been initially implemented in networking and telecommunication applications (Bertsekas & Gallager, 1992), and is recognized as one of the applicable fairness criteria in many similar areas. Nevertheless, it should be noted that, as reported by (Bertsimas *et al.*, 2011), a pure Max-Min rule may result in a significant decrease in system efficiency. Therefore, a trade-off between the efficiency and fairness, by means of setting different κ and ρ, is also worth exploring in the future work.

C.2 Iterative model execution

With Constraints (C.4)-(C.8) further included, the DCB model can be re-executed to perform the iterative optimization process. Assume at the start of the $(\tau+1)$ th time period, i.e., $\underline{T}(\tau+1)$, the capacity matrix is estimated to largely change from current status of the time period of $T(\tau)$, and requires for a new round of delay assignment.

$$
w_k^f(\tau+1) = w_k^f(\tau) \quad \forall f \in F, \forall k \in K_f, \dot{T}_k^{P(k,1)}(\tau) < \underline{T}(\tau+1), \tag{C.4}
$$

$$
\begin{aligned}
x^j_{k,\dot{T}_k^j(\tau)-1}(\tau+1) = y^j_{k,\dot{T}_k^j(\tau)-1}(\tau+1) = 0 \quad \forall k \in K_f, \\
\forall j \in P_k : \dot{T}_k^j(\tau) < \underline{T}(\tau+1),
\end{aligned} \tag{C.5}
$$

$$
\begin{aligned}
x^j_{k,\dot{T}_k^j(\tau)}(\tau+1) = y^j_{k,\dot{T}_k^j(\tau)}(\tau+1) = w_k^f(\tau) \quad \forall f \in F, \forall k \in K_f, \\
\forall j \in P_k : \dot{T}_k^j(\tau) < \underline{T}(\tau+1),
\end{aligned} \tag{C.6}
$$

$$
\begin{aligned}
x^{j'}_{k,\dot{T}_k^{j'}(\tau)-1}(\tau+1) = y^{j'}_{k,\dot{T}_k^{j'}(\tau)-1}(\tau+1) = 0 \quad \forall k \in K_f, \forall i \in [1, n_k - 1], \\
\dot{T}_k^{P(k,i)}(\tau) < \underline{T}(\tau+1), \dot{T}_k^{P(k,i+1)}(\tau) \geq \underline{T}(\tau+1),
\end{aligned} \tag{C.7}
$$

$$
\begin{aligned}
&x^{j'}_{k,\dot{T}^{j'}_k(\tau)}(\tau+1) = y^{j'}_{k,\dot{T}^{j'}_k(\tau)}(\tau+1) = w^f_k(\tau) \quad \forall f \in F, \forall k \in K_f, \\
&\forall i \in [1, n_k - 1], \dot{T}^{P(k,i)}_k(\tau) < \underline{T}(\tau+1), \dot{T}^{P(k,i+1)}_k(\tau) \geq \underline{T}(\tau+1).
\end{aligned} \tag{C.8}
$$

Then, Constraint (C.4) enforces that, once the aircraft has taken off, its selected trajectory is fixed. Constraints (C.5) and (C.6) specify that the values, prior to $\underline{T}(\tau+1)$, of the decision variables derived from the current round of optimization are assigned to those new decision variables defined in the same domains. Constraints (C.7) and (C.8) stipulate that for specifically the aircraft in the air at time $\underline{T}(\tau+1)$, the decision variables subject to the new round of optimization start from the next position after finishing their current flight segment linked by (j, j'). This is because the remaining distance within the segment might be not long enough to realize the amount of delay recovery and linear holding previously provided by airlines, which, however, is based on the calculation by an entire segment.

C.3 Retrieve airspace capacity

The following Algorithm C.1 presents a procedure to establish the static sector scheme according to the DDR2 database, where the required source files include: 1) OpeningScheme.cos, 2) Configuration.cfg, and 3) Airspace.spc, for the same AIRAC date.

Algorithm C.1: *Retrieve static collapsing scheme for elementary sectors*

```
for e in elementary_sector_list do
    for t in time_period_list do
        for a in area_control_center_opening_list do
            for cf in configuration_list[a][t] do
                for s in operating_sector_list[cf] do
                    if s in elementary_sector_list then
                        if s == e then
                            collapse_scheme[e][t] = s
                    else if s in collapsed_sector_list then
                        for c in collapsed_sector_list[s] do
                            if c == e then
                                collapse_scheme[e][t] = s
```

As for mapping the operating capacities to the set of matched collapsed sectors, some extra sources are needed, such as 4) TrafficVolume.ntfv, 5) Activation.nact, and 6) Capacity.ncap. See below for a detailed illustration to the procedure.

Procedure of generating the operating capacities of active sectors in different time periods

def Generation-of-Active-Sector-and-Capacity**:**

open 'OpeningScheme.cos' and 'Configuration.cfg'**:**

Create a dictionary of each ACC's opening scheme mapping to its associated elementary and/or collapsed sectors

open 'Airspace.spc'**:**

Create a dictionary of each collapsed sector's belonging elementary sectors

for elementary sector **in** list-of-designed-positions**:**

 # the list contains all the elementary sectors that the scheduled trajectories traverse

for period **in** list-of-time-periods:

 # the list contains all the time periods taken into the case study

Cross reference between the ACC's dictionary and collapsed sector's dictionary

Fill in a data frame (frame-of-elementary-sector)

 # the frame shows for each elementary sector what the operating sector (being itself or grouped into some collapsed sector) it will be during each period of time

open 'TrafficVolume.ntfv' and 'Activation.nact'**:**

Create a dictionary of each elementary/collapsed sector's associated Traffic Volume(s) (TV)

Remove those not activated *# with only one activated TV remained for each sector*

open 'Capacity.ncap'**:**

Create a dictionary of each unit's capacity and capacity-active period(s)

for item, time **in** frame-of-elementary-sector**:**

if item **in** list-of-units **and** time **in** list-of-unit-active-times**:**

 # search in the above capacity-dictionary

item**.append**(unit's capacity)

elif item **in** list-of-traffic-volumes**:** *# i.e., traffic-volume-dictionary.keys()*

tv = traffic-volume-dictionary[item][i] *# i.e., name of the traffic volume*

if tv **in** list-of-units **and** time **in** list-of-unit-active-times**:**

item**.append**(tv's capacity)

return Data-Frame-of-Active-Sector-and-Capacity

Starting properly is half done.

— Catalan Proverb

D

Involvement of a flight in Collaborative ATFM

This appendix presents the involvement of airspace users in the iterative procedures, under the proposed Collaborative ATFM framework, in collaboration with the Network Manager. It is shown via an example of a specific flight (LIRF-EGLL) extracted from the scenario simulated for the numerical experiments in Chapter VI. As in the same way, two route modes, i.e., structured route and free route, are considered.

D.1 Submission of trajectory options

Figs. D-1(a) and D-2(a) show the lateral route of the initial trajectory for Case-SR and Case-FR respectively. As discussed in Sec. VI.2.1, the initial trajectory should reflect the most-preferred trajectory, minimizing the aircraft direct operating cost, for the airspace user. The traversed elementary sectors are highlighted in the two figures, whilst the vertical profile of the trajectory intersecting with those sectors is as shown in Figs. D-1(c) and D-2(c).

For each of the traversed elementary sectors, the control point is defined at the entry position. Through a primary hotspot detection process (recall Sec. VI.2.3) conducted by the Network Manager, comparing the traffic demand (of the initial trajectories) and airspace capacity for different time periods, sector LFEEHR (see Figs. D-1(a) and D-1(c)) and sector LFEEKF (see Figs. D-2(a) and D-2(c)) are identified as the hotspot areas to be avoided for this particular flight, in Case-SR and Case-FR respectively.

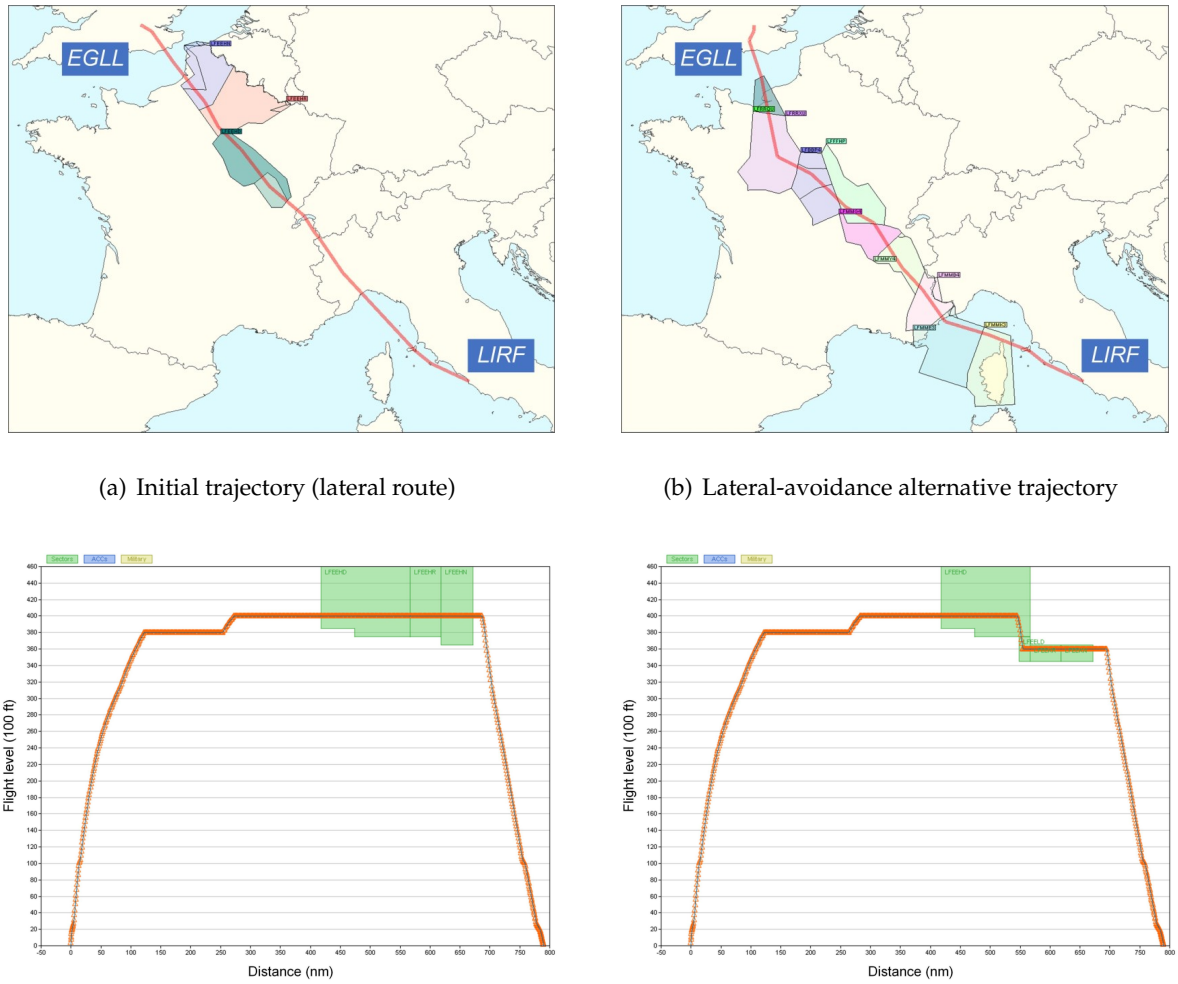

(a) Initial trajectory (lateral route)

(b) Lateral-avoidance alternative trajectory

(c) Initial trajectory (vertical profile)

(d) Vertical-avoidance alternative trajectory

Figure D-1: *Airspace user's submitted trajectory options for the specific flight (LIRF-EGLL) in Case-SR, including the initially scheduled trajectory, the lateral- and vertical-avoidance alternative trajectories.*

With the detailed avoidance information received (recall Sec. VI.2.3), the airspace user then produces the lateral-avoidance (see Figs. D-1(b) and D-2(b)) and vertical-avoidance (see Figs. D-1(d) and D-2(d)) alternative trajectories to precisely evade the corresponding sectors, using the aircraft trajectory optimization techniques introduced in Sec. VI.2.4. Taking the extra cost into account (see Table D-1), the airspace user thereafter decides to submit all the three trajectory options to the Network Manager, as well as the preferences for different measures of the timeline adjustments (recall Sec. VI.2.5).

D.2 Trajectory selection and delay assignment

Subsequently, the DCB is initiated by the Network Manager, generating the optimal solution of trajectory options and timeline adjustments, in such a way to minimize the overall deviation with respect to the airspace users' initial trajectories (recall Sec. VI.3). Eventually, the vertical-avoidance alternative trajectory is selected for the particular flight in Case-SR (see green line in Fig. D-3(a)),

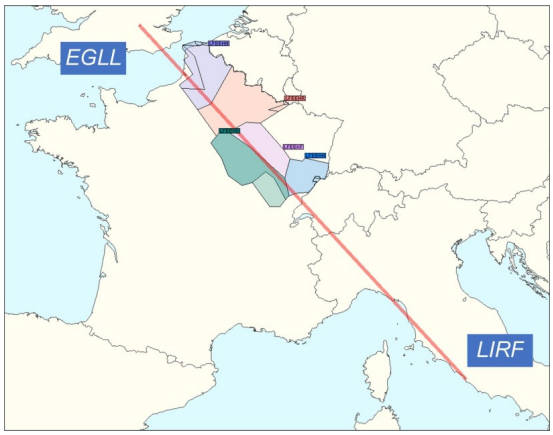

(a) Initial trajectory (lateral route)

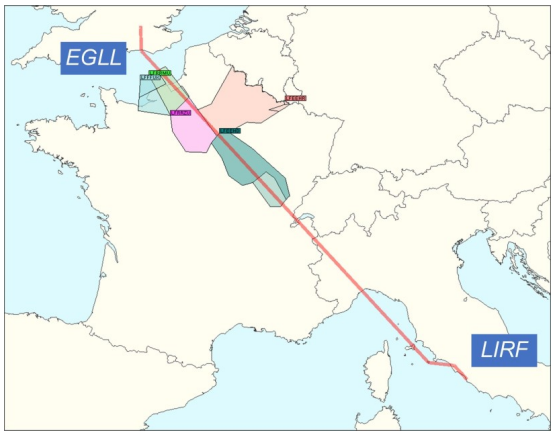

(b) Lateral-avoidance alternative trajectory

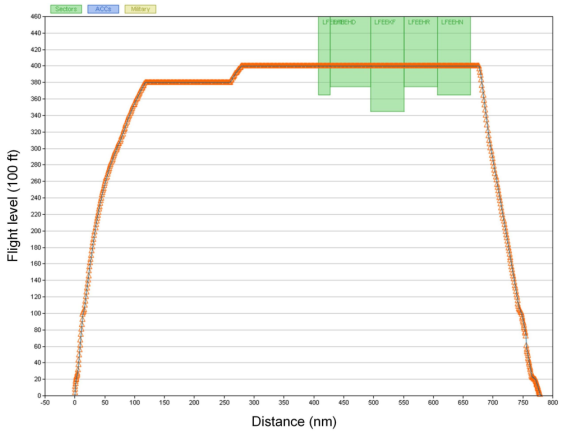

(c) Initial trajectory (vertical profile)

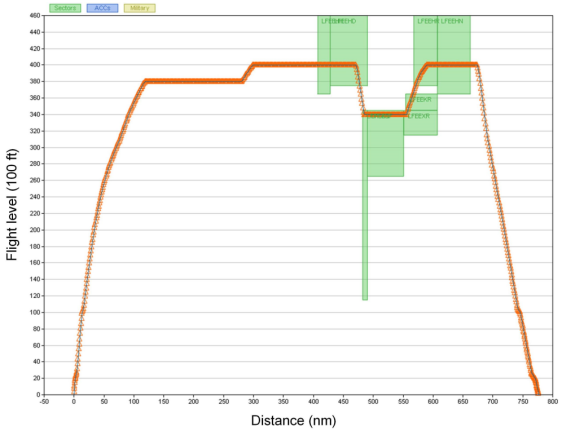

(d) Vertical-avoidance alternative trajectory

Figure D-2: *Airspace user's submitted trajectory options for the specific flight (LIRF-EGLL) in Case-FR, including the initially scheduled trajectory, the lateral- and vertical-avoidance alternative trajectories.*

Table D-1: *Costs of all trajectory options and delay management on the selected trajectory.*

Cases	Options	Fuel (kg)	Charges (euro)	E. Fuel (kg)	E. Charges (euro)	E. Time (min)				
						GH	AH	LH	DR	AD
Case-SR	Initial	4529	1359	0	0	-	-	-	-	-
	Lateral	4666	1370	137	11	-	-	-	-	-
	Vertical	4548	1359	19	0	10	0	0	-3	7
Case-FR	Initial	4473	1386	0	0	-	-	-	-	-
	Lateral	4505	1399	32	13	0	0	0	0	0
	Vertical	4544	1386	71	0	-	-	-	-	-

based on which 10 min of ground holding is imposed and 3 min of delay recovery is allowed. In Case-FR, on the other hand, the lateral-avoidance trajectory is chosen (see blue line in Fig. D-3(b)), while no further timeline adjustment is required. For different selected trajectories, the 4-D intersection (between trajectory and airspace) information varies accordingly, as shown in Fig. D-3(a) and Fig. D-3(b) respectively.

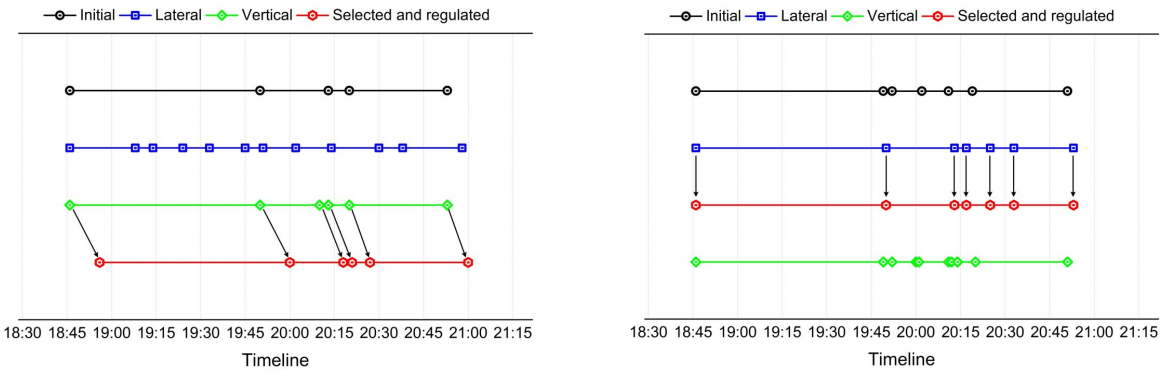

(a) Case-SR (b) Case-FR

Figure D-3: *Timeline of each trajectory along different defined positions (i.e., origin and destination airport, as well as entry point of all elementary sectors the trajectory traverses).*

Table D-2: *3-Dimensional information along different defined positions in Case-SR.*

Initial	LIRF	LFEEHD	LFEEHR	LFEEHN	EGLL						
Dep. dist.	0 NM	418 NM	566 NM	618 NM	790 NM						
Inter.FL	FL0	FL400	FL400	FL400	FL0						
Inter.lat.	41°48′01″	46°52′13″	48°40′47″	49°22′53″	51°27′25″						
Inter.lon.	12°14′20″	5°46′41″	3°16′49″	2°32′24″	-0°23′46″						
Lateral	LIRF	LFMMK3	LFMME3	LFMMB4	LFMMY4	LFMMG4	LFFFHP	LFBBP4	LFRRXU	LFRRQU	LFRRQS	EGLL
Dep. dist.	0 NM	131 NM	181 NM	252 NM	314 NM	396 NM	437 NM	510 NM	592 NM	698 NM	751 NM	848 NM
Inter.FL	FL0	FL380	FL380	FL380	FL400	FL400	FL400	FL400	FL400	FL400	FL345	FL0
Inter.lat.	41°48′01″	42°57′12″	43°17′08″	43°45′41″	44°35′57″	45°40′58″	46°15′47″	46°55′01″	47°44′41″	49°07′46″	49°58′14″	51°27′25″
Inter.lon.	12°14′20″	9°45′05″	8°42′50″	7°14′37″	6°25′33″	5°16′09″	4°44′57″	3°18′03″	1°40′28″	0°23′26″	0°03′02″	-0°23′46″
Vertical	LIRF	LFEEHD	LFEELD	LFEEKR	LFEEKN	EGLL						
Dep. dist.	0 NM	418 NM	551 NM	567 NM	618 NM	790 NM						
Inter.FL	FL0	FL400	FL375	FL360	FL360	FL0						
Inter.lat.	41°48′01″	46°52′10″	48°30′36″	48°40′48″	49°22′50″	51°27′25″						
Inter.lon.	12°14′20″	5°46′45″	3°33′10″	3°16′48″	2°32′26″	-0°23′46″						

Table D-3: *3-Dimensional information along different defined positions in Case-FR.*

Initial	LIRF	LFEEHH	LFEEHD	LFEEKF	LFEEHR	LFEEHN	EGLL			
Dep. dist.	0 NM	408 NM	426 NM	495 NM	550 NM	607 NM	781 NM			
Inter.FL	FL0	FL400	FL400	FL400	FL400	FL400	FL0			
Inter.lat.	41°48′01″	47°02′14″	47°16′48″	48°07′21″	48°47′42″	49°27′57″	51°27′25″			
Inter.lon.	12°14′20″	6°10′12″	5°50′58″	4°42′17″	3°45′04″	2°45′46″	-0°23′46″			
Lateral	LIRF	LFEEHD	LFEEHR	LFRRZU	LFRRMU	LFRRMS	EGLL			
Dep. dist.	0 NM	419 NM	571 NM	598 NM	648 NM	701 NM	797 NM			
Inter.FL	FL0	FL400	FL400	FL400	FL400	FL345	FL0			
Inter.lat.	41°48′01″	46°45′52″	48°37′41″	48°56′52″	49°32′02″	50°09′01″	51°27′25″			
Inter.lon.	12°14′20″	5°39′31″	3°04′15″	2°35′54″	1°42′31″	0°44′15″	-0°23′46″			
Vertical	LIRF	LFEEHH	LFEEHD	LFFFAR	LFEEUF	LFEEXR	LFEEKR	LFEEHR	LFEEHN	EGLL
Dep. dist.	0 NM	407 NM	428 NM	484 NM	490 NM	551 NM	558 NM	571 NM	607 NM	781 NM
Inter.FL	FL0	FL400	FL400	FL345	FL340	FL340	FL344	FL375	FL400	FL0
Inter.lat.	41°48′01″	47°02′18″	47°17′38″	47°58′56″	48°04′00″	48°47′59″	48°52′50″	49°02′40″	49°28′29″	51°27′25″
Inter.lon.	12°14′20″	6°10′53″	5°50′42″	4°54′55″	4°47′54″	3°45′49″	3°38′48″	3°24′29″	2°46′14″	-0°23′46″

References

AIRBUS. 1993. *Flight crew operation manual (FCOM): A320, version 1.3.1*. 3.04.10. 26, 30

AIRBUS. 1998. *Getting to grips with the cost index, issue II. flight operations support and line assistance (STL)*. 2 edn. Airbus Customer Services Directorate, Blagnac, Toulouse, France. 25, 27, 85

AIRLINES FOR AMERICA. 2016. *U.S. Passenger Carrier Delay Costs*. Tech. rept. 1

AIRSERVICES AUSTRALIA. 2007. *Airservices Australia annual report 2006-2007*. Tech. rept. 17

BALAKRISHNAN, HAMSA. 2007. Techniques for reallocating airport resources during adverse weather. *Pages 2949–2956 of: 46th IEEE conference on decision and control*. IEEE. 21

BALAKRISHNAN, HAMSA, & JUNG, YOON. 2007. A framework for coordinated surface operations planning at Dallas-Fort Worth International Airport. *In: Proceedings of the AIAA guidance, navigation and control conference*. 55

BALL, MICHAEL, BARNHART, CYNTHIA, DRESNER, MARTIN, HANSEN, MARK, NEELS, KEVIN, ODONI, AR, PETERSON, EVERETT, SHERRY, LANCE, TRANI, ANTONIO, & ZOU, BO. 2010a. Total delay impact study: a comprehensive assessment of the costs and impacts of flight delay in the United States. University of California, Berkeley. Institute of Transportation Studies. 1, 18

BALL, MICHAEL O, HOFFMAN, ROBERT L, & KNORR, DAVE. 2000. Assessing the benefits of collaborative decision making in air traffic management. *In: Proceedings of the 3rd USA/Europe ATM R&D Seminar*. 19

BALL, MICHAEL O, CHEN, CHIEN-YU, HOFFMAN, ROBERT, & VOSSEN, THOMAS. 2001. Collaborative decision making in air traffic management: Current and future research directions. *Pages 17–30 of: New concepts and methods in air traffic management*. Springer. 23

BALL, MICHAEL O, HOFFMAN, ROBERT, ODONI, AMEDEO R, & RIFKIN, RYAN. 2003. A stochastic integer program with dual network structure and its application to the ground-holding problem. *Operations research*, **51**(1), 167–171. 20, 21

BALL, MICHAEL O, HOFFMAN, ROBERT, LOVELL, DAVID, & MUKHERJEE, AVIJIT. 2005. Response mechanisms for dynamic air traffic flow management. *In: Proceedings of the 6th USA/Europe ATM R&D Seminar*. 19

BALL, MICHAEL O, HOFFMAN, ROBERT, & MUKHERJEE, AVIJIT. 2010b. Ground delay program planning under uncertainty based on the ration-by-distance principle. *Transportation science*, **44**(1), 1–14. 5, 15, 23

BARMORE, BRYAN. 2006. Airborne precision spacing: A trajectory-based aprroach to improve terminal area operations. *Pages 1–12 of: Proceedings of the 25th IEEE/AIAA digital avionics systems conference (DASC)*. IEEE. 17

BARNHART, CYNTHIA, BERTSIMAS, DIMITRIS, CARAMANIS, CONSTANTINE, & FEARING, DOUGLAS. 2012. Equitable and efficient coordination in traffic flow management. *Transportation science*, **46**(2), 262–280. 23

BARNIER, NICOLAS, & ALLIGNOL, CYRIL. 2009. 4d-trajectory deconfliction through departure time adjustment. *In: 8th USA/Europe ATM R&D Seminar*. 19

BAYEN, ALEXANDRE M, RAFFARD, ROBIN L, & TOMLIN, CLAIRE J. 2004. Eulerian network model of air traffic flow in congested areas. *Pages 5520–5526 of: Proceedings of the 2004 American Control Conference*, vol. 6. IEEE. 22

BELKOURA, SEDDIK, PEÑA, JOSÉ MARIA, & ZANIN, MASSIMILIANO. 2016. Generation and recovery of airborne delays in air transport. *Transportation research part C: Emerging technologies*, **69**, 436–450. 16

BERTSEKAS, DIMITRI, & GALLAGER, ROBERT. 1992. *Data networks*. Vol. 2. Prentice-Hall International. 23, 138

BERTSIMAS, DIMITRIS, & GUPTA, SHUBHAM. 2015. Fairness and collaboration in network air traffic flow management: an optimization approach. *Transportation science*, **50**(1), 57–76. 22, 23, 68, 71

BERTSIMAS, DIMITRIS, & PATTERSON, SARAH STOCK. 1998. The air traffic flow management problem with enroute capacities. *Operations research*, **46**(3), 406–422. 22, 64, 68, 92, 95, 99

BERTSIMAS, DIMITRIS, & PATTERSON, SARAH STOCK. 2000. The traffic flow management rerouting problem in air traffic control: A dynamic network flow approach. *Transportation science*, **34**(3), 239–255. 22

BERTSIMAS, DIMITRIS, FARIAS, VIVEK F, & TRICHAKIS, NIKOLAOS. 2011. The price of fairness. *Operations research*, **59**(1), 17–31. 23, 106, 138

BETTS, J. 2010. *Practical methods for optimal control and estimation using nonlinear programming*. Second edn. Society for Industrial and Applied Mathematics. 17, 31

BETTS, JOHN T, & CRAMER, EVIN J. 1995. Application of direct transcription to commercial aircraft trajectory optimization. *Journal of guidance, control, and dynamics*, **18**(1), 151–159. 17

BILIMORIA, K. 2016. Analysis of additional delays experienced by flights subject to ground holding. *In: Proceedings of the AIAA aviation technology, integration, and operations conference*. 7, 54, 57

BOLIĆ, TATJANA, CASTELLI, LORENZO, COROLLI, LUCA, & RIGONAT, DESIRÉE. 2017. Reducing atfm delays through strategic flight planning. *Transportation research part E: Logistics and transportation review*, **98**, 42–59. 67, 85

CAO, YI, & SUN, DENGFENG. 2012. A parallel computing framework for large-scale air traffic flow optimization. *IEEE transactions on intelligent transportation systems*, **13**(4), 1855–1864. 23

CASTELLI, L, BOLIĆ, T, COSTANZO, S, RIGONAT, D, MARCOTTE, E, & TANNER, G. 2015. Modulation of en-route charges to redistribute traffic in the european airspace. *In: Proceedings of the 5th SESAR Innovation Days*. 20

CASTELLI, LORENZO, PESENTI, RAFFAELE, & RANIERI, ANDREA. 2011. The design of a market mechanism to allocate air traffic flow management slots. *Transportation research part C: Emerging technologies*, **19**(5), 931–943. 20

CHANG, KAN, HOWARD, KEN, OIESEN, RICK, SHISLER, LARA, TANINO, MIDORI, & WAMBSGANSS, MICHAEL C. 2001. Enhancements to the FAA ground-delay program under collaborative decision making. *Interfaces*, **31**(1), 57–76. 19

CIVIL AVIATION ADMINISTRATION OF CHINA. 2016. *Statistics of key performance indicators for China's civil aviation industry*. 2

CLARKE, JOHN-PAUL B, HO, NHUT T, REN, LILING, BROWN, JOHN A, ELMER, KEVIN R, ZOU, KATHERINE, HUNTING, CHRISTOPHER, MCGREGOR, DANIEL L, SHIVASHANKARA, BELUR N, TONG, KWOK-ON, *et al.* 2004. Continuous descent approach: Design and flight test for Louisville International Airport. *Journal of aircraft*, **41**(5), 1054–1066. 17

COOK, ANDREW. 2007. *European air traffic management: principles, practice, and research*. Ashgate Publishing, Ltd. 19, 98

COOK, ANDREW J, & TANNER, GRAHAM. 2011. *European airline delay cost reference values*. Tech. rept. 25

COOK, ANDREW J, & TANNER, GRAHAM. 2015. *European airline delay cost reference values: Updated and extended values*. Tech. rept. 18

COOK, LARA S, & WOOD, BRYAN. 2010. A model for determining ground delay program parameters using a probabilistic forecast of stratus clearing. *Air traffic control quarterly*, **18**(1), 85. 5, 15

CRUCIOL, LEONARDO L.B.V., DE ARRUDA, ANTONIO C., WEIGANG, LI, LI, LEIHONG, & CRESPO, ANTONIO M.F. 2013. Reward functions for learning to control in air traffic flow management. *Transportation research part C: Emerging technologies*, **35**, 141 – 155. 21

DALMAU, RAMON, & PRATS, XAVIER. 2015. Fuel and time savings by flying continuous cruise climbs: Estimating the benefit pools for maximum range operations. *Transportation research part D: Transport and environment*, **35**, 62–71. 17

DALMAU, RAMON, & PRATS, XAVIER. 2017. Assessing the impact of relaxing cruise operations with a reduction of the minimum rate of climb and/or step climb heights. *Aerospace science and technology*, **70**, 461–470. 17, 85

DALMAU, RAMON, MELGOSA, MARC, VILARDAGA, SANTI, & PRATS, XAVIER. 2018. A fast and flexible aircraft trajectory predictor and optimiser for atm research applications. *In: Proceedings of the 8th international conference for research in air transportation (ICRAT)*. 18, 31, 84, 85

DELAHAYE, DANIEL, & PUECHMOREL, STÉPHANE. 2000. Air traffic complexity: towards intrinsic metrics. *In: Proceedings of the 3rd USA/Europe ATM R&D Seminar*. 87

DELGADO, LUIS. 2015. European route choice determinants. *In: Proceedings of the 11th USA/Europe ATM R&D Seminar*. 18, 94

DELGADO, LUIS, & PRATS, XAVIER. 2012. En route speed reduction concept for absorbing air traffic flow management delays. *Journal of aircraft*, **49**(1), 214–224. 5, 16, 25, 26, 33, 34, 47, 121

DELGADO, LUIS, & PRATS, XAVIER. 2013. Effect of wind on operating-cost-based cruise speed reduction for delay absorption. *IEEE transactions on intelligent transportation systems*, **14**(2), 918–927. 11, 16, 25, 26

DELGADO, LUIS, & PRATS, XAVIER. 2014. Operating cost based cruise speed reduction for ground delay programs: Effect of scope length. *Transportation research part C: Emerging technologies*, **48**, 437–452. 5, 16, 25, 26

DELGADO, LUIS, PRATS, XAVIER, & SRIDHAR, BANAVAR. 2013. Cruise speed reduction for ground delay programs: A case study for San Francisco International Airport arrivals. *Transportation research part C: Emerging technologies*, **36**, 83–96. 5, 16, 25, 26, 43, 57

EUROCONTROL. 2015. *European ATM master plan*. Tech. rept. Ed. 2015. 3

EUROCONTROL. 2016. *Optimised airspace users operations: Step 1 business trajectory final OSED 2016*. Tech. rept. Ed. 00.05.01. 3

EUROCONTROL. 2017. *All-causes delay and cancellations to air transport in Europe*. Tech. rept. CODA Digest 2016, CDA-2017-005. Network Manager. 1

EUROCONTROL. 2017. *ATFCM operations manual - network operations handbook*. Tech. rept. Ed. 21.0. 19

EUROCONTROL. 2017. *SESAR 2020 concept of operations edition 2017*. Tech. rept. PJ.19-02. 3

EUROCONTROL. 2018a. *ATFCM users manual - network manager*. Tech. rept. Ed. 22.0. 19

EUROCONTROL. 2018b. *DDR2 reference manual for general users*. Tech. rept. Version 2.9.5. 87

EVANS, ANTONY D, & LEE, PAUL U. 2016. Analyzing double delays at newark liberty international airport. *In: Proceedings of the 16th AIAA aviation technology, integration, and operations conference*. 11, 54

FAA. 2009. *Traffic Flow Management in the National Airspace System*. Tech. rept. FAA-2009-AJN-251. Federal Aviation Administration. 2, 18, 44

FAA. 2014. *Collaborative Trajectory Options Program (CTOP): Document Information*. Tech. rept. AC 90-115. Federal Aviation Administration. 2, 20

FAA. 2015. *Instrument procedures handbook, FAA-h-8083-16a, chapter 3, arrivals*. 17

FAA. 2016. *Nextgen implementation plan*. Tech. rept. 3

FAA. 2016. *Pilot's handbook of aeronautical knowledge, FAA-h-8083-25a, chapter glossary, holding pattern*. 56

FAA. 2017. *Air traffic by the numbers*. Federal Aviation Administration Air Traffic Organization. 60

GAMS Development Corporation. 2013a. *GAMS - The Solver Manuals, GAMS Release 24.2.1*. Washington, DC, USA. 31

GAMS Development Corporation. 2013b. *General Algebraic Modeling System (GAMS) Release 24.2.1*. http://www.gams.com/. Washington, DC, USA. 31

Gardi, Alessandro, Sabatini, Roberto, & Ramasamy, Subramanian. 2016. Multi-objective optimisation of aircraft flight trajectories in the ATM and avionics context. *Progress in aerospace sciences*, **83**, 1–36. 18

Grabbe, Shon, & Sridhar, Banavar. 2003. Modeling and evaluation of miles-in-trail restrictions in the national air space. *In: AIAA guidance, navigation, and control conference and exhibit*. 18

Grabbe, Shon, Sridhar, Banavar, Mukherjee, Avijit, & Morando, Alexander. 2011. Traffic management advisor flow programs: an Atlanta case study. *Pages 8–11 of: Proceedings of the AIAA guidance, navigation, and control conference*. 54

Günther, T, & Fricke, H. 2006. Potential of speed control on flight efficiency. *Pages 197–201 of: Proceedings of the 2nd international conference on research in air transportation (ICRAT), belgrade, serbia*, vol. 1. 17

Hart, Peter E, Nilsson, Nils J, & Raphael, Bertram. 1968. A formal basis for the heuristic determination of minimum cost paths. *IEEE transactions on systems science and cybernetics*, **4**(2), 100–107. 86

Hoffman, Robert, & Ball, Michael O. 2000. A comparison of formulations for the single-airport ground-holding problem with banking constraints. *Operations research*, **48**(4), 578–590. 21

Holloway, Stephen. 2008. *Straight and level: Practical airline economics*. Ashgate Publishing, Ltd. 18

Inniss, Tasha R, & Ball, Michael O. 2004. Estimating one-parameter airport arrival capacity distributions for air traffic flow management. *Air traffic control quarterly*, **12**, 223–252. 5, 15

International Civil Aviation Organization. 1994. *Manual of the ICAO standard atmosphere: Extended to 80 kilometres (262 500 feet)*. International Civil Aviation Organization. 30

International Civil Aviation Organization. 2016. *Global air navigation plan (2016-2030), Doc 9750-an/963, fifth edition*. Tech. rept. 3

Janić, Milan, & Tošić, Vojin. 1982. Terminal airspace capacity model. *Transportation research part A: General*, **16**(4), 253–260. 87

Jin, Li, Cao, Yi, & Sun, Dengfeng. 2013. Investigation of potential fuel savings due to continuous-descent approach. *Journal of aircraft*, **50**(3), 807–816. 17

Jones, James C, Lovell, David J, & Ball, Michael O. 2013. En route speed control methods for transferring terminal delay. *In: Proceedings of the 10th USA/Europe ATM R&D Seminar*. 17

Jones, James C, Lovell, David J, & Ball, Michael O. 2015. Combining control by CTA and dynamic en route speed adjustment to improve ground delay program performance. *Pages 1–10 of: Proceedings of the 11th USA/Europe ATM R&D Seminar*. 8, 17

Khadilkar, Harshad, & Balakrishnan, Hamsa. 2014. Network congestion control of airport surface operations. *Journal of guidance, control, and dynamics*, **37**(3), 933–940. 55

Kim, Amy, & Hansen, Mark. 2015. Some insights into a sequential resource allocation mechanism for en route air traffic management. *Transportation research part B: Methodological*, **79**, 1–15. 20

Kirkman, Worth, Gaydos, Travis, & Weitz, L. 2014. Optimizing metering for trajectory timing uncertainty. *In: Proceedings of the AIAA guidance, navigation, and control conference*. 17

Klooster, Joel, Torres, Sergio, Earman, Daniel, Castillo-Effen, Mauricio, Subbu, Raj, Kammer, Leonardo, Chan, David, & Tomlinson, Tom. 2010. Trajectory synchronization and negotiation in trajectory based operations. *In: Proceedings of the 25th IEEE/AIAA digital avionics systems conference*. IEEE. 32

KOPARDEKAR, PARIMAL, BILIMORIA, KARL, & SRIDHAR, BANAVAR. Initial concepts for dynamic airspace configuration. *In: Proceedings of the 7th AIAA aviation technology, integration and operations conference (atio*. AIAA. 9

LIBBY, MARK, BUCKNER, JAMES, & BRENNAN, MICHAEL. 2005. *Operational concept for Airspace Flow Programs (AFP)*. Tech. rept. FAA Air Traffic Oranization, Systems Operations Services. 2, 19, 44

LULLI, GUGLIELMO, & ODONI, AMEDEO. 2007. The European air traffic flow management problem. *Transportation science*, **41**(4), 431–443. 22

MAJUMDAR, ARNAB, OCHIENG, WASHINGTON, & POLAK, JOHN. 2002. Estimation of European airspace capacity from a model of controller workload. *The journal of navigation*, **55**(3), 381–403. 87

MENON, P K, SWERIDUK, G D, LAM, T, DIAZ, GM, & BILIMORIA, KARL D. 2006. Computer-aided Eulerian air traffic flow modeling and predictive control. *Journal of guidance, control, and dynamics*, **29**(1), 12–19. 22

MENON, PADMANABHAN K, SWERIDUK, GREGORY D, & BILIMORIA, KARL D. 2004. New approach for modeling, analysis, and control of air traffic flow. *Journal of guidance, control, and dynamics*, **27**(5), 737–744. 22

MEYER, JOHN ROBERT, & OSTER, CLINTON V. 1981. *Airline deregulation: the early experience*. Auburn House. 18

MILLER, MARY ELLEN, & HALL, WILLIAM D. 2015. Collaborative trajectory option program demonstration. *Pages 1C1–8 of: Proceedings of the 34th IEEE/AIAA digital avionics systems conference (DASC)*. IEEE, Prague, Czech Republic. 2, 20

MOLINA, MARTIN, CARRASCO, SERGIO, & MARTIN, JORGE. 2014. Agent-based modeling and simulation for the design of the future european air traffic management system: the experience of cassiopeia. *Pages 22–33 of: International conference on practical applications of agents and multi-agent systems*. Springer. 20

MORGENSTERN, OSKAR, & VON NEUMANN, JOHN. 1953. *Theory of games and economic behavior*. Princeton university press. 20

MORRISON, STEVEN, & WINSTON, CLIFFORD. 2010. *The economic effects of airline deregulation*. Brookings Institution Press. 18

MUKHERJEE, AVIJIT, & HANSEN, MARK. 2007. A dynamic stochastic model for the single airport ground holding problem. *Transportation science*, **41**(4), 444–456. 21, 69

MUKHERJEE, AVIJIT, & HANSEN, MARK. 2009. A dynamic rerouting model for air traffic flow management. *Transportation research part B: Methodological*, **43**(1), 159–171. 18, 22, 44

NUIC, A, & MOUILLET, V. 2014. *User manual for the base of aircraft data (BADA) family 4, EEC Technical/Scientific Report*. Eurocontrol Experimental Centre, Bretigny-sur-Orge, France. 86

ODONI, AMEDEO R. 1987. The flow management problem in air traffic control. *Pages 269–288 of: Flow control of congested networks*. Springer. 21

PILON, NADINE, COOK, ANDREW, RUIZ, SERGIO, BUJOR, ANDRADA, & CASTELLI, LORENZO. 2016. Improved flexibility and equity for airspace users during demand-capacity imbalance. *In: Proceedings of the 6th SESAR Innovation Days*. 20

POURTAKLO, NASIM VAKILI, & BALL, MICHAEL. 2009. Equitable allocation of enroute airspace resources. *In: Proceedings of the 8th USA/Europe ATM R&D Seminar*. 2, 5

PRATS, XAVIER, & HANSEN, MARK. 2011. Green delay programs: absorbing ATFM delay by flying at minimum fuel speed. *In: Proceedings of the 9th USA/Europe ATM R&D Seminar*. 5, 16

PRATS, XAVIER, PUIG, VICENC, & QUEVEDO, JOSEBA. 2011a. Equitable aircraft noise-abatement departure procedures. *Journal of guidance, control, and dynamics*, **34**(1), 192–203. 23

PRATS, XAVIER, PUIG, VICENC, & QUEVEDO, JOSEBA. 2011b. A multi-objective optimization strategy for designing aircraft noise abatement procedures. case study at girona airport. *Transportation research part D: Transport and environment*, **16**(1), 31–41. 23

REBOLLO, JUAN, & BRINTON, CHRIS. 2015. Brownian motion delay model for the integration of multiple traffic management initiatives. *In: Proceedings of the 11th USA/Europe ATM R&D Seminar*. 54

RICHETTA, OCTAVIO. 1991. *Ground holding strategies for air traffic control under uncertainty*. Ph.D. thesis, Massachusetts Institute of Technology. 15, 21

RICHETTA, OCTAVIO, & ODONI, AMEDEO R. 1993. Solving optimally the static ground-holding policy problem in air traffic control. *Transportation science*, **27**(3), 228–238. 21

RICHETTA, OCTAVIO, & ODONI, AMEDEO R. 1994. Dynamic solution to the ground-holding problem in air traffic control. *Transportation research part A: Policy and practice*, **28**(3), 167–185. 21

RIOS, JOSEPH, & ROSS, KEVIN. 2010. Massively parallel Dantzig-Wolfe decomposition applied to traffic flow scheduling. *Journal of aerospace computing, information, and communication*, **7**(1), 32–45. 22, 71

ROBERSON, BILL. 2007. Fuel conservation strategies: cost index explained. *Boeing aero quarterly*, **2**, 26–28. 25, 85

ROBINSON, MICHAEL, DELAURA, RICH, MARTIN, B, EVANS, JAMES E, & WEBER, MARK E. 2009. Initial studies of an objective model to forecast achievable airspace flow program throughput from current and forecast weather information. *Pages 1–19 of: Aviation, range and aerospace meteorology special symposium on weather-air traffic management integration, AMS annual meeting*. 19

RODIONOVA, O., ARNESON, H., SRIDHAR, B., & EVANS, A. 2017 (Sept). Efficient trajectory options allocation for the ollaborative trajectory options program. *Pages 1–10 of: Proceedings of the 36th IEEE/AIAA digital avionics systems conference (dasc)*. 20

RUIZ, SERGIO, PIERA, MIQUEL A, NOSEDAL, JENARO, & RANIERI, ANDREA. 2014. Strategic de-confliction in the presence of a large number of 4D trajectories using a causal modeling approach. *Transportation research part C: Emerging technologies*, **39**, 129–147. 17

SCHUMMER, JAMES, & VOHRA, RAKESH V. 2013. Assignment of arrival slots. *American economic journal: Microeconomics*, **5**(2), 164–85. 21

SHERALI, HANIF D, HILL, JUSTIN M, MCCREA, MICHAEL V, & TRANI, ANTONIO A. 2011. Integrating slot exchange, safety, capacity, and equity mechanisms within an airspace flow program. *Transportation science*, **45**(2), 271–284. 19, 20

SMEDT, DAVID DE, BRONSVOORT, JESPER, & MCDONALD, GREG. 2013. Controlled time of arrival feasibility analysis. *In: Proceedings of the 10th USA/Europe ATM R&D Seminar*. 5

SOLER, MANUEL, OLIVARES, ALBERTO, STAFFETTI, ERNESTO, & ZAPATA, DANIEL. 2012. Framework for aircraft trajectory planning toward an efficient air traffic management. *Journal of aircraft*, **49**(1), 341–348. 18

SRIDHAR, BANAVAR, SHETH, KAPIL S, & GRABBE, SHON. 1998. Airspace complexity and its application in air traffic management. *In: Proceedings of the 2nd USA/Europe ATM R&D Seminar*. 87

SUN, DENGFENG, & BAYEN, ALEXANDRE M. 2008. Multicommodity eulerian-lagrangian large-capacity cell transmission model for en route traffic. *Journal of guidance, control, and dynamics*, **31**(3), 616–628. 22

SUN, DENGFENG, STRUB, ISSAM S, & BAYEN, ALEXANDRE M. 2007. Comparison of the performance of four eulerian network flow models for strategic air traffic management. *Networks and heterogeneous media*, **2**(4), 569. 22

SUN, DENGFENG, CLINET, ALEXIS, & BAYEN, ALEXANDRE M. 2011. A dual decomposition method for sector capacity constrained traffic flow optimization. *Transportation research part B: Methodological*, **45**(6), 880–902. 23

SWAROOP, PREM, ZOU, BO, BALL, MICHAEL O, & HANSEN, MARK. 2012. Do more us airports need slot controls? a welfare based approach to determine slot levels. *Transportation research part B: Methodological*, **46**(9), 1239–1259. 21

TERRAB, M, & ODONI, AR. 1993. Strategic flow control on an air traffic network. *Operations research*, **41**(1), 138–152. 21

TERRAB, MOSTAFA, & PAULOSE, SAAJU. 1992. Dynamic strategic and tactical air traffic flow control. *Pages 243–248 of: IEEE international conference on systems, man and cybernetics*. IEEE, Chicago, USA. 21

TOMLIN, CLAIRE, PAPPAS, GEORGE J, & SASTRY, SHANKAR. 1998. Conflict resolution for air traffic management: A study in multiagent hybrid systems. *IEEE transactions on automatic control*, **43**(4), 509–521. 17

US DEPARTMENT OF TRANSPORTATION. 2015. *Beyond traffic: Trends and choices 2045*. Tech. rept. 1

US DEPARTMENT OF TRANSPORTATION. 2016a. *Airline on-time statistics*. Tech. rept. 1

US DEPARTMENT OF TRANSPORTATION. 2016b. *The future of the NAS*. Tech. rept. 3

VELA, ADAN, SOLAK, SENAY, SINGHOSE, WILLIAM, & CLARKE, JOHN-PAUL. 2009. A mixed integer program for flight-level assignment and speed control for conflict resolution. *Pages 5219–5226 of: Proceedings of the 48th IEEE conference on decision and control*. IEEE. 17

VOSSEN, THOMAS, & BALL, MICHAEL. 2006a. Optimization and mediated bartering models for ground delay programs. *Naval research logistics (NRL)*, **53**(1), 75–90. 20

VOSSEN, THOMAS W. M., HOFFMAN, ROBERT, & MUKHERJEE, AVIJIT. 2012. *Air traffic flow management*. Boston, MA: Springer US. Pages 385–453. 19

VOSSEN, THOMAS WM, & BALL, MICHAEL O. 2006b. Slot trading opportunities in collaborative ground delay programs. *Transportation science*, **40**(1), 29–43. 20

VRANAS, PETER B, BERTSIMAS, DIMITRIS J, & ODONI, AMEDEO R. 1994. The multi-airport ground-holding problem in air traffic control. *Operations research*, **42**(2), 249–261. 21

WEI, P, CAO, Y, & SUN, D. 2013. Total unimodularity and decomposition method for large-scale air traffic cell transmission model. *Transportation research part B: Methodological*, **53**, 1–16. 23

WIELAND, FREDERICK, HUNTER, GEORGE, & SHERRY, LANCE. 2008. Assessing NextGen's susceptibility to gaming strategies. *In: AIAA modeling and simulation technologies conference and exhibit*. 21

WORLD METEOROLOGICAL ORGANIZATION. 1994. *A guide to the code form fm 92-ix ext. GRIB*. Edition 1. 86

XIONG, JING, & HANSEN, MARK. 2009. Value of flight cancellation and cancellation decision modeling: ground delay program postoperation study. *Transportation research record: Journal of the transportation research board*, 83–89. 18

XU, YAN, ZHANG, HONGHAI, LIAO, ZHIHUA, & YANG, LEI. 2016. A dynamic air traffic model for analyzing relationship patterns of traffic flow parameters in terminal airspace. *Aerospace science and technology*, **55**, 10–23. 17, 87

YANG, LEI, YIN, SUWAN, HAN, KE, HADDAD, JACK, & HU, MINGHUA. 2017. Fundamental diagrams of airport surface traffic: Models and applications. *Transportation research part B: Methodological*, **106**, 29–51. 87

ZELINSKI, SHANNON, & LAI, CHOK FUNG. 2011. Comparing methods for dynamic airspace configuration. *Pages 3A1–1 of: Proceedings of the 30th IEEE/AIAA digital avionics systems conference (DASC)*. IEEE, Seattle, WA, US. 92

ZHAO, WENJING, ALAM, SAMEER, & ABBASS, HUSSEIN A. 2013. Evaluating ground–air network vulnerabilities in an integrated terminal maneuvering area using co-evolutionary computational red teaming. *Transportation research part C: Emerging technologies*, **29**, 32–54. 17